Enhancing the effect of Tumour necrosis factor - Related Apoptosis Inducing Ligand (TRAIL) in malignant pleural mesothelioma

Dr Doraid Alrifai

CRUK Clinical Training Research Fellowship

Lungs for Living Research Centre

UCL Respiratory

University College London

A submission for the degree of Doctor of Philosophy (PhD)

Declaration

I, Doraid Alrifai, confirm that the work described in this thesis is my own. Where work performed with others is included appropriate acknowledgment is made.

Acknowledgements

As I sit and begin this literary voyage describing some of my efforts; success and failure, it is not possible to make a start without recognising those that have educated, supported and inspired me.

I begin with Professor Sam Janes, my primary supervisor who has hosted me in his laboratory since March 2017. I've struggled to find many people with such rapidly growing success yet a level of humility that can't be quantified. His immense kindness and endless support regardless of his colossal workload has provided me with great motivation and confidence when I have needed it the most. Alongside Professor Janes, my secondary supervisor Dr Martin Forster has provided a level of encouragement in equal measure. Allowing me to work within his department reviewing patients participating in early phase clinical trials, Dr Forster has allowed me to discover the crucial bridge between clinical research and patient care, the latter my ultimate inspiration for undertaking this PhD. His advice, technical support, experience, scientific and clinical knowledge has helped me carry this thesis forward.

My friend, 'high level' scientist, fellow family man and at times life coach Dr Krishna Kolluri has been the most influential colleague I have ever encountered. I am unable to find enough adjectives to describe him. It is very rare in life to find a truly selfless person but in Krish I can honestly say he fits that mould to a tee (or T depending on your English). Finding a balance between completing a PhD, performing clinical work and my biggest job being a father to two young children has been made easy by working alongside Krish. His guidance, patience and true kindness will never be forgotten. His contribution to my professional development is incalculable. There are so many other people in the lab to thank but I am

likely to significantly eat up the word count by acknowledging each member equally. In particular Dr Yuki Ishii and Dr Neelu Kumar have been instrumental during my stay. Like Krish, Yuki has spent countless hours teaching me basic bench techniques, spending time discussing my experimental approach and guiding me through my thesis. I have benefitted greatly from Neelu over the years (this includes pre-PhD where we were once youthful doctors!) from both her lab and clinical experience. A trusted colleague and friend who I turn to when things go wrong. Others within the lab who require particular mention include Dr Rob Hynds (help with PDX models), Dr Kyren Lazarus, Dr Celine Denais (both microscope support), Dr Adam Pennycuick (bioinformatics support) and finally Dr Deepak Chandrasekharan who offered all sorts of advice with a pinch of sarcasm always. Sample acquisition has been crucial to support this work and so I thank a huge clinical team in particular Dr Sonia Cherian, Dr Toby Hillman, Mr David Lawrence, Mr Achilles Antonopoulos and Mr Sofoklis Mitsos who have all helped in providing tumour samples amongst others. Dr Ayad Eddaoudi kindly assisted in cell sorting using flow cytometry and the team from the UCL school of pharmacy who include Dr Richard Angell, Dr Ben Allsop and Dr Trevor Askwith have been incredibly helpful. I must not forget Dr Nnenna Kanu, based at the UCL Cancer Institute, who has provided essential input to the DNA damage work performed.

Without the help of my mother Yasamin Alrifai and father Dr Luay Alrifai I can be certain I would never have made it. Their constant and unremitting support, love, care and most importantly time is immeasurable. They really are truly special people who I aspire to become one day. My brother Zaid and his wife Katie also deserve mention. Where I have shown at times my stress and angst, Zaid has been the voice of reason. Although we gregariously race to see who achieves most in life I really do respect his opinion and reach

out to him when I need him (I am not sure if he really knows this). In addition, my in-laws have hugely influenced me from my mother and father in law Sauad and Hassan Elreda right down to my siblings in law who I hold in the highest regard; Dr Loreen Elreda, Dr Syed Hussain (and their high flying children Amir and Emma), Dr Danny Elreda, Dr Lauren Molloy Elreda, Neggme Elreda and my eldest niece in law Maya Jaafar.

This brings me to the end; however one truly special person and 2 smaller people deserve the greatest credit of all. My wife Donna and children Amelia and Ali are the most important people in my life. Where I questioned my aptitude and withering confidence throughout this process, Donna would dismiss and correct this act of 'self-deprecation'. The early days where she would sit next to and comfort me when things were going wrong to days of celebration standing by my side when things finally went right. Days in the lab where it was falling apart and lonely late trips back home after chaotic working days were made easy when I got back to Donna. A genuinely loving intelligent individual whose dedication to her own craft sometimes took a back seat when I needed her support the most. I'm certain this was not possible without her and my beautifully chaotic children. Love you all.

Finally, this thesis is a tribute to all the patients suffering with cancer who have offered their precious time to participate in this work. Thank you, Cancer Research UK, for supporting this work.

Abstract

Malignant pleural mesothelioma (MPM) is a cancer which originates from the pleura, a layer lining the lungs. The prognosis is bleak as patients who receive standard of care chemotherapy have a median overall survival of approximately 12 months. Tumour necrosis factor - Related Apoptosis Inducing Ligand (TRAIL) is a protein involved in activating the extrinsic apoptosis pathway via engagement with death receptors located on the surface of cells. Following activation of this intracellular cascade, cells undergo apoptosis. We have previously shown that when MPM cells have loss of function mutations in BRCA-1 associated protein 1 (BAP1) they sensitise to TRAIL. BAP1 is involved in several other key cellular functions such as DNA damage response, cell cycle regulation, cell growth and differentiation. Moreover, TRAIL selectively seeks out transformed cells and activates apoptosis making this a therapy of great interest. Methods of utilising TRAIL include recombinant TRAIL (rTRAIL) or through lentiviral transduction of mesenchymal stromal cells expressing TRAIL on their surface (MSCTRAIL).

The work I present in this thesis attempts to amplify the effect of TRAIL exploiting key areas that govern its function. I show *in vitro* that BAP1 plays a non-critical role in homologous recombination and by attempting to exploit this through synthetic lethality using PARP inhibition, a marginal differential response is seen between mutant and wild type cell lines. In addition, I explore the relationship between TRAIL and the immune system. I go on to show that a strong anti-tumour synergistic relationship exists between host immune cells and TRAIL, validated through the development of a syngeneic platform using pleural effusion derived cell lines and matched immune cells from the same patient. Finally, I present work evaluating the role of heat shock protein 90 (HSP90) inhibition and TRAIL confirming a synergistic relationship between the two.

Impact statement

The findings I present have great clinical significance. MPM is a disease with limited therapeutic options. Furthermore, biomarker enrichment is lacking in MPM meaning treatment is offered to all comers rather than those who are likely to benefit. Sparing drug toxicity to those with this disease, unlikely to respond, is paramount.

My work suggests that BAP1 has a limited role in identifying patients likely to benefit from PARP inhibition. It indicates that its relationship with BRCA1 may be an area for further research development. Synthetic lethality in the context of BRCA1 mutations has revolutionised the treatment of breast and ovarian cancer and if this can be recapitulated in MPM in the context of BAP1 this could change a subgroup of these patients lives.

The immense synergistic signal I report between MSCTRAIL and circulating immune cells opens up many options for patients considering immune targeted therapy. The impact of this on the scientific community could be huge given MSCs are considered immune privileged. With the advent of immune checkpoint blockade this could change the way we treat MPM in the future.

Finally, HSP90 inhibition has demonstrated impressive response rates in early phase clinic trials in MPM. This has shown to be associated with upregulation of death receptors in other tumour types, a tumour microenvironment key to TRAIL sensitivity. The low toxicity profile predicted with TRAIL / MSCTRAIL makes this an ideal therapeutic addition in a disease with few options.

Abbreviations

ADI-PEG 20	Pegylated Arginine Deiminase
AR	Anetumab Ravtansine
ASC	Active Symptom Control
ASXL	Additional sex combs-like
ATM	Ataxia telangiectasia mutated gene
ATR	Ataxia telangiectasia and Rad3 related
BAP1	BRCA1 – associated protein 1
BRCA	BReast CAncer gene
BSA	Bovine Serum Albumin
BSC	Best Supportive Care
CDK	Cyclin Dependent Kinase
CDKN2A	Cyclin Dependent Kinase Inhibitor 2A
CHK1	Checkpoint kinase 1
COSMIC	Catalogue of Somatic Mutations in Cancer
CT	Computed Tomography
CTLA-4	Cytotoxic T-lymphocyte-associated protein 4
cFLIP	cellular FLICE-like inhibitory protein
DDR	DNA Damage Response
DMSO	Dimethyl sulfoxide
DNA	Deoxyribonucleic acid
DSB	Double Strand Break
DUB	Deubiquitinase
EAP	Expanded Access Program
EPP	Extrapleural Pneumonectomy

EZH2	Enhancer of Zeste Homolog 2
FAK	Focal Adhesion Kinase
FADD	FAS associated death domain
FBS	Fetal Bovine Serum
FGFR	Fibroblast Growth Factor Receptor
FISH	Fluorescence In Situ Hybridization
FOXK1	Forkhead Box Transcriptional Factor 1
FOXK2	Forkhead Box Transcriptional Factor 2
Gy	Gray
HBM	HCF Binding Motif
HDAC	Histone Deacetylase
HP1	Heterochromatin Protein 1
HR	Homologous Recombination
HCF-1	Host Cell Factor 1
HMGB1	High Motility Group protein B1
H2A	Histone 2A
ICI	Immune Checkpoint Inhibition
IHC	Immunohistochemistry
IR	Ionising Radiation
KD	Knockdown
KO	Knock out
kV	Kilovolt
LATS 1/2	Large tumour suppressor kinase 1 and 2
LOH	Loss of heterozygosity
mA	miliamp

MAPS	Mesothelioma Avastin cisPlatin Pemetrexed Study
MARS	Mesothelioma and Radical Surgery
MDC1	Mediator of DNA Damage Checkpoint Protein 1
MiST	Mesothelioma Stratified Therapy
MJD	Machado Josephin Domain
MPM	Malignant Pleural Mesothelioma
MSC	Mesenchymal Stromal Cells
MSCTRAIL	Mesenchymal Stromal Cells expressing TRAIL
MT	Mutant
MTT	3-(4,5-dimethylthiazol-2-yl)-2,5-diphenyltetrazolium bromide
mTOR	Mammalian Target of Rapamycin
NF2	Neurofibromatosis Type 2
NF-KB	Nuclear Factor Kappa-light chain enhancer of activated B cells
NHEJ	Non-Homologous End Joining
NLS	Nuclear Localising Signals
NSCLC	Non-Small Cell Lung Cancer
ORR	Overall Response Rate
OS	Overall Survival
PARP	Poly ADP (Adenosine Diphosphate) – Ribose Polymerase
PBMC	Peripheral Blood Mononuclear Cell
PBS	Phosphate Buffered Saline
PcG	Polycomb Group
PCR	Polymerase Chain Reaction
PD	Progressive Disease
PD-1	Programmed Cell Death Protein 1

PDGFR	Platelet Derived Growth Factor Receptor
PD L1	Programmed Death-Ligand 1
PET-CT	Positron emission tomography – computed tomography
PI3K	Phosphatidylinositol 3-kinase
PFA	Paraformaldehyde
PR	Partial Response
PRC1	Polycomb Repressive Complex 1
PRC2	Polycomb Repressive Complex 2
PR-DUB	Polycomb Repressive Deubiquitinase
Rb	Retinoblastoma Protein
RPMI	Roswell Park Memorial Institute
SV40	Simian Virus 40
TACTICAL	Targeted Stromal Cells Expressing TRAIL as a Therapy for Lung Cancer
TAI	Telomeric Allelic Imbalance
TAZ	Transcriptional Co-activator with PDZ- Binding Motif
TBE	Tris/Borate/EDTA
TCGA	The Cancer Genome Atlas
TP53	Tumour Protein 53
TRAIL	Tumour Necrosis Factor Related Apoptosis Inducing Ligand
UCH	Ubiquitin Carboxy-terminal Hydrolase
UCL	University College London
UCLH	University College London Hospitals
USP	Ubiquitin Specific Proteases
OTU	Ovarian Tumour Proteases
UV	Ultraviolet

VATS	Video Assisted Thoracoscopic Surgery
VEGFR	Vascular Endothelial Growth Factor Receptor
WT	Wild type
WT1	Wilms' Tumour 1
Yap	Yes-associated Protein
YY1	Ying Yang 1
µl	Microlitre

Table of figures

Contents

1 INTRODUCTION

Malignant pleural mesothelioma (MPM) is a devastating illness with a history blighted with clinical trials offering little in the way of improvement in survival.

The mesothelium, a monolayer of mesodermal cells, is crucially supported by connective tissue in the thorax (1). Its ability to abnormally divide, driven by a plethora of genomic alterations in a pro-oncogenic inflammatory environment is thought the basis of MPM. This over simplified description of the development of pleural mesothelioma has been dissected over time to gain a greater understanding of the pathobiology and genomic landscape of MPM; a guide for the search of new and novel therapies.

1.1 Aetiology of MPM

Since its pre-malignant recognition, several occupational fibres such as crocidolite and amosite, collectively termed asbestos, have been withdrawn from routine use in numerous countries (2). As a result, we are beginning to see a decline in mortality worldwide in some of these participating countries such as the United Kingdom. Based on differing regional legislation, worldwide incidence rates are likely to vary from country to country, which is further compounded by the variation in data collection from diagnostic coding to registration of death (3, 4). Detailing historical exposure is a notorious business heavily relying on sufferers who need to remember key events of diagnostic interest for the data recorder (5). Despite the wide latency period of 20 – 50 years many countries continue to demonstrate an increase in the incidence of MPM which is in part due to ongoing exposure to asbestos both

in developed countries where its previous use remains tattooed in society and in developing countries where its prohibition remains lackadaisical (6). Other ‘unregulated malignancy causing fibres’ are likely to exist which adds further complexity to this paradigm of abolishment of MPM where asbestos has been banned (7).

Although occupational exposure to asbestos is clearly associated with malignancy other examples of fibre encounters have equally shown a profound relationship with cancer. A multinational analysis of 18 studies reported an association between domestic exposure of asbestos and cancer influenced by both the type of fibre and its length (8). Other fascinating accounts of environmental exposure to these carcinogenic fibres have included well described research in the Cappadocian area in Turkey (9, 10), Mexico (11) and some regions in the United Stated of America (12).

Other causes of MPM which have received widespread attention includes exposure to contaminated polio vaccines with simian virus 40 (13) and the presence of asbestos in talc baby powder (14). These reports have been serially challenged over the years with no clear robust relationship identified between exposure and cancer.

The mechanism underlying the cause of MPM through asbestos exposure remains largely unknown. The slow development of a pro-oncogenic inflammatory environment driven by oxygen radicals and high motility group protein B1 (HMGB1) activates mesothelial nuclear factor kappa-light chain enhancer of activated B cells (NF-KB) and phosphatidylinositol 3-kinase (PI3K). This unfavourable environment is thought in part to contribute to MPM, however its universally agreed that this is not the full story (15, 16).

Moreover, the development of MPM appears to be largely somatic, however a subset of cases are driven by germline mutations. BRCA1 associated protein-1 (*BAP1*) is implicated as are other DNA repair genes (17). It has recently been recognised that a pre-malignant state exists. Loss of BAP1 and other genomic alterations in a single layer of untransformed mesothelial cells has shown to predict the development of mesothelioma (18).

1.2 Diagnosis of MPM

The most common presenting symptoms of MPM are breathlessness and chest pain caused by a reactive pleural effusion, tumour encasement of the lung or invasion into the chest wall. Fatigue, anorexia, weight loss, sweats and malaise are also often present as a result of circulating cytokines. Some patients are asymptomatic in the early stages resulting in incidental diagnoses. Less commonly are symptoms secondary to distant metastases, which has been thought to be a rare phenomenon. This has recently been disputed through post mortem studies (19, 20).

Radiological imaging plays a key role in diagnosis; chest radiography, thoracic ultrasound, contrast enhanced computed tomography (CT) and positron emission tomography – CT (PET-CT) are all utilised to guide acquisition of tissue +/- pleural fluid for histopathological assessment (19).

A number of diagnostic serum biomarkers including mesothelin, osteopontin and fibulin 3 have been evaluated but found to be of limited clinical use (21-23). Definitive diagnosis therefore requires histological assessment of primary tumour tissue obtained via medical thoracoscopy or video assisted thoracoscopic surgery (VATS). Where this is difficult,

cytological assessment of pleural fluid can be considered although outcomes from this can be highly variable and diagnosis of the sarcomatoid subtype rarely possible, as a result of a lack of shedding of these cell types into the pleural cavity. Overlap between benign mesothelial proliferation and epithelioid MPM exists (24). The gold standard diagnostic tool is histological evaluation of tissue obtained via biopsy. There are three distinct morphological subtypes of MPM: epithelioid (50-60%), sarcomatoid (10%) and biphasic (30-40%), the latter representing a mixed histological picture of the former two. Epithelioid is associated with a more favourable prognosis compared with sarcomatoid (25, 26).

Ancillary studies central to MPM diagnosis include immunohistochemistry (IHC). Despite this crucial addition to complement the diagnostic workup, there is not a marker that offers both 100% sensitivity and specificity. Calretinin is considered the most commonly used marker however other markers which offer diagnostic value include the gene product of Wilms' tumour 1 (WT1), mesothelin, cytokeratin 5 or 5/6, D2-40 (podoplanin) and thrombomodulin (24). Antibodies to detect these diagnostic markers are used in conjunction with the clinical, radiological and morphological picture. Other antibodies under consideration include GATA3, a transcriptional factor used to differentiate sarcomatoid MPM from lung adenocarcinoma (27). IHC to detect BAP1 is emerging as an important staining method in the diagnosis of MPM. In non-malignant cells, BAP1 is detected in both nucleus and cytoplasm. In malignant cells, where mutations in BAP1 exist in up to 60% of cases, a loss in nuclear staining can be seen as well as sparing of cytoplasmic staining in some cases (a result of mutations within the nuclear localising signal (NLS) causing truncated versions of BAP1) (28). This is becoming a useful and reliable method to support a diagnosis of MPM in this context, however offers little benefit where BAP1 is expressed in MPM, as

its also expressed in normal cells. Mutations appears more prevalent in epithelioid and biphasic subtypes compared with sarcomatoid (29).

Finally, deletions in P16 (CDKN2A), detected using fluorescence in situ hybridization (FISH) have been seen in up to 70% of MPM cases. This is particularly relevant to the epithelioid MPM subtype although is associated with any pathological subtype of MPM (30).

1.3 Staging and prognosis of MPM

The importance of accurately classifying the stage and prognosis of MPM is critical when treatment options and prognosis are to be considered.

As described, there are several radiological modalities that offer a means to accurately stage MPM, although caveats for each of these exist. Contrast enhanced CT is commonly used to evaluate the extent of disease both locally and distally. PET-CT and magnetic resonance imaging (MRI) have been shown to add value where CT falls short. Tissue sampling approaches such as mediastinoscopy are also used in selected cases and centres where uncertainty arises (31-34).

A number of staging classifications for MPM exist, all of which have limitations for routine clinical use. The 8th edition of the International Association for the Study of Lung Cancer (IASLC) TNM (Tumour, Nodes, Metastases) classification is the most widely used as recommended by the International Mesothelioma Interest Group. Tumour assessment is the most challenging of these and several approaches have been explored to accurately and relevantly depict the extent of tumour invasion (35).

T	Primary tumour
TX	Primary tumour cannot be assessed
T0	No evidence of primary tumour
T1	Tumour involves ipsilateral parietal or visceral pleura only, with or without involvement of visceral, mediastinal or diaphragmatic pleura
T2	Tumour involves the ipsilateral pleura (parietal or visceral pleura), with at least one of the following: Invasion of diaphragmatic muscle Invasion of lung parenchyma
T3	Tumour involves ipsilateral pleura (parietal or visceral pleura), with at least one of the following: Invasion of endothoracic fascia Invasion onto the mediastinal fat Solitary focus of tumour invading soft tissues of the chest wall Non-transmural involvement of the pericardium
T4	Tumour involves the ipsilateral pleura (parietal or visceral pleura), with at least one of the following: • Chest wall, with or without associated rib destruction (diffuse or multifocal) • Peritoneum (via direct transdiaphragmatic extension) • Contralateral pleura • Mediastinal organs (oesophagus, trachea, heart, great vessels) • Vertebra, neuroforamen, spinal cord • Internal surface of the pericardium (transmural invasion with or without a pericardial effusion)
N	**Regional lymph nodes**
NX	Regional lymph nodes cannot be assessed
N0	No regional lymph node metastasis
N1	Metastases to ipsilateral intrathoracic lymph nodes (includes ipsilateral bronchopulmonary, hilar, subcarinal, paratracheal, aortopulmonary, paraoesophageal, peridiaphragmatic, pericardial fat pad, intercostal and internal mammary nodes)
N2	Metastases to contralateral intrathoracic lymph nodes. Metastases to ipsilateral or contralateral supraclavicular lymph nodes
M	**Distant metastasis**
M0	No distant metastasis
M1	Distant metastasis

Figure 1. 1 - 8th edition of the TNM classification for pleural mesothelioma; IASLC (Staging Handbook in Thoracic Oncology, 2nd edition)

Stage IA	T1	N0	M0
Stage IB	T2, T3	N0	M0
Stage II	T1, T2	N1	M0
Stage IIIA	T3	N1	M0
Stage IIIB	T1, T2, T3	N2	M0
	T4	ANY N	M0
Stage IV	ANY T	ANY N	M1

Figure 1. 2 - Staging system for pleural mesothelioma based on 8th edition of the TNM classification (Staging Handbook in Thoracic Oncology, 2nd edition)

Often, median overall survival (OS) is quoted at 9-12 months in cases of advanced unresectable MPM. Prognosis is dictated not just by distribution of disease but also by histopathological parameters (36). It is well documented that the epithelioid subtype carries the best prognosis with some studies quoting a median OS of 14 months compared with its sarcomatoid counterpart, which reports a lower median OS of around 4 months (25, 26). Furthermore, other methods of predicting prognosis have emerged from a deep learning model; MesoNet, which has been shown to predict outcomes based on stromal inflammation, cellular diversity and vacuolisation (37).

Germline mutations have also been shown to offer much improved survival benefits. Patients with inherited heterozygous mutations in BAP1 experience a median OS of around 5 years whereas other non-BAP1 germline variants have reported extended survival up to 9 years. Furthermore, these germline mutations tend to be associated with a non-aggressive histological phenotype almost always representing epithelioid morphology (38).

1.4 Management of MPM

Patients who undergo treatment for MPM are carefully selected for either a radical approach, in other words to achieve surgical tumour clearance and ultimately long-term remission or a more palliative approach of managing symptoms and extension of good quality of life.

Conventionally treatment modalities include surgery, radiotherapy and systemic offerings such as chemotherapy, anti-angiogenics, targeted small molecule inhibitors and immunotherapy. Clinical data has emerged over the past few decades in support of each of these with broadly limited success.

Surgery

Surgical intervention for MPM has remained a contentious issue since its inception. Randomised trial data is yet to robustly support this strategy with efforts ongoing to define its role.

Surgery is reserved for those with adequate physiological reserve and amenable to complete macroscopic resection. Caveats to surgery include the importance of intra-operative assessment of 'normal' pleura, the extent of nodal dissection and the hopeless attempts at microscopic clearance. As these issues remain unaddressed, many of the clinical trials attempting to answer whether a particular surgical approach is valid remain clouded (39).

The UK led Mesothelioma and Radial surgery (MARS) randomised feasibility study recruited 112 patients from 12 centres with pathologically confirmed MPM. 50 patients went on to receive induction platinum based chemotherapy followed by either extrapleural

pneumonectomy (EPP) and post-operative radiotherapy or no surgery in a 1:1 ratio. Of the 24 randomised to EPP, only 16 successfully completed surgery. A hazard ratio of 1.90 (95% CI 0.92-3.93, p=0.082) extended to 2.75 (1.21 - 6.26, p=0.016) when adjusted for age, sex, stage and histological subtype. A damning hazard ratio further compounded by a reduced median OS and quality of life highlighted the need to readdress this therapeutic modality for patients with MPM (40). Selection bias was a particular concern as only patients who responded to chemotherapy (stable disease or better) were able to proceed to surgery, leaving half of patient not able to enrol into surgery despite randomisation. Moreover, patients in the non-surgical arm has survival rates higher than expected from historical studies. The ongoing randomised MARS2 study is evaluating the role of extended pleural decortication (EPD) versus no surgery following induction chemotherapy (NCT02040272). The British Thoracic Society (BTS) guidelines state that partial pleurectomy (PP) and extended pleurectomy/decortication (EPD) should not be offered and EPD only within a clinical trial (19).

Radiotherapy

Radiotherapy has a limited role in MPM. The SAKK 17/04 phase II study investigated patients who underwent induction chemotherapy and EPP with or without adjuvant hemi-thoracic radiotherapy. No improvement in relapse free survival was reported, although these results have been criticised based on low numbers and variable radiotherapy approaches (41). Both the SMART and PIT open label phase III studies evaluated the role of radiotherapy as a prophylactic following surgical and large bore pleural procedures. The negative results have led to widespread abandonment of radiotherapy in this context (42, 43). SYSTEMS-2 is an ongoing randomised study evaluating the correct dose of radiation to palliative areas of disease (44).

Systemic anti-cancer therapy

Chemotherapy

Historical studies from early clinical trials have demonstrated meek survival outcomes. A variety of chemotherapy agents have been tested in patients with MPM, teasing out cisplatin therapy as the most efficacious treatment, albeit with a marginal improvement in survival. This has led to many combination studies seeking out clinical synergism. A landmark study, which has shaped modern treatment of MPM is the phase III EMPHACIS trial, evaluating the role of cisplatin (75mg/m2) with or without the anti-folate agent pemetrexed (500mg/m2). The authors reported a 12.1 month improvement in median OS in the combination arm versus 9.3 months in those who received cisplatin alone (p=0.020). Response rates to treatment were also superior at 41.3% compared with 16.7% (p<0.0001). Grade 3 and 4 toxicity was worse in the combination arm (28% v 2% neutropenia, nausea 15% v 6%)), significantly mitigated by use of vitamin B12 and folic acid supplementation (45). In an attempt to avoid some of the characteristic side effects of cisplatin such as central and peripheral sensory neuropathy, a comparison of its use with the more tolerable carboplatin in combination with pemetrexed was reviewed through the international expanded access program (EAP). Safety and efficacy data were reported in 3000 patients who had not previously received chemotherapy. 12-month survival rates were almost identical between cisplatin (63%) and carboplatin (64%) (46). This activity is reflected in several other single arm phase II studies combining carboplatin with pemetrexed (47, 48). Raltitrexed has also been shown to be a worthy substitute of pemetrexed. MOS of 11.4 months compared to 8.8 months with cisplatin alone (HR 0.76, p=0.048) (49).

Other combinations with platinum agents have fared less well. Gemcitabine, a routinely used antimetabolite in other cancers such as lung and hepatobiliary malignancies, has been

explored in a number of trials. Following its reported single agent use (50), phase II activity was confirmed when combined with a higher dose of cisplatin (100mg/m2). Almost half of the patients had a partial response, with only 2 recorded to have progressed of the 21 patients treated. This has since been supported by a further multicentre study presenting similar findings with a marginally improved median OS of 11.2 months (51, 52).

Anti-microtubule agents such as vinca alkaloids and taxanes have also been investigated in combination with cisplatin. Initial activity seen with vinorelbine led to evaluation of this family of drugs in a phase III study (53). The largest of these is the multicentre MS01 study which evaluated the benefit of MVP (mitomycin, vinblastine and cisplatin), vinorelbine and active symptom control (ASC). As a result of poor patient accrual, the study required treatment arm modification resulting in an amalgamation of all chemotherapy agents into one arm to be compared against ASC. This resulted in a non-significant improvement in overall survival in the ASC + chemotherapy arm (HR 0.89 p=0.29), although following exploratory analysis the use of vinorelbine with ASC suggested a trend towards improvement OS (54). The relevance of this study in the current era remains questionable given the front-line chemotherapy recommendation is now pemetrexed and platinum. Furthermore, vinorelbine in combination with oxaliplatin, in a small phase II study, offered a median overall survival of only 8.8 months accompanied by a 1 year survival of 27% (55). The relationship between taxanes and platinums is less well defined with best evidence seen in a small French phase II study of 18 patients reporting a median OS of 12 months accompanied by only 1 partial response (56). Other combinations have been equally underwhelming. HDAC inhibitors, topoisomerase inhibitors and anthracyclines have all been tested in clinical trials with jaded outcomes (57-60).

Antiangiogenic therapy

Bevacizumab, a monoclonal antibody targeting vascular endothelial growth factor-A (VEGF) has shown mixed results in MPM. Following initial failure to demonstrate a survival advantage (61) bevacizumab was investigated in the Mesothelioma Avastin Cisplatin Pemetrexed Study (MAPS), where treatment naive MPM patients were randomised to pemetrexed (500mg/m2) and cisplatin (75mg/m2), with or without the anti-angiogenic agent bevacizumab (15mg/kg). Median OS was longer in the bevacizumab arm compared with chemotherapy alone (18.8 v 16.1 months, HR 0.77, p=0.0167). This may be on account of patient selection bias as those enrolled where under strict eligibility criteria including the omission of patients with cardiovascular comorbidities (62).

Nintedanib, an oral multi angiokinase inhibitor targeting the intracellular domains of VEGFR 1-3, fibroblast growth factor receptor (FGFR) and platelet derived growth factor receptors (PDGFR); α and β, is used in patients with adenocarcinoma of the lung (63). In a phase II study, 87 patients with advanced MPM were randomly assigned to chemotherapy with or without nintedanib. Benefit was seen in patients with epithelioid pathology, who received nintedanib, reporting a non-statistically significant median OS of 20.6 months versus 15.2 months (HR 0.70, p=0.197) (64). A follow up phase III study failed to demonstrate any clinically meaningful improvement in survival and its use is therefore not recommended at present (65). A phase II study exploring the role of nintedanib monotherapy in previously treated patients did not meet its primary endpoint of progression free survival (PFS) (66). Other small molecule multi-kinase agents targeting VEGFR have demonstrated limited activity to date (67, 68).

There remain global differences in the prescribing of first line chemotherapy, with some only offering doublet platinum chemotherapy given its modest survival advantage, lower expense and toxicity compared with the anti-angiogenic combination.

Arginine deprivation

A proportion of mesotheliomas are unable to convert citrulline to arginine; catalysed by argininosuccinate synthetase 1 (ASS1). This epigenetic silencing of ASS1 and resultant deficiency in arginine leads the malignant mesothelial cell to seek out exogenous arginine from the extracellular environment to replace this lost supply. MPM becomes addicted to arginine and is therapeutically cut off using pegylated arginine deiminase (ADI-PEG 20), based on an enzyme involved in catalysing the conversion of arginine back to citrulline and ammonia (69, 70). Following validation in these preclinical models, a proof of concept molecularly stratified window of opportunity randomised phase II ADAM trial was launched comparing ADI-PEG 20 to best supportive care (BSC) reporting an improved median PFS of 1.2 months (3.2 v 2.0 months respectively, HR 0.56, p=0.03) (71).

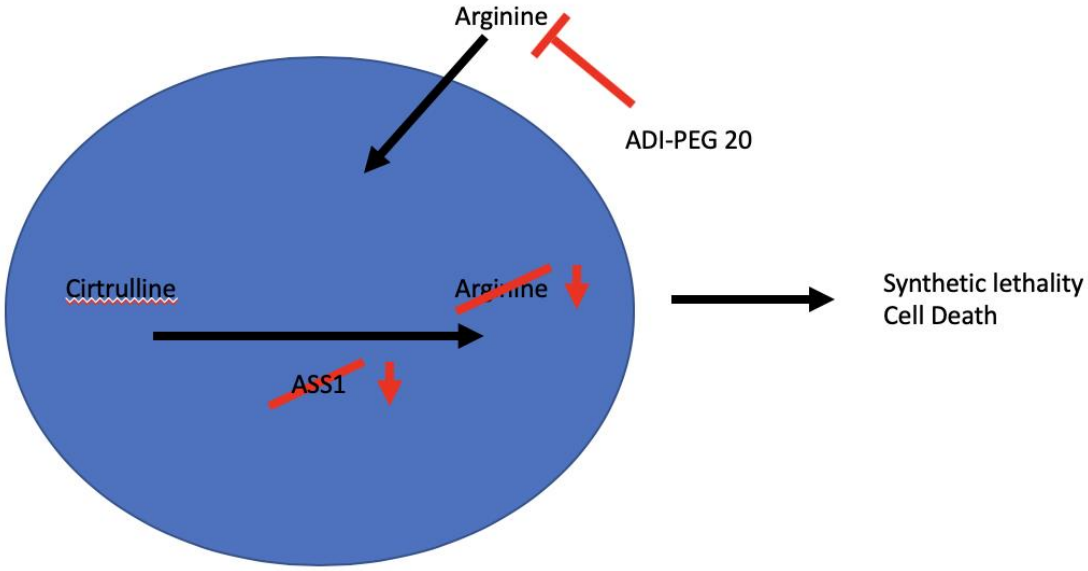

Figure 1. 3 - Exogenous arginine addiction in MPM

The rationale to study the combination of ADI-PEG 20 and antifolates is supported by data confirming that reduction in ASS1 is associated with antifolate resistance (72). Beddowes et al attempted to study this relationship in a phase 1 dose finding exercise. ADI-PEG 20 was added to standard of care chemotherapy (cisplatin and pemetrexed). 38 patients were screened (17 were identified as ASS1 deficient – 45%). 9 patients deemed eligible were eventually enrolled (5 MPM, 4 non-small cell lung cancer), achieving at least stable disease. 7 of these 9 patients achieved a partial response. Of the 5 MPM patients, 4 achieved a partial response (30% or greater tumour size reduction measured by CT) regardless of pathological subtype (73). This has triggered the ATOMIC-Meso study, a phase III clinical trial evaluating the role of ADI-PEG 20 in combination with pemetrexed and platinum chemotherapy in non-epithelioid MPM (NCT02709512).

Immunotherapy

Effective immunosurveillance aids against the development and progression of malignancy yet the ability of cancer to evade this promotes its survival and dissemination. MPM is seldom referred to as an 'immunogenic' tumour. The mutational landscape appears crucial when predicting response to immune checkpoint blockade (ICB), as the highest mutationally burdened tumours respond best. MPM offers a low burden of mutation (<2 mutations per megabase) leading many to believe the likelihood of response to ICB is low (74-76).

Studies evaluating the migration of immune cells have demonstrated differences in survival outcomes. Tumour microenvironments with an increased inflammatory component are associated with a better prognosis (77). Furthermore, the migration of effector T and B cells has been shown to be associated with an improved survival when compared with tumours with less infiltration or components of the immune system that promote tumourigenesis such as tumour associated macrophages (78).

Tumour cells upregulate cell surface inhibitory ligands that bind to corresponding co-inhibitory receptors, also known as immune checkpoints, on immune cells triggering their down regulation. This inherent defence mechanism against an immune based attack has been studied at length in an attempt to exploit this pathway leading to tumour cell death. The most studied of these inhibitory receptors are CTLA-4, programmed cell death – 1 (PD-1) and its natural ligand programmed death ligand 1 (PD-L1) (74). Inhibition of these receptor interactions has yielded remarkable clinical results for tumours such as malignant melanoma persuading researchers to explore these interactions in other cancers including MPM. A study exploring dual inhibition of CTLA-4 and PD-1 in malignant melanoma has reported a substantially improved median overall survival of almost 60% at 3 years, a far cry away from

its infamous prognosis. Kaplan Meier curves continue to plateau suggesting a long term survival outcome, although only time will tell whether these patients have been cured (79). Expression of PD-L1, shown to be a predictive biomarker of response to anti-PD-1 therapy is found to have high expression (> 50%) in under 10% of MPM, although over two thirds are associated with non-epithelioid pathology (p=0.0001). It has been shown that patients with high PD-L1 expression are associated with poorer prognosis (80, 81).

Clinical results from single agent CTLA-4 inhibition are negative. The large placebo controlled phase IIb DETERMINE trial of the anti CTLA-4 monoclonal antibody tremelimumab showed no benefit in the second or third line setting. 571 patients with previously treated advanced MPM were randomised to tremelimumab (n=382) or placebo (n=189). Median OS in the intention-to-treat population did not differ (7·7 v 7·3 months respectively; HR 0.92, p= 0.41) (82).

Many studies have focused on the PD-1/PD-L1 axis as these offer more promise. Initial results from the phase Ib KEYNOTE-028 trial of the anti PD-1 antibody pembrolizumab in 25 patients with previously treated PD-L1 positive (>1%) MPM revealed a PR in 5 (20%) patients and stable disease in 13 (52%). Stable disease in the immunotherapy space can represent long term durable response like other tumour types. Median OS was reported as 18 months, however no discernible relationship between PD-L1 and response rate was demonstrated (83). Phase II studies such as NivoMes and MERIT provide further support for inhibiting PD-1 (84). Phase III studies have been less generous. The PROMISE-meso study compared pembrolizumab with chemotherapy (gemcitabine or vinorelbine) in unselected pre-treated advanced MPM revealing no benefit in the anti PD-1 arm (85). The phase III double-

blinded CONFIRM trial looks to address this by comparing nivolumab to placebo in 336 patients. PD-L1 expression is a pre-planned stratification factor (NCT03063450).

Combining immune checkpoint blockade with chemotherapy was evaluated in the Durvalumab with First-Line Chemotherapy in Mesothelioma (DREAM) study. This was a single arm, phase II trial of 54 treatment naive MPM patients (82% epithelioid) looking to establish activity, safety and tolerability of durvalumab, an antibody targeting PD-L1, in combination with standard of care chemotherapy; pemetrexed and cisplatin. The median progression free survival was 6.9 months with a duration of response of 6.5 months. The highest grade 3-5 toxicities were 13% neutropenia and 11% nausea (86).

An alternative approach has been to combine the immune checkpoint inhibitors anti CTLA-4 and anti PD-1, with recently published promising results. The open label phase II MAPS2 study randomised 125 patients to either the combination of ipilimumab (anti CTLA-4 inhibitor) and nivolumab (n=62) or nivolumab alone (n=63), following first line chemotherapy. Although the study was not powered to compare arms, in the intention to treat analysis, 40% of patients in the nivolumab arm and 52% in the dual checkpoint inhibition arm achieved disease control at 12 weeks, an early signal of activity. Median overall survival reached 11.9 and 15.9 months respectively (87). Using the same combination of drugs, the single arm phase II INITIATE trial treated 34 patients with dual immune checkpoint inhibition resulting in 68% achieving disease control at 12 weeks (10 PR and 13 stable disease) (88). The combination arms reported grade 3-4 toxicity of 26% and 34% in the two studies respectively, whereas 14% was found in the single agent arm of MAPS2. Cautious analysis of results is needed as the control arm in MAPS2 is not deemed standard of care.

Other immune modulating agents have been explored in MPM. Agents targeting mesothelin, an antigen found on the surface of mesothelial cells, have progressed furthest toward the clinic. A single arm phase II study of the anti-mesothelin monoclonal antibody amatuximab in combination with chemotherapy demonstrated an encouraging median OS of 14.8 months and an impressive disease control rate of 90% in 89 patients. We are yet to see a randomised phase III study (89).

Anetumab ravtansine (AR), an anti-mesothelin IgG1 antibody conjugated to the maytansinoid tubulin inhibitor DMR, has reported activity in a phase I study of 16 MPM patients. A PR of 31% and stable disease of 44% has been reported with a durable response defined as greater than 600 days in 5 patients (n=16) (90). Although this prompted a phase II study in mesothelin overexpressing MPM (n=248) randomising patients to either AR or vinorelbine, the trial failed to meet its primary endpoint of progression free survival (91).

Other approaches, such as a recent phase I clinical trial of intra-pleural 2nd generation chimeric antigen receptor T (CAR-T) cells targeting mesothelin in 19 MPM patients has reported noteworthy results. For patients who demonstrated persistence of CAR-T cells anti PD-1 therapy was offered. 2 patients demonstrated a complete metabolic response and a further 9 had disease control (92). Several other immune modulating therapies have been explored with mixed results (93-98).

Examining the role of the immune system *in vitro* can be technically challenging. Extraction of immune cells from a host used for bench-based assays can provide some important information, however several caveats exist when comparing to *in vivo* / human based experiments. Using peripheral blood mononuclear cells (PBMCs) with an assumed

population of cells based on historical experiments introduces margins of error as does the use of these cells in unrelated recipients. As described in the results chapters later in the thesis, standardised immune based PBMC assays were used, however the requirement to develop a syngeneic platform to mitigate this non-self effect was necessary. Volunteer cells can be used as a screening tool to justify moving to a syngeneic model. Extraction of pleural effusion based immune cells can be used however the number and quality of cells are likely to be much lower for assays that require validation and technical repetition. Again, as you will see from the results section both PBMCs and immune cells from pleural effusions were extracted. Pleural effusion samples can be rich in important proteins that govern the immune response both inhibitory and excitatory, hence exploration of this space is important (99). Immune cells found in the peripheral blood may have a role in MPM as evidenced by recent studies looking at neutrophil to lymphocyte ratios (100, 101).

1.5 Commonly identified genomic aberrations in MPM

A germline predisposition to cancer has been identified in many models (102). Heterozygous mutations in *BAP1* are most recognised as implicated in MPM, both germline and somatic (103). Other germline mutations have also been shown to be associated with MPM such as tumour suppressor protein 53 (*p53*) and *BReast CAncer* 2 (*BRCA2)* gene, the former, infamous for causing Le Fraumeni syndrome (104).

The publicly available 'The Cancer Genome Atlas' (TCGA) provides a further demonstration of the genomic landscape of MPM. An updated report in 2018 studied 74 primary treatment naive MPM cases subjected to whole exome sequencing, copy number analysis, mRNA sequencing, non-coding RNA profiling, DNA methylation and reverse phase protein arrays

(76). Mutational burden was highlighted as low evidenced by a somatic mutation rate of < 2 mutations per megabase, a relatively low proportion when compared to other tumour types (75). The clinical implications of this could be profound as mutational burden has been explored as a surrogate marker for response to immune checkpoint inhibition (105). Surprisingly, no genomic signatures were associated with asbestos nor were there differences between DNA breaks and oxidative stress between exposure and non-exposure to asbestos. As expected, 57% of cases were found to have mutations in *BAP1*. Other frequently reported mutations included *CDKN2A, NF2, p53, LATS2 and SETD2*. Although reviewers have been critical of the depth of sequencing undertaken by the TCGA group, which equated to 30 sequence reads, similar findings have been demonstrated in studies that have covered up to 100 sequence reads (106). Further work exploring the combination of alternative investigatory modalities such as next generation sequencing (NGS) and high density arrays have added to this landscape including copy number alterations, point mutations and chromothripsis, the latter an exploratory marker for immunogenicity (107, 108). Recent excitement in the use of immunomodulatory drugs have not fared as well in MPM, although evidence is mounting supporting the idea of an immune response to tumour related neoantigens (109).

It has recently transpired that just over 1 in 10 diagnoses of MPM are associated with a germline mutation, although this is more likely in the younger and non-pleural mesothelioma subtypes (104). This encourages debate as to whether we should consider clinically screening individuals who are diagnosed with MPM or a disease associated with the BAP1 syndrome such as uveal melanoma. This conversation is outside the scope of this thesis but is a meaningful subject matter when considering the long-term management of these patients and their families (110). As our understanding of this genomic landscape in MPM continues to

grow, the scientific / clinical community have taken the opportunity to therapeutically target these aberrations. Although as discussed MPM is associated with a low somatic mutation rate, there are several tumour suppressor genes (TSGs) which are disabled leading to the activation of several oncogenic pathways (76). Among those TSGs identified as most frequently inactivated are *BAP1*, *CDKN2A* and *NF2*. Targeting pathways regulated by these genes therefore offers promise.

BRCA associated protein-1 (BAP1)

Its familial relationship with MPM was brilliantly outlined by Dr Michele Carbone who visited remote villages in Cappadocia, Turkey. He had observed an extraordinary mortality rate reporting half of the villagers dying of MPM. Certain families were preferentially affected whilst others were spared. Through a sequence of carefully planned experiments in similarly affected families in the United States of America, Carbone and his team were able to clearly demonstrate an association between germline mutations in *BAP1* and MPM. This inherited genomic anomaly was re-termed BAP1 cancer syndrome on account of the development of other types of cancers including uveal melanoma (111, 112). Somatic aberrations in *BAP1* have been shown to be as high as 60% in MPM playing an active role in the development and progression of this invariably fatal illness (108, 113-115).

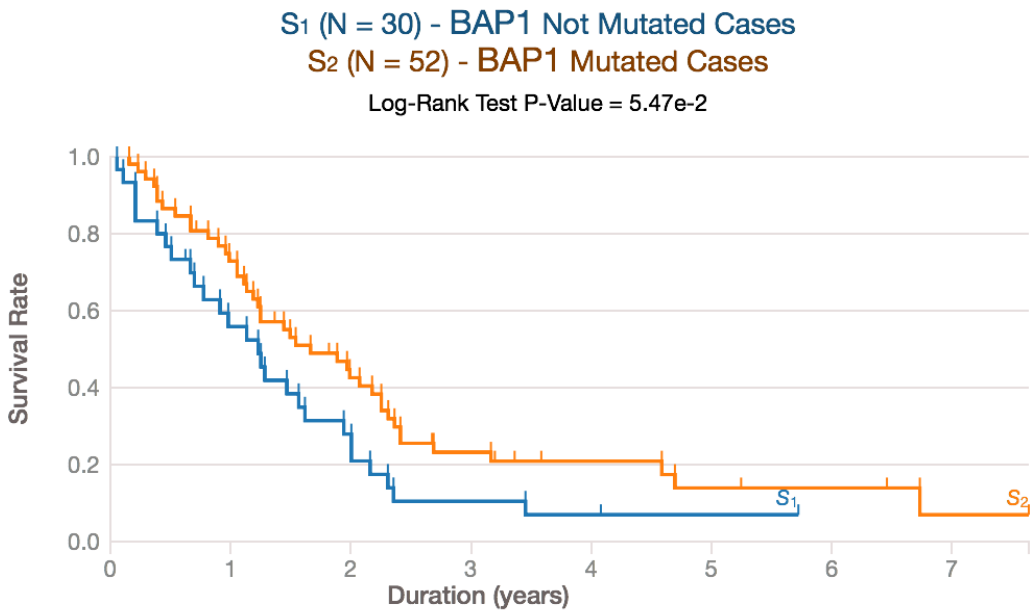

Figure 1. 4 – MPM and somatic mutations (TCGA)

BAP1 and its function

BAP1 is crucial in embryo development and data reporting homozygous deletion of *BAP1* leads to failure to thrive (116). It is frequently found to be deleted in cancer which supports its role as a tumour suppressor gene. Its recognised promiscuity in several cellular functions creates a great challenge for researchers who have endeavoured to decipher its exact behaviour (117, 118).

BAP1 is located on chromosome 3 at position 21.1 (3p21.1) encoding for a 729 amino acid sized protein weighing 90kDa. The *BAP1* gene consists of several domains including an N-terminus catalytic domain (ubiquitin carboxy-terminal hydrolase (UCH)), a C-terminal domain containing two nuclear localising signals (NLS) promoting nuclear residency, a HCF binding motif (HBM) allowing for host cell factor 1 (HCF-1) binding and a BRCA1 binding domain adjacent to the C-terminal domain. Multiple phosphorylation sites promote FOXK1

binding and DNA damage repair (117, 119). Each domain governs a function of BAP1 and mutations within these regions will affect its ability to complete this function.

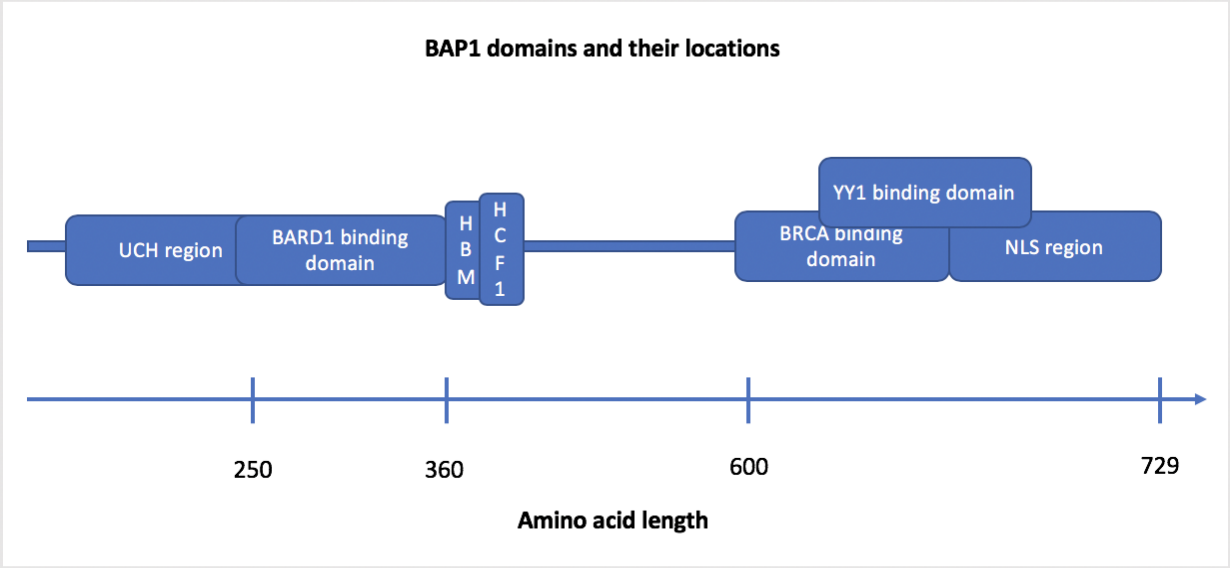

Figure 1. 5 - BAP1 gene and its relevant domains.

It was initially found to interact with the RING finger domains of *BRCA1 and BARD1* (120). As a ubiquitin ligase, BRCA1 was believed to auto-ubiquitinate and subsequently regulated by the deubiquitinating function of BAP1, however this was later disproved (121). It is thought BAP1 deubiquitinates BARD1 modulating the BRCA1-BARD1 E3 ligase activity, a likely explanation for the role of *BAP1* in DNA damage response (122).

Principally, ubiquitination is a process of ubiquitin binding to proteins altering their behaviour (123). One outcome of poly-ubiquitination is the proteasomal degradation of proteins, a process regulated by deubiquitinating enzymes, termed DUBs (124). The C terminus domain of ubiquitin binds to the lysine residues of target proteins, catalysed by a

selection of enzymes which work in a synchronised fashion; E1 (ubiquitin activation), E2 (ubiquitin conjugation) and E3 (ligase function). E1 activates ubiquitin via hydrolysation of ATP, which then conjugates ubiquitin to a target protein with the help of E3. Following poly-ubiquitination, the protein is labelled for degradation and cleared accordingly (125, 126).

As a deubiquitinating enzyme, BAP1 reverses the ubiquitination process by cleaving the bond between the C terminus of ubiquitin and the lysine residues (118). Its relationship between key protein partners is centred upon this deubiquitinating ability mediating DNA damage response (127), the cell cycle (128), cellular pluripotency / differentiation (129) and cell death (130, 131). This ability to contribute to the post translational modification of proteins (based on the degree of ubiquitination) allows for the diverse effects seen upon key cellular processes, making it an exciting molecular target.

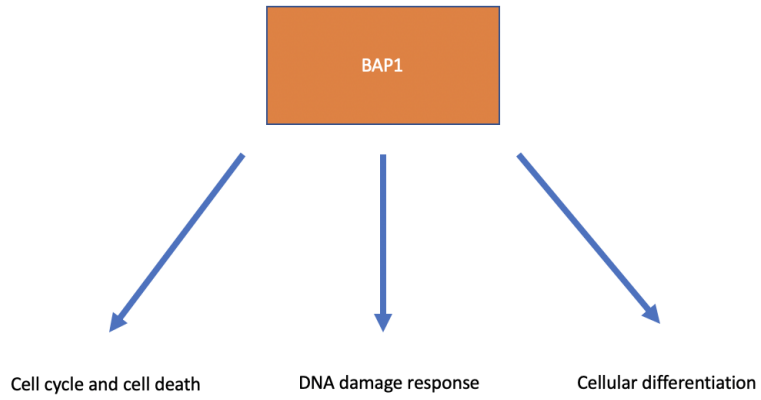

Figure 1. 6 - BAP1 and its functions

There are almost a hundred deubiquitinating enzymes in the literature classified into either cysteine proteases or metalloproteases. The cysteine proteases include ubiquitin specific proteases (USPs), ubiquitin C terminal hydrolases (UCHs), Machado Josephin domain proteases (MJDs) and ovarian tumour proteases (OTU). BAP1 is the largest member of the

UCH family, which is comprised of 3 other enzymes; UCLH1, UCLH3 and UCLH5/37. The metalloprotease superfamily (Jab1/mov34/Mpr1 Pad1 N-terminal + (MPN+)) bind zinc hence their name.

One of the most important interactions reported is that of BAP1 and the ASX subunits of the Polycomb group proteins (PcG); Polycomb repressive deubiquitinase (PR-DUB). This partnership exerts its influence on transcription via deubiquitination of histone 2A (H2A), balanced by ubiquitination via BRCA1 or polycomb repressive complex 1 (PRC1), playing a key role in DNA damage repair (132). The transcriptionally repressive polycomb repressive complex 2 (PRC2) is of particular relevance in MPM as enhancer of zeste homolog 2 (EZH2), a key component of PRC2 has been targeted in MPM (133, 134).

Transcriptional regulation is a key feature of BAP1. In support of this hypothesis, it achieves this through its nuclear relationships with several partner proteins which assist recruitment of BAP1 to the genome given it has no direct DNA binding ability. Equally, HCF-1 interacts with the genome via transcriptional regulators that bind DNA directly. In the nucleus, BAP1 binds HCF-1 via its HBM binding domain. It deubiquitinates HCF-1 at lysine residue 48 (K48) (135). This BAP1-HCF-1 relationship is thought to modulate transcription by recruiting chromatin modifying enzymes such as E2F family members (136, 137). BAP1 and HCF-1 bind to another transcriptional regulator; ying yang 1 (YY1) to form a ternary complex; a critical regulator of gene expression. Its recruitment to the promoter of the COX7C gene controls expression of a mitochondrial respiratory chain protein (128).

The forkhead box transcriptional factors (FOXK1 and 2) are a key set of proteins involved in BAP1 mediated gene regulation. Their ability to directly binding to DNA using their forkhead winged helix-turn-helix DNA-binding domain gives this protein the opportunity to

bring BAP1 to the genome (138). Following phosphorylation at threonine 493, a critical step in BAP1s interaction with DNA bound FOXK2, a HCF-1 bound BAP1 can negatively regulate FOXK2 target genes through its deubiquitinating function (138). Interestingly however in the event of a mutation in the HCF-1 binding motif the repression of FOXK2 continues suggesting its redundant activity in the regulation of FOXK2 (139). The catalytic domain of *BAP1* is deemed important in regulating the expression of genes involved with FOXK2 such as MCM3 (138).

O-linked N-acetylglucosamine (OGT) has been shown to be deubiquitinated by PR-DUB. Its role in transcription is centred upon its ability to catalyse the addition of N-acetylglucosamine to serine or threonine residues. Its relationship with BAP1 and HCF-1 promotes recruitment of further target proteins to mediate transcription (140). The role of their relationship on gluconeogenesis has also been documented (141).

Several other proteins have been shown to be directly engaged with BAP1, such as INO80 a protein directly involved in chromatin remodelling, amongst others.

Cell cycle regulation is another important documented function of BAP1. Its modulation of S phase is supported by several studies demonstrating its ability to both promote and inhibit this stage of the cell cycle (118, 122). Data has also emerged implicating the BAP1-HCF-1 complex in cell cycle regulation, however work in this field remains in its infancy (135). Work to elucidate the exact role *BAP1* has on the cell cycle remains ongoing with a school of thought believing the deubiquitinating function of BAP1 influences this.

BAP1 and cancer

BAP1 exerts much of its influence against cancer through its catalytic and NLS domains. Studies have shown when they are abrogated through genetic modification BAP1 loses its tumour suppressor function (29, 118).

It remains unclear how mutations in BAP1 lead to cancer. Various theories are supported by numerous studies. Heterozygous mutations in *BAP1* in non-malignant cells have a predilection to develop into cancer. One theory is due to a metabolic drive towards cancer established *in vitro* where MPM was found to be associated with aerobic glycolysis and lactate secretion. A relationship so robust a metabolic model was developed able to accurately predict BAP1 status (142). Its role in epigenetic regulation of pluripotency and cell differentiation is thought another mechanism of carcinogenesis (143). In addition, BAP1 influences cell death in a number of ways. Work from our lab has shown that loss of function mutations in *BAP1* upregulate death receptors, priming cells for apoptosis (144). Sensitisation of mesothelioma cells to TRAIL *in vitro* and *in vivo* was robustly demonstrated and is due to be studied in a phase II clinical trial exploring the role of standard of care chemotherapy with or without mesenchymal stromal cells expressing TRAIL. Other explored mechanisms include modulation of the IP3R3 channel, which regulates the transport of calcium from the endoplasmic reticulum to the mitochondria (130) and its inhibition of ferroptosis, a metabolically mediated cell death process (131).

A plethora of studies have targeted BAP1 in both the pre-clinical and clinical setting. Some of the agents explored include histone deacetylase (HDAC) inhibitors, EZH2 inhibitors, poly ADP ribose polymerase (PARP) inhibitors and death receptor agonists. Use of BAP1 as a

predictive biomarker of response to these drugs allows for patient stratification and sparing of toxicities in patients unlikely to respond.

Following the identification that HDAC expression is dependent on the type of cell that translates it, it has been shown that HDAC2 is inhibited in *BAP1* mutated MPM cell lines through transcriptional abundance. HDAC1 expression increases in an attempt to compensate for this loss which in turn has been shown to sensitise to HDAC inhibitors (145). Unfortunately, this has not translated into the clinic. The Vorinostat in Patients with Advanced Malignant Pleural Mesothelioma who Have Progressed on Previous Chemotherapy (VANTAGE 014) study failed to demonstrate an improved survival benefit in all comers (146).

Mutant BAP1 has been shown to increase trimethylation at histone H3 (H3K27me3), EZH2 and enhanced repression of PRC2. When EZH2, the only methyltransferase to histone H3, is inhibited in a *BAP1* mutant setting, this leads to reduced tumour growth (133). Preliminary results from a phase II multicentre clinical trial of the EZH2 inhibitor tazemetostat in MPM tumours with inactive BAP1 offers cautious optimism. Of 74 patients recruited and initiated on treatment, 31 patients (51%) achieved disease control at 12 weeks, of which 2 achieved partial response (PR) (134).

BAP1 and DNA damage response

BAP1 and its role in DNA damage response remains poorly understood. Its critical function in homologous recombination has been questioned and is unlikely to have the same influence compared with crucial partners such as BRCA1, despite its close-knit relationship. Given its function in regulating transcription it is fitting that it has been investigated for its role in the repair of DNA.

Repair of double strand DNA breaks is a complex endeavour. When a break occurs, it triggers recruitment of essential repair proteins to the site of damage. It is thought recruitment of these proteins is governed by a ubiquitin mediated signalling cascade (147). One of the early steps in repair involves heterochromatin protein 1 (HP1) -beta (CBX1) which binds methylated histone H3 on lysine 9 (H3K9me) altering the structure of the chromatin (148).

As a result, H2AX, a critical histone in the repair pathway becomes phosphorylated on serine 139 as a result of the double strand break forming γH2AX. As this can also occur during physiological states the presence of γH2AX does not necessarily represent a double strand break, however its comparable quantification can be useful in well designed assays (149, 150). This additional attempt at chromatin modification allows for the recruitment of other proteins necessary to instigate DNA repair. γH2AX binds mediator of DNA damage checkpoint protein 1 (MDC1), which then mobilises RING finger E3 ubiquitin ligases (RNF8 and RNF168) to this complex (151, 152). Following a process of ubiquitination including RNF168 which assists ubiquitin formation on K63 of H2AX (153), BRCA1 and p53 are enlisted, which are crucial in dictating the manner in which the break is repaired; homologous recombination (HR) or non-homologous end joining (NHEJ) respectively (154, 155). The technique in which DNA is repaired is crucial as the former is the preferred option given its

complex yet reliable method of repair compared with NHEJ which is simple but error prone. A careful replication of DNA and re-joining through a step wise approach leads to few errors and robust DNA repair compared with NHEJ which involves a crude re-assembly of the dissected strands by directly linking them back together. As one would expect, the latter is thought to carry high error risk. Further proteins assemble at the site including Mre11, RAD50 and Nbs1 (MRN complex), RAD51 a protein crucial in homologous recombination promoting strand invasion and ataxia telangiectasia mutant (ATM) (156, 157). As more and more proteins join the fray the chromatin continues to decondense and prepare the site for repair.

Of these proteins, poly-ADP ribose polymerase (PARP) has garnered the greatest attention over the years, as a result of its critical role in *BRCA* mutated breast and ovarian cancer (158-160). Like the other proteins, PARP has a key role in chromatin modification and is involved in several repair pathways including homologous recombination and base excision repair (161). Double strand breaks are detected by PARP leading to a process of PARylation. In union with NAD+, poly ADP ribose (PAR) chains are formed and attach to target proteins (including PARP itself) assisting in the recruitment of key partners to double strand breaks such as p53, BRCA1, γH2AX and BARD1 (162, 163). PARP then loses affinity for the resected area and pulls away, allowing the repair process to continue (164).

A fundamental aspect of PARP1 is the repair of single strand breaks. Where PARP1 is deficient, single strand breaks are unable to repair due to stalled replication forks. Double strand breaks accumulate which are repaired through the homologous recombination pathway, and so cells become overly reliant on this mechanism. PARP1 is also involved in NHEJ, alternative NHEJ (aNHEJ) and single strand annealing (SSA) (165). NHEJ is the most

studied of these error-prone pathways. PARP1 is overexpressed in several cancers (166, 167). Invariably the process of carcinogenesis is driven by a deficiency in a DNA repair pathway allowing for sustained mutagenesis and aberrant cell division. *BRCA1/2* is the best example of this as germline mutations in these genes are associated with a predisposition to breast and ovarian cancer (102). More recently other tumour types have shown faults in these genes and subsequent homologous recombination including prostate cancer (168). These malignant cells become reliant on a compensatory pathway such as base excision repair and targeting these pathways form the basis of synthetic lethality.

The successful attempt at exploiting synthetic lethality has be shown in breast and ovarian cancer. Mutations in *BRCA1/2* lead to homologous recombination deficiency (HRD) and a dependence on an alternative method of DNA repair. PARP mediated repair has been shown to be implicated in these tumours and through pharmacological PARP inhibition exquisite cell death has been demonstrated (169).

PARP inhibition works principally by inhibiting PARylation of essential proteins. This leads to a concept termed PARP trapping where PARP is firmly bound to double strand breaks leading to replication fork collapse and no reliable method of repair (170). Other mechanisms underpinning PARP trapping have been explored (171). This ultimately leads to stagnation of PARP-DNA complexes interfering with the ability to repair DNA, leading to cell death (172).

Deubiquitination is thought to play a key part in this process, although much work still needs to be completed to elucidate its exact role. Other than catalysing the ubiquitin formation on K63 of H2AX other members of the deubiquitinating family influence DNA damage repair. The transcriptional repressor PRC1 is involved in mono-ubiquitination of H2A on K119

which is implicated in DNA damage response and gene expression. By enforcing silencing of transcription at the ends of double strand breaks, repair can be facilitated quicker (173, 174). DUBS have also been implicated in RAD51 recruitment (175) as has BRCC36 (176), a DUB which modulates ubiquitination of key repair proteins. The broad nature of DUBs makes deciphering its exact role a challenging assignment.

The role of *BAP1* in DNA repair remains uncertain despite a growing understanding. Its interaction with the RING finger domains of *BRCA1 and* BARD1 inform us of some involvement (120). It is thought BAP1 deubiquitinates BARD1 modulating the BRCA1-BARD1 E3 ligase activity, a supportive argument for the role of *BAP1* in DNA damage response (122).

A key initial step in the DNA repair process is phosphorylation of BAP1 at serine 592 by ATM, which later dephosphorylates on completion of repair (119). A landmark study exploring DNA repair in *BAP1* knockout (KO) chicken DT40 cell lines has shown that this KO *in vitro* model is sensitive to DNA damaging agents including ionising radiation. The authors suggest the deubiquitinase activity of BAP1 is important in assembling the key proteins for homologous recombination such as RAD51 and that migration of BAP1 to sites of double strand breaks is dependent on where mutations exist in *BAP1* (127).

BAP1 and its role in MPM is even less well understood. BAP1 is thought to mediate PARP dependant migration of PR-DUB to sites of damage, which is involved in the repair process and is phosphorylated by ATM at the time of DNA damage (177). Work performed by Srinivasan et al suggests pharmacologically inhibiting PARP, regardless of *BAP1* status or the type of PARP inhibitor used, leads to cell death. Unfortunately, only 6 cell lines were

used (only 3 reported in the main manuscript) with no genetic knockdown models making interpretation of their findings problematic (178). If this theory holds true and PARP inhibition is effective across all cell lines, this could suggest that HRD is implicated in most cases of MPM regardless of whether *BAP1* is mutated or not. Furthermore, a few years ago a study identifying a specific isoform of BAP1 affecting its catalytic domain suggested sensitivity to PARP inhibition in MPM. This splice variant was found lacking 12 amino acids from the catalytic region compared with full length BAP1. The cell viability results were limited to the ZL-55 MPM cell line transfected to express the identified BAP1 isoform, however results were unconvincing only accentuated when PI3K-MTOR inhibition was employed i.e. BRCA inhibition (179). Another more recent study again explores this relationship between olaparib sensitivity and *BAP1* mutated MPM and although a correlation is again made only 3 cell lines were used for the preliminary work and 90 fixed frozen paraffin embedded (FFPE) samples to complement this and identify a 'BRCAness' like phenotype correlating with survival. This is supported by further work consolidating the role of the existence of DNA damage response genes and improved survival (180, 181). The pre-clinical work up of *BAP1* in DNA repair remains inadequate which is the basis behind the lack of robustness of this relationship. In my opinion, there is no consensus whether mutations in BAP1 clearly lead to synthetic lethality when PARP inhibition is employed.

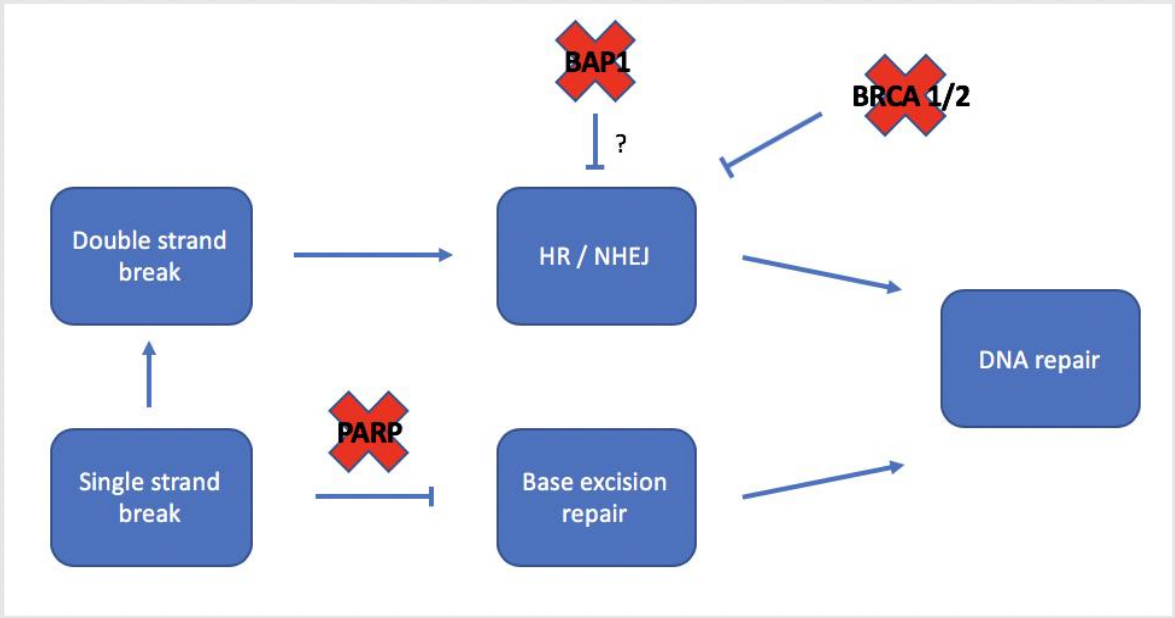

Figure 1. 7 – Compensatory DNA repair pathways in BRCA mutations

Studies are currently underway to compare the clinical role mutations in *BAP1* have in cancer compared with *BRCA1*. The homologous recombination pathway they share has triggered similarly designed studies exploring synthetic lethality using PARP inhibitors. This has invited some discussion given the expected non-crucial role BAP1 is likely to have in homologous recombination. A phase II study of the PARP1/2 inhibitor olaparib is underway; patient response will be correlated with somatic mutations in *BAP1* and germline mutations in DNA repair genes (NCT03531840). In addition, a phase II clinical trial of the PARP1/2 inhibitor niraparib in *BAP1* and other DDR pathway deficient neoplasms, including MPM, also continues (NCT03207347). VIM an open label randomised phase II trial of oral vinorelbine versus active symptom control, looks to explore the relationship between *BRCA1* and its speculative sensitivity to vinka alkaloids, an essential regulator of the spindle assembly checkpoint (NCT02139904). Almost 40% of MPM cases lack BRCA1 expression (182).

Other heavily investigated DNA damage response agents such as ataxia telangiectasia mutated gene (ATM) / ataxia telangiectasia and Rad3 related (ATR) / checkpoint kinase 1 (CHK1) inhibitors are yet to find a place in MPM (183).

Other important genomic aberrations

Cyclin-dependent kinase inhibitor 2A (CDKN2A)

Recent studies have identified homozygous deletion of the 9p21 locus encompassing *cyclin-dependent kinase inhibitor 2A (CDKN2A)* in approximately half of MPM cases (115, 184). Alternative methods of detecting deletions such as fluorescence *in situ* hybridization reveal rates as high as 80% (30, 185, 186). Within the same exon, two unique proteins p14 (ARF) and p16 (INK4a) are encoded via alternate reading frames. Both proteins mediate regulation of tumour suppressing pathways centred upon p53 and retinoblastoma protein (Rb) respectively (187). p14 facilitates p53 activation which in turn promotes cell cycle arrest and apoptosis by interruption of cyclin-cyclin dependent kinase (CDK) complexes (188). p16 inhibits cyclin-dependent kinases 4 and 6 (CDK4/6) which inactivate the Rb / E2 factor (E2F) complex also leading to cell cycle arrest (189, 190). Thus, p14 (ARF) and p16 (INK4a) halt tumour growth through alternative pathways and when lost predispose to cell cycle dysregulation and carcinogenesis (189, 191, 192). Therapies impeding these oncogenic pathways are an area of active interest with supportive preclinical data. Re-expression of the p16(INK4a) gene product in p16 deficient cell line and human mesothelioma xenograft mouse models has demonstrated inhibition of CDK4/6 and phosphorylation of Rb leading to cell death (193, 194). The CDK4/6 inhibitor ribociclib, licensed for use in metastatic breast

cancer, is currently being tested in a phase II clinical trial in solid tumours including MPM (NCT02187783).

NF2

Inactivating mutations of *neurofibromatosis type 2 (NF2)* are seen in 40-50% of MPM (115, 195). *NF2*, located on chromosome 22q12, encodes the scaffolding protein merlin. Located in the plasma membrane, merlin communicates with local integrins mediating several pathways dysregulated in cancer such as cellular migration, invasion and adhesion (196). It also governs the activity of several proteins involved in cell growth arrest via cell contact inhibition. Of these proteins, the most studied is Yes-associated protein (YAP), a key player in the Hippo signalling pathway that controls organ size during development and proliferation. Merlin also recruits large tumour suppressor kinase 1 and 2 (LATS1/2), responsible for inactivation of YAP and its homolog; transcriptional co-activator with PDZ-binding motif (TAZ). Inactivation of merlin therefore leads to constitutive upregulation of YAP/TAZ and activation of the Hippo pathway, commonly seen in MPM (197). Therapeutic targeting of this axis is in its early stages and there are no clinical trials to date. Agents have however shown preclinical activity and are in further development (198, 199).

Merlin inactivation also upregulates mammalian target of rapamycin (mTOR) signalling, a pathway frequently activated in cancer and implicated in MPM development (200, 201). A phase II study of the mTOR inhibitor everolimus in 59 previously treated advanced MPM patients reported limited activity. Only 2% demonstrated a response with a 2.9 month median PFS and 6.3 month median OS (202). A phase I study of the dual class-I PI3K and mTOR kinase inhibitor apitolisib in 120 patients with advanced solid tumours showed PR in only 3

of 33 patients with MPM (203). Newer generations of dual PI3K/mTOR inhibitors however remain in development and are being tested in clinical trials (NCT01655225).

Merlin negatively regulates focal adhesion kinase (FAK), a protein involved in motility and cell survival, upregulated in many cancers including MPM (204). Despite early promise in MPM (205, 206), a phase II trial studying the role of the FAK inhibitor (VS-6063) defactinib in merlin deficient pre-treated MPM led to early termination (NCT01870609) (207). A subsequent phase II window of opportunity study of pre-surgical MPM candidates treated with defactinib recorded an overall response rate (ORR) of 13%. This modest response however was correlated with an increase in CD4 and CD8 T cell infiltration and a decrease in immunosuppressive cell infiltration (208). This immunomodulatory relationship has since triggered a phase I clinical trial of defactinib in combination with pembrolizumab, a monoclonal antibody against programmed cell death protein 1 (PD-1) (NCT02758587).

Despite a surge in understanding in the biology of MPM, this is yet to translate into meaningful survival outcomes for patients. Much is promised through these clinical trials and only time will tell whether the therapeutic agents materialise into licensed treatment for these unfortunate individuals.

1.6 Mesenchymal stromal cells (MSC)

The definition of mesenchymal stromal cells (MSCs) remains a contentious issue, although several attempts have been made to characterise them (209).

These mesodermal originating multipotent cells can be sourced from a variety of sites including bone marrow, adipose tissue and umbilical cord. Their task of differentiating into adipocytes, chondrocytes and osteocytes contributes to the development of a central support network for tissue. The differences between these cells and their underlying function remains poorly understood (210).

These cells lack characteristic differentiation surface markers which makes both distinguishing them from other MSCs and other unrelated cell types a great challenge. They express three markers; CD73, CD90, CD105 but lack essential haematopoetic surface markers such as CD45, CD34, CD14 or CD11b, CD31, CD79 alpha, CD19 and HLA-DR (211). Furthermore, it is also well documented that they lack the necessary machinery to perform antigen presentation including MHC II and co-activating signals CD80/86 and CD40 (212). MSCs grow into a fibroblast like shape, are adhesive to plastic in standardised culture conditions and display ‘plasticity’ meaning in the presence of growth factors these cells can differentiate into adipocytes, chondrocytes and osteocytes (209, 213).

Not all undifferentiated cells develop into these subtypes, a representation of their heterogeneity despite their similarity pre-differentiation. Other cell markers have been explored but remain investigational.

The primary role of MSCs is to facilitate tissue repair by differentiation into appropriate cell types, regeneration of the extracellular matrix and re-vascularisation of insulted areas. At the site of local injury, where inflammation initially promotes an immune response, MSCs are mobilised to promote tissue repair. The mechanism underlying this is poorly understood but one theory implicates CD44 expressing MSCs interacting with hyaluronic acid, produced at the site of damage (214). In response to the release of inflammatory mediators such as IFNγ and TNF A, MSCs release a plethora of their own mediators which fosters cellular regeneration (215). This cross talk between the tumour microenvironment and MSCs is what is thought to dictate the fate of cancer.

Assessment of these cells has drawn criticism based on several assays performed *ex vivo* rather than *in vitro*. This inconsistency across the board is reflected in varying experimental results. Historical co-culture experiments performed have had variable differences in the cell to cell ratios between MSCs and cancer / immune cells. This irregularity may reflect the differences in results and ultimately questions the impact MSCs have on the immune system. As a guide, MSC: leukocyte ratio of up to 1:10 has shown greatest inhibitory potential on immune cells, although in reality the ratio is likely to be far less *in vivo* (216).

The combination of its 'immune-privileged' status and ability to conduct repair at inflammatory sites has been a source of investigation in diseases such as acute graft versus host disease. Taking advantage of this unique property, use of allogeneic MSCs as 'off the shelf' therapy has been explored in this setting in hundreds of clinical trials.

MSCs and cancer

These basic principles have been mirrored in cancer. Like sites of tissue injury, migration towards cancer cells is well documented; a property that has generated much excitement. The tumour microenvironment largely relies on a hypoxic atmosphere to fuel growth. Signals such as hypoxia – inducible factor 1 (HIF-1), stromal cell derived factor 1 (SDF1), VEGF and chemokine receptor 4 (CXCR4) lead to MSC homing as do growth factors including endothelial growth factor - A (EGF-A) and fibroblast growth factor (FGF) (217, 218). Interruption of these homing pathways has led to reduced recruitment of MSCs to tumour tissue and thus reduced tumour development. Moreover, MSCs have also been shown to regulate the AKT pathway which contributes to mobilisation of MSCs (219).

On arrival, MSCs commit to a path of either supporting tumour progression or regression, influenced by a number of inflammatory mediators. Numerous mechanisms of tumour progression have been explored confirming the role MSCs have on epithelial mesenchymal transition (EMT) (220), angiogenesis (221) and differentiation into a 'cancer associated fibroblast' like phenotype (also colloquially known as tumour associated MSC) (222), through a process of gene regulation and cytokine release. Pro-tumourogenic factors such as hepatocyte growth factor (HGF) and insulin like growth factor 1 (IGF1) as well as proangiogenic cytokines such as VEGF, TGFB (pro and anti-tumourogenic) and IL-6 have been shown to be implicated in this process. In addition, they have been shown to modulate the immune system promoting an immune evasive atmosphere, stimulating the development of cancer (223-225). In contrast, MSCs have led to tumour regression *in vitro*. Both bone marrow and umbilical cord MSCs have led to anti-tumour effects (226, 227).

MSCs and their relationship with the immune system

To maintain tissue homeostasis in the context of acute injury, MSCs need to find a balance between repair of damaged tissue and termination of the immune response to avoid a chronic inflammatory site. The latter becomes a fundamental problem in cancer where a robust immune response is necessary to promote tumour cell clearance. This balance is governed by several factors, driven by IFNγ, including indoleamine 2,3 dioxygenase (IDO), nitric oxidase 2 (NOS2), prostaglandin E2 (PGE2), arginase 1 and 2 (ARG1 and ARG2), HGF, TGFB and many more (228). IDO inhibition induces immunosuppression via kynurenine synthesis, a method which has led to mixed results in the clinic (229). Its role as a secreted factor of MSCs promotes tissue repair including tumour cell development. TGFß, another growth factor which offers both protective and tumour promoting properties interferes with the expression of NKG2D, expressed on immune cells, disrupting anti-tumour effector function as well promoting the function of Tregs (228).

The type of mesenchymal stromal cell may play a pivotal role in its relationship with the immune system. A good level of evidence suggests there is no clear consensus between immune-modulatory properties of bone marrow MSCs and other types of MSCs derived from umbilical cord or adipose tissue (230, 231). This physiological balance between stimulation and inhibition is driven by the microenvironment it exists within. This driving force towards a particular phenotype can be tumour specific and data supporting its immunosuppressive role in breast cancer may not necessarily cross over into MPM (232).

Lack of antigen presentation machinery; MHC I (low) and II (absent) are thought to be a significant reason for their immune-privileged status. The lack of ability to present foreign

antigen makes these cells an ‘off the shelf’ possibility if harnessed in the correct manner (211).

MSCs are thought to affect the immune system through several mechanisms. The current paradigm suggests MSCs affect maturation of antigen presenting cells including their cell differentiation and availability of accessory molecules including CD80 and CD86 (232). They have also been shown to downregulate T and NK cells, whilst upregulating immunosuppressive cells such as regulatory T cells (Treg) and myeloid derived suppressor cells (MDSC) (233). Their immunosuppressive impact can be demonstrated further by expression of immune based proteins. When activated by cytokines such as IFNγ, MSCs have the ability to upregulate MHC I and II to a lesser extent (234). Other proteins can be overexpressed on their surface in parallel including the co-inhibitory ligand to PD-1; PD-L1. ICAM1 and VCAM1 have also been shown to upregulate supporting the idea that cell to cell contact also influences immunosuppression (235, 236).

MSCs have influence across both the innate and adaptive immune system.

MSCs interact with the complement system promoting migration to sites of injury as well as protection against targeting and destruction. They promote neutrophil migration and survival via cytokines and chemokines (237). Their relationship with NK cells is tenuous. As well as harbouring the ability to downregulate their function they are also liable to death by activated NK cells through MICA-B and ULBP interactions. Their ability to reduce IFNγ production and activating receptors, NKp30 and NKG2A leads to this diminished response (238). As described above, dendritic cells are also affected through both monocyte development and activation, which results in ineffective T cell function (239). MDSCs are found to be more

prevalent in the presence of MSCs; an inherently immune-inhibitory cell type (240). Macrophages are also affected regulating their differentiation to M1 and M2 via IL6 (241). There is also emerging data suggesting a role between gamma delta T cells and MSCs (242).

As described earlier, the adaptive immune system is particularly relevant in cancer. Several mechanisms exist supporting an immunosuppressive MSC phenotype; found to downregulate B and T cells through the release of immunosuppressive mediators including IDO and iNOS (228). Despite this, there is little but available evidence to suggest MSCs play an immune stimulatory role supporting the paradigm for a bi-directional approach (243).

Toll like receptors (TLRs) play a key role in MSC behaviour based on the expression of particular types of TLRs. Depending on which receptors are activated, an MSC can either display an immunosuppressive or immune-stimulatory phenotype. TLR 3 and 4 have been found to promote secretion of cytokines which both lead to MSC immunosuppression and immune-stimulation. Further evidence supports the changeable immuno-phenotype of MSCs (244).

The spectrum of inflammation is key to which phenotype MSCs adopt. Tumour microenvironments with a low level of inflammation (IFNγ / TNF alpha) are likely to have an immuno-stimulatory phenotype as opposed to a heavily inflamed site where MSCs are expected to function in an immune-inhibitory role. A dynamic phenotype has also been shown as inflammation levels pick up (Waterman et al) providing importance to the composition of the microenvironment (245).

It is therefore clear that depending on the tumour microenvironment, MSCs will adopt a particular persona which either drives tumour progression or leads to impedance of its development.

Mesenchymal stromal cells and cancer treatment

MSC derived exosomes have invited controversy over the years. MSCs can release intracellular material in the form of exosomes, which includes mRNA, micro RNA as well as other proteins. Micro RNA delivery in particular has shown in studies to be anti-tumourogenic where tumours lack a particular micro RNA fundamental to cancer growth (246). This remains a work in progress.

MSCTRAIL

MSCs have long been touted as a potential vehicle for anti-cancer therapy. Its immune privileged status allows for allogeneic transfer of these cells with little in the way of a host reaction given its perceived lack of immunogenicity. Its homing capability to sites of injury / cancer add further value to this potential targeted treatment modality (210).

MSCs have been found to clear *in vivo* very quickly, however animal studies have shown their migration and persistence in tumours, building a further case to use these cells as therapeutic vehicles (247). Preclinically, drugs such as paclitaxel, known largely for their undesirable toxicity profile have been selectively transported to tumours (248).

Through transfection with adenovirus, MSCs have been made capable of expressing IFNγ and IFNß, the latter demonstrating tumour cell kill and upregulation of key components of the immune system such as NK cells (249).

Our laboratory has shown through a similar method that lentiviral transduction of MSCs expressing TNF related apoptosis inducing ligand (TRAIL) on its cell surface induces cell death in a lung cancer mouse model (250).

Other transfection methods such as herpes simplex virus thymidine kinase (HSV-TK) expressing a suicide gene have been explored (251). Interleukin and chemokine delivery to the tumour microenvironment has yielded positive findings, prompting an anti-tumour immune response. Carriage of IL-12 and IL-18 to sites of malignancy have offered promise as has delivery of CX3C chemokine fractalkine (CX3CL1) (252-254).

MSC mouse models

In vivo models have great limitations as murine MSCs have a significantly different behaviour to human MSCs. This disparity between MSCs generates great discourse when applying murine MSC knowledge to human models.

Clinical trials of MSCs in cancer

The **TACTICAL** study; a trial born from our laboratory uses umbilical cord derived MSCs transduced to express full length TRAIL on its surface (MSCTRAIL) in the treatment of adenocarcinoma of the lung. Patients receive front-line standard of care chemotherapy;

pemetrexed and platinum, in combination with the anti-PD1 agent pembrolizumab alongside MSCTRAIL. This phase I/II clinical trial, currently at the dose finding phase, will look to proceed to a cohort expansion phase including 46 patients randomised to receive standard of care therapy or standard of care therapy with MSCTRAIL (NCT03298763).

The phase II portion of TACTICAL will run in parallel with our phaSe IIa randomised controlled TRiAl of firsT line chemotherapy with/without MSCTRAIL in BAP1 mutatEd maliGnant pleural mesothelIoma Cases (STRATEGIC), exploring the use of the same standard of care chemotherapy with or without MSCTRAIL in MPM. The emergence of immune checkpoint blockade may modify the treatment pathway in these patients which may require study modification.

The issue of course lies with using MSCs, a cell type known to negatively regulate the immune system with immune checkpoint blockade, which conversely galvanises the immune system.

Other human clinical studies include TREATME1, a phase I/II trial delivering HSV-TK MSCs, trials in ovarian cancer using IFNß expressing MSCs and prostate cancer. The trial was terminated prematurely due to assumed poor accrual (NCT02008539).

1.7 Tumour necrosis factor Related Apoptotic Inducing Ligand (TRAIL)

Also known as APO2 ligand, TRAIL is a type II transmembrane protein comprising of 281 amino acids. Its relationship with cell surface death receptors leads to activation of the extrinsic (or external) apoptosis pathway and ultimately cell mediated apoptosis (255).

There are 5 recognised death receptors which can potentially interact with TRAIL. Death receptor 4 (TRAIL – R1 or DR4) and death receptor 5 (TRAIL – R2 or DR5) are the most studied as when bound to TRAIL trigger a signal from the extracellular receptor domain to the nucleus activating apoptosis. The other receptors lack the basic requirements to induce apoptosis. TRAIL-R3 and TRAIL-R4 are also known as decoy receptors. When TRAIL binds to the extracellular domains of these receptors, apoptosis is not induced as they lack an appropriate intracellular domain required to carry this signal forward. The other receptor, osteoprotegerin, is not expressed on the cell surface so despite its ability to bind TRAIL, it is unable to trigger cell mediate apoptosis and is considered redundant (256).

Its role in cancer has been studied extensively. TRAIL targets transformed cells but spares 'normal' cells, a unique property which is not well understood (257). This cancer specific feature has garnered huge interest in using TRAIL as a therapy against cancer. As a result of this, a further advantage in contrast to currently used treatment modalities, such as chemotherapy, is its low comparable toxicity profile. The mechanism underlying this cancer cell selectivity remains controversial. Some believe there are differences between expression of death receptors between normal and transformed cells; DR4 and DR5 highly expressed on the latter, while others believe that death receptors located in lipid raft areas of a cell

membrane induce apoptosis compared with receptors that are not. Other theories have also been suggested (258).

TRAIL and cell death

On binding to the extracellular domain of a death receptor, TRAIL activates the first step of the external apoptosis pathway. Death receptors trimerise together which triggers intracellular recruitment of the FAS associated death domain protein (FADD) (259). Further intracellular proteins congregate to this adaptor protein including pro-caspase 8, forming the multi protein complex death inducing signaling complex (DISC) (260). Caspase 3 is subsequently activated triggering apoptosis (261).

An alternative cell death mediated pathway; intrinsic (or internal) apoptosis pathway, is facilitated by p53 and BAX/BAK promoting the release of cytochrome c (Cyt c) from mitochondria. Cyt c activates caspase 9 via apoptotic protease-activating factor 1 (APAF-1) which leads to activation of a further cascade of caspases leading to apoptosis (262).

Both apoptotic pathways share an intimate association via the protein BID, allowing for simultaneous activation of both pathways (263, 264). This is seen as a potential therapeutic approach. Combination studies using TRAIL and chemotherapeutic agents such as cisplatin and pemetrexed, activating the internal apoptotic machinery, have demonstrated therapeutic synergy (265, 266).

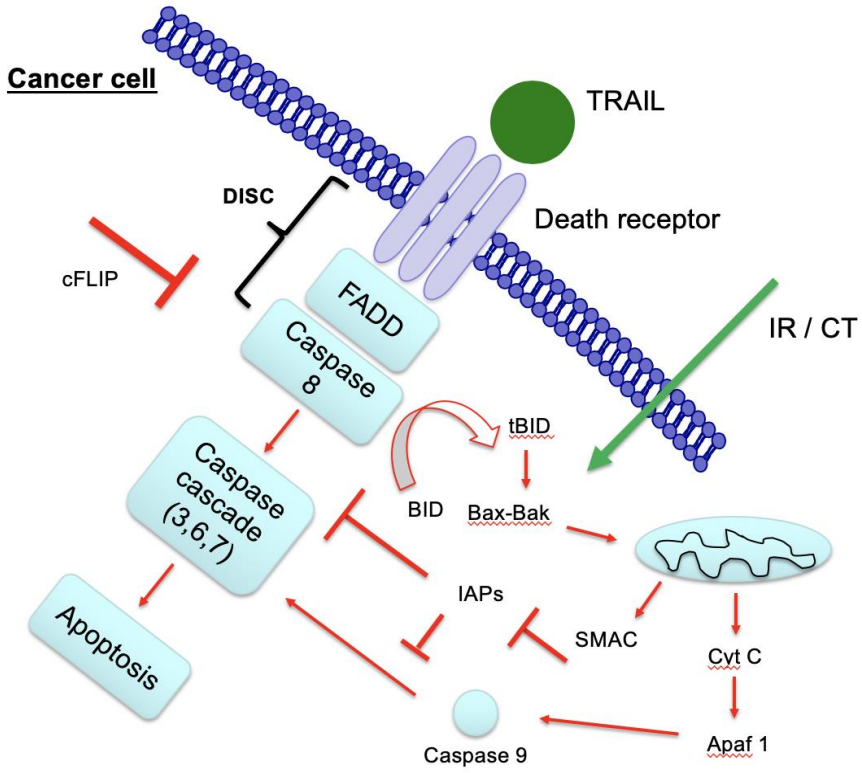

Figure 1. 8 - Schematic illustrating both extrinsic and intrinsic apoptosis pathways

TRAIL resistance has been studied implicating intracellular proteins such as cellular FLICE-like inhibitory protein (cFLIP) and inhibitors of apoptosis proteins (IAPs) as responsible proteins. In brief, cFLIP is an inactive homologue of caspase 8 and 10, expressed in tumour cells, which binds to FADD competitively inhibiting caspase binding and apoptosis. Chemotherapeutic agents such as cisplatin have been shown to inhibit cFLIP (267). The IAP family comprises of a number of proteins including XIAP and survivin, which are overly expressed in cancer cells and antagonised by second mitochondria-derived activator of caspases (SMAC). B cell lymphoma 2 (BCL-2) another important set of anti-apoptotic proteins regulates mitochondrial outer membrane permeabilisation (MOMP). A balance is struck between anti-apoptotic and pro-apoptotic BCL-2 proteins, the former inhibiting MOMP (268, 269).

1.8 Heat shock protein 90 (HSP90)

Heat shock proteins are molecular chaperones which ensure correct and efficient folding of proteins avoiding degradation. Heat shock protein 90 (HSP90), a cytoplasmic chaperone protein weighing 90 kDA combines with other chaperone proteins forming a complex known as the HSP90 chaperone machine. Its main function is to stabilise client proteins. Like BAP1 its role in chromatin modification and transcriptional regulation is being studied. It has recently been implicated in MPM (270).

In unstressed cells, HSP90 plays an important role in protein folding and ubiquitination through maintenance of the 26S proteasome (271). There is some work looking at its relationship with the glucocorticoid receptor; upregulation of the receptor gene in the absence of glucocorticoid has been shown (272). Its role in cancer has recently received a lot attention as it stabilises proteins critical to tumour growth. Its overexpression in several cancer subtypes signifies poor prognosis and progressive disease, however it has also led exploration as a target for treatment (273, 274).

HSP90 interacts with a variety of proteins involved in carcinogenesis including oncogenic intracellular signaling pathways, angiogenesis and apoptosis. As the name suggests, HSPs provide protection of proteins under thermal stress. There are 5 HSP90 genes that encode for 5 protein isoforms; HSP90-α1, HSP90-α2, HSP90-ß, endoplasmin / GRP-94 and TRAP1 (TNF receptor – associated protein 1) (275). HSP90 executes it functions through several mechanisms including direct ATP binding (cleaving ATP to ADP and phosphate), which is being studied as a therapeutic target and a direct protein binding site facilitating folding and transport of proteins.

HSP90 is composed of three domains. The alpha domain (N domain) comprises the ATP binding region and binding sites for other binding proteins such as HSP70 (also a region for drug binding), the middle (M domain) domain is a site for target proteins to bind whilst further chaperone proteins are able to bind to this site and finally the carboxy terminal domain (C domain) which allows for further drug binding, chaperone binding and dimerisation. The N domain is targeted by all HSP90 inhibitors and is the main mechanism of action for inhibiting HSP90 function (276).

Some of these chaperone proteins effect the rate of the HSP cycle (namely the binding of ATP to this binding site, interaction of chaperone proteins, dimerisation of HSP90 molecules and eventual ATP hydrolysis), facilitate recruitment of key substrates (e.g. TAH1 and PIH1 help recruit RVB1 and RVB2 which are involved in transcriptional regulation) and are involved in ubiquitination such as catalysing E3. Understanding these 'co-chaperones' is key to learning about cancer progression and resistance of HSP90 inhibitors particularly as some cancers will over-express these co-chaperones; a further therapeutic target (270).

Post translational modifications (PTM) also affects the function of HSP90 and its interaction with these licensed inhibitors. Hyperphosphorylation and dephosphorylation are both recognised features of PTM driving angiogenesis (277), cell cycle regulation (278) and apoptosis (279). Acetylation of HSP90 has suggested increased sensitivity to HDAC inhibitors (280) whilst S-Nitrosylation inhibits the effects of HSP90 in normal cells (281).

HSP90 influences gene expression by regulating the co-chaperone protein heat shock transcription factor 1 (HSF1). HSP90 inhibition can upregulate HSF1, a transcriptional factor implicated in regulation of cell survival genes. Transcriptional factors such as IRF1 are also upregulated by HSP90, a key tumour suppressor factor (282). Its involvement in chromatin

modulation has been described earlier with genes such as TAH1 and PIH1 which help recruit RVB1 and RVB2 involved in transcriptional regulation (283). PRMT5, an important enzyme in arginine metabolism (arginine methyltransferase) and chromatin modification is modified by HSP90 leading to its inhibition when HSP90 is inhibited (284).

HSP90 has a direct relationship with DNA. It participates in stabilisation of DNA polymerase and where inhibited leads to increased sensitivity to DNA damaging treatment. This adds further evidence for their use alongside DNA damaging therapeutics given their effect on WEE1 and DNA polymerase. WEE1, a client protein of HSP90, is known to regulate the G2/M cell cycle checkpoint. via phosphorylation of CDK1. Its ability to phosphorylate a tyrosine reside in the N domain affects drug binding but promotes recruitment of client proteins such as HER2 and RAF1 (278). Clinical data supporting HSP90 inhibition with DNA damaging agents such as radiation (285), topoisomerase inhibitors (286) or antimetabolites such as gemcitabine (287) have offered modest responses.

Its role in apoptosis is unclear. Recent data supports the idea of tipping the balance towards apoptosis by triggering upregulation of pro-apoptotic pathway proteins such as BID, BIK and PUMA and downregulation of BCL-2 family members when HSP90 is inhibited (288).

HSP90 and malignant pleural mesothelioma

The most studied HSP90 inhibitor, 17-allylamino-17-demethoxygeldanaycin (17-AGG) is a less toxic derivative of its predecessor geldanamycin. Its predilection to cancer cells has been demonstrated with a greater than 100 times affinity for transformed cells than normal cells (289). AKT, a critical intracellular protein in the PI3K/AKT pathway is upregulated in many cancers including MPM. AKT is stabilised by HSP90 which promotes oncogenic signaling in

transformed cells. *In vitro* studies have shown HSP90 inhibition leads to G1 or G2/M cell cycle arrest and apoptosis in MPM associated with reduction in AKT and survivin levels (290). Other studies have shown synergy between standard of care chemotherapy; pemetrexed and cisplatin and the 2nd generation HSP90 inhibitor ganetespib (20 times more potent than the first generation HSP90 inhibitor 17-AGG), confirming greater apoptosis when combined with chemotherapy and altering the 'senescence' associated secretome resulting in an increase in cytokines including IL8, a cytokine later confirmed to be associated with an increase in AKT and FAK signaling. This has been validated further in an *in vivo* model using MSTO-211H mouse xenografts and intraperitoneal administration of treatment reporting a synergistic effect between ganetespib and chemotherapy whilst also confirming IL8 secretion as a proxy for response (291).

HSP90 inhibition in colon cancer leads to upregulation of DR5, a key component in TRAIL, inducing apoptosis. This upregulation may pave the way for combination therapy using HSP90 inhibitors and TRAIL in BAP1 mutant MPM, given its previously documented sensitivity in our laboratory (144, 292).

HSP90 and relevant clinical trials

Inhibition of HSP90 in clinical trials has shown much promise including significant activity against MPM. The first HSP90 inhibitor was clinically introduced in 1999 (NCT00093821) (293). Following several studies, a phase I clinical trial demonstrating clinical activity when ganetespib was combined with pemetrexed and cisplatin is currently being explored in a phase II study (NCT01590160). 27 patients were treated in the phase I study reporting a

partial tumour response of 61%, a response rate far higher than historical control data for doublet chemotherapy alone (294).

Despite our rapidly growing understanding of MPM, from its complex genomic landscape to clinical trial results, we are still yet to offer patients anything more meaningful than doublet chemotherapy. The initially reported study by Vogelzang et al in 2003 remains standard of care for patients with several exciting prospects on the cusp of entry into the patient's treatment pathway.

1.9 Hypothesis and aims

This knowledge base provides an understanding of MPM and how it correlates with targeting apoptosis through TRAIL binding. I have shown this relationship is governed by the tumour suppressor gene BAP1. A plethora of targets are available to study, in an attempt to amplify the TRAIL effect on cancer cells.

I hypothesise that I can strengthen the impact of TRAIL in MPM in several ways. I believe BAP1, through its involvement in homologous recombination (HR), modulates sensitivity to PARP inhibition and subsequently to TRAIL. Moreover, I believe TRAIL sensitisation can also be augmented through HSP90 inhibition and finally despite the plethora of data suggesting MSCs are immuno-suppressive I believe that this is not entirely the case based on limitations of historical assays and the changeable phenotype MSCs undergo. I therefore provide a further hypothesis that cell mediated death using TRAIL 'vehicled' using MSCs are likely to overcome the impact of the MSC immune suppressive phenotype in a cancer cell environment.

My aims are as follows:

- Explore the relationship between BAP1 and HR in the context of PARP and TRAIL sensitivity (Results chapter I)
- Examine the synergistic relationship between MSCTRAIL and PBMCs, validated using a syngeneic platform I developed (Results chapter II)
- Study the potentially synergistic relationship between HSP90 inhibitor ganetespib and TRAIL in BAP1 mutated MPM (Results chapter III)

2 MATERIALS AND METHODS

2.1 General chemicals, solvents, and plasticware

All chemicals used were of analytical grade or above and obtained from Sigma Aldrich (Poole, UK) unless otherwise stated. Water used for preparation of buffers was distilled and deionised (ddH_2O) using a Millipore water purification system (Millipore R010 followed by Millipore Q plus; Millipore Ltd., MA, US). Polypropylene centrifuge tubes and pipettes were obtained from Becton Dickenson (Oxford, UK).

2.2 List of drugs, reagents and antibodies

Antibody	FC	Clone	Cat. No.	Manufacturer	Dilution
CD105	APC	43A4E1	130-094-926	Miltenyi Biotec	1 in 50
CD90	PE/CY7	5.00E+10	328123	Biolegend	1 in 50
CD73	PE-Vio-770	AD2	130-104-225	Miltenyi Biotec	1 in 50
Annexin V	AF647	N/A	640912	Biolegend	1 in 100
DAPI	N/A	N/A	D9542	Sigma Aldrich	2ug / ml
DiI	N/A	N/A	V22885	Thermo Fisher	1 in 100
CD2 / 3 / 28 beads	N/A	N/A	10970	Stemcell technology	1 in 40
Anti PD-1	N/A	EH12.2H7	329946	Biolegend	1 in 50
PD-L1 (CD274)	APC	MIH1	17-5983-42	Life Technologies Ltd	1 in 50
PD-L1 (CD274)	N/A	29E.283	329716	Biolegend	1 in 50
CTLA-4 (CD152)	N/A	BNI3	369602	Biolegend	1 in 50
CTLA-4 (CD152)	N/A	L3D10	349923	Biolegend	1 in 50
AF488 donkey anti-rabbit IgG	N/A	N/A	A-21206	Invitrogen	1 in 400
CD45 (TIL) MicroBeads	N/A	N/A	130-118-780	Miltenyi Biotec	1 in 5
BAP1	N/A	N/A	SC28383	Santa Cruz Biotechnology	1 in 200
TRAIL	N/A	N/A	Ab47230	Abcam	1 in 10
a-tubulin	N/A	N/A	9099S	Cell Signaling Technology	1 in 2000
Gamma H2AX	AF647	2F3	613408	Biolegend	1 in 400
RAD51	N/A	N/A	AB63801	Abcam	1 in 600
HRP conjugated antibody	N/A	N/A	7074	Cell Signaling Technology	1 in 2000

Figure 2. 1 - List of antibodies

All drugs used were reconstituted in DMSO, as per manufacturer instructions. All drugs were passed through a 0.22uM filter.

Drugs	Stock concentration	Solvent	Cat no	Manufacturer
Olaparib	1mM	DMSO	CAY10621	Cambridge Bioscience
MK-4827	1mM	DMSO	CAY10621	Cambridge Bioscience
BMN673	1mM	DMSO	CAY19782	Cambridge Bioscience
AZD0156	5mM	DMSO	HY-100016	MedChemExpress
AZD6738	1mM	DMSO	HY-19323	MedChemExpress
Ganetespib	10mM	DMSO	HY 15205	Insight biotechnology Ltd
Human recombinant TRAIL	10 ug/ml	PBS	310-04	Peprotech
IDO	1mM	DMSO	206931	MedKoo Biosciences Inc

Figure 2. 2 - List of drugs

Reagents / buffers	Stock concentration	Catalogue number	Manufacturer
Red Lysis buffer	10X	5831-100	Cambridge Bioscience
Ethanol	100%	10644795	Fischer Scientific
Polybrene	4mg/ml	638133	Sigma Aldrich
D-luciferin	10mg/ml	2591-17-5	Regis Technologies Inc
Human IL2	500units/ml	500-M02	Peprotech Ltd
Human FICCOLL-Paque Plus	< 0.12 Eu/ml	17-1440-02	VWR International Ltd
Thiazolyl Blue Tetrazolium Bromide (MTT)	5mg/ml	M2128	Sigma Aldrich

Figure 2. 3 - Other relevant reagents and buffers

2.3 Cell culture

All culture media, L-Glutamine (L-Glut), Fetal Bovine Serum (FBS), 50U/ml penicillin and 50µg/ml streptomycin antibiotics (PS), 5mM sodium pyruvate, (SP), Trypsin/EDTA were purchased from Invitrogen (Paisley, UK) unless otherwise stated. FBS required batch testing prior to purchase, switched June 2019. Sterile tissue culture flasks and plates were purchased from Nunc (Roskilde, Denmark) unless otherwise stated. Cells were cultured in varying sizes of flasks (T25 (25cm^2 surface area), T75 (75cm^2) and T175 (175cm^2)) in an infrared direct heat (37 degrees) 5% CO2 incubator.

Established cell lines

Cancer cells were grown in Roswell Park Memorial Institute (RPMI) cell culture media 1640 supplemented with 4mM L-Glutamine, 10% FBS, 1% PS and SP. Cell lines used included lung cancer (A549), breast cancer (MDA-MB-231), 2 sets of malignant pleural mesothelioma cell lines and embryonic kidney (293T). MPM cell lines were acquired from either MesoBank UK, Papworth (8T) or the Wellcome Trust Sanger Institute, Cambridge, UK (MST0-211H (CRL2081), H226, MPP89, H513, H2869, H2810, H2818, H2803, H28, H2731 and H2804). 293T, A549 and MDA-MB-231 were obtained from Cancer Research UK (CRUK). H226 cells were a kind gift from Professor Peter Szlosarek (Barts Cancer Institute, London). Cell lines acquired from MesoBank were cultured in RPMI, 5% FBS, 1% PS, 1% Hepes buffer and 1% SP.

Location	Cell line	Type
Wellcome Trust Sanger Institute, Cambridge, UK	CRL2081	Biphasic mesothelioma
	H226	Squamous cell carcinoma, mesothelioma
	MPP89	Epithelioid mesothelioma
	H513*	Mesothelioma (unspecified)
	H2869	Biphasic mesothelioma
	H2373	Sarcomatoid mesothelioma
	H2810	Epithelioid mesothelioma
	H2795	Epithelioid mesothelioma
	H2591	Epithelioid mesothelioma
	H2589	Mesothelioma (unspecified)
	H2818	Epithelioid mesothelioma
	H2803	Mesothelioma (unspecified)
	H28	Sarcomatoid mesothelioma
	H2731	Sarcomatoid mesothelioma
	H2804	Mesothelioma (unspecified)
MesoBank UK, Papworth	8T	Biphasic mesothelioma
Other	A549	Lung adenocarcinoma
	MDA-MB-231	Breast adenocarcinoma
	PC9	Lung adenocarcinoma

Figure 2. 4 - list of cancer cell lines used

Culture media was changed every 3 days and cells grown to 80% confluency before cell splitting was undertaken. Splitting cells was performed by washing cells using phosphate-buffered saline (PBS), adding 0.05% trypsin in EDTA and incubating for 2 minutes or until cells detached from the surface of the flask, in a 5% CO2 incubator. On detachment, culture media was added to the cell suspension followed by collection into a 15ml falcon tube. Cells underwent centrifugation at 300G for 5 minutes. Supernatant was removed from the tube leaving a pellet of cells which was resuspended in the appropriate culture media and seeded back into a new flask at an appropriate concentration depending on future experimental

planning. On completion of cell line work, cells were stored long term in liquid nitrogen. Once cells were formed into a pellet post centrifugation, 1ml of freezing media was added (50% RPMI, 40% FBS and 10% dimethyl sulfoxide (DMSO)) and the solution of cells were then transferred into a cryovial and placed in an isopropanol freezing container. The container was initially frozen in a -80 freezer for 24-48 hours followed by transfer of cryovials to liquid nitrogen for longer term storage. On re-use, cells were thawed in a water bath at 37 ^{0}C, RPMI media added and cells centrifuged at 300G for 5 minutes. Supernatant was then removed and cells deposited into appropriately sized flasks based on the assay planned.

Mesenchymal Stromal Cells (MSCs)

Pre-purchased human adult MSCs (passage 1) from the Texas A&M Health Science Center were used. Cells were cultured in α-minimum essential medium (αMEM) supplemented with 4mM L-Glutamine, 50U/ml penicillin, 50µg/ml streptomycin and 16% FBS.

Cells were seeded at 400-500 cells/cm^2 into T175 flasks, grown to 80% confluency before cell splitting was undertaken. Splitting cells was performed by washing cells using phosphate-buffered saline (PBS), adding 0.05% trypsin in EDTA and incubating for 2 minutes or until cells have detached from the surface of the flask, in a 5% CO2 incubator. On detachment, αMEM was added to the cells followed by collection into a 15ml falcon tube. Cells underwent centrifugation at 300G for 5 minutes. Supernatant was removed from the tube leaving a pellet which was resuspended in αMEM. Cells were counted and 400-500 cells / cm^2 were seeded back into a T175 flask. On completion of cell line work, cells were stored long term in liquid nitrogen. Once cells were formed into a pellet post centrifugation, 1ml of

freezing media was added (50% αMEM, 40% FBS and 10% dimethyl sulfoxide (DMSO)) and the solution of cells were then transferred into a cryovial and placed in an isopropanol freezing container. The container was initially frozen in a -80 freezer for 24-48 hours followed by transfer of cryovials to liquid nitrogen for longer term storage. On re-use, cells were thawed in a water bath at 37 ^{0}C, αMEM media added and cell centrifuged at 300G for 5 minutes. Supernatant was then removed and cells deposited into T175 at 400-500 cells / cm^{2}.

Cell lines derived from pleural effusion samples

See section 2.3 for development of these cell lines. Cells were cultured in Dulbecco's Modified Eagle Medium: Nutrient Mixture F-12 (DMEM/F12) supplemented with 4mM L-Glutamine, 50U/ml penicillin, 50µg/ml streptomycin and 10% FBS.

Cells were collected and seeded at 1 million cells per T75 flask. Cells were reviewed 24 hours following cell seeding and cells were washed with PBS and media replaced to remove tissue debris and non-adherent cells such as immune cells. Culture media was changed every 3 days until cells are grown to 80-90% confluency. Splitting cells was performed by washing cells using PBS, adding 0.05% trypsin in EDTA and incubating for 3-5 minutes or until cells detached from the surface of the flask, in a 5% CO2 incubator. On detachment, DMEM/F12 was added to the cells followed by collection into a 15ml falcon tube. Cells underwent centrifugation at 300G for 5 minutes. Supernatant was removed from the tube leaving a pellet which was resuspended in DMEM/F12. Cells were counted and seeded back into a T75 flask at an appropriate fraction. On completion of cell line work, cells were stored long term in liquid nitrogen. Once cells were formed into a pellet post centrifugation, 1ml of freezing media was added (50% DMEM/F12, 40% FBS and 10% dimethyl sulfoxide (DMSO)) and

the solution of cells were then transferred into a cryovial and placed in an isopropanol freezing container. The container was initially frozen in a -80 freezer for 24-48 hours followed by transfer of cryovials to liquid nitrogen for longer term storage. On re-use, cells were thawed in a water bath at 37 ^{0}C, DMEM/F12 media added and cells centrifuged at 300G for 5 minutes. Supernatant was then removed and cells deposited into an appropriately sized flask.

2.4 Development of cell lines from pleural effusions

Patients were identified with suspected or confirmed malignant pleural effusions. This was done in two ways. Firstly, cardiothoracic cases were screened on a weekly basis in parallel with cardiovascular and respiratory teams to identify suitable patients who were to undergo VATS procedures at Westmoreland Street Hospital, London. In addition, cases were screened prior to a weekly intra-pleural chest drain list at University College Hospital London. Patients with suspected malignant pleural mesothelioma in particular were sought out. Patients were provided with a patient information sheet and a consent form to complete if in agreement. The consent form provided depended on the procedure to be undertaken (see supplementary). This was filed in the conventional way in the patients notes.

A blood sample was then obtained and taken back to the lab for PBMC isolation (see section 2.5). Once the procedure was complete the pleural effusion sample was taken to the laboratory for cell isolation. Effusion samples were collected either as serous or haemorrhagic fluid.

On return to the laboratory the samples were placed in a tissue culture hood and diluted in 50% PBS in a 50ml falcon tube. They were then subjected to centrifugation at 300G for 10 minutes. Supernatant was then removed with a remaining pellet of cells. 1X red lysis buffer (Cambridge Bioscience 10X) was added to the pellet in a 1 in 10 ratio and incubated at room temperature for 5 minutes. Once the incubation period was complete the cells were subjected to a further cycle of centrifugation at 300G for 10 minutes. Cells were counted and seeded at 500000 per T75 flask and 1000000 per T175 flask in DMEM / F12 media. Flasks were placed in a CO2 driven incubator. Following 24 hours, cells were assessed and fresh media replaced to eliminate any debris.

2.5 Isolation of peripheral blood mononuclear cells

Blood samples were taken from patients and transported to a tissue culture hood in the laboratory for PBMC isolation. 10ml of blood was deposited in a 50ml falcon tube. This was done in several tubes depending on the amount of blood obtained. Samples were diluted in 10ml of plain RPMI media at room temperature. Underlaying of Human Ficoll-Paque Plus (Sigma Aldrich) was then undertaken. A sterile glass pasteur pipette was placed in the 20ml of solution and 10ml of Human Ficoll-Paque Plus was placed through the glass pipette, which deposits to the bottom of the falcon tube forming a 10ml layer of clear Ficoll fluid beneath the 20ml of blood / media. The 30ml solution was subjected to high speed centrifugation (760G at 10 minutes with no brakes at room temperature). On completion, a buffy coat appeared above a layer of blood and clear Ficcoll fluid. The top layer of plasma was carefully suctioned and using a P1000 pipette the buffy coat extracted and deposited in a 15ml falcon tube. These cells were then mixed with chilled complete RPMI media 2-3 times the volume of the buffy coat and subjected to a further cycle of centrifugation at 460G for 6 minutes at 4

degrees. On completion, a pellet of cells formed. Supernatant was removed and the cells were washed again with complete RPMI at the centrifugation parameters as the last. Cells were then counted and frozen using 1ml of freezing media (45% complete RPMI media, 45% FBS and 10% DMSO. The cells were then transferred into a cryovial and placed in an isopropanol freezing container. The container was initially frozen in a -80 freezer for 24-48 hours followed by transfer of cryovials to liquid nitrogen for longer term storage. On re-use, cells were thawed in a water bath at 37 ^{0}C, media of choice (depending on the assay) was added and cells centrifuged at 300G for 5 minutes.

2.6 Magnetic activating cell sorting

Magnetic activated cell sorting (MACS) was used to positively select CD45+ cells from pleural effusion samples.

Once cells from pleural effusion samples were collected for tissue culture the remaining cells were subject to CD45+ isolation. Cells were counted and collected up to 10^{7}. Cells were then centrifuged at 300G for 5 minutes followed by complete removal of supernatant. 80µl of 0.5% FBS/PBS buffer and 20µl of CD45 conjugated microbeads - CD45(TIL) microbeads (Miltenyi Biotec, 130-118-780) was added to the pellet of cells. Cells and microbeads were incubated for 15 minutes at 2-8^{o}C. Once incubation was complete the sample was made up to 500µl with buffer.

A magnet was set up, with a column holder. A LS column (Miltenyi Biotec 130-042-401) was placed on the magnet and rinsed with 3ml of buffer. The cell suspension was then run through the column with magnetically bound CD45+ cells attracted to the magnetic region

and the non-magnetised CD45- cells collected into a falcon tube. The CD45+ bound column was then washed twice with 2ml of buffer. The column was then removed from the magnet and flushed with 3ml of buffer collecting all the magnetically bound cells. Cells were stored at -80^{o}C using pre-prepared freezing media (50% RPMI, 40% FBS and 10% dimethyl sulfoxide (DMSO)).

2.7 Lentivirus production and transduction

A full length TRAIL expressing lentiviral vector (pCCL-CMV-flT) was developed in our lab prior to this work. In short, the lentiviral plasmid pCCL-c-Fes-GFP was acquired. The c-Fes promoter was deleted by enzymatic digestion and replaced by a CMV promoter to allow for constitutive activation of TRAIL. The GFP sequence was replaced by full length TRAIL leading to pCCL-CMV-flT.

293T cells were seeded in x6 T175 flasks and cultured in standard conditions until a confluency of 80-90% was achieved. For each T175 flask, 20ug of transfer plasmid (pCCL-CMV-flT), 7ug pMD2.2 and 13ug pCMV-dR8.74 (packaging plasmids) were added to 1ml of 150mM sodium chloride solution. This was initially subjected to vortex mixing for 10 seconds and passed through a 0.2ul filter. In a separate falcon tube, 80ul of the transfection reagent JetPEI was added to 1ml of 150mM sodium chloride per T175 flask. This was subjected to vortex mixing for 10 seconds. Both mixtures were then added together and vortexed for 10 seconds followed by incubation at room temperature for 30 minutes.

Once incubation of the plasmid transfection mixture was complete, 2ml of solution with 13ml of DMEM media were added to each flask of cells and incubated for 4 hours. Media was

changed thereafter with 20ml of DMEM. The virus rich media was collected on day 1 and 2, subjected to ultracentrifugation (17,000 rpm using SW28 rotor, Optima LE80K Ultracentrifuge, Beckman) for 2 hours at 4°C. The virus was then resuspended in DMEM and frozen at -80°C into small aliquots to avoid repeated freeze thaw cycles.

To identify a viral titre that transduces enough cells effectively, a titration exercise was performed. 50,000 293T cells were seeded into a 12 well plate. Following 24 hours of incubation, viral dilutions were added to each well (2, 1, 0.5, 0.25, 0.125µl) with polybrene 4µg/ml. Following 48 hours of incubation, cells were collected via trypsinisation, underwent centrifugation, counted, incubated with a phycoerythrin (PE) conjugated mouse anti-human anti TRAIL antibody (Abcam, Ab47230 1:10) and subjected to flow cytometry using a FACS LSRII flow cytometer for TRAIL expression. Percentage of TRAIL expressing cells was measured for each viral titration. The viral titre was calculated as per below:

$$\text{Volume of virus (virus particles/ml)} = \frac{\text{no. of cells x fraction of cells transduced}}{\text{volume of virus (ml)}}$$

2.8 DNA isolation

A PureLink Genomic DNA Kit (Thermo Fisher Scientific) was used to extract DNA. Cells were collected via trypsinisation and subjected to centrifugation at 300G for 5 minutes. Supernatant was removed completely and the samples were made up to 200µl of PBS. 20µl of Proteinase K and 20µl of RNase A were added followed by brief vortex mixing. Following 2 minutes of incubation at room temperature, 200µl of PureLink Genomic Lysis / Binding Buffer was added followed by vortex mixing for 5 seconds to achieve homogeny. Samples

were incubated for 10 minutes in a 55ºC water bath to promote protein digestion. On completion, 200µl of 100% ethanol was added to the lysate and subjected to 5 seconds of vortex mixing. Samples were transferred to a spin column provided by the manufacturer and collection tube. Samples were subject to centrifugation (10,000G for 1.5 minutes). The supernatant was removed (collection tube discarded and replaced) and the spin column placed in a new collection tube. The DNA was washed twice with provided wash buffers prior to elution into a sterile 1.5ml Eppendorf. 50µl of a genomic elution buffer was added to the spin column and the DNA was collected following a final centrifugation step (maximum speed, 1.5 minutes). DNA was frozen at -20ºC for future use.

2.9 Co-culture experiments

Cells were collected from confluent flasks (80% or more) following washing with PBS and trypsinisation (0.05% EDTA). Cells were subject to centrifugation (300G in 5 minutes). Supernatant was removed and cells reconstituted in fresh complete media. Cells were counted and seeded at the desired concentration.

Following 24 hours of incubation, cells were treated with agents of choice constituted in the complete media. Desired concentrations were calculated and measured in pre-existing media.

Cancer cells were either pre-labelled with DiI or transduced to express genes such as luciferase prior to seeding. Cells were assessed based on the type of assay e.g. cell viability, apoptosis, bioluminescence etc

2.10 Cell viability assay

MTT assay

An MTT assay is a colorimetric assay used to measure the metabolic activity of a cell. The yellow 3-(4,5-dimethylthiazol-2-yl)-2,5-diphenyl tetrazolium bromide (MTT) is reduced to purple formazan by intracellular NAD(P)H- dependant enzymes in living cells. When cells were cultured and treated, 10uL of MTT reagent (Sigma Aldrich) was added to 100uL of media per well and incubated for 3 hours. Following the incubation period, the media and MTT solution was removed and 100µl of DMSO was added which dissolves the insoluble formazan into a purple colour. The more purple a well becomes the more viable it is deemed. Absorbance of this coloured solution was measured at a wavelength of 570nm using a spectrophotometer.

Luciferase assay

Bioluminescence is the production and emission of light energy in a living organism. Cells can be transduced to express the firefly luciferase gene, an oxidative enzyme causing bioluminescence. Luciferase catalyses the oxidation of luciferin (aided by O2 and ATP) to oxyluciferin in an electronically excited state. This leads to the release of a photon of light allowing oxyluciferin to return back to baseline activity, causing bioluminescence.

Cancer cells were transduced to express luciferase. They were seeded in 96 well plates at desired concentrations and treated with a drug agent of choice. Following a decided upon incubation / treatment period, luciferin (Regis technologies Inc. USA) was added to the cells (150 u/ml) for 5 minutes and bioluminescence recorded using a microplate reader.

2.11 Apoptosis Assay

Cells were initially collected from culture flasks following trypsinisation and centrifugation (300G in 5 minutes) to form a cell pellet. Cells were counted and labelled with 1% DiI (PBS). Cells were incubated with DiI for 15 minutes and washed twice to remove unbound DiI. Following the second wash and centrifugation (300G at 5 minutes) cells were counted and seeded in a 96 well plate at the desired concentration. Cells were incubated for 24 hours following which cells were treated with the agents / cells of choice. Once the treatment period was completed, the cells were subjected to flow cytometry assessment using a FACS LSRII flow cytometer.

The media from the treatment plate was transferred to corresponding wells in a V shaped 96 well plate. The wells were washed with PBS and transferred to the corresponding wells of the V shaped plate. The cells then underwent trypsinisation and following detachment were transferred to the corresponding wells in the V shaped plate, topped up with complete RPMI media. The V shaped plate was subjected to centrifugation (300G in 5 minutes) and the supernatant subsequently removed. If any non-apoptosis conjugated antibodies were needed these were then added at pre-optimised concentrations and incubated in the dark for 15 minutes. Cells were then washed in PBS twice and stained with Annexin V antibody (Biolegend - AF647, 1:100) and DAPI (Sigma, 2µg /ml). Cells were then transferred to the flow cytometry machine for analysis.

Phosphatidlserine is normally cytoplasmic, however when a cell undergoes apoptosis it is mobilised to the cell surface where Annexin V binds to it. In addition, it is also able to bind cytoplasmic phosphatidlserine where the cell membrane has been disrupted in late apoptosis. DAPI is able to bind in the nucleus at this point indicating late apoptosis.

2.12 Western blot

Cells of interest were cultured in T75 flasks to a confluency of 80-90%. Cells were collected via trypsinisation and underwent centrifugation (300G for 5 minutes) to create a pellet of cells. Supernatant was removed. Cells were lysed using 100µl radioimmunoprecipitation assay (RIPA) buffer mixed with a protease inhibitor cocktail (AEBSF, Aprotinin, Bestatin, E64, Leupeptin, Pepstatin in DMSO). The cells were incubated at 4ºC for 30 minutes. The suspension underwent centrifugation (13000rpm) for 10 minutes at 4ºC. The protein rich supernatant was then collected and quantified using a bicinchoninic acid (BCA) assay.

BCA assay

A BCA protein assay is a standardised experiment which is fundamentally used to ensure equal amounts of protein are loaded for assessment. Proteins reduce copper from Cu^2 to Cu^+ which turns purple in the presence of bicinchoninic acid. 2000µg/ml of BSA in PBS was made and serially diluted to 20µg/ml. 20µl of each was deposited in a 96 well plate from row A to H. 20µl of protein / cell lysate was added to separate wells. 180µL of BCA working solution was added to each of these wells to make 200µl in total. The plate was the incubated in a 5% CO2 driven incubator for 30 minutes followed by assessment of absorbance using a spectrophotometer at 562nm. Absorbance was compared with the standards from A-H to form a straight line graph (y=mx+c). The concentration required for each sample was derived from this.

Development of immune-reactive bands

Once the protein has been quantified per sample, it is diluted in distilled H_2O and 5X laemmli buffer (10% SDS, 20% glycerol, 3.125mM Tris-base pH 6.8, 50mM Dithiothreitol (DTT), in

dH2O with bromophenol blue). Cells were incubated for 10 minutes at 70 degrees and placed back on ice. 25µl of each sample were loaded on a 4-12% Bis-Tris gel (Invitrogen NuPAGE). 5µl of PageRuler pre-stained protein ladder (Thermo Scientific) was used as a reference. The gel was filled with a running buffer (0.25M Tris-base, 1.92M Glycine, 1% SDS, in dH2O) and 150V applied. Once separation was complete the gel was taken out of the cassette and transferred on to a nitrocellulose membrane. Protein transfer was facilitated using the iBlot transfer system for 7 minutes (program 3). Once completed the protein transfer was assessed using Tris-buffered saline Tween (TBST) (20mM Tris-base, 150mM NaCl, 0.1% Tween 20). Blots were incubated in dry milk in TBST for 1 hour followed by incubation with primary antibody in BSA (5%) and TBST overnight at 4^{o}C. The following day the blots were washed 3 times (TBST) and incubated in HRP conjugated secondary antibody for 1 hour at room temperature. On completion the blot was washed (TBST) and incubated in 1ml of Luminata western HRP chemiluminescence reagent (Millipore) for 3 minutes. On completion, blots were read using ImageQuant LAS 4000 (GE Healthcare).

2.13 RNA interference

To knock down BAP1 expression in cell lines, short hairpin RNAs (shRNAs) were used. A mir30-based GIPZ lentiviral vector (Dharmacon) was used which expressed shRNA. In simple terms, the GIPZ hairpin is taken up by cells leading to BAP1 knockdown.

The acquired bacteria expressing lentiviral vectors (Dharmacon, UCL RNAi library) were grown and expanded in LB broth, followed by plasmid extraction and generation of virus as described section 2.5. Following transduction with the generated virus, cell lines were

cultured and treated with puromycin, a selection strategy to maintain only BAP1 knockdown cell lines. These were confirmed using western blotting (see section 2.9). The clone used in this thesis was BAP1 (V2LHS_4147).

2.14 Immunofluorescence

Two methods of immunofluorescence were used for detection of γH2AX.

Coverslip based

A 6 well plate was prepared with 3 circular clear coverslips added to each well. 250,000 cells per well were seeded in 2ml of complete RPMI media. Following 24 hours of incubation cells were adherent to the coverslips and each removed and placed in 3 separate 24 well plates with 250uL of complete RPMI media. Cells were pharmacologically treated and / or irradiated at the desired time point and radiation dose. Plates were placed back in a 5% CO2 driven incubator.

At the desired timepoint the plates with adherent cells on the cover slips were washed with PBS, fixed with PTEMF (20mM PIPES pH 6.8, 0.2% Triton X-100, 1mM $MgCl_2$, 10mM EGTA and 4% paraformaldehyde) for 15 minutes, washed thereafter and blocked with primary antibody in the dark overnight. Blocking involved 1-hour incubation of 250µl of 3% BSA/PBS per well, followed by the addition of antibody (AF647 conjugated γH2AX 1:400, Biolegend) and unconjugated RAD51 1:600, Abcam rabbit ab63801).

The following day involved washing of cells, application of 250µl of 3% bovine serum albumin (BSA) / PBS with 0.25% of secondary antibody (AF488, donkey, anti-rabbit, Life Technologies) incubated in the dark for 1 hour. 500ul of DAPI in PBS (10µg/ml) was added

to the cells for 5 minutes. Cells were washed and left in dH2O to avoid crystallisation. Coverslips were carefully lifted out of the plates and mounted onto transparent slides for microscopy assessment.

Plate based

Cells were seeded in a 96 well plate at the desired concentration in complete RPMI media. Following 24 hours of incubation, cells were treated pharmacologically. 48 hours following incubation cells were fixed with 4% paraformaldehyde for 10 minutes, washed with PBS and permeabilised with Triton X-100 (Sigma) for 10 minutes followed by incubation of AF647 conjugated primary antibody (γH2AX 1:1000) overnight in 3% BSA/PBS at 4ºC. Cells were washed with Triton X-100 the following day and incubated with Hoechst 33342 (0.2µg/ml, Abcam) for 1 hour at 4ºC. Cells were read using the Cytation 3 Cell Multi-Mode Reader.

2.15 Granzyme B ELISA

Granzyme B is a serine protease released by granules predominantly from cytotoxic T cells and natural killer (NK) cells. In conjunction with perforin, granzyme B promotes apoptosis through targeting caspases, mostly caspase 3. An increase in granzyme B is associated with cytotoxic T cell activity.

Release of granzyme B was measured using an Enzyme Linked ImmunoSorbent Assay (ELISA) (LEGEND MAX^{TM}, Biolegend). Cells were cultured in a 96 well plate. Following 24 hours of incubation, cells were treated with PBMCs plus other types of treatment. Following a further 48 hours of incubation, the media was collected (which contained released granzyme B) and stored.

Standards were initially prepared by taking 15µl of the 600pg/ml provided standard and diluting in 485µl assay buffer to make a final volume of 500µl. This was serially diluted 6 times by 1:2. A pre-coated mouse monoclonal anti-human granzyme B antibody 96 well strip plate was provided. This was initially washed in assay buffer and adequately dried. 50µl of assay buffer was then added to each well that will receive either a standard dilution or sample. This was followed by adding 50µl of each standard and 50µl of sample to separate wells made up with assay buffer, akin to a BCA assay. Samples with granzyme B bind to the antibodies coated in the well.

The plate was sealed and incubated for 2 hours at room temperature on a mechanical rocker (200 rpm). On completion, the contents were discarded and the plate washed 4 times with wash buffer. Granzyme B detection antibody solution was added to each well and incubated for a further 1 hour at room temperature on a mechanical rocker. The antibody binds to the bound granzyme B. Once completed, the contents were discarded and the plate was washed 4 times with wash buffer. 100µl of Avidin-HRP E solution was added to each well and incubated for 30 minutes on a mechanical rocker. This binds to the secondary antibodies. Once completed, the plate was washed 5 times with wash buffer and 100µl of substrate solution F was added and incubated for 30 minutes in the dark. Wells with granzyme B turn blue; the more enzyme the more obvious the colour. Once the colour change has occurred the process was terminated by adding 100µl of stop solution turning the colour from blue to yellow. The plate was then read at 450nm using a spectrophotometer.

2.16 Ionising radiation

Cells were subjected to irradiation using the AGO HS 320 kV x-ray machine at the UCL Cancer Institute. Cells were placed on a bullseye in a radiation field and settings calibrated to achieve the desired radiation dose. Dosage was selected for each plate and calculated based on the voltage (kV), current (mA), distance from probe and duration of treatment. On completion of irradiation of the plates, they were returned back to the tissue culture room / incubator for subsequent treatment if appropriate.

2.17 HR assay

Homologous Recombination Assay Kit (Norgen Biotek Corp) is a sensitive tool for measuring homologous recombination in mammalian cells. The assay is based on the ability of mammalian cells to repair transfected plasmids via strand invasion (homologous recombination).

Cells were seeded at 75,000 cells in 3 wells of a 12 well plate. Following 24 hours of incubation, transfection of the plasmids occurred in each of the wells. The first well underwent transfection with a positive control plasmid (420bp), the second well with a negative control; dI-2 plasmid (183bp) and the third with two partner plasmids; dI-1 (563bp) and dI-2 (183bp). The cells and plasmids were incubated for a further 24 hours to allow for transfection to occur. The plasmids were then subjected to DNA isolation (see section 2.11) and measured accordingly using a Nanodrop One (Thermo Fisher Scientific). Samples were then amplified using PCR and products were detected using gel electrophoresis.

Transfection of plasmids

The TransIT-X2 transfection reagent (Mirus Bio LLC) was used for transfection of plasmid DNA. Serum free media; Opti-MEM (Thermo Fisher Scientific) was incubated in an Eppendorf with 1ug of plasmid and 1µl of TransIT-X2. Samples were incubated for up to 30 minutes. Following a change of complete RPMI media, each of these samples were deposited in each well and allowed to incubate to encourage transfection.

PCR

Following the addition of REDTaq ReadyMix PCR Reaction Mix (Sigma Aldrich) to each of the samples plus PCR grade nuclease free water (Thermo Fisher) and both the assay primer (detects HR product) and universal primer mixtures (detects each plasmid as a quality assurance step) supplied by the manufacturer, the samples were run on an MJ Research PTC 225 Thermal Cycler to amplify the samples (denaturation 95^{o}C for 3 minutes, then 95^{o}C for 15 seconds, 65^{o}C for 15 seconds and 72 for 15 seconds). This was cycled 35 times followed by a final cycle of 72^{o}C for 5 minutes. Samples were rested at 4^{o}C until ready for use / storage at -20^{o}C.

Gel electrophoresis

A 1% agarose gel was created using a concentration of 1.5g/100ml agarose solution. 150ml of Tris/Borate/EDTA (TBE) buffer solution was added and heated using a microwave until the agarose dissolved. Once the solution cooled down, GelRed Nucleic Acid Gel Stain (Biotium) was added and mixed well. The solution was then poured into a confined casting tray with a well comb to create wells for sample deposition. Following cooling, the gel solidifies, and the well comb was carefully removed. The casting tray was placed in a gel box connected to a voltage source via electrodes and the box was filled with TBE up to the

maximum limit. 5µl of DNA loading dye (New England BioLabs) was loaded into the first well followed by each post amplified sample (10µl). The voltage was run at 85 volts over 45-60 minutes or until the samples ran their vertical course along the gel.

2.18 Apoptosis Array

A membrane-based sandwich immunoassay; Proteome Profiler Human Apoptosis Array Kit (R&D systems - ARY009) was used. A collection of 35 apoptosis associated related proteins were assessed. Cells were seeded in a 6 well plate at the desired cell count. Following 24 hours of incubation cells were treated with agents of choice. Cells were lysed on ice and collected into Eppendorf tubes using the manufacturers lysis buffer. Cell lysates were subjected to centrifugation at 14000 G for 10 minutes at 4^{o}C. On completion, quantification of protein was performed using a BCA assay (see 2.8.1). A multi-well multi-dish supplied by the manufacturer was used and the desired number of membranes added to each well. Membranes were blocked for 1 hour followed by the addition of cell lysate to each well as required. Wells were incubated overnight on a rocker at 2-8^{o}C. The following day, a cocktail antibody mix was added, followed by streptavidin-HRP and a chemi-reagent mix (chemiluminescent substrate) all supplied by the manufacturer. Membranes were analysed using ImageQuant LAS 4000.

2.19 Statistics and software used

All co-culture assays were performed at least in triplicate unless otherwise stated and represented as mean values with standard error. Results were predominantly analysed using GraphPad Prism (GraphPad Software, CA, USA) and Microsoft Excel v16.0 (Microsoft, Washington, USA) unless otherwise stated. For multiple groups assessed longitudinally (dose response curves) repeated measures analysis of variance (ANOVA) was used. For comparison between two paired groups a student's t-test was used and for three groups two way ANOVA with multiple comparisons was used; Tukey, Bonferroni and Sidak tests were used. P values were recorded and used as a measure of statistical significance. A p-value of 0.05 or less was deemed statistically significant.

RESULTS CHAPTER I

Exploring the sensitivity of BAP1 mutated malignant pleural mesothelioma to PARP inhibition and TRAIL

Hypothesis

I hypothesise that BAP1 mutated MPM leads to homologous recombination (HR) deficiency and subsequent sensitisation to the combination of PARP inhibition and TRAIL.

3 RESULTS I EXPLORING THE SENSITIVITY OF BAP1 MUTATED MALIGNANT PLEURAL MESOTHELIOMA TO PARP INHIBITION AND TRAIL

3.1 Mutations in BAP1 are associated with DNA repair

78 MPM samples were analysed from The Cancer Genome Atlas (TCGA) catalogue to assess for the highest frequency of genomic aberrations in MPM.

Loss of function mutations in BAP1 feature highest followed by NF2 and p53. These samples do not have matched normal pleural tissue controls to compare with, a limitation to the mesothelioma cohort, however these mutated genes are thought to be contributory to the development of MPM. It is well documented that a combination of diagnostic modalities can identify defects in BAP1 which include Sanger sequencing, Multiplex Ligation Dependant Probe Amplification, copy number analysis and cDNA sequencing. IHC is the technique of choice in the clinic.

The frequency of mutations in BAP1 is high

To understand the mutational landscape of MPM, The Cancer Genome Atlas (TCGA) was used to collect data on 78 exome sequenced samples. The most frequent mutations were tabulated and represented in graphical form. The commonest mutations identified were BAP1, followed by NF2, p53 and SETD2. Several other genes were identified to be aberrant including genes involved in DNA repair such as ATR.

(figure 3.1).

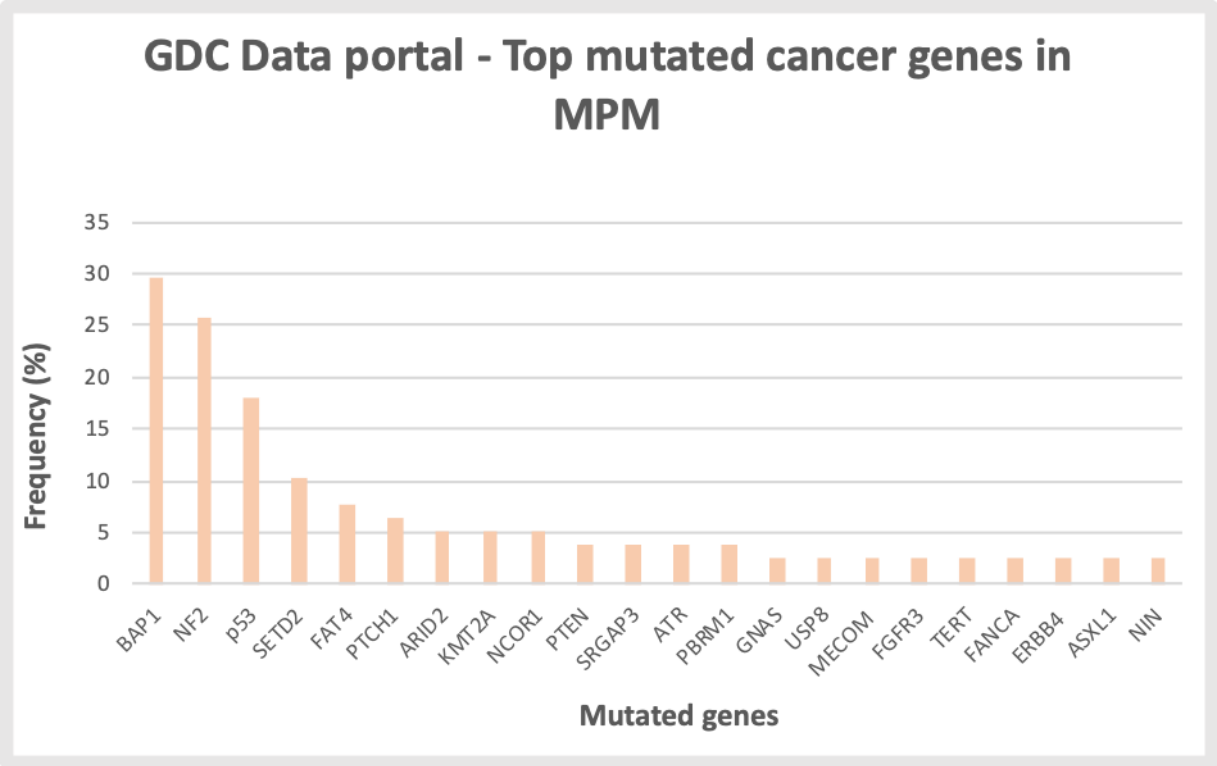

Figure 3. 1 – Top mutated cancer genes in MPM

Other types of genome aberrancy relevant to MPM include copy number alteration (CNA). This structural variation in chromosomes involves alterations in the number of copies of a region of DNA, leading to either duplication or deep / shallow deletion. Screening the TCGA

data shows us that CDKN2A is the commonest gene to be subject to CNA. Over 55% of CNA cases from the updated TCGA review were shown to involve CDKN2A. BAP1 is less frequently affected by this (76).

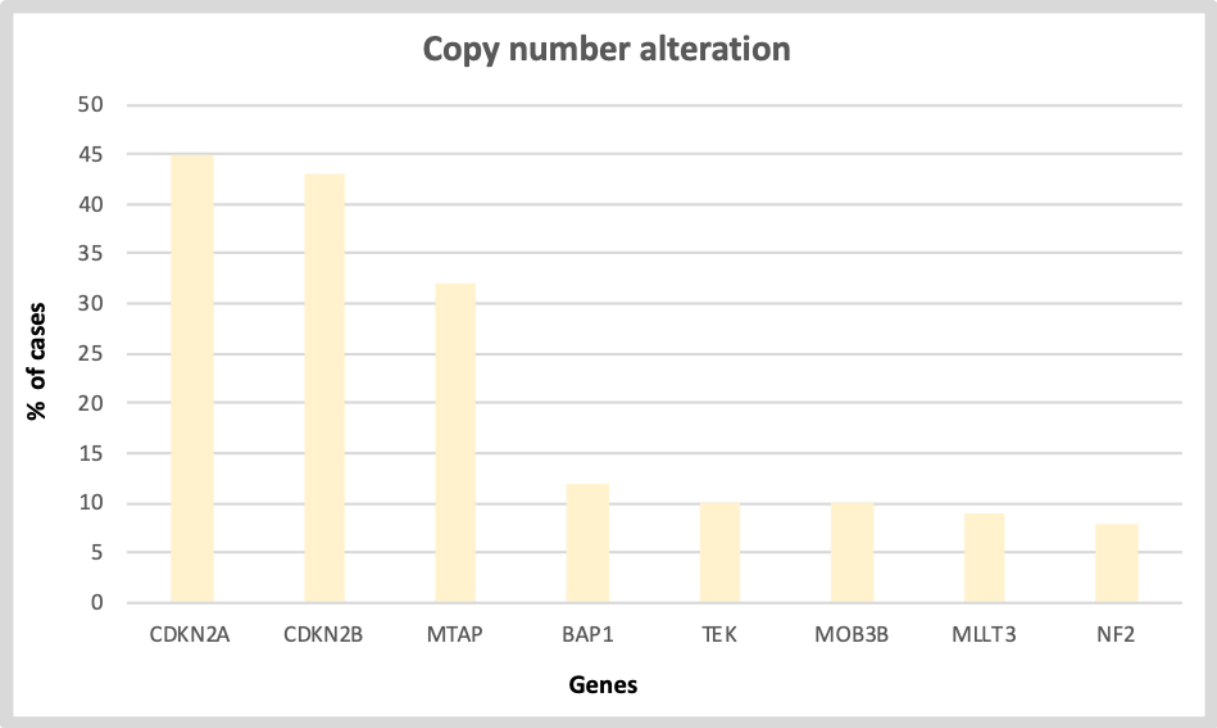

Figure 3. 2 - Genes with the highest copy number alteration in MPM.

MPM is linked to mutations in genes associated with DNA damage repair

A combination of TCGA and patient sequenced data collected from Guo et al (115) was reviewed for mutations in genes associated with DNA damage repair. DNA repair genes selected were identified from several papers (295-298). The pathways reviewed include base excision repair, mismatch excision repair, nucleotide excision repair, homologous recombination and non-homologous end joining. Other genes included in the repair machinery include genes involved in DNA - topoisomerase cross links, DNA polymerases, ubiquitination and modification, chromatin structure including ubiquitination, genes associated with sensitivity to DNA damaging agents (e.g. ATM, Werner syndrome helicase / 3' – exonuclease (WRN), replication protein A 4 (RPA4) and other genes such as p53, CHK1/2.

The frequency of mutations in these genes were then reviewed in 109 patients. BAP1 was shown to be the commonest aberrant gene involved in DNA repair followed by p53. Mutations in the RAD family of genes included RAD51, a crucial protein in homologous recombination. Most of these genes are mutated sub 5%.

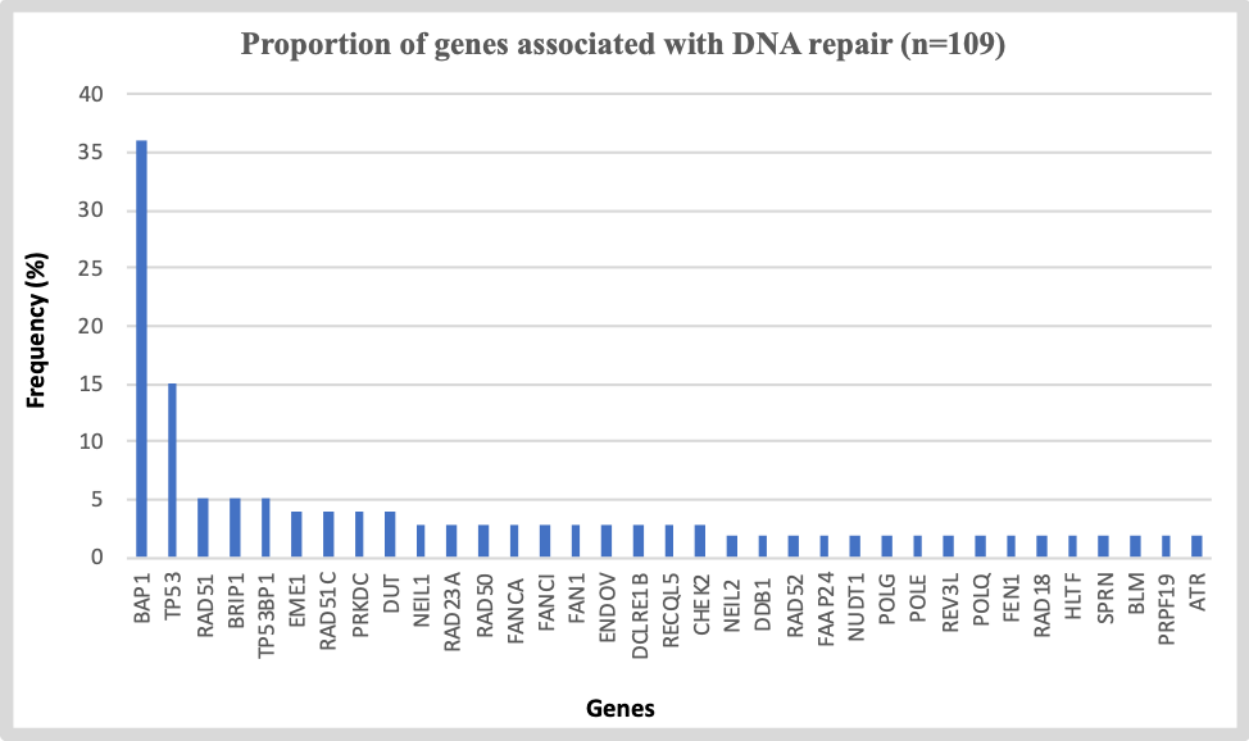

Figure 3. 3 - Genes involved in DNA damage repair in MPM.

3.2 Mutations in BAP1 influence DNA repair

Mutations in BAP1 are associated with a higher burden of DNA damage

Burden of DNA damage was measured using γH2AX. When double-strand breakage occurs, phosphorylation of H2AX leads to γH2AX. Following repair of DNA, γH2AX recedes confirming DNA restoration. γH2AX is therefore used as a surrogate for DNA repair

To understand how BAP1 relates to DNA damage I initially tested 6 MPM cell lines (3 BAP1 wild type – CRL2081, H2803, MPP89 and 3 BAP1 mutant – H2804, H2731, H28) and measured baseline γH2AX in the absence of DNA damaging treatment. Cells were seeded at 3000 per well in a 96 well plate. At 48 hours immunostaining was performed on each well to determine both percentage of positive γH2AX nuclei and foci per nuclei of γH2AX. Cells were fixed, permeabilised and stained with anti - γH2AX antibodies (see methods section) and read using the microplate reader, Cytation™ 3.

There was a non-statistically significant difference between BAP1 mutant and wild type cell lines.

Baseline DNA damage quantified as foci per nuclei of yH2AX in BAP1 mutant and wild type MPM cell lines

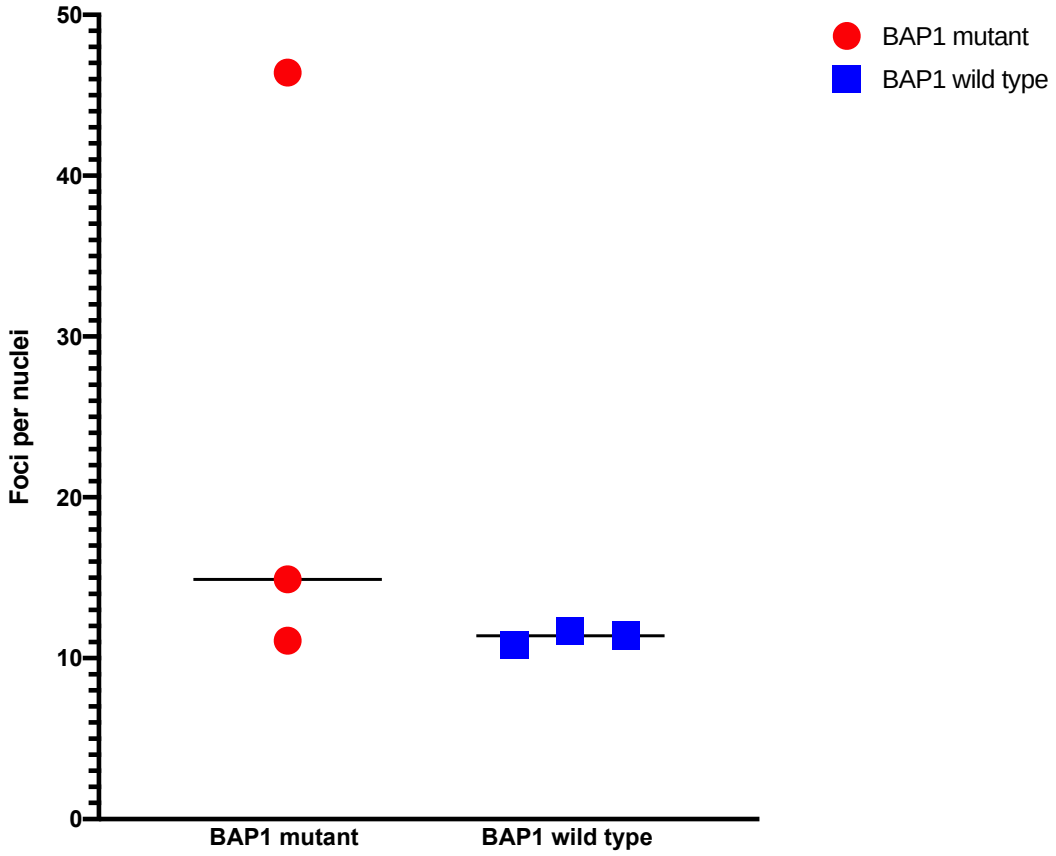

Baseline DNA damage quantified as total yH2AX in BAP1 mutant and wild type MPM cell lines

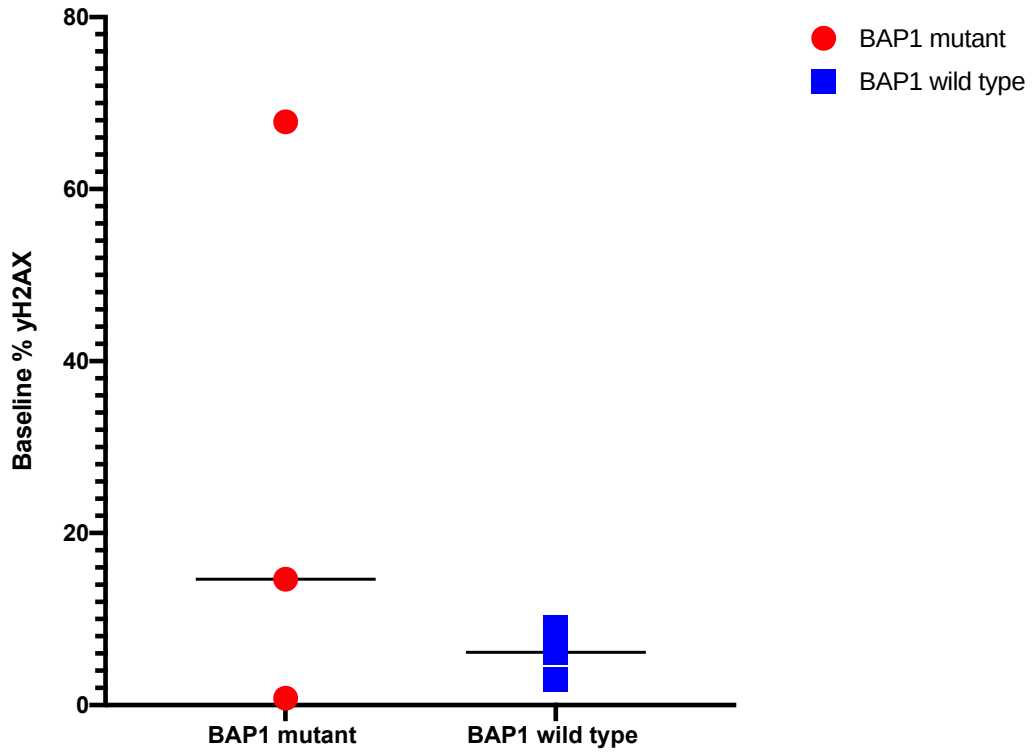

Figure 3. 4 – Baseline DNA damage measured as foci per nuclei and total number of foci

6 MPM cell lines tested (x3 BAP1 mutant (red) and x3 BAP1 wild type (blue)). Cell lines were cultured in a 96 well plate for 48 hours followed by fixing, permeabilisation and staining with a γH2AX antibody (1:1000, AF647). The nuclear stain was read using a microplate reader, Cytation™ 3. Foci per nuclei and % γH2AX were collectively measured in BAP1 mutant and wild type cell lines. Paired t test p=0.3693 and p=0.3756 respectively between mutant and wild type cells.

DNA damage is increased in BAP1 mutant MPM when induced by ionising radiation

Ionising radiation induces double-strand breaks and subsequent repair in robust cell lines. Cells vulnerable to DNA damage due to deficient repair pathways either seek alternatives to repair or undergo cell death. If BAP1 has a driver role in DNA repair, then mutations which inactivate its function will lead to a persistent rise in γH2AX. 6 MPM cell lines (3 BAP1 wild type – CRL2081, H2803, MPP89 and 3 BAP1 mutant – H2804, H2731, H28) were tested compared with baseline γH2AX in the absence of DNA damaging treatment. Cells were seeded at 3000 per well in a 96 well plate. Following 24 hours of incubation, they were subjected to ionising radiation at 1.5 and 5Gy. At 48 hours immunostaining was performed on each well to determine both percentage of positive γH2AX nuclei and foci per nuclei of γH2AX. Cells were fixed, permeabilised, stained with anti - γH2AX antibodies (see methods section) and read using the microplate reader, Cytation™ 3.

There are various ways to measure γH2AX in a sample. Both percentage of positive cells compared to unstained and foci per nuclei are widely accepted. Both are measured here in the 6 cell lines. 2 out of 3 cell lines mutant for BAP1 (H2804 + H2731) demonstrated higher γH2AX at baseline (no radiation – untreated control) and 48 hours following ionising radiation. The persistence of γH2AX is thought to signify the inability of the cell to repair itself accentuated by radiation. Little γH2AX was detected at baseline and following radiation in the other BAP1 mutant cell line; H28. The other cell lines did not demonstrate any increases following irradiation.

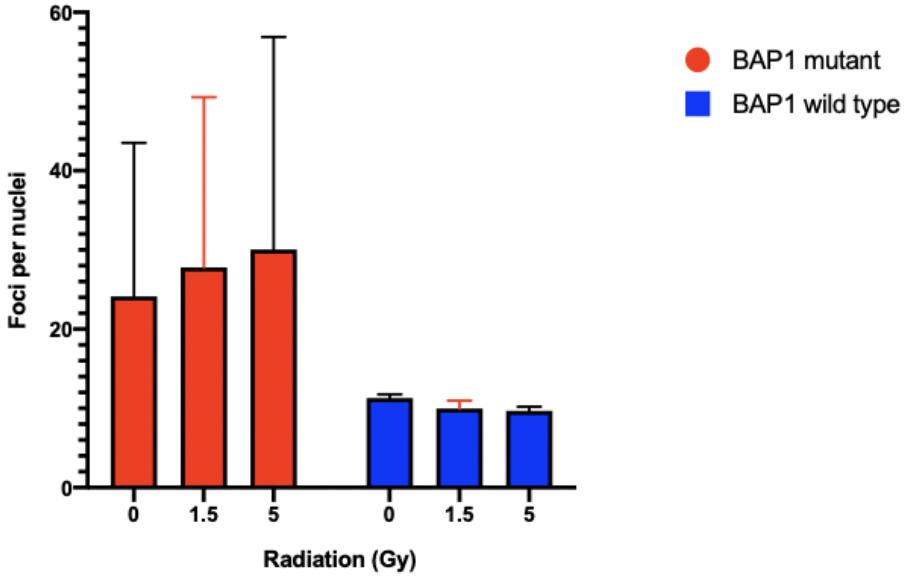

Figure 3. 5 – Mean foci per nuclei of BAP1 mutant and wild type MPM cell lines subjected to ionising radiation

6 MPM cell lines tested (3 BAP1 mutant (H2804, H2731, H28) and 3 BAP1 wild type (CRL2081, H2803, MPP89)). Cell lines were cultured in a 96 well plate and subjected to ionising radiation at 24 hours. Cells were fixed, permeabilised and stained with a γH2AX antibody (1:1000, AF647). The nuclear stain was read using a microplate reader, Cytation™ 3. Foci per nuclei of γH2AX in BAP1 mutant and wild type cells was collectively measured. Paired t tests were used to compare BAP1 mutant and wild type at separate radiation doses (5Gy p= 0.3251, 1.5Gy p= 0.2829 and no radiation p=0.03693)

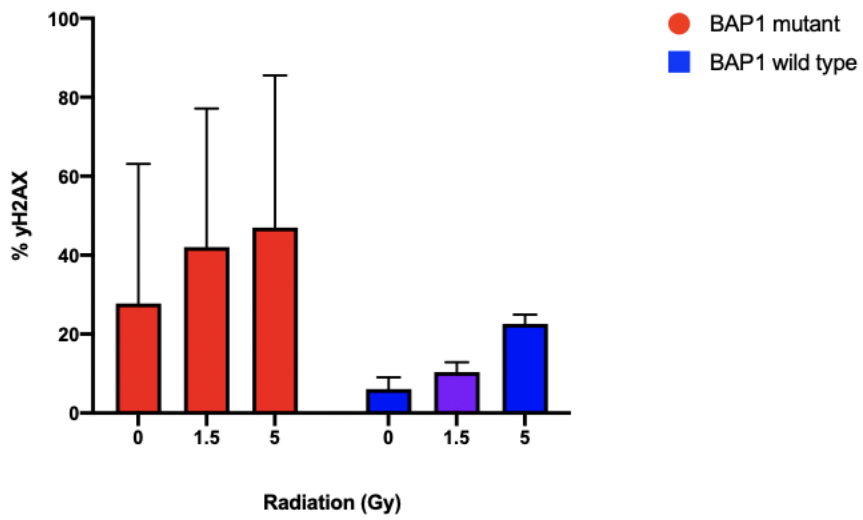

Figure 3. 6 – % positive γH2AX of BAP1 mutant and wild type MPM cell lines subjected to ionising radiation at 1.5 and 5Gy.

6 MPM cell lines tested (3 BAP1 mutant (H2804, H2731, H28) and 3 BAP1 wild type (CRL2081, H2803, MPP89)). Cell lines were cultured in a 96 well plate and subjected to ionising radiation at 24 hours. Cells were fixed, permeabilised and stained with a γH2AX antibody (1:1000, AF647). The nuclear stain was read using a microplate reader, Cytation™ 3. Percentage γH2AX was measured. Paired t tests were used to compare BAP1 mutant and wild type at separate radiation doses (5Gy p=0.3645, 1.5Gy p=0.2624 and no radiation p=0.3756)

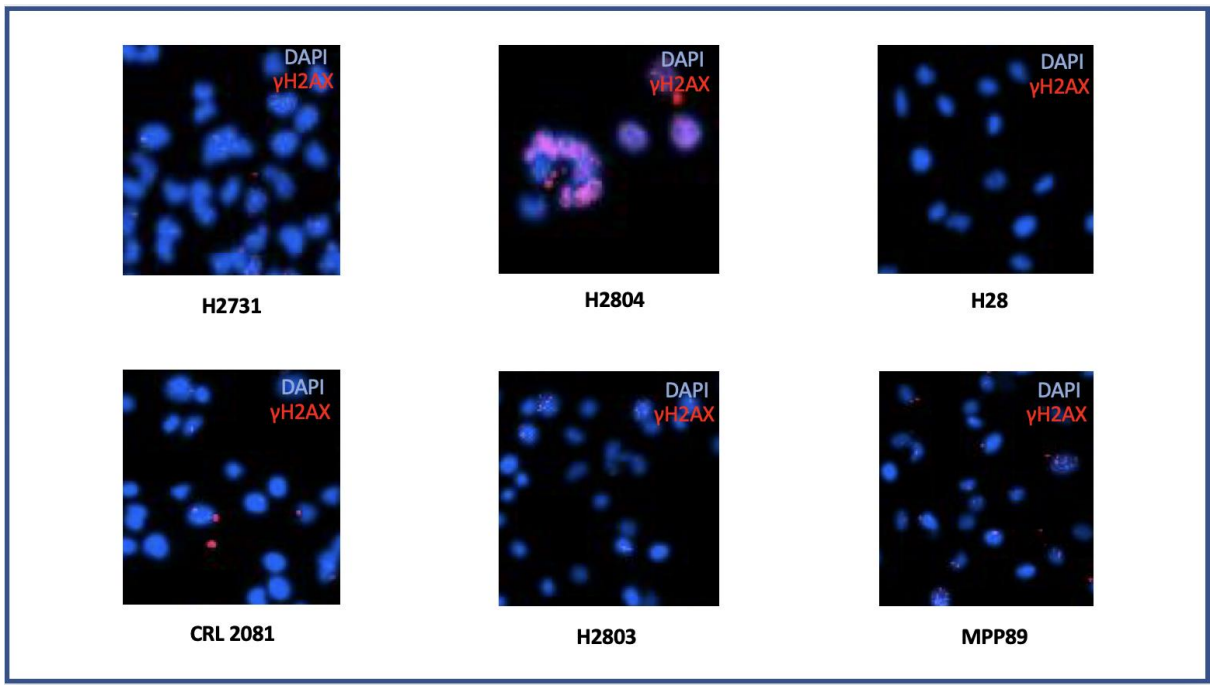

Figure 3. 7 – Captured immunofluorescent images at baseline of 6 MPM cell lines

Baseline immunofluorescent images of the 6 examined cell lines including DAPI and γH2AX staining. Blue = DAPI, red = γH2AX. H2804 stains very strong for γH2AX

Genetic knockdown of BAP1 leads to impaired DNA repair

Other critical proteins are involved in HR such as RAD51, a protein involved in DNA strand invasion. RAD51 can be measured in a similar way to γH2AX using immunofluorescence. Detection of RAD51 signifies the cells intention of undertaking homologous recombination.

H2869 shBAP1 and empty vector cells were seeded in 6 well plates at 250,000 per well. 3 circular coverslips were placed in each well with care to avoid them overlapping. Following 24 hours of incubation the coverslips were inspected for cell adherence and removed and placed upright in separate 24 well media filled plates. Plates were separately treated with

either no radiation (untreated control) or 5Gy then at 3 and 21 hours pre-fixation. Cells were then permeabilised and stained with γH2AX (1:1000, AF647) and RAD51 (1:600) antibodies. A secondary antibody was used for RAD51 (1:400, FC488). Coverslips were carefully removed and mounted on section slides, later read on a Leica DM6000 CS microscope.

Foci per nuclei was calculated for each coverslip using ImageJ. Results demonstrated below (Figure 3 22) show both γH2AX and RAD51 foci per nuclei for each cell line. At 0 hours γH2AX levels were higher in the BAP1 knockdown cell line compared with its empty vector counterpart. As time from radiation lengthened, the γH2AX levels continued to rise in both BAP1 knockdown and empty vector cell lines, although higher in the former, signifying a greater burden of damage and impaired repair. By 21 hours, γH2AX is expected to return back to baseline in HR competent cells supporting the premise that BAP1 knockdown cells harbour greater DNA burden, although the empty vector construct also demonstrated increased γH2AX levels not entirely consistent with this theory.

In parallel, RAD51 levels were measured almost 3 times higher at baseline compared with the shBAP1 cell line suggesting an impaired ability to repair upfront. RAD51 increases very little from 0 to 3 hours (9%) followed by a more significantly delayed increase by 21 hours (41%). In comparison, a small increase in empty vector foci is seen in RAD51 at 3 hours (9%) followed by a further small decline at 21 hours (2%). These results demonstrate that the BAP1 knockdown cell line suffers ongoing DNA damage and a poorer efficiency of repair compared with the empty vector construct. In addition, RAD51 has a higher baseline level and changes very little over the course of radiation treatment, suggesting little change in DNA damage.

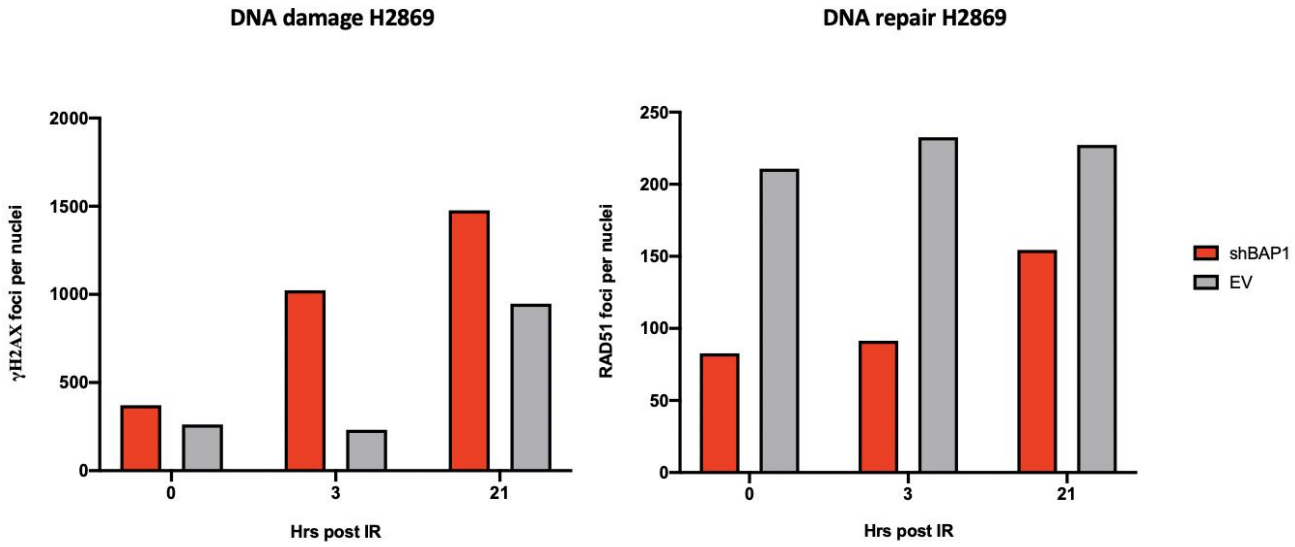

Figure 3. 8 – DNA damage in shBAP1 H2869

shBAP1 H2869 and empty vector constructs irradiated at 3 and 21 hours pre-fixation and compared with untreated control (0 hours). Immunostaining was performed requiring fixation, permeabilisation and antibody staining using γH2AX and RAD51. No error bars or statistics are provided for this set of results as they were only produced once.

No irradiation delivered

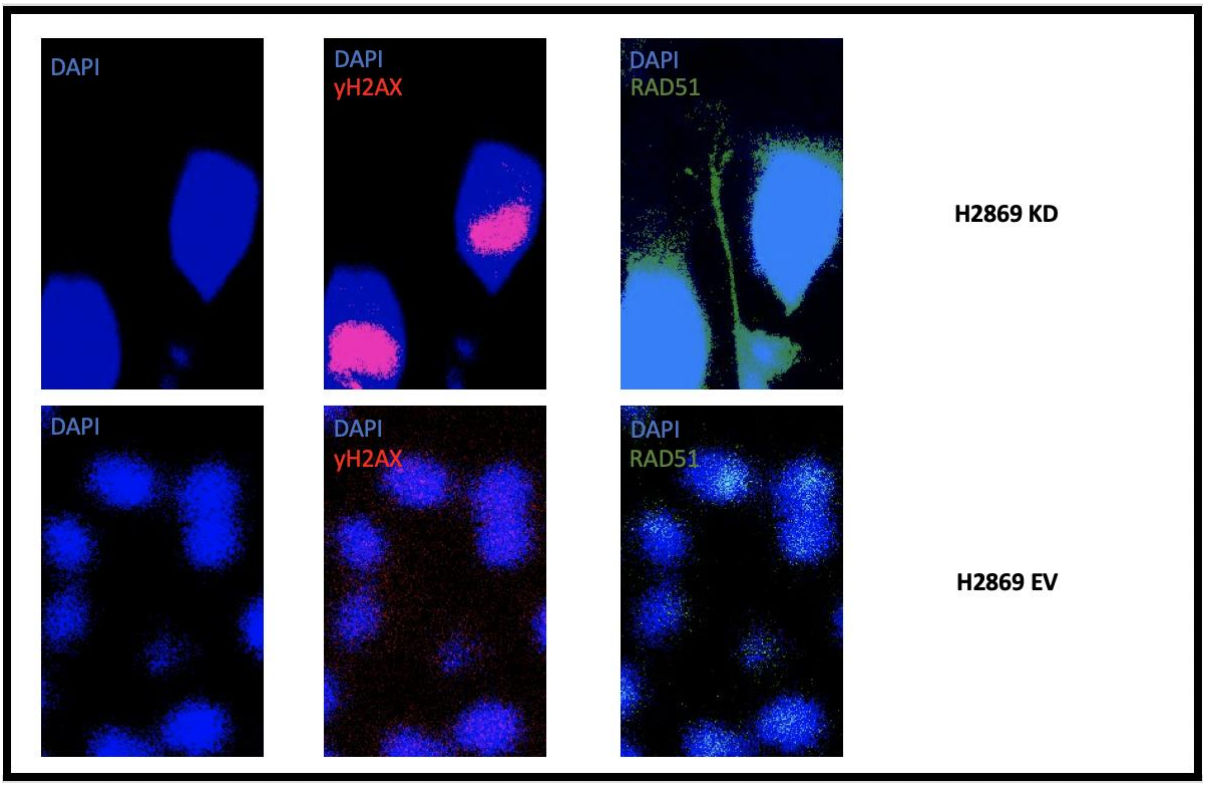

3 hours post irradiation

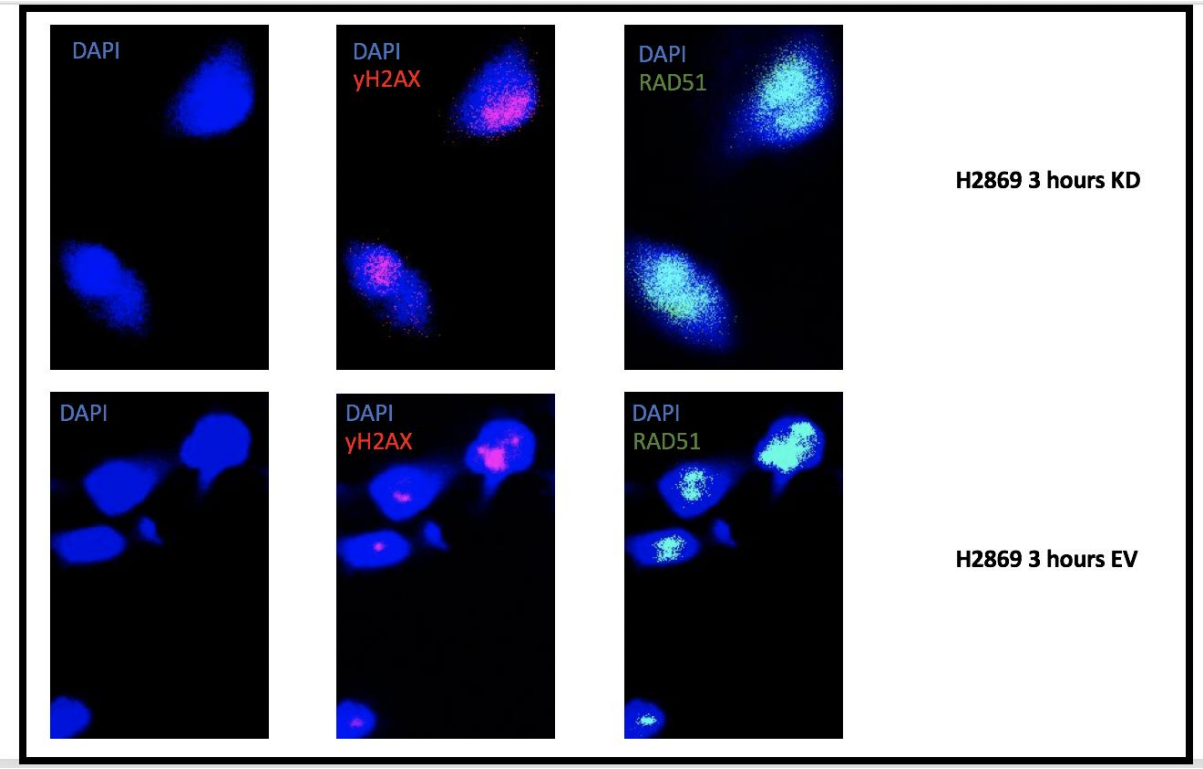

21 hours post irradiation

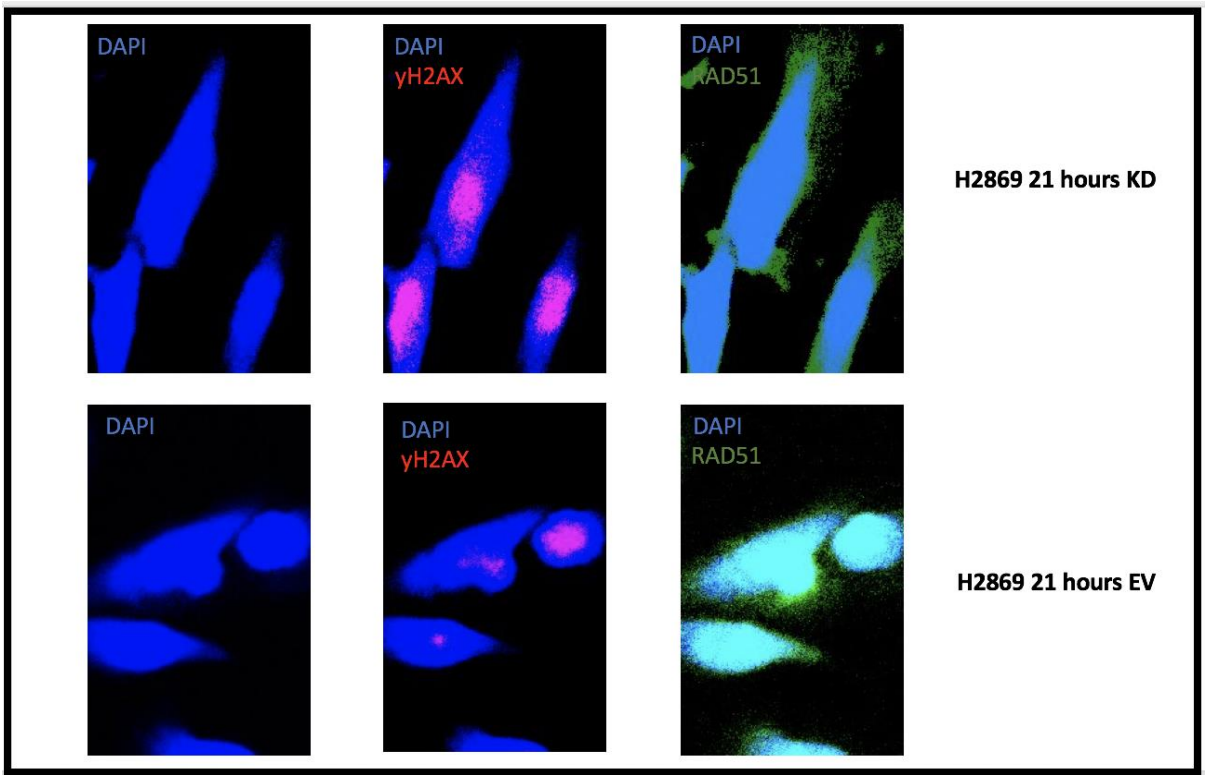

Figure 3. 9 – Captured immunofluorescent images of shBAP1 and empty vector cells subjected to irradiation

Images obtained following analysis (Fiji; ImageJ software). Channels included DAPI (blue), γH2AX (red) and RAD51 (green). The final image (composite) is an amalgamation of the 3 channels. Magnification 63X. Cell lines: H2869 shBAP1 (BAP1 knockdown cell line) and empty vector. Images taken of non-irradiated, following 3 hours and following 21 hours of irradiation (Assisted by Dr Kyren Lazarus)

3.3 Functional assessment of BAP1 in homologous recombination

Functional assay to assess homologous recombination an ongoing effort

Assessing the importance of BAP1 in homologous recombination posed a great challenge. I looked at assessing the functional ability of a cell line to conduct homologous recombination. The assay selected principally used a set of 2 plasmids, co-cultured in a cell line with proficient homologous recombination. In a proficient cell line this should lead to strand invasion of one plasmid with the other and its subsequent repair. A positive control plasmid (homologous recombination product) and a negative control plasmid (culture of just 1 plasmid) were used to validate the result. As a quality assurance step, primers were used for detection of individual plasmids to ensure transfection took place. Several cell lines were subject to this assay with varying results. Following a determined concerted effort using over 10 cell lines, H2731 was the only cell line to successfully be completed meaning I was unable to determine the functional capacity of BAP1 in HR using this assay.

This effort is ongoing in a separate piece of work, however due to the COVID19 pandemic this has been delayed significantly.

A)

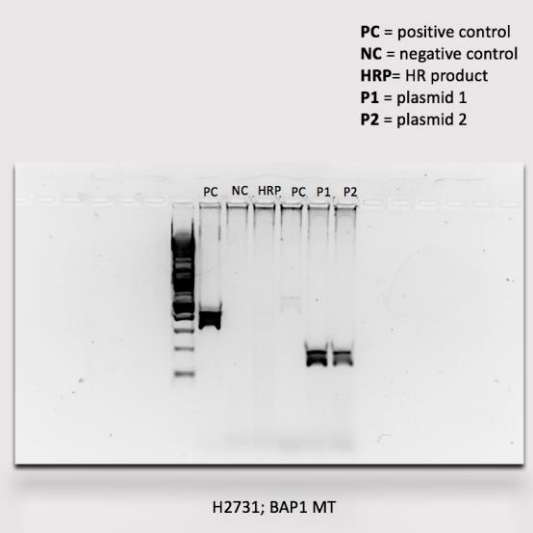

B)

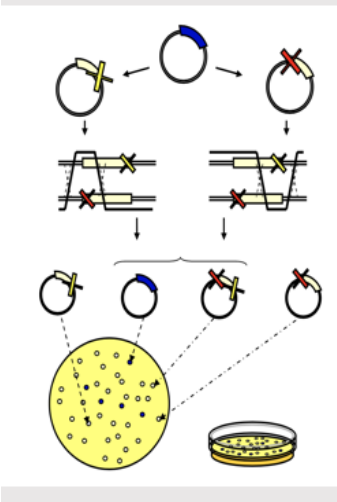

Figure 3. 10 – Homologous recombination assay

A) Demonstrates the results following gel electrophoresis of H2731. The furthest column to the left represents the ladder. The cell line was unable to produce a product of homologous recombination suggesting it was unable to perform HR B) A schematic of the assay demonstrating transfection of 2 mutated plasmids supplied by the assay kit; when co-cultured together leads to repair via homologous recombination in a proficient cell line

3.4 Loss of function mutations in BAP1 sensitise to the PARP inhibition *in vitro*

In support of the above data, BAP1 is reported to be frequently mutated and involved in DNA repair. It is speculated BAP1 plays a role in homologous recombination but, unlike BRCA, its loss is predicted not to impede the DNA repair pathway significantly suggesting its role as a passenger in the repair process.

This section demonstrates modest *in vitro* findings supporting BAP1 in DNA repair. Markers of DNA damage (γH2AX) and repair (RAD51) were measured in knockdown cell line models demonstrating increased DNA damage and reduced efficiency to repair DNA in BAP1 knockdown constructs.

Cell viability data shows a marginal differential response between BAP1 wild type and mutant MPM cell lines when treated with the PARP inhibitor; olaparib. Genetic knockdown models of BAP1 show similar findings. Use of ionising radiation to increase double strand breakage burden and exploit the use of PARP inhibition did not increase the loss of cell viability in mutant cell lines. Furthermore, although I was unable to demonstrate the importance of the catalytic domain, which governs deubiquitination, by knocking down the expression of BRCA1 I was able to demonstrate sensitivity to PARP inhibition, a finding yet to be reported in the literature. I report my findings below.

Mutant BAP1 MPM cells are more sensitive to olaparib than wild type

MPM cell lines were selected based on their BAP1 mutational status as identified through the Catalogue Of Somatic Mutations In Cancer (COSMIC) database. 4 BAP1 mutant and 4 BAP1 wild type cells lines were treated with a dose range of olaparib and cell viability assessed by MTT assay. MDA-MB-231, a frequently used BAP1 wild type breast cancer reference cell line in our laboratory was included at the time to balance the groups while further BAP1 wild type cells were sourced. A suitable BRCA mutated control cell line (with historic sensitivity to PARP inhibition) was sourced at the time (HCC1937), however following several reliability issues its continued use was abandoned and no further suitable BRCA mutated control cell line found.

MPM cell lines	BAP1 status
H2804	-
H28	-
H2731	-
H226	-
8T*	-
H2373	+
H2803	+
H2810	+
H2818	+
H2869	+
H513	+
MPP89	+
CRL 2081	+

Figure 3. 11 – COSMIC database and their BAP1 status: mutant (-) and wild type (+)

Cells were seeded at 3000 per well of a 96 well plate. Following 24 hours of incubation, cells were treated in triplicate with a dose range of olaparib from 0 - 100μM. Following a further

72 hours incubation cell viability of all cells was measured using an MTT assay. Results were normalised to the untreated arm of the assay. Results showed that cell lines with mutations in BAP1 had a reduced cell viability compared with their BAP1 wild type counterparts. Interestingly, the BAP1 wild type cell line H2810 demonstrated the greatest sensitivity, although reasons behind this remain unknown.

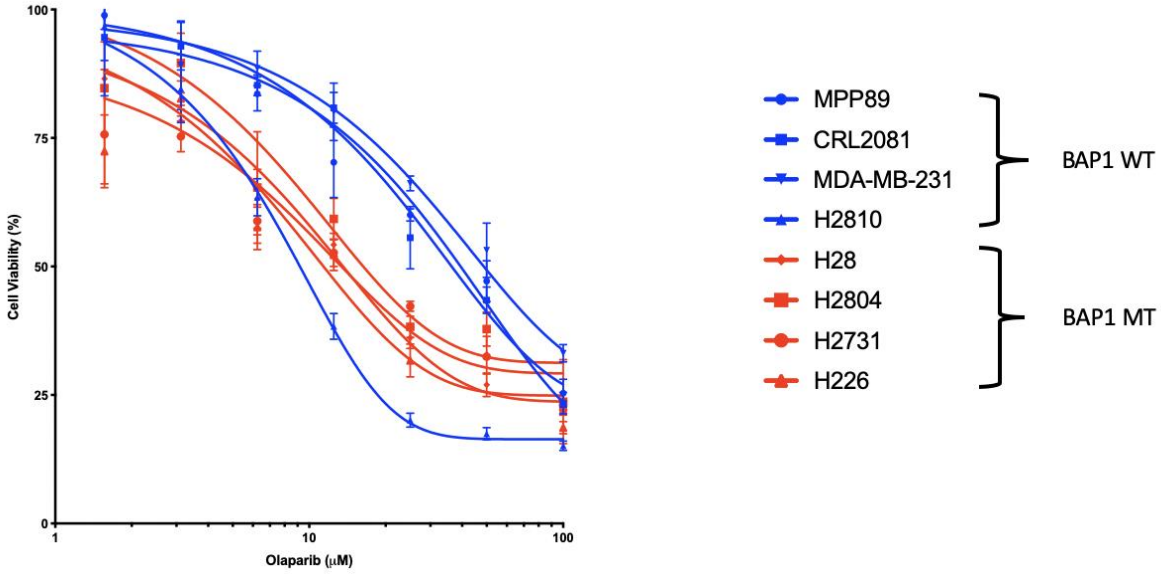

Figure 3. 12 – Cell viability of BAP1 mutant and wild type MPM cell lines

8 cell lines (4 BAP1 wild type (black) and 4 BAP1 mutant (red)) were cultured in a 96 well plate. Cell viability measured using an MTT assay. Cells were treated with a dose range of olaparib 0 - 100μM in triplicate (logarithmic scale). Two way ANOVA was used to statistically compare BAP1 mutant and wild type cell lines (p=0.0002)

To validate this further, measuring cell counts using Hoechst 33342 was performed (see 2.14, plate based). 6 similar cell lines were seeded at 3000 cells per well of a 96 well plate. Following 24 hours of incubation, cells were treated in triplicate with a dose range of olaparib from 0 - 100μM. Cell count was reported at the end of this time period using an automated fluorescence microplate reader, Cytation™ 3. Similar to the cell viability assay data, lower percentage cell counts per dose of olaparib were associated with BAP1 mutant cell lines. A differential response is less convincing here.

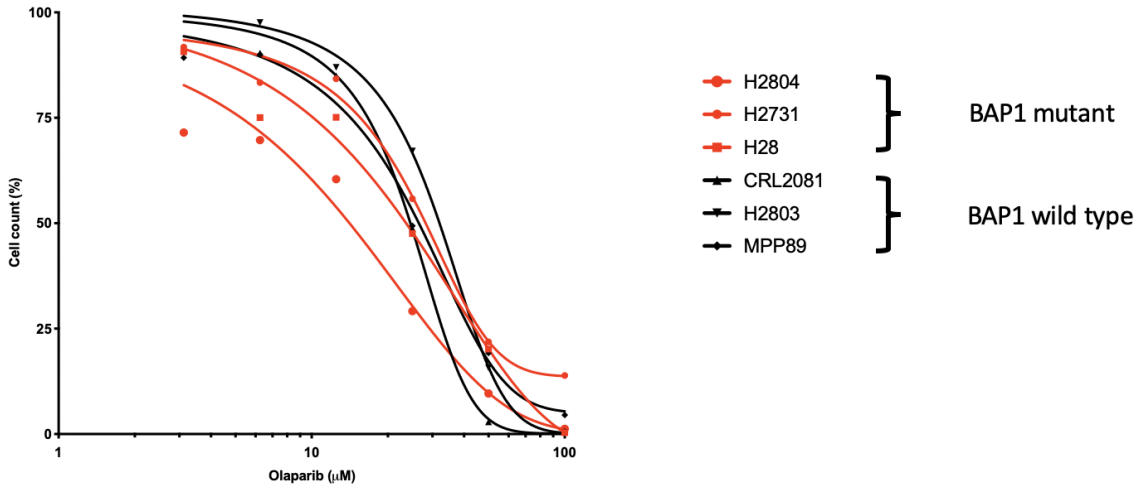

Figure 3. 13 - Measure of cell death in BAP1 mutant and wild type MPM cell lines

Hoechst staining of 6 MPM cell lines (BAP1 wild type (black) and 3 BAP1 mutant (red)) were cultured in a 96 well plate. Cells were treated with a dose range of olaparib 0 - 100μM in triplicate. Percentage cell count for each cell line was measured as a surrogate for cell death. Two way ANOVA was used to statistically compare BAP1 mutant and wild type cell lines p=0.0129.

Knockdown of full length BAP1 leads to increased sensitivity to olaparib

shRNA BAP1 knockdown cell line models were used to evaluate the above. Four BAP1 wild type cell lines were transduced with BAP1 shRNA and empty vector shRNA (see methods section). Cells were seeded at 3000 per well of a 96 well plate. Following 24 hours of incubation, cells were treated in triplicate with a dose range of olaparib from 0 - 100μM. Following a further 72 hours incubation, cell viability of all the cells was measured using an MTT assay. Results were normalised to the untreated arm of the assay. Results showed that the knockdown cell lines of H2869 and H513 were associated with a lower cell viability compared with their empty vector counterparts. It later became apparent that H513 was in fact not a pure mesothelioma cell line but a contaminant with adeno-squamous features.

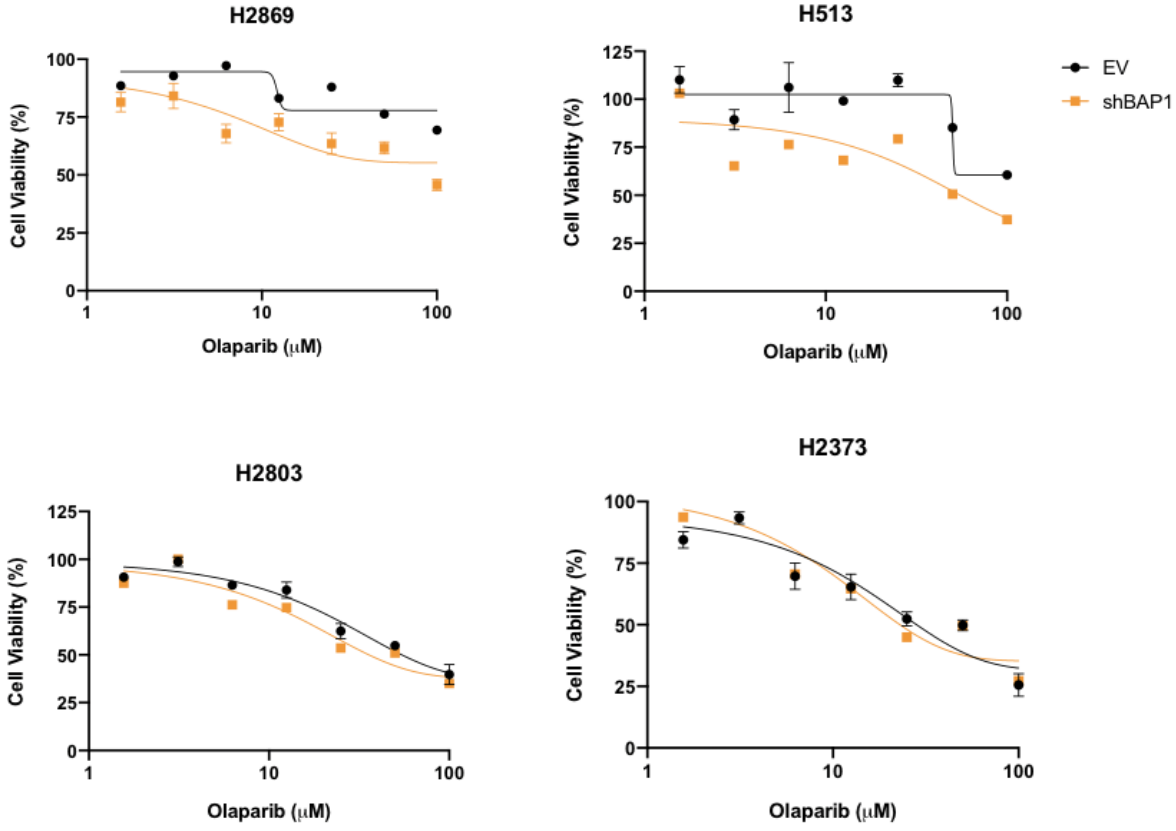

Figure 3. 14 - Cell viability of BAP1 shRNA knockdown MPM cell lines

4 cell lines were tested with BAP1 shRNA knockdown (orange) and empty vector (black) constructs. Cell lines were cultured in a 96 well plate. Cells were treated with a dose range of olaparib 0 - 100μM in triplicate. Cell viability assay measured using an MTT assay at 72 hours. Two way ANOVA was used to statistically analyse the difference between empty vector and knockdown model at each dose range (H2869 p=0.0002, H513 p<0.0001, H2803 p=0.2390, H2373 p=0.2390).

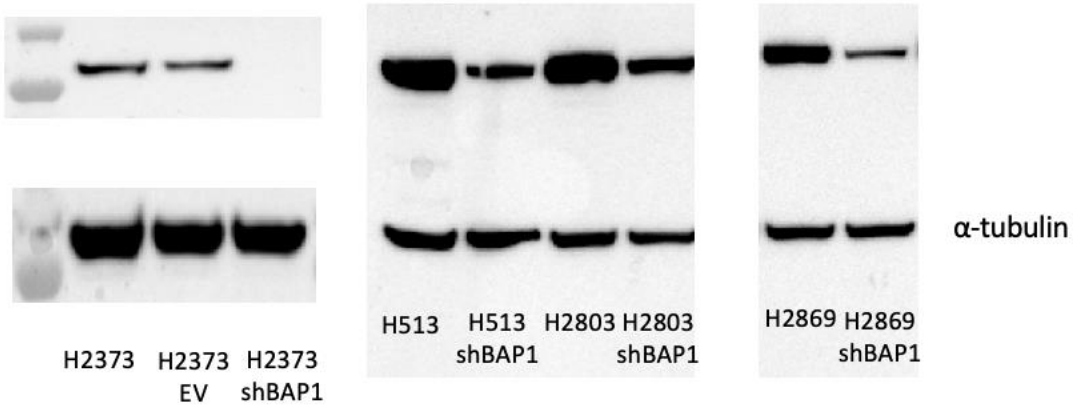

Figure 3. 15 – Western blot data supporting the 4 shBAP1 cell lines

Ionising radiation does not lead to increased sensitivity to olaparib in MPM cells transduced with BAP1 shRNA

As the differential response was modest, I attempted to amplify this by generating a greater double-strand break burden using ionising radiation. In a normal cell, as double-strand breaks increase, HR upregulates repair of the cells DNA. In a HR deficient system, this is not repaired and the cell seeks an alternative repair pathway as described in the literature review. Base excision repair, an alternative option to repair DNA can be targeted by olaparib leading to a greater synthetic lethal effect.

The H2869 shRNA BAP1 knockdown cell line was used. Cells were seeded at 3000 per well in a 96 well plate. Following 24 hours of incubation, cells were treated in triplicate with a dose range of olaparib from 0 - 100μM. Cells were then treated with ionising radiation delivered at 5Gy. Following a further 72 hours incubation, cell viability of all cells was recorded using an MTT assay. Results were normalised to the untreated arm of the assay. Results showed no clear difference in cell viability between untreated and 5Gy of radiation (statistically non-significant). Cells were also irradiated first and treated with olaparib after but this also did not show any difference (data not shown).

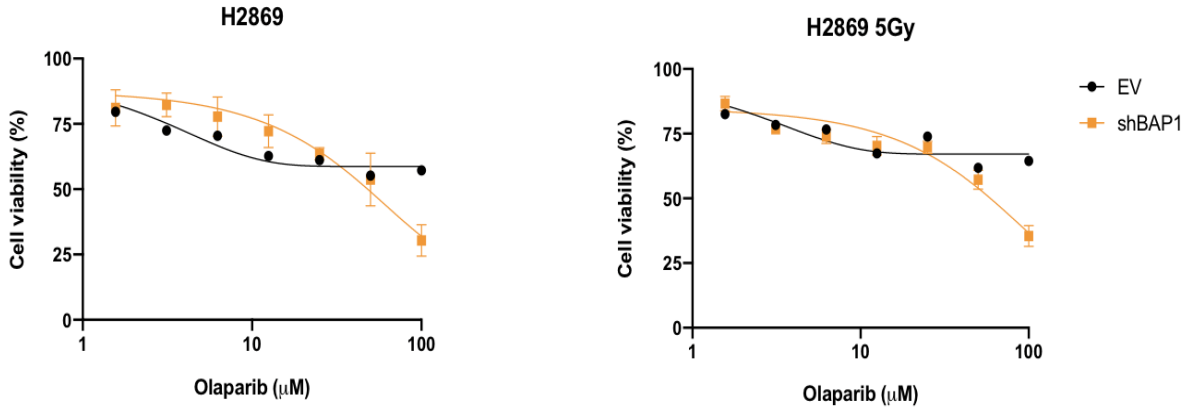

Figure 3. 16 - Effect of ionising radiation on cell viability of H2869 shBAP1

Differences in relative cell viability (%) between empty vector and shRNA BAP1 knockdown cell lines. Cell lines were cultured in a 96 well plate and treated with a dose range of olaparib 0 - 100μM in triplicate. Cells were either spared of ionising radiation or treated with 5Gy. Cell viability measured using an MTT assay at 72 hours. Two way ANOVA was used to compare 0 and 5Gy in the shBAP1 cell line only confirming a non-statistically significant p value of 0.2362. Comparisons between EV and shBAP1 with no radiation ($p<0.0001$) and 5Gy ($p<0.0001$) also analysed.

Loss of the deubiquitinase function of BAP1 does not result in increased sensitivity to olaparib

Deubiquitination is thought to play a role in DNA repair but it's function in this space remains unclear, in particular in MPM.

H226, an MPM cell line with homozygous deletion of BAP1 was transduced with a BAP1 construct with an inactive catalytic domain (C91A) and a wild type construct (BAP1 WT).

Cells were seeded at 3000 per well in a 96 well plate. Following 24 hours of incubation, cells were treated in triplicate with a dose range of olaparib from 0 - 100μM. Following a further 72 hours incubation cell viability of all the cells was measured using an MTT assay. Results were normalised to the untreated arm of the assay. Results showed no differences in cell viability between the parental null BAP1 cell line, wild type BAP1 and inactive BAP1 (C91A). Issues around the inactive BAP1 cell line later became apparent and have since been discarded.

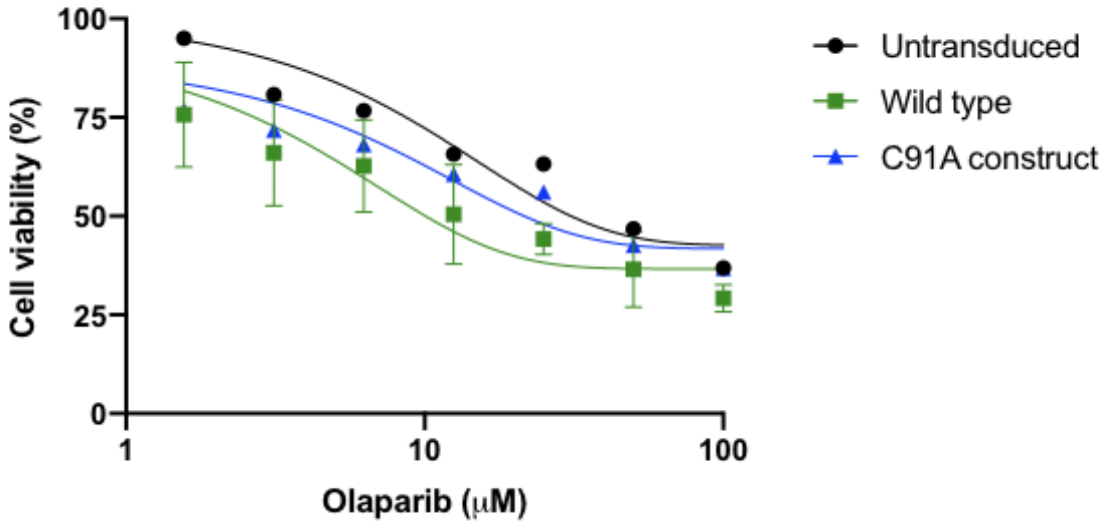

Figure 3. 17 - Cell viability of BAP1 mutant (untransduced), BAP1 wild type and the catalytically inactive H226 MPM cell line

Differences in relative cell viability (%) between BAP1 mutant,, wild type and catalytically inactive (C91A) H226 cell line. Cell lines were cultured in a 96 well plate and treated with a dose range of olaparib 0 - 100μM in triplicate. Cell viability measured using an MTT assay at 72 hours, Tukey's multiple comparison test: untransduced v wild type adjusted p=0.0001, untransduced v C91A construct adjusted p=0.0108 and wild type v C91A construct adjusted p=0.0095

Loss of the BRCA1 binding region of BAP1 sensitises to olaparib

The BRCA1 binding domain is an important region for BRCA1/BARD1 interaction. BRCA1 is critical to homologous recombination. Disruption of this interaction may inhibit DNA repair. The parental H226 cell line was transduced with a BAP1 construct with deletion of the BRCA binding site (BAP1 BRCA). This cell line, the parental cell line, H226 WT and H226 C91A were tested. Cells were seeded at 3000 per well in a 96 well plate. Following 24 hours of incubation, cells were treated in triplicate with a dose range of olaparib from 0 - 100μM. Following a further 72 hours incubation, cell viability was measured using an MTT assay. Results were normalised to the untreated arm of the assay. Results showed sensitivity to olaparib when cells lacked the BAP1 BRCA binding domain.

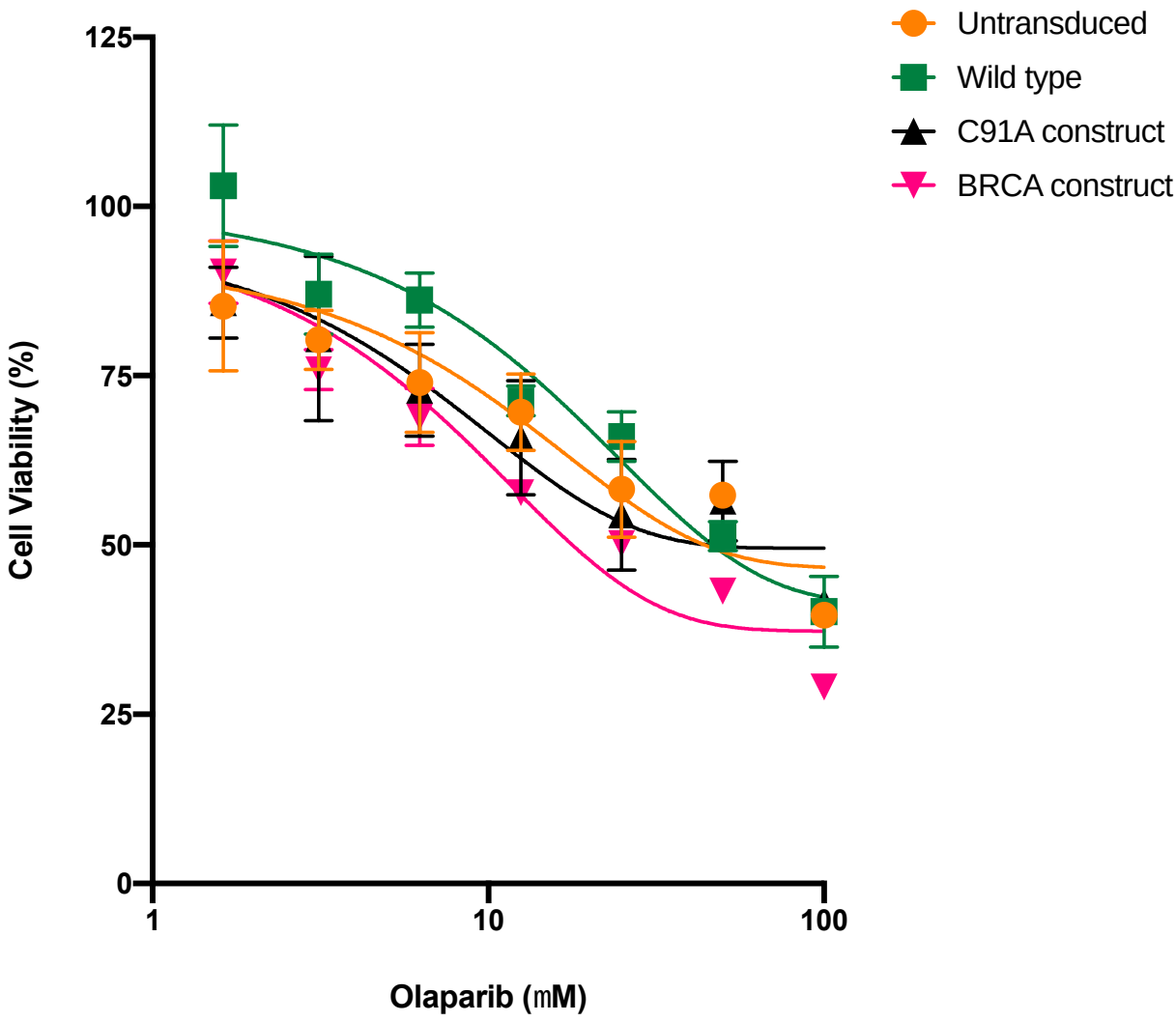

Figure 3. 18 - Cell viability of H226 cell constructs

Differences in relative cell viability (%) between untransduced, BAP1 wild type, C91A and mutated BRCA binding site cell lines. Cell lines were cultured in a 96 well plate and treated with a dose range of olaparib (0 - 100μM) in triplicate. Cell viability was measured using an MTT assay at 72 hours. Tukey's multiple comparison BRCA construct v untransduced adjusted p=0.0477, BRCA construct v untransduced adjusted p=0.0002 and BRCA construct v C91A construct adjusted p=0.1051.

A dose between 20μM (BAP1 BRCA binding domain construct) - 50μM plus (others) led to a 50% loss of cell viability (IC50). 50μM was explored further, represented in the scatter plot below. The lost BAP1 BRCA binding domain cell line demonstrated the greatest loss of cell viability at 50μM.

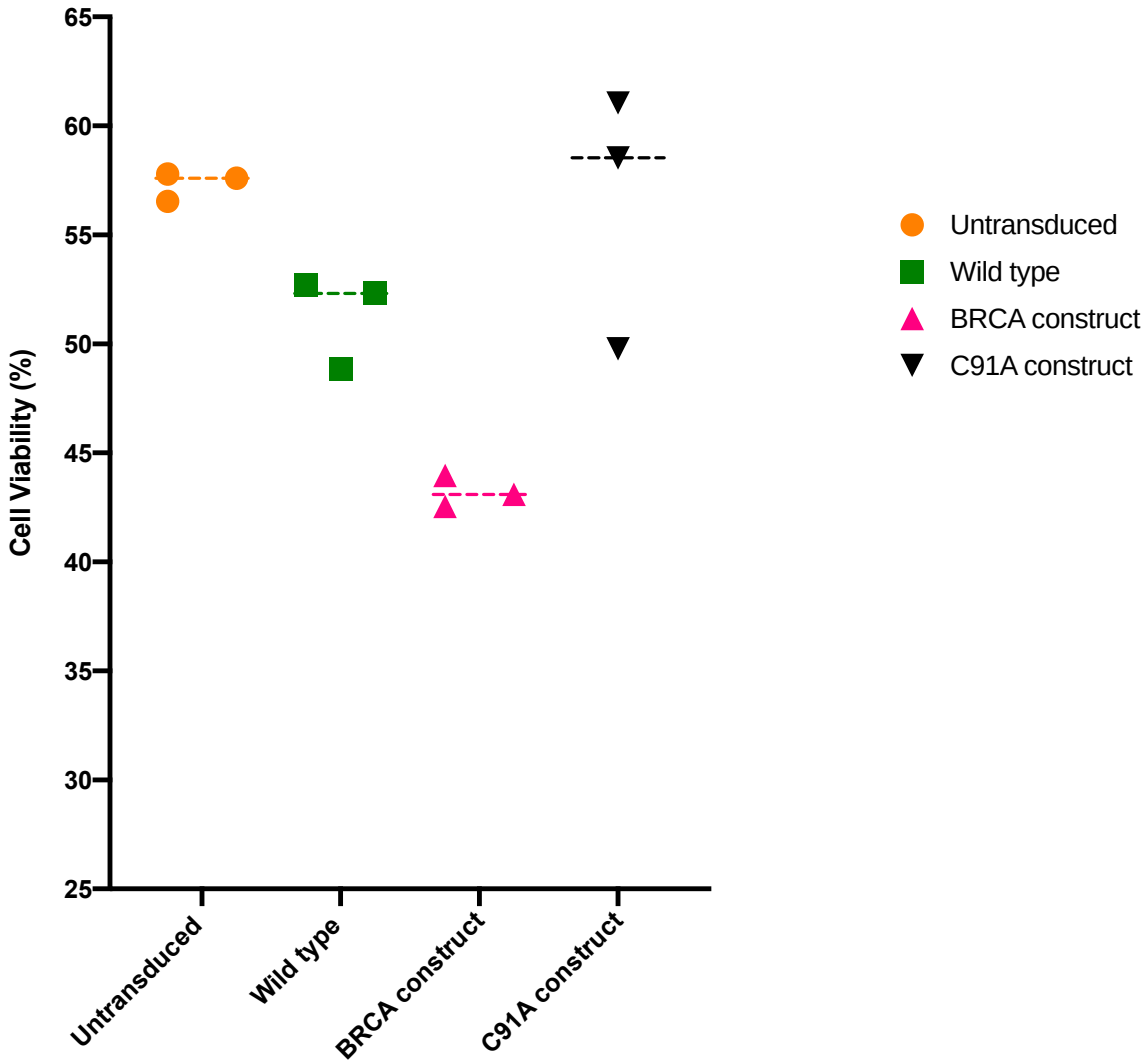

Figure 3. 19 - Cell viability assay using 50μM of olaparib in H226 cell line constructs

Differences in relative cell viability (%) between untransduced H226 (BAP1 mutant), BAP1 wild type, BAP1 mutated BRCA binding domain and inactive BAP1 catalytic domain. Cell lines were cultured in a 96 well plate and treated with 50μM of olaparib in triplicate. Cell viability was measured using an MTT assay at 72 hours. Tukey's multiple comparisons: BRCA construct v untransduced adjusted p=0.0020, BRCA construct v BAP1 wild type adjusted p=0.0310 and BRCA construct v c91A construct adjusted p=0.1375.

shRNA knockdown of BAP1 leads to increased sensitivity to other PARP inhibitors in MPM

Sensitivity was extended to other third generation PARP inhibitors. Talazoparib and niraparib, two newer agents in development, were tested using the knockdown cell line models.

The shRNA H2869 BAP1 knockdown cell line was used. Cells were seeded at 3000 per well in a 96 well plate. Following 24 hours of incubation, cells were treated in triplicate with a dose range of olaparib from 0 - 100μM. Following a further 72 hours incubation, cell viability of all the cells was measured using an MTT assay. Results were normalised to the untreated arm of the assay. Results showed that both niraparib and talazoparib led to reduced cell viability at higher doses in the BAP1 knockdown compared with the untransduced cell line, although this was not supported by statistical significance when talazoparib was used. Potency was higher at lower concentrations compared with olaparib.

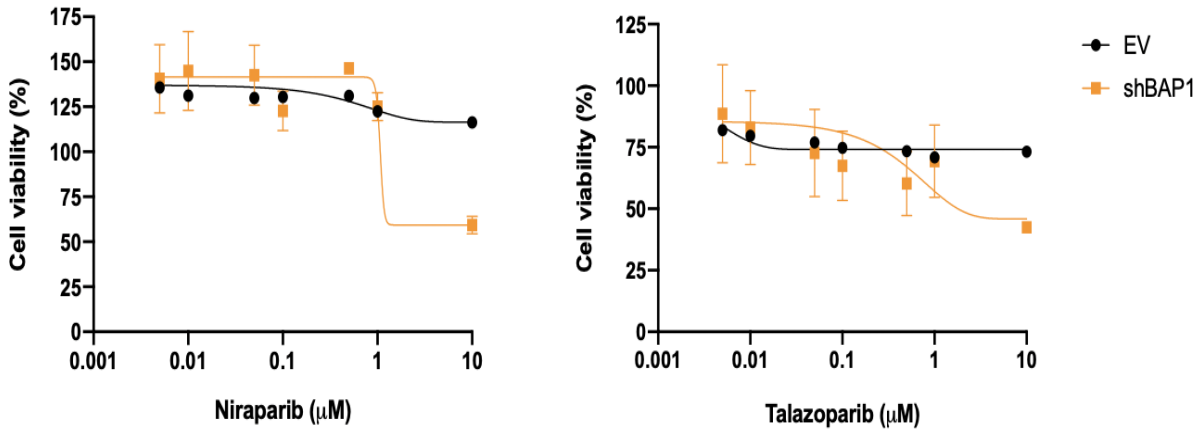

Figure 3. 20 – Cell viability of H2869 shBAP1 using alternative PARP inhibitors

Sensitivity to other PARP inhibitors was assessed using a BAP1 shRNA knockdown (orange) and empty vector (black) cell line model. Cells were cultured in a 96 well plate and treated with a dose range of niraparib (0.001 – 10μM) and talazoparib (0.001 – 10μM), in triplicate. Cell viability was measured using an MTT assay at 72 hours. Two way ANOVA was used to statistically analyse the difference between empty vector and knockdown model (niraparib $p<0.0001$ and talazoparib $p=0.2617$.

Further homologous recombination modulating agents under clinical investigation fail to show sensitisation in BAP1 mutant MPM

Other targets of DNA repair machinery under assessment and making progress in the clinic include ATM and ATR. Small molecule inhibitors targeting these proteins were each tested in 4 MPM cell lines (x2 BAP1 mutant – H2731 and H2804and x2 BAP1 wild type H2373 and H2818). Cells were seeded at 3000 per well in a 96 well plate. Following 24 hours of incubation, cells were treated in triplicate with a dose range of an ATM inhibitor (AZD0156) from 0 - 100μM and an ATR inhibitor (AZD6738) from 0 – 10μM. Dose ranges were selected based on previous *in vitro* studies examining these agents in similar settings (299, 300). Following a further 72 hours of incubation, cell viability of all the cells was measured using an MTT assay. Results were normalised to the untreated arm of the assay. Results showed no difference between BAP1 mutant and wild type cell lines when treated with either agent.

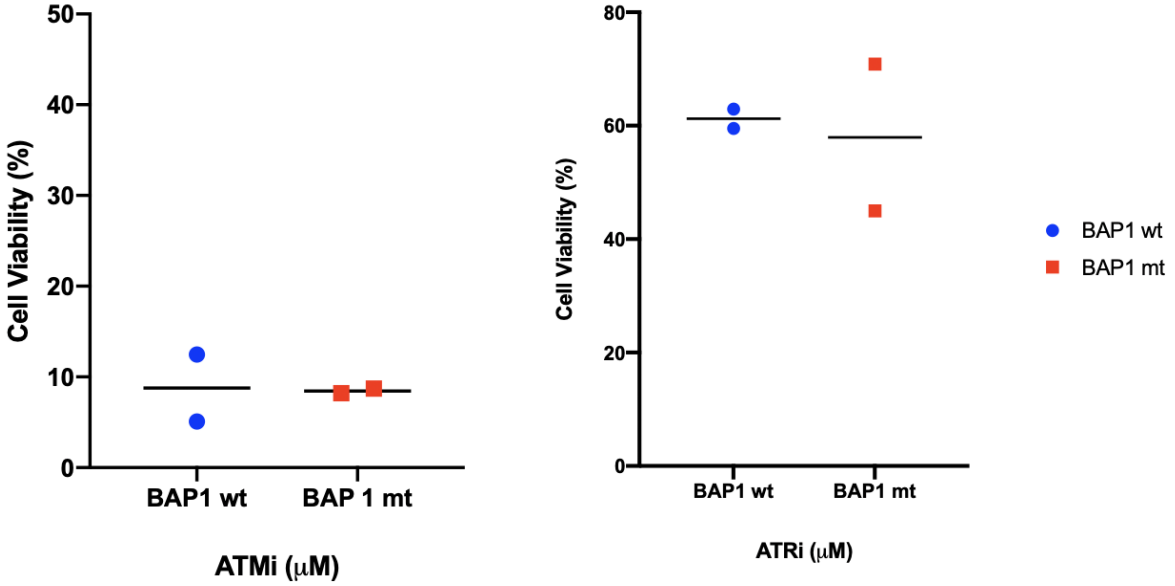

Figure 3. 21 - Cell viability of MPM cell lines using ATR and ATM inhibitors

4 cells lines (2 BAP1 mutant, 2 BAP1 wild type) were cultured in a 96 well plate and treated with a dose range of ATMi (AZD0156) from 0 - 10μM and ATRi (AZD6738) from 0-100μM in triplicate. Cell viability was measured using an MTT assay. Paired T test was used comparing BAP1 mutant and wild type cell lines (ATMi p=0.7366, ATRi p=0.0394)

3.5 Mutations in BAP1 sensitise to TRAIL and olaparib

As described earlier, data we published in January 2018 confirmed that loss of function mutations in BAP1 led to sensitisation to TRAIL (144). This has since triggered the development of a clinical trial currently in the pipeline. Given the role BAP1 may have in homologous recombination, the use of PARP inhibitors with TRAIL is studied in this section. Data demonstrated here shows mutations in BAP1 lead to sensitivity to olaparib.

Recombinant TRAIL and olaparib lead to greater loss of cell viability in BAP1 mutated MPM

Using the H2869 shBAP1 cell line and its empty vector counterpart, cells were seeded at 3000 per well in a 96 well plate. Following 24 hours of incubation cells were treated in triplicate with a dose range of olaparib and a fixed dose of 100ng/ml of TRAIL, a reference dose optimised and used in our previous work. Cells were analysed 72 hours later measuring cell viability using an MTT assay.

Results showed a reduction in cell viability at higher doses of olaparib when combined with TRAIL. H2869 shBAP1 and TRAIL reported the highest reduction in cell viability when combined with olaparib.

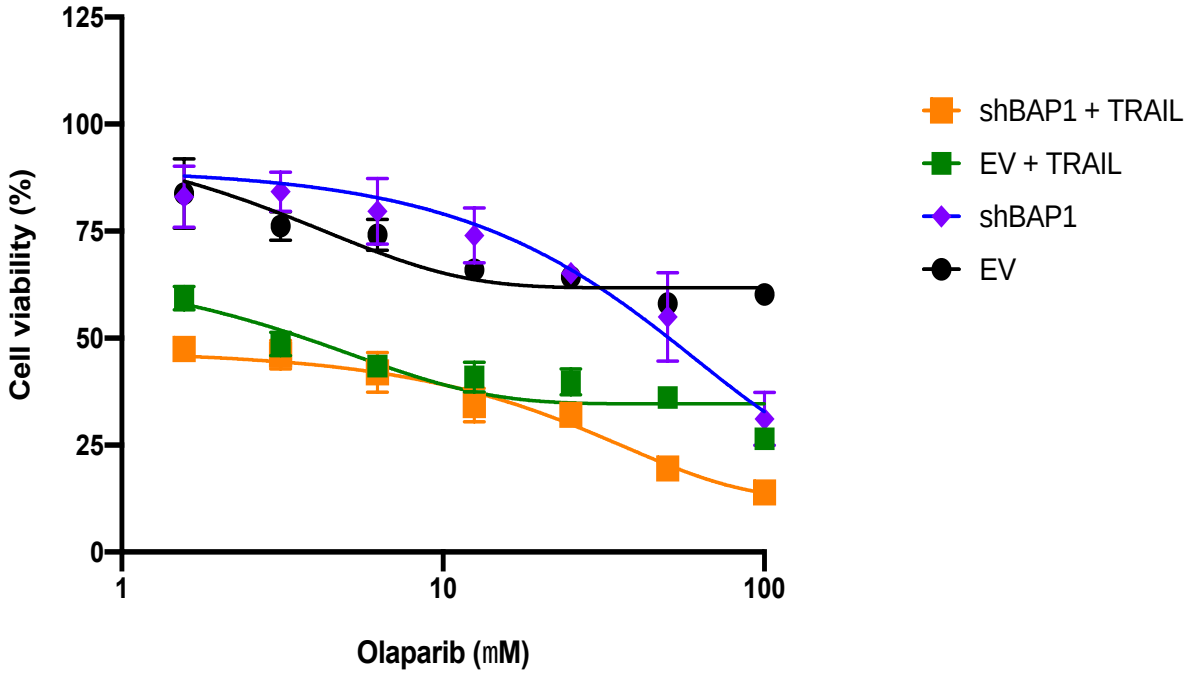

Figure 3. 22 – Cell viability of H2869 cell constructs treated with olaparib and TRAIL

H2869 shBAP1 and empty vector cell lines were cultured in a 96 well plate. Cells were treated with a dose range of olaparib 0 - 100μM in triplicate and TRAIL 100ng/ml. Cell viability was measured using an MTT assay at 72 hours. Tukey's multiple comparison test: shBAP1 + TRAIL v shBAP1 p <0.0001, shBAP1 + TRAIL v EV p <0.0001 and shBAP1 + TRAIL v EV + TRAIL p 0.0174)

Using the H226 cell line models described earlier (untransduced (BAP1 mutant), BAP1 wild type, mutation in BAP1 BRCA binding domain and a newly developed catalytically inactive C91A cell line), cells were seeded at 3000 per well in a 96 well plate. Following 24 hours of incubation cells were treated in triplicate with a dose range of olaparib and a fixed dose of 100ng/ml of TRAIL. Cells were analysed 72 hours later measuring cell viability using an MTT assay.

Results showed mutations in BAP1 were associated with a greater loss of cell viability compared with wild type. Mutations in BAP1 BRCA binding domain led to a further fall in cell viability, however H226 C91A was associated with the greatest drop in cell viability.

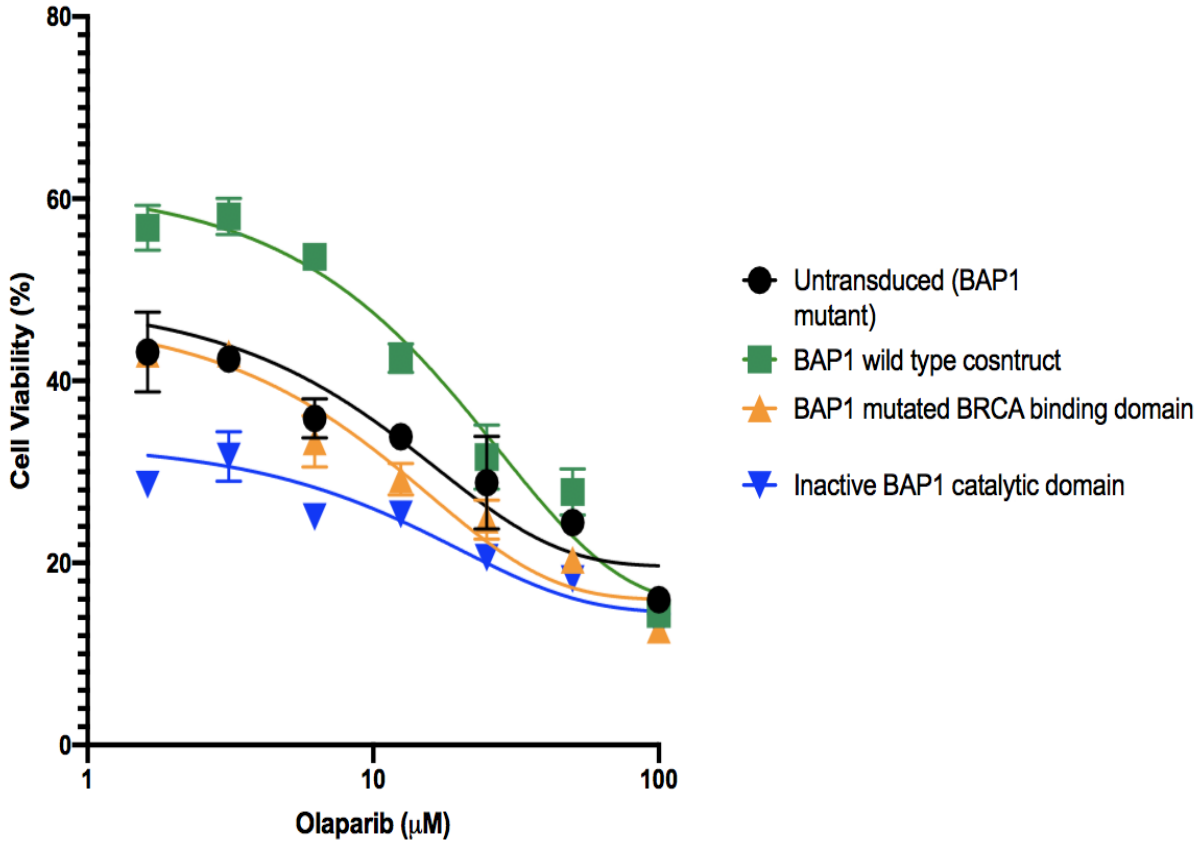

Figure 3. 23 - Cell viability of H226 cell constructs treated with olaparib and TRAIL

H2226 cell line constructs were cultured in a 96 well plate. Cells were treated with a dose range of olaparib 0 - 100μM in triplicate and TRAIL 100ng/ml. Cell viability was measured using an MTT assay at 72 hours. Tukey's multiple comparison test: inactive BAP1 binding domain v untransduced adjusted p=0.0020, inactive BAP1 binding domain v BAP1 wild type construct adjusted p=0.0360, inactive BAP1 binding domain v BAP1 mutated BRCA binding domain adjusted p=0.0226.

3.6 Discussion

Mutations in BAP1 influence DNA repair

The data demonstrated here shows BAP1 correlates with critical proteins involved in DNA repair such as RAD51 and γH2AX best illustrated using shBAP1 cells (Fig 3.8). Knocking down expression of BAP1 and reviewing its longitudinal relationship to RAD51 and γH2AX was key to supporting this theory. The pattern of repair was unexpected as 3 hours post irradiation one would expect a rising γH2AX and RAD51, however by 21 hours both should have fallen suggesting repair of DNA damage. Nevertheless, it provided support for greater DNA damage burden and inefficient repair in the BAP1 knockdown model. Other proteins could have been reviewed but given the critical nature of these two in HR they were thought acceptable enough to demonstrate the point. Although this supports its involvement in HR it doesn't inform us to what degree. Equally, any involvement in other repair pathways remains unanswered when measuring these proteins.

Functional assessment of HR in a panel of BAP1 mutant and wild type cell lines remains unknown. Several technical issues arose with the assay over months with ongoing inconsistent results. The integrity of the assay came under question given the inconsistencies. A number of reasons can be offered for this. 75,000 cells were cultured in a 12 well plate. Following transfection of the relevant plasmids the cells were collected post trypsinisation however as the cell number remained low the pellet of cells was often barely visible leading to low quantity of plasmid extraction and subsequent absence of bands on gel electrophoresis post PCR. In addition, the lack of validation of successful transfection of plasmids provided further uncertainty leaving me to abandon the assay due to lack of confidence. Prior to

acquisition of this kit, despite its recommendation, it has been used very little in the literature and problems with the experimental steps were apparent from the offset.

Other ways of measuring HR efficiency exist. The most clinically relevant is the FDA approved myChoice assay, developed my Myriad. This looks at BRCA1/2 variants including an assessment of genomic stability including loss of heterozygosity, telomeric allelic imbalance and large-scale state transitions. This tool is clinically validated and is being explored in MPM.

Loss of function mutations in BAP1 sensitise to the PARP inhibition *in vitro*

The concept of synthetic lethality has been exploited in breast and ovarian cancer. By targeting compensatory DNA repair pathways in cancer cells with deficient homologous recombination, cancer cells succumb to death. Mutations in key proteins that govern homologous recombination are likely to be targets for PARP inhibition. Other than mutations in the tumour suppressor gene BRCA there are no other predictive biomarkers of response to PARP inhibitors. Exploration of BAP1 in this space is poorly understood and other than a diagnostic tool it has no role in predicting response to DNA modulating agents.

Challenging the idea of its clinical importance required a series of experiments. Firstly, delineating a relationship between BAP1 and mutations in genes associated with DNA damage response was important going forward. Although several genes were identified through TCGA data, many of these were neither critical nor frequent highlighting a questionable significance to their relationship.

Following this, identification of whether mutations in BAP1 actually make a difference was the next step. Using a series of cell lines stratified for mutations in BAP1 yielded a statistically significant difference in cell viability and cell death when treated with olaparib. MDA-MB-231 was initially included in this group of cell lines to numerically balance the groups as further MPM cell lines were sourced. It offered an initial glimpse at seeing another tumour types tested in these experiments suggesting this therapy could be extended to other BAP1 mutant tumours regardless of their origin. An outlier to this H2810, a BAP1 wild type cell line, demonstrated the greatest reduction in cell viability. Exploring the exome data through COSMIC no mutations sensitising to PARP inhibition were found including mutations in the BRCA gene. In particular, mutations in the tumour suppressor gene TP53 were found but unlikely to implicate its sensitivity to PARP inhibition.

To validate this further BAP1 gene expression was knocked down re-testing the theory. Using 4 cell lines, 2 exhibited a reduction in cell viability compared with their respective control arms. The shBAP1 MPM cell lines H2803 and H2373 failed to demonstrate any differential response. The knockdown efficiency was satisfactory meaning the empty vector cell line is particularly sensitive to olaparib regardless of BAP1 expression. Other than APC, no other meaningful mutations were noted through COSMIC and no mutations rendering the cell line sensitive to PARP inhibition were found. Knockdown of BAP1 was not necessarily that convincing in these assays, which could be explained by either the requirement of a total knock out of the protein or in fact BAP1 alone is not enough to lead to a significantly synthetic lethal effect.

Disappointingly, I was unable to demonstrate an augmented PARP inhibition effect *in vitro* when BAP1 mutated cell lines were subjected to ionising radiation. Although H2869 shBAP1 had lower cell viability at higher olaparib doses, ionising radiation had no additional impact. It's unclear why this was the case despite earlier showing that ionising radiation led to increased DNA damage and inhibited RAD51 a proxy for HR. Resistance to irradiation may well be a result of robust double strand break repair independent of BAP1. COSMIC confirms an ATM mutation in the cell line, however given the volatility of these cell lines its likely further genes are affected as they frequently divide and transfer into new flasks. In addition, cells which harbour inherent mutations or those designed to reduce gene expression of BAP1 do not compare with an absent full length *BAP1* gene. Truncated versions of BAP1 and/or low expression of the BAP1 protein may still be able to contribute to functional processes. CRISPR-Cas9 of BAP1 has been attempted several times over the years in our lab with limited success. Those with homozygous mutations in BAP1 lead to failure to thrive and cells with full BAP1 knockout die, making it very challenging to explore this in DNA repair pathways (116).

Use of other commonly used PARP inhibitors; niraparib and talazoparib showed increasing loss of cell viability at higher concentrations, although the latter agent was associated with a non-statistically significant outcome. An opportunity to run this assay again using higher concentrations and fresh/newly purchased compounds was limited by time.

Knockdown of both inactive catalytic domain and the BAP1 BRCA binding domain support sensitivity to PARP inhibition, the latter a finding yet to be reported in MPM (Fig 3.18 and 3.19). By interfering with BRCA binding, this crucial step in DNA repair is halted and then exploited using PARP inhibition. This implies the interaction between BAP1 and BRCA is

important in DNA damage response. A niche but robust target which if explored could open up therapeutic opportunities for patients with MPM. Exploiting the understanding that BAP1 mutated cell lines leads to sensitisation to TRAIL and these cell lines are also sensitive to PARP inhibition, combining both agents led to the best reduction in cell viability. These two targets with minimal side effects should be validated using apoptosis assays and explored *in vivo*.

In summary, several experiments have shown sensitivity to PARP inhibition when BAP1 is mutated, in particular when the BRCA binding domain is affected. Tumours with mutations in BAP1, in particular in the BRCA binding domain, may benefit from PARP inhibition and TRAIL.

RESULTS CHAPTER II

The host immune system enhances the effect of mesenchymal stromal cells expressing TRAIL

Hypothesis

MSCTRAIL is synergistic when combined with host immune cells outweighing the inherent immunoregulatory role of MSCs in MPM

4 RESULTS II THE HOST IMMUNE SYSTEM ENHANCES THE EFFECT OF MESENCHYMAL STROMAL CELLS EXPRESSING TRAIL

Patients with advanced mesothelioma are predominantly managed with palliative chemotherapy. Ongoing research highlights the importance of immune checkpoint blockade in MPM (86, 87). It is expected that patients will soon receive immune checkpoint inhibition as standard of care in this disease.

Pre-clinical evidence shows that MPM responds well to TRAIL, in particular when cancer cells harbour mutations in the BAP1 gene (144). Clinical use of recombinant TRAIL is limited given it has a half-life of 30-60 minutes *in vivo* (301). Delivering TRAIL using a vector such as MSCs has been explored with success (MSCTRAIL). The half-life of MSCTRAIL is far longer and combined with its ability to home to tumours and activate apoptosis, makes this a very attractive option in MPM.

A balance emerges between MSCTRAIL directed apoptosis and its subsequent stimulation of an immune response and downregulation of the immune system via the inherent phenotypic behaviour of MSCs (228). This alliance between MSC mediated TRAIL expression and immune stimulation is hoped to outweigh the inhibition of the immune response leading to a synergistic relationship, supporting the hypothesis.

4.1 Development of MSCTRAIL

Development of virus

A full-length TRAIL expressing lentiviral vector (pCCL-CMV-flT) was previously developed in our lab. In short, the lentiviral plasmid pCCL-c-Fes-GFP was procured. The c-Fes promoter was deleted by enzymatic digestion and replaced by a CMV promoter to allow for constitutive activation of TRAIL. The GFP sequence was replaced by full-length TRAIL leading to pCCL-CMV-flT.

Viral production is key given the incapacity of virus to replicate independently. This is done with the help of 293T cells. Lentiviral vectors first require packing into liposomes prior to delivery into cells. 293T cells were initially cultured for 24 hours. A transfection reagent was incubated with the TRAIL construct and packaging plasmids (see methods). Complete culture media was replaced with serum free media, as this improves transfection efficiency (formation of DNA with cationic liposomes) and the transfection mixture carefully added and incubated with the cells. Media was changed after 4 hours. The virus rich media was collected thereafter on day 1 and 2, filtered and frozen in to small aliquots for repeated use to avoid continuous freeze thaw cycles.

Fresh cultured 293T cells were seeded in a 12 well plate at 50,000 cells per well and cultured for 24 hours. On day 2, serial doses of virus plus polybrene (neutralises the cell membrane charge allowing for transfection) were incubated with the cells (1, 0.5, 0.25, 0.125, 0.06µl). Following 48 hours of incubation, cells were collected via trypsinisation, centrifugation (300G for 5 minutes), counted, incubated with a PE conjugated anti TRAIL antibody and subjected to flow cytometry for TRAIL expression. Percentage of TRAIL expressing cells

was measured for each viral titration. The volume of virus was calculated as per below. Assistance was offered by Dr Krishna Kolluri.

$$\text{Volume of virus (IU/ml)} = \frac{\text{no. of cells x fraction of cells transduced}}{\text{volume of virus (ml)}}$$

TRAIL expression depending on viral volume

	Cell count	Virus (μl)	TRAIL expression (%)	Titre IU/μl
Day 1	100,000	0.06	18.3	305000
	100,000	0.125	27.5	220000
	100,000	0.25	53.3	213200
	100,000	0.5	66.8	133600
	100,000	1	84.3	84300

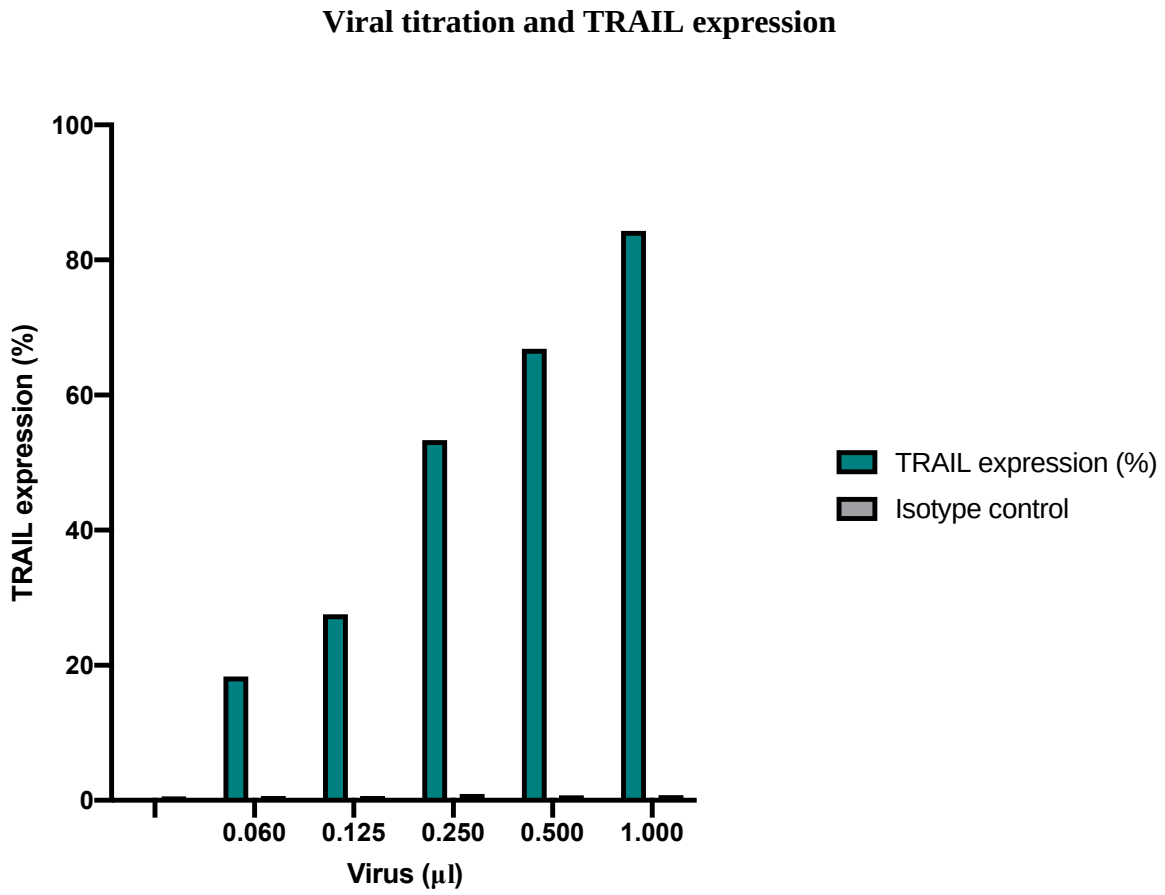

Figure 4. 1 – TRAIL expression and the associated viral titration

Multiplicity of infection (MOI) was used as a benchmark for transfection. This is a measure of the number of viral particles entering a cell. To achieve 86.5% infection (MOI 2) 84,300 IU/µl is needed.

Transduction of MSCs and confirmation of expression

MSCs were initially cultured in complete αMEM media, and transduced with viral particles aiming for an MOI of 2. Virus and polybrene were added to complete αMEM media which was exchanged at 4 hours. Similar to the above, cells were collected via trypsinisation, counted, washed, stained with a PE conjugated anti TRAIL antibody and subjected to flow cytometry to assess TRAIL expression. Successful transduction of MSCTRAIL was achieved up to 99%.

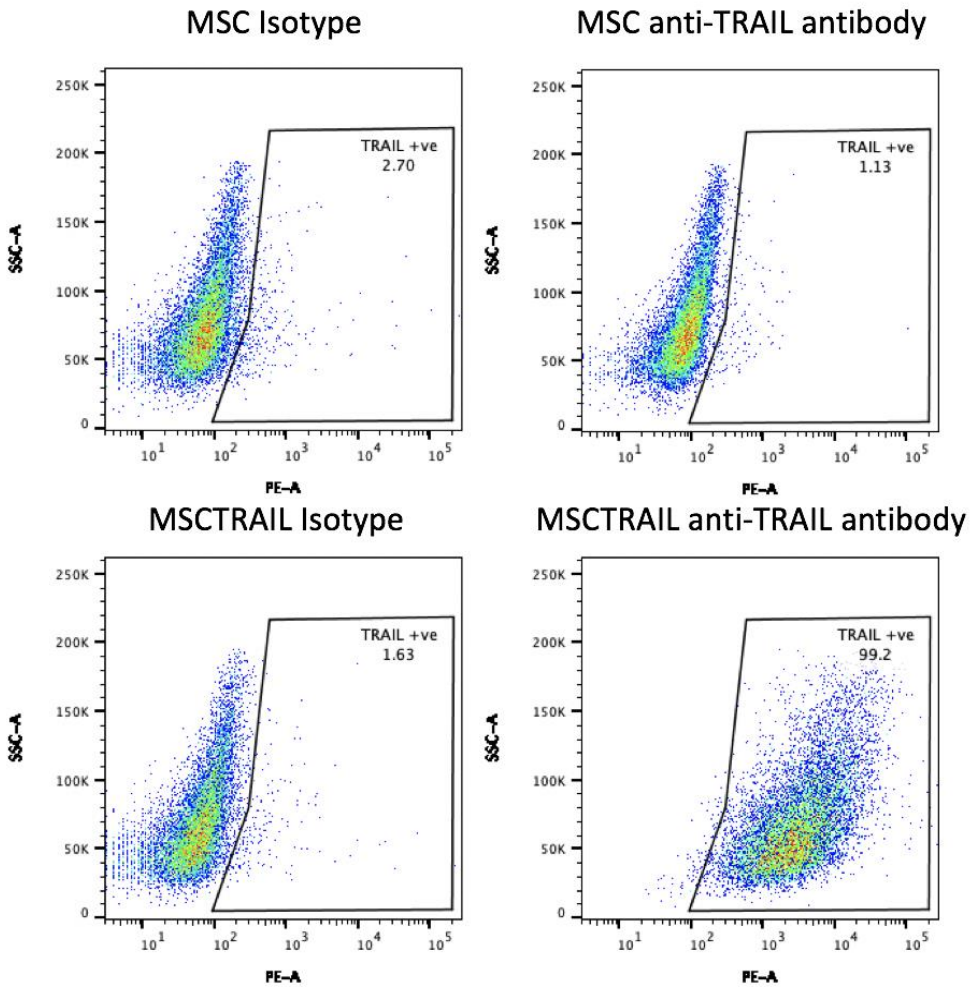

Figure 4. 2 – TRAIL expression following viral transduction of MSCs

Untransduced MSCs (negative control) and transduced MSCs (MSCTRAIL) were assessed for TRAIL expression using a PE conjugated antibody against TRAIL.

4.2 Identification of synergy between MSCTRAIL and immune cells

To begin, demonstrating a synergistic relationship between MSCTRAIL and volunteer (allogeneic) peripheral blood mononuclear cells (PBMCs) relied upon complex co-culture experiments measuring cell viability and apoptosis. Monoclonal antibodies targeting the PD-L1/PD-1 axis was studied guided by clinical application of PD-L1 expression. These experiments are detailed below.

Characterisation of PD-L1 expression

Characterisation of cell types planned for use in co-culture experiments were undertaken. Anti PD-1 therapy is contingent on PD-L1 expression on tumour cells. Data shows that cells with higher expression of PD-L1 i.e. a greater immune-inhibitory signal, experience a greater response following anti PD-1 therapy (74).

MSCs and MSCTRAIL express high levels of PD-L1

MSCs and MSCTRAIL cultured cells were collected via trypsinisation and stained with APC conjugated and isotype control antibodies targeting PD-L1 (latter = negative control). Cells underwent flow cytometry to detect PD-L1 expression. Both MSCs and MSCTRAIL expressed high levels of PD-L1; 99.6 and 97.2% respectively.

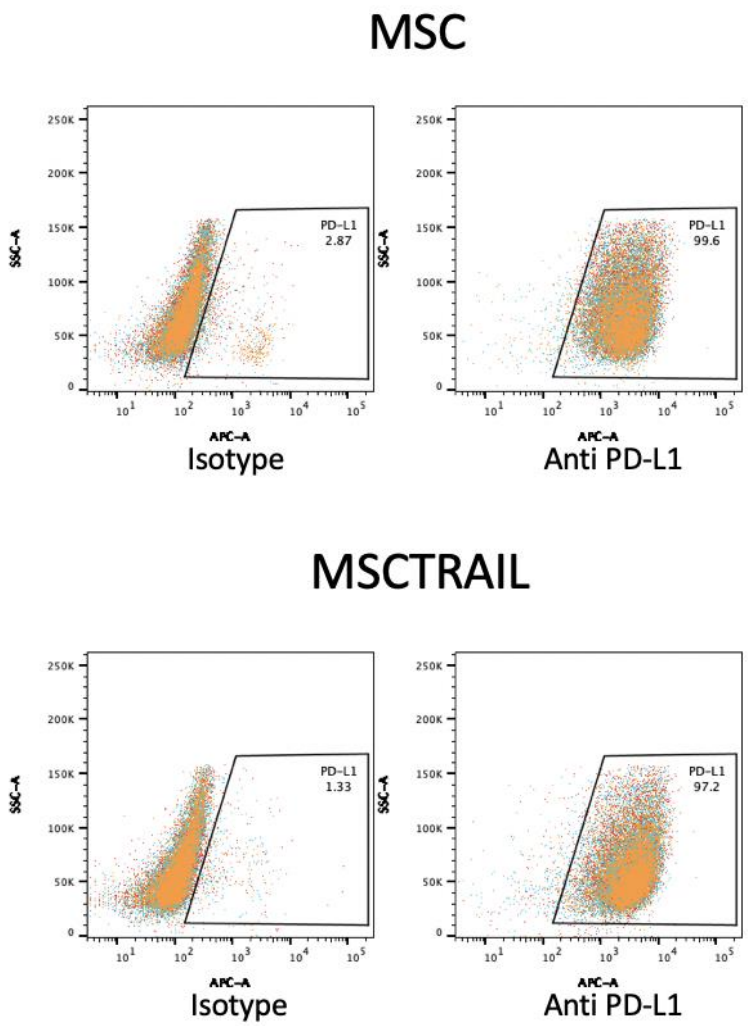

Figure 4. 3 – MSC and MSCTRAIL expression of PD-L1

Cells were stained with an APC conjugated anti PD-L1 antibody and an isotype control.

A549 does not express PD-L1 and MDA-MB-231 expresses PD-L1

A549 and MDA-MB-231 were reference cell lines used for the preliminary work. Characterisation of these cells was performed similar to the above. Cells were cultured, collected via trypsinisation and stained with the same APC conjugated antibody and isotype control antibody targeting PD-L1 (negative control). Cells underwent flow cytometry to detect PD-L1 expression. A549 expressed low levels of PD-L1 (4.65%) and MDA-MB-231 expressed high levels (98.3%). Assistance was offered by Dr Krishna Kolluri.

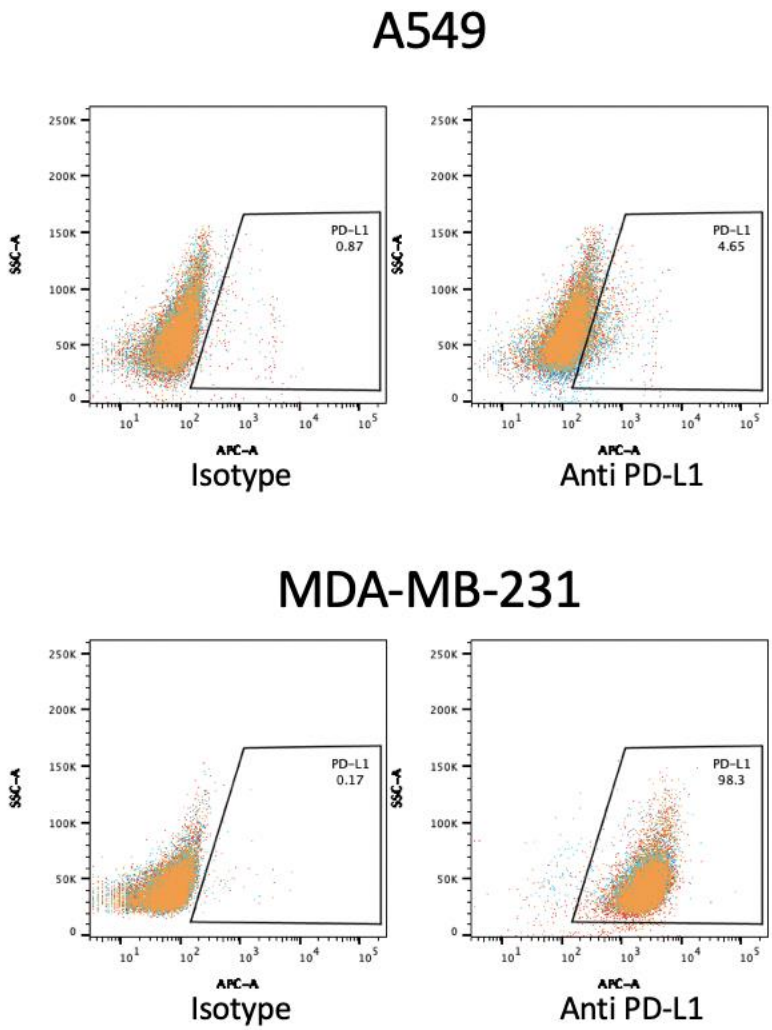

Figure 4. 4 - Cancer cell expression of PD-L1

A549 and MDA-MB-231 cells stained with an anti PD-L1 antibody conjugated to APC and an isotype control.

MSCs and volunteer PBMCs survive in co-culture experiments

Cell viability of MSCs in the presence of volunteer PBMCs

Cell viability can be measured in several ways. Cells labelled to express luciferase can be used in co-culture studies enabling the measurement of bioluminescence, a proxy for cell viability. MSCs (GFP), A549 (mStrawberry) and MDA-MB-231 (mStrawberry) previously transduced in our lab to express luciferase were used in the following experiments.

In the first instance it was crucial to identify whether MSCs and immune cells could survive together *in vitro*. These following studies confirm each group thrives and avoids cell death from the other.

Luciferase labelled MSCs (2500 per well) were initially seeded in a 96 well plate in triplicate. Following 24 hours of incubation, 200,000 volunteer PBMCs were added. Bioluminescence was recorded at days 1, 2, 3, 5 and 7. Uncharacterised volunteer PBMCs were isolated from healthy volunteers and the same sample was used for each assay with no mixing between assays.

MSCs and PBMCs remained viable thriving under these conditions, more so in the former, a product of MSCTRAIL mediated targeted apoptosis of PBMCs. On balance, PBMCs had little effect on MSCs / MSCTRAIL.

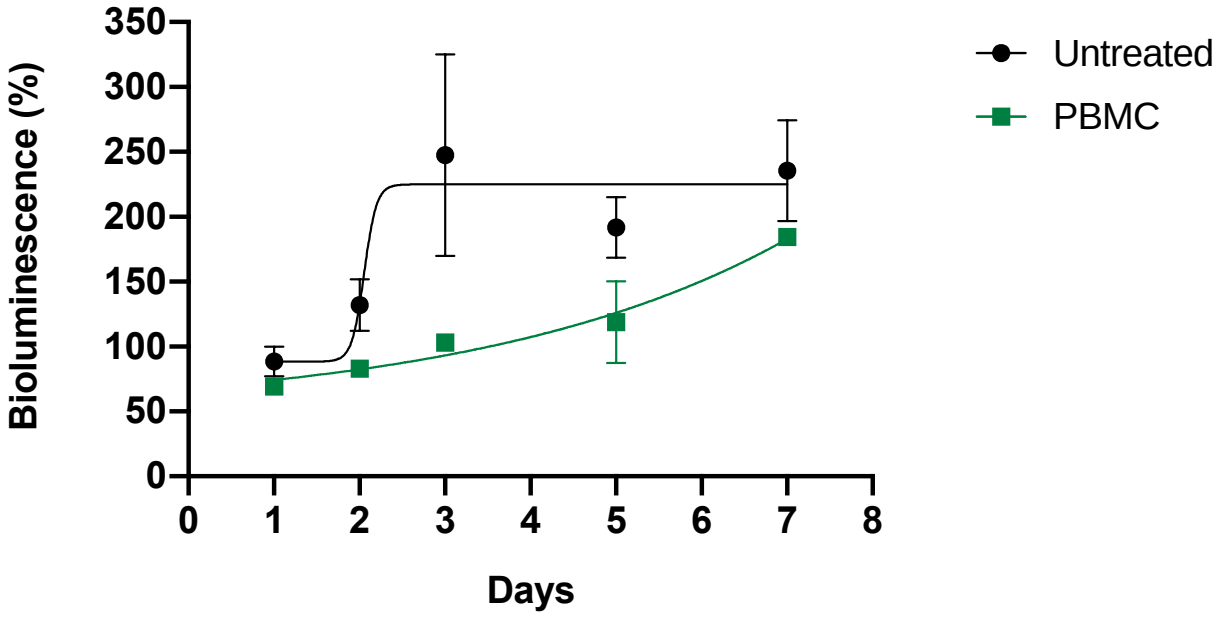

Figure 4. 5 - MSC viability over 7 days

MSCs co-cultured with PBMCs over 7 days. Untreated MSCs and MSCs cultured with allogeneic PBMCs thrived in vitro. Two way ANOVA comparing both untreated MSCs and combined with PBMCs p=0.0270

MSC viability was further assessed when cancer cells were co-cultured with luciferase labelled MSCs. 3000 cells per well of A549 were cultured in triplicate in a 96 well plate. 24 hours following this MSCs (2500 / well) and volunteer PBMCs (200,000 per well) were added. Bioluminescence was recorded on days 1, 2, 3, 5 and 7. Cell viability reduced as the week progressed supporting the approach to assess synergy in the first few days to avoid MSCs succumbing to *in vitro* cell death and obscuring the overall outcome. Cell viability increased when MSCs were cultured with A549, however division was stunted when cultured

with PBMCs. Some loss in cell viability was noted towards the end of the week in the PBMC co-culture arm.

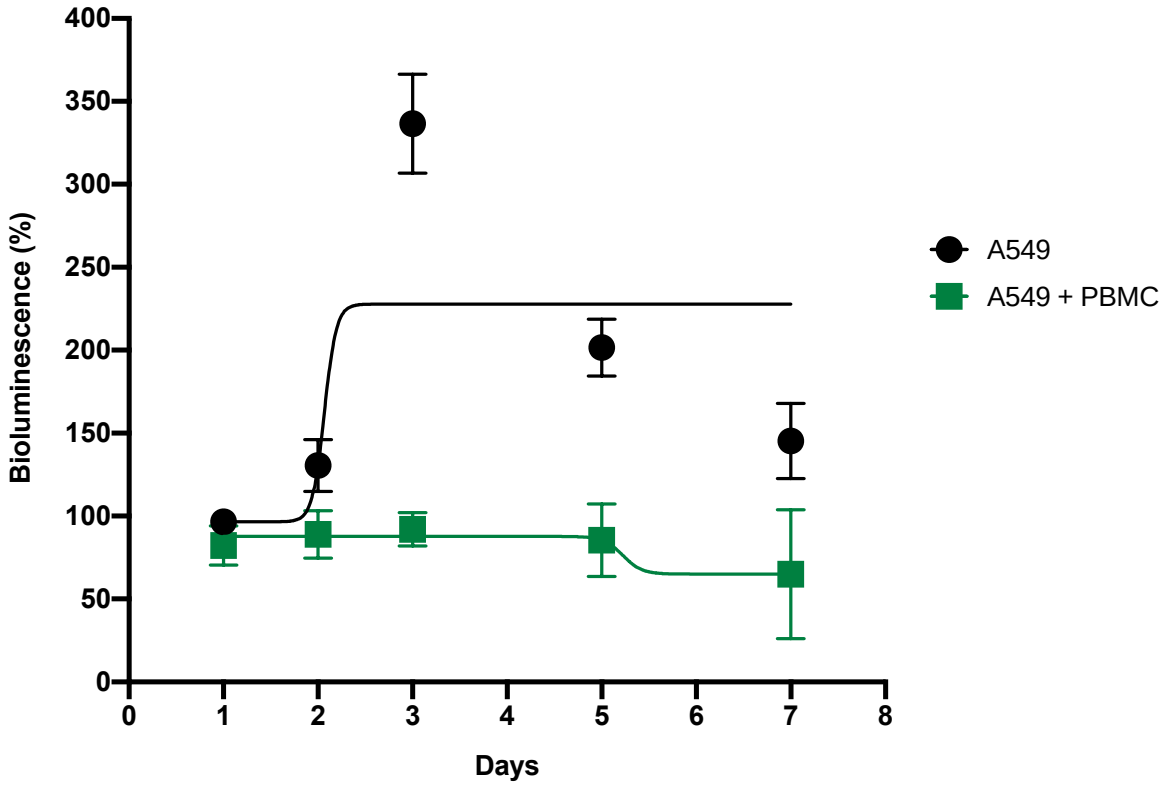

Figure 4. 6 - MSC viability over 7 days when co-cultured with cancer cells

Co-culture of MSCs, PBMCs and the cancer cell line A549 over 7 days. Bioluminescence was recorded on a microplate reader at intervals throughout the week. Two way ANOVA comparing interaction between MSC and A549 and in combination with PBMCs $p<0.0001$

MSCTRAIL and volunteer PBMCs

To assess the impact of MSCTRAIL on PBMCs, a cell death assay was performed. MSCTRAIL was initially labelled with DiI prior to co-culture for 24 hours (5000 per well) with increasing doses of PBMCs in a ratio of 1:2, 1:4, 1:8, 1:30, 1:40 and 1:50 in a 96 well plate. At 48 hours, cells were collected via trypsinisation into dedicated flow cytometry tubes, stained with DAPI and Annexin V antibody (cell death markers), and subjected to flow cytometry to measure apoptosis. Cell death increased by only 6% from untreated MSCTRAIL to 1:50.

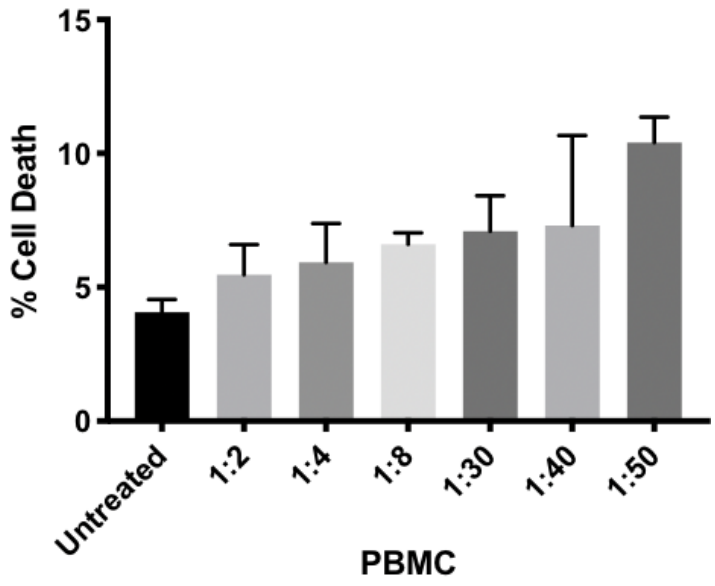

Figure 4. 7 – Cell death of MSCTRAIL with an increasing ratio of PBMCs

DiI labelled MSCTRAIL (5000 / well) co-cultured with an increasing ratio of PBMCs over 48 hours. Cells were subjected to flow cytometry. Cell death was measured using DAPI and Annexin V. Paired t test comparing untreated with 1:50 p=0.0005.

The effect of MSCTRAIL on PBMCs was assessed using a similar cell death assay. Apoptosis of PBMCs was measured at 48 hours. PBMCs were labelled with DiI prior to co-culture (100,000 per well) with increasing doses of MSCTRAIL in a ratio of 1:2, 1:4, 1:8, 1:30, 1:40 and 1:50 in a 96 well plate. At 48 hours, cells were collected via trypsinisation into dedicated flow cytometry tubes, stained with DAPI and Annexin V antibody and subjected to flow cytometry to measure cell death. Cell death increased by 10% from untreated PBMCs to 1:50.

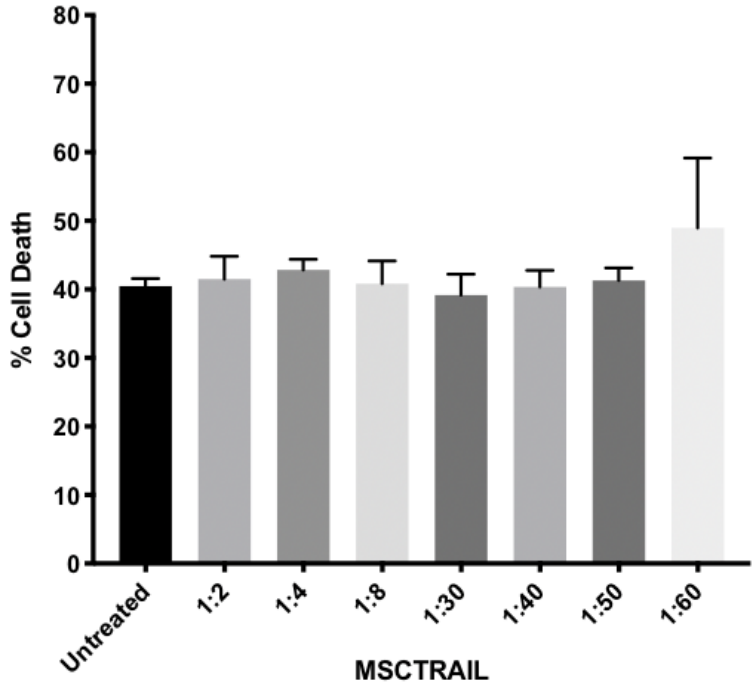

Figure 4. 8 - Cell death of PBMCs with an increasing ratio of MSCTRAIL

DiI labelled PBMCs (100,000 cells / well) co-cultured with an increasing ratio of MSCTRAIL over 48 hours. Cells were subjected to flow cytometry. Cell death was measured using DAPI and Annexin V. Paired t test comparing untreated with 1:60 p=0.2243

The MSC cell count between the luciferase and cell death assays are explained by the length of the assays. To allow for growth within the well over a longer period of time, 2500 cells were seeded as opposed to 5000 per well in the shorter 48-hour cell death assay which allowed for higher numbers to be assessed without leading to early confluency and clouding of results.

Both cell viability and cell death assays demonstrate acceptable losses, enough to proceed to further study the synergistic relationship between MSCTRAIL and PBMCs.

A synergistic anti-cancer relationship exists between MSCTRAIL and volunteer / allogeneic immune cells

In both assays it was shown that both MSCTRAIL and PBMCs experienced some loss however this was deemed acceptable to take the experiments forward. Luciferase assays were performed at 5 and 7 days to assess cell viability.

Assessment at 5 days and over is too late to see an effect

PC9, a non-small cell lung cancer cell line was used to determine whether 5 or 7 days were best. PC9 was transduced to express luciferase. Cells were seeded at 3000 per well in a 96 well plate in triplicate. Following 24 hours of incubation cells were co-cultured with MSCTRAIL and PBMCs. Bioluminescence was measured following a further 5 and 7 days of incubation. Bioluminescence was undetectable when treated with MSCTRAIL and PBMCs suggesting much of the activity happens earlier than 5 days. To explore this further, subsequent experiments were performed over a 7 day period.

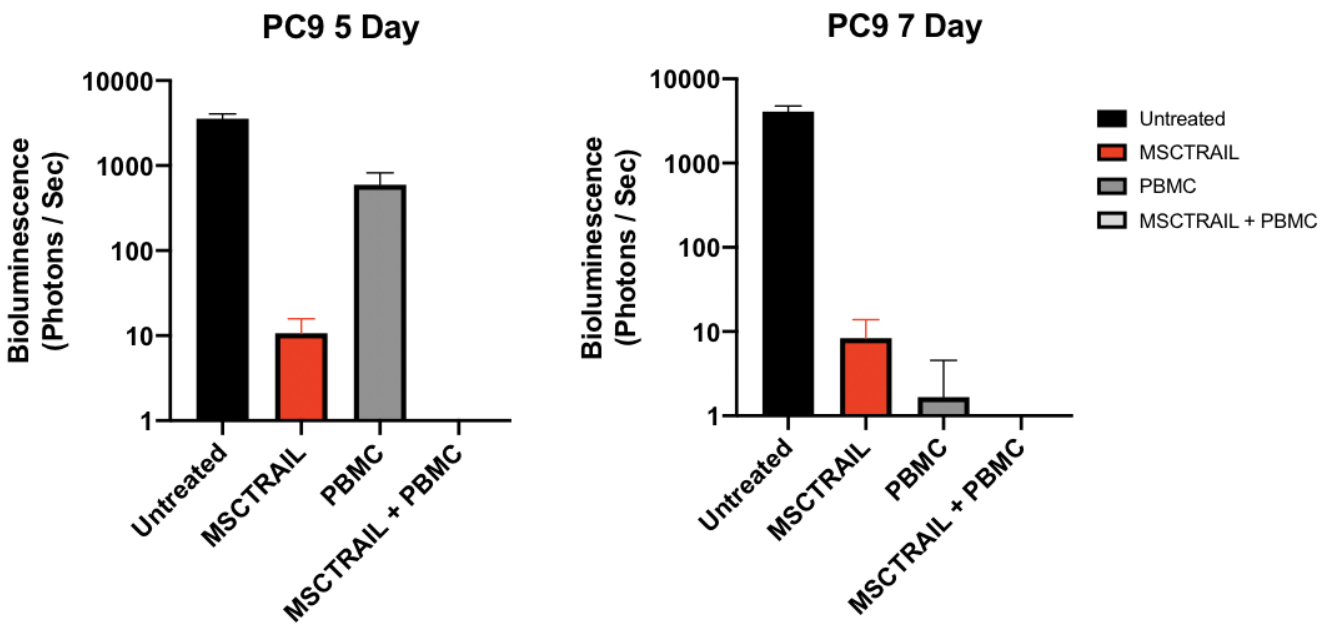

Figure 4. 9 – 5 and 7-day luciferase cell viability assay of PC9 cell line

PC9 co-cultured with MSCTRAIL and PBMCs. Bioluminescence was measured at 5 and 7 days. Tukey's multiple comparisons: 5 day assay - untreated v MSCTRAIL adjusted p value 0.0172, untreated v PBMC adjusted p value 0.0215 and untreated v MSCTRAIL + PBMC adjusted p value 0.0172. 7 day assay – untreated v MSCTRAIL adjusted p value 0.0239, untreated v PBMC adjusted p value 0.0235 and untreated v MSCTRAIL + PBMC adjusted p value 0.0235.

A synergistic relationship exists between MSCTRAIL and PBMCs in non-mesothelioma cell lines

A549 and MDA-MB-231 luciferase labelled cell lines were used. A549, a regularly used reference cell line in our lab, is known to be TRAIL resistant, a property which suits an assay like this as overcoming this resistance provides value to the synergistic signal.

A549 was cultured at 3000 cells per well of a 96 well plate in triplicate. Following 24 hours of incubation cells were co-cultured with MSCs (5000/well), MSCTRAIL (5000/well) and PBMCs (200,000/well). Bioluminescence was measured at 1, 2, 3, 5 and 7 days. A549 cultured alone, with MSCs or MSCTRAIL demonstrated increasing cell viability. When cultured with PBMCs cell viability reduced considerably compared to the 'mono-arms' (demonstrated as a slight reduction), however when co-cultured with MSCTRAIL and PBMCs a huge reduction is seen on the logarithmic scale below. This impact was augmented even further when 5μM of cisplatin was added, the backbone chemotherapy treatment for MPM.

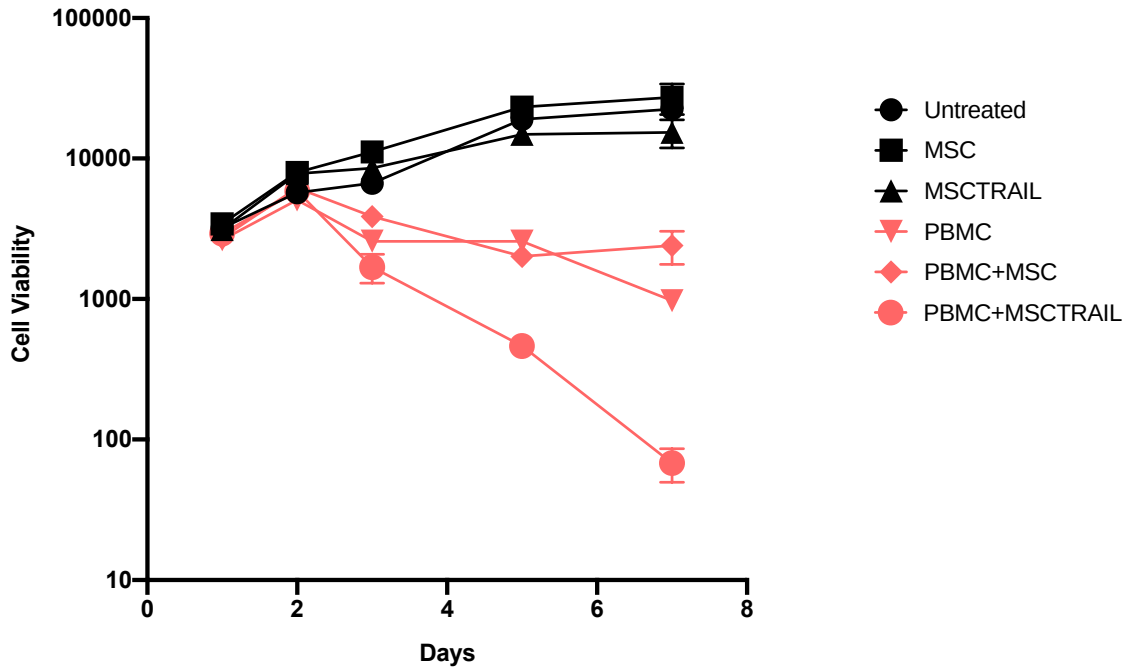

Figure 4. 10 – A549 co-cultured with MSC, MSCTRAIL and PBMCs

A549 co-cultured with MSC, MSCTRAIL and PBMCs. Bioluminescence was recorded at 1,2,3,5 and 7 days. Tukey's multiple comparison: untreated v MSCTRAIL adjusted p=0.1609, untreated v MSC adjusted p<0.0001, untreated v PBMC adjusted p <0.0001, untreated v MSC+PBMC adjusted p<0.0001 and untreated v MSCTRAIL+PBMC p<0.0001.

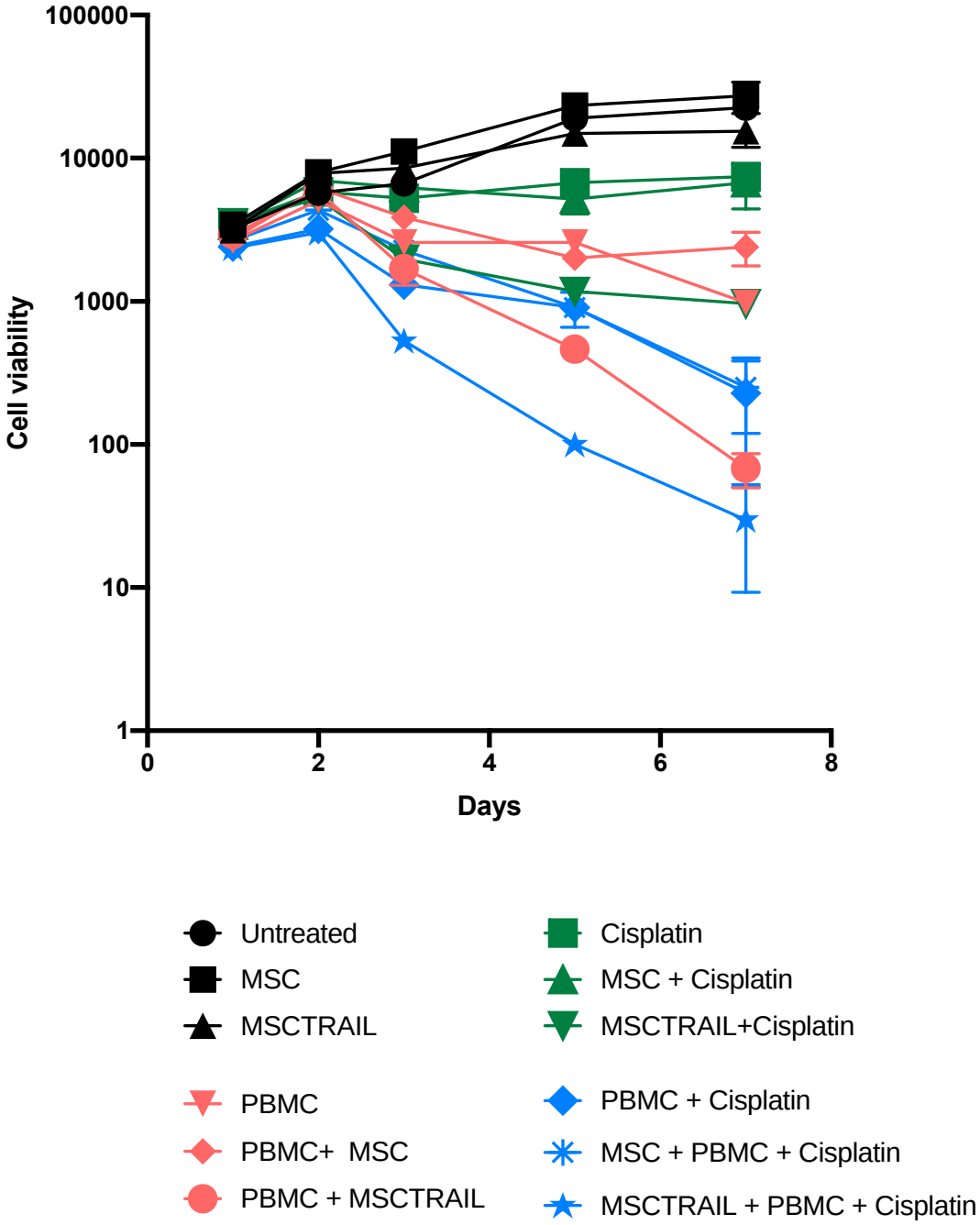

Figure 4. 11 - A549 cell line co-cultured with MSC, MSCTRAIL, PBMCs and cisplatin

A549 co-cultured with MSC, MSCTRAIL, PBMCs and cisplatin. Bioluminescence was recorded at 1,2,3,5 and 7 days. Tukey's multiple comparison: untreated v PBMC adjusted p <0.0001, untreated v MSCTRAIL adjusted p=0.0610, untreated v MSCTRAIL + PBMC adjusted p <0.0001 and untreated v MSCTRAIL + PBMC + cisplatin adjusted p <0.0001.

This was reproducible using the TRAIL sensitive MDA-MB-231 cell line. MDA-MB-231 was cultured at 3000 cells per well in a 96 well plate in triplicate. Following 24 hours of incubation cells were co-cultured with MSCs (5000/well), MSCTRAIL (5000/well) and PBMCs (200,000/well). Bioluminescence was measured at 1, 2, 3, 5 and 7 days. MDA-MB-231 cultured alone, with MSCs or MSCTRAIL demonstrated increasing cell viability. When cultured with PBMCs cell viability reduced, however when co-cultured with MSCTRAIL and PBMCs a huge reduction is again seen on the logarithmic scale. This impact was augmented even further when 5μM of cisplatin was added, the backbone chemotherapy treatment for MPM, although cell viability ended at the same point without cisplatin at 7 days. Assistance was offered by Dr Krishna Kolluri.

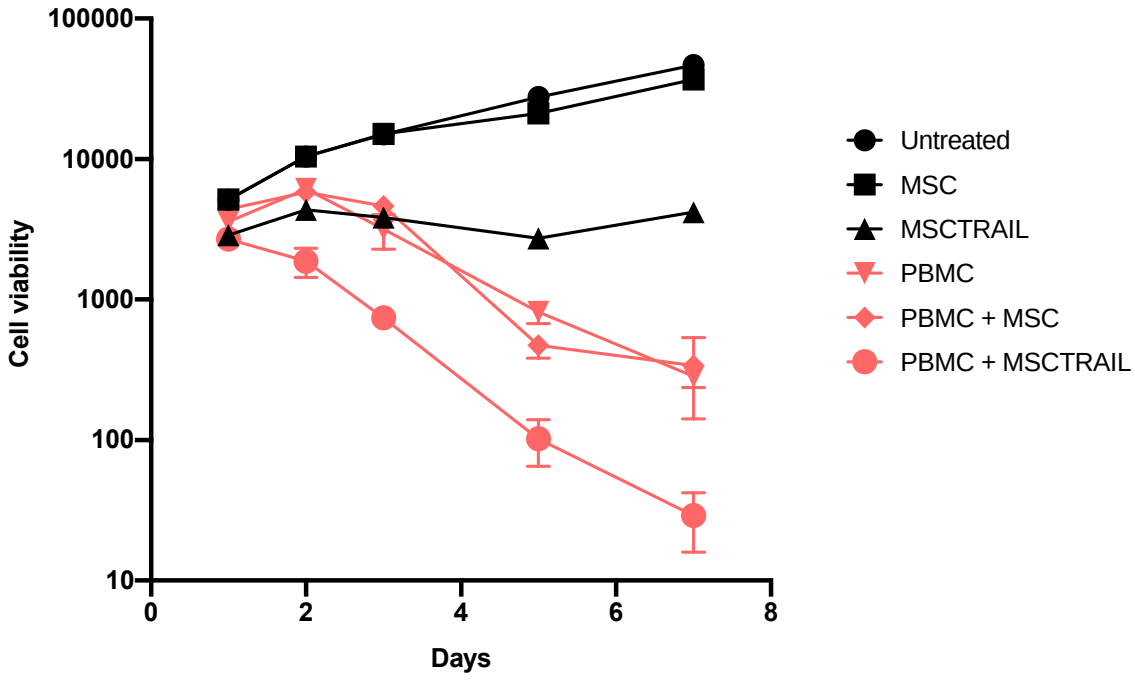

Figure 4. 12 - MDA-MB-231 cell line co-cultured with MSC, MSCTRAIL and PBMCs

MDA-MB-231 co-cultured with MSC, MSCTRAIL and PBMCs. Bioluminescence was recorded at 1,2,3,5 and 7 days. Tukey's multiple comparison: untreated v MSCTRAIL adjusted p<0.0001, untreated v MSC adjusted p<0.0001, untreated v PBMC adjusted p <0.0001, untreated v MSC+PBMC adjusted p<0.0001 and untreated v MSCTRAIL+PBMC p<0.0001.

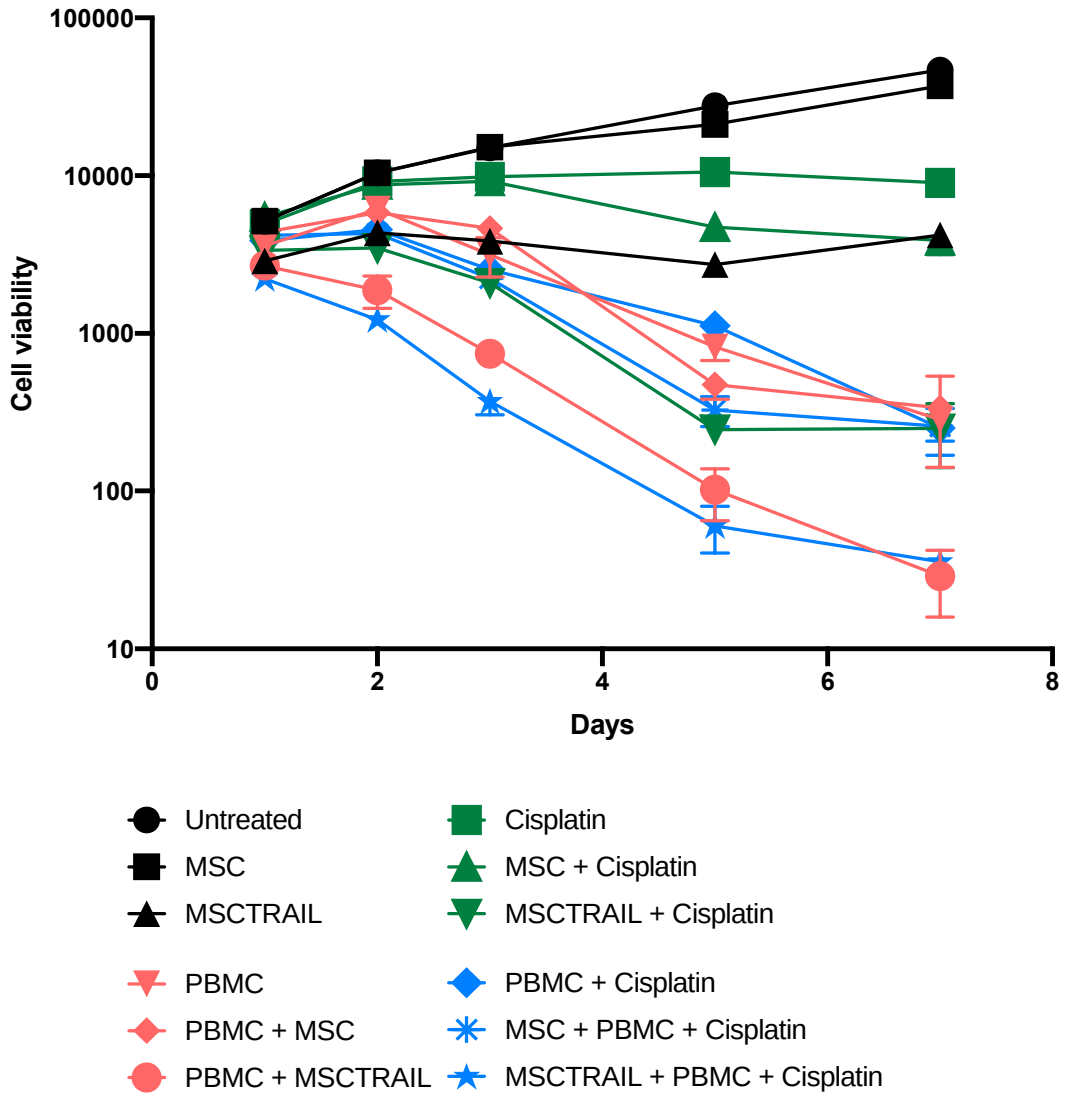

Figure 4. 13 – MDA-MB-231 co-cultured with MSC, MSCTRAIL, PBMCs and cisplatin

MDA-MB-231 co-cultured with MSC, MSCTRAIL, PBMCs and cisplatin. Bioluminescence was recorded at 1,2,3,5 and 7 days. Tukey's multiple comparison: untreated v PBMC adjusted p <0.0001, untreated v MSCTRAIL adjusted p<0.0001, untreated v MSCTRAIL + PBMC adjusted p <0.0001 and untreated v MSCTRAIL + PBMC + cisplatin adjusted p <0.0001.

The scale of the fall in cell viability was particularly impressive, however an allogeneic effect cannot be excluded. A non-self immune response, as a result of the use of volunteer PBMCs, towards these cancer cells is the most important criticism to this assay. Developing a syngeneic model would require a concerted effort but would address this issue.

MSCTRAIL and volunteer PBMCs demonstrate synergy in MPM

This allogeneic synergistic relationship extended into MPM demonstrated in a panel of cell lines found to be resistant to TRAIL.

Like the previous luciferase assays, MPM cell lines transduced to express luciferase were seeded in a 96 well plate at 3000 cells / well. Following 24 hours of incubation, cells were treated with MSCs (5000/well), MSCTRAIL (5000/well), volunteer PBMCs (200,000/well) and cisplatin 5μM. Bioluminescence wad recorded over 3 days (days 1,2,3), a measure of cell viability. Findings were similar to the non MPM cell lines. Cell viability increased in the untreated / MSC / MSCTRAIL alone arms, declined when MSCTRAIL and allogeneic PBMCs were co-cultured and declined even further when cisplatin was added.

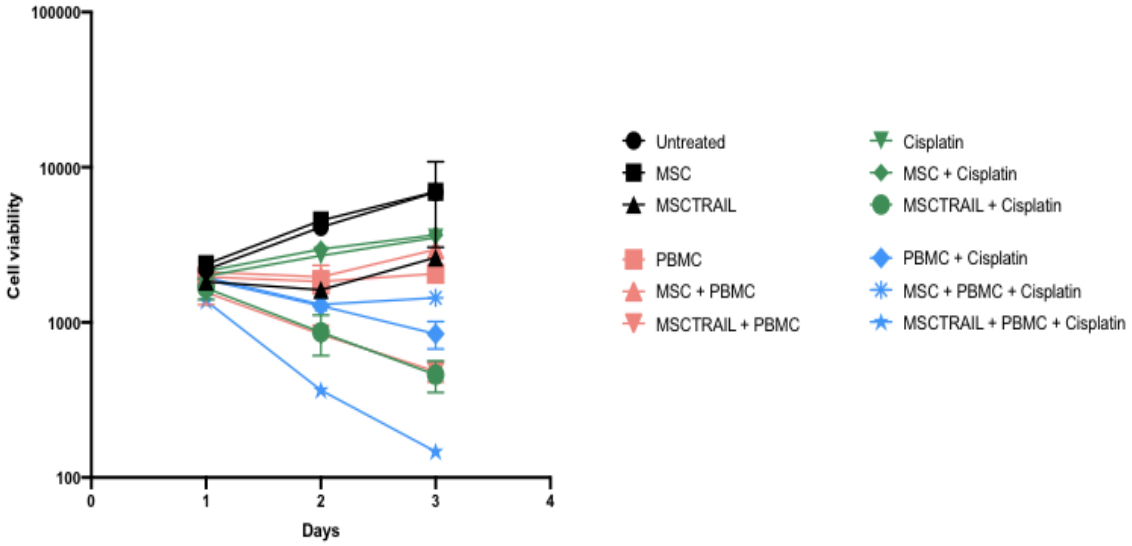

Figure 4. 14 – H513 co-cultured with MSC, MSCTRAIL, PBMCs and cisplatin

*Luciferase labelled H513 co-cultured with MSC, MSCTRAIL, PBMCs and cisplatin. Bioluminescence was recorded at 1, 2 and 3 days. Tukey's multiple comparison: untreated v PBMC adjusted p <0.0001, untreated v MSCTRAIL adjusted p<0.0001, untreated v MSCTRAIL + PBMC adjusted p <0.0001 and untreated v MSCTRAIL + PBMC + cisplatin adjusted p <0.0001.** this cell line has since been shown to have adeno-squamous features*

The MPM cell line H226 was co-cultured in the same way under the same conditions. The relationship was reproducible. Cell viability increased in the untreated / MSC / MSCTRAIL alone arms, declined when MSCTRAIL and allogeneic PBMCs were co-cultured and declined even further when cisplatin was added.

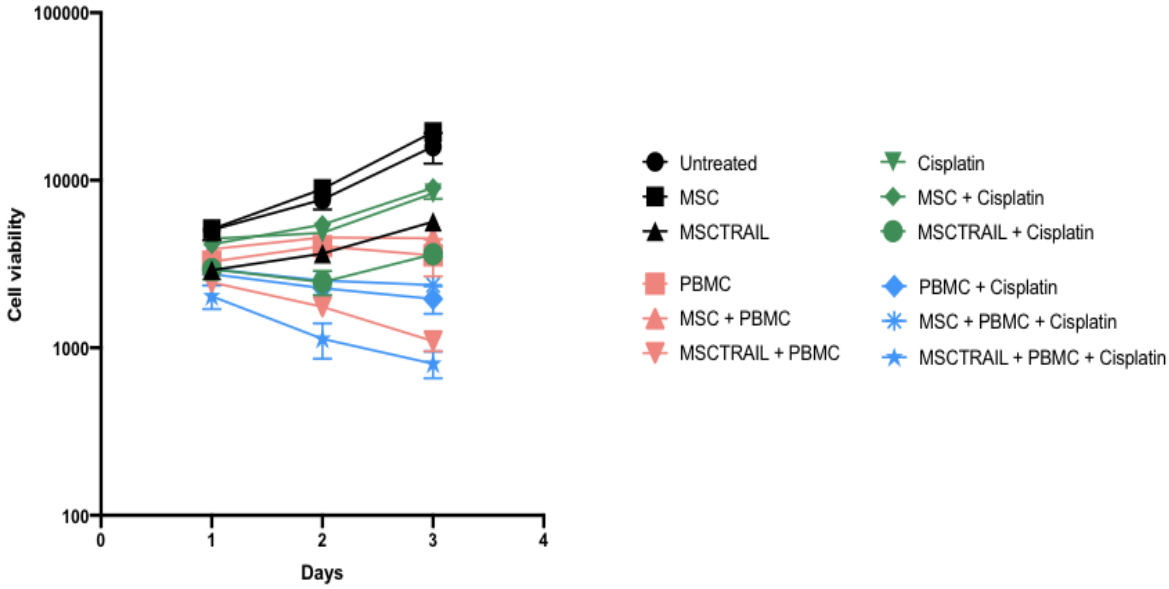

Figure 4. 15 – H226 co-cultured with MSC, MSCTRAIL, PBMCs and cisplatin

Luciferase labelled H226 co-cultured with MSC, MSCTRAIL, PBMCs and cisplatin. Bioluminescence was recorded at 1, 2 and 3 days. Tukey's multiple comparison: untreated v PBMC adjusted p <0.0001, untreated v MSCTRAIL adjusted p<0.0001, untreated v MSCTRAIL + PBMC adjusted p <0.0001 and untreated v MSCTRAIL + PBMC + cisplatin adjusted p <0.0001.

MPP89 was co-cultured in the same way under the same conditions. The relationship again was shown to be reproducible. Cell viability increased in the untreated / MSC / MSCTRAIL alone arms, declined when MSCTRAIL and allogeneic PBMCs were co-cultured and declined even further when cisplatin was added.

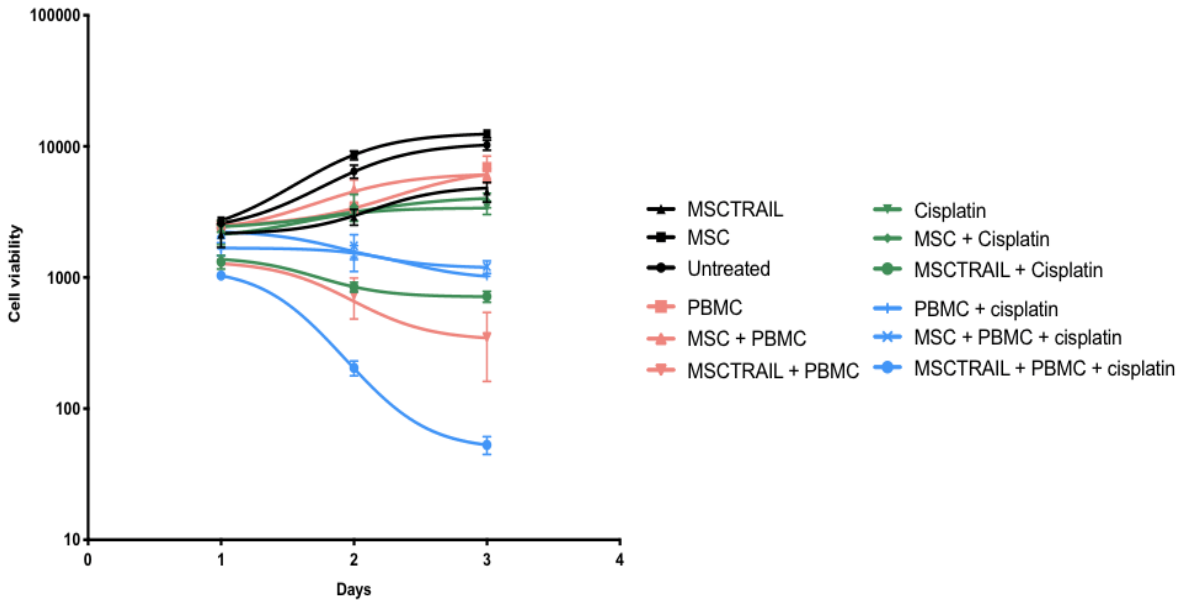

Figure 4. 16 – MPP89 co-cultured with MSC, MSCTRAIL, PBMCs and cisplatin

Luciferase labelled MPP89 co-cultured with MSC, MSCTRAIL, PBMCs and cisplatin. Bioluminescence was recorded at 1, 2 and 3 days. Tukey's multiple comparison: untreated v PBMC adjusted p <0.0001, untreated v MSCTRAIL adjusted p<0.0001, untreated v MSCTRAIL + PBMC adjusted p <0.0001 and untreated v MSCTRAIL + PBMC + cisplatin adjusted p <0.0001.

Unsuccessful but ongoing apoptosis assay of MPM cell lines

Mesothelioma cell lines express extracellular MSC markers which is a great challenge when subjecting these cells to assays necessitating differentiation between the two groups of cells. As well as clear differentiation markers, apoptosis assays also depend on the reliable labelling of cells of interest. DiI has routinely been used throughout this thesis, however other equally credible stains are used. This is particularly pertinent where cell types are a challenge to label e.g. DiI staining has leaked on several occasions compromising the end result. This remains a work in progress and was significantly limited by COVID19 and the closure of the lab.

I present the some of the initial pre COVID19 work up prior to further optimisation at a later stage. To understand in greater detail the shared MSC characteristics between the two groups, cells were subjected to flow cytometry and stained with the MSC markers CD73, CD90 and CD105 using conjugated antibodies. Cells were cultured, harvested via trypsinisation, centrifuged to pellet formation, washed, stained with the appropriate conjugated antibodies and assessed.

A screening process therefore ensued of 8 TRAIL resistant mesothelioma cell lines absent for one of the three MSC surface markers; CD73, CD90 and CD105. This would allow for clear distinction between mesothelioma cells and MSCs at the point of analysis for flow cytometry studies. The use of TRAIL resistant cells would be more likely to demonstrate a synergistic signal then if all cells succumbed to MSCTRAIL from the outset.

Cell line	PD-L1 (%) APC	CD73 PE CY7	CD90	CD105
MPP89	+	+	-	+
H226	+	+	-	+
H513	+	+	-	+
H2795	+	+	+	+
H2373	-	+	+	+
H2869	differential expression	+	differential expression	+
H2818	-	+	differential expression	+
H2591	-	+	+	+

Figure 4. 17 - Table of MPM cell lines analysed

List of MPM cell lines analysed for PD-L1, and MSC markers (CD73, CD90, CD105). MPP89, H226 and H513 were found to be CD90 negative.

Antibody	Fluorochrome
CD105	APC
CD90	PE/CY7
CD73	PE-Vio-770

Figure 4. 18 - List of conjugated antibodies used during the screening phase

H513 flow cytometry screen

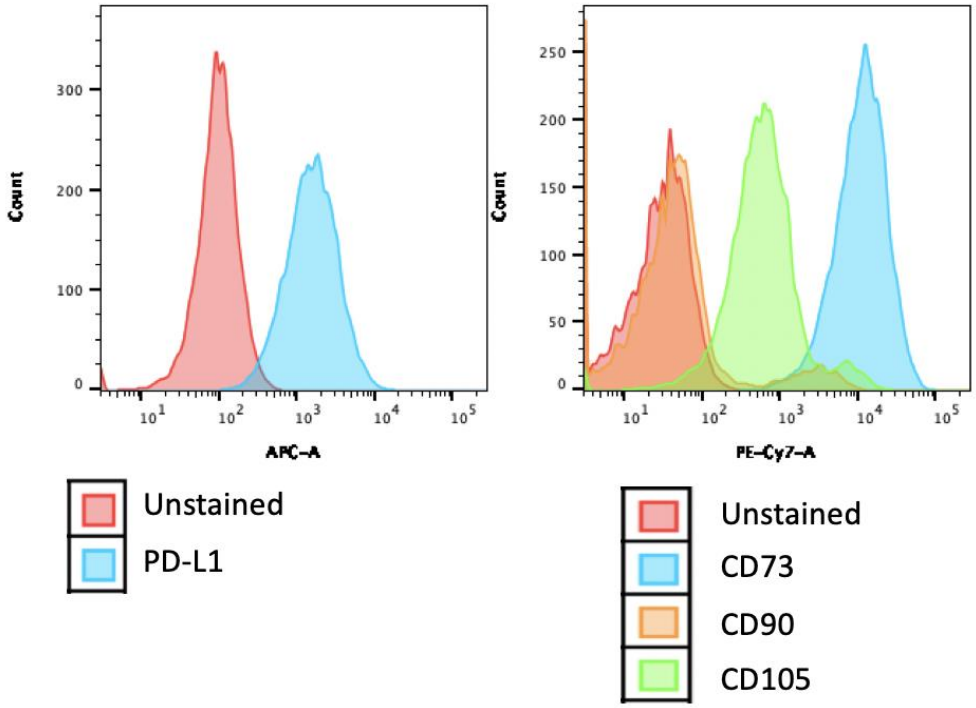

H226 flow cytometry screen

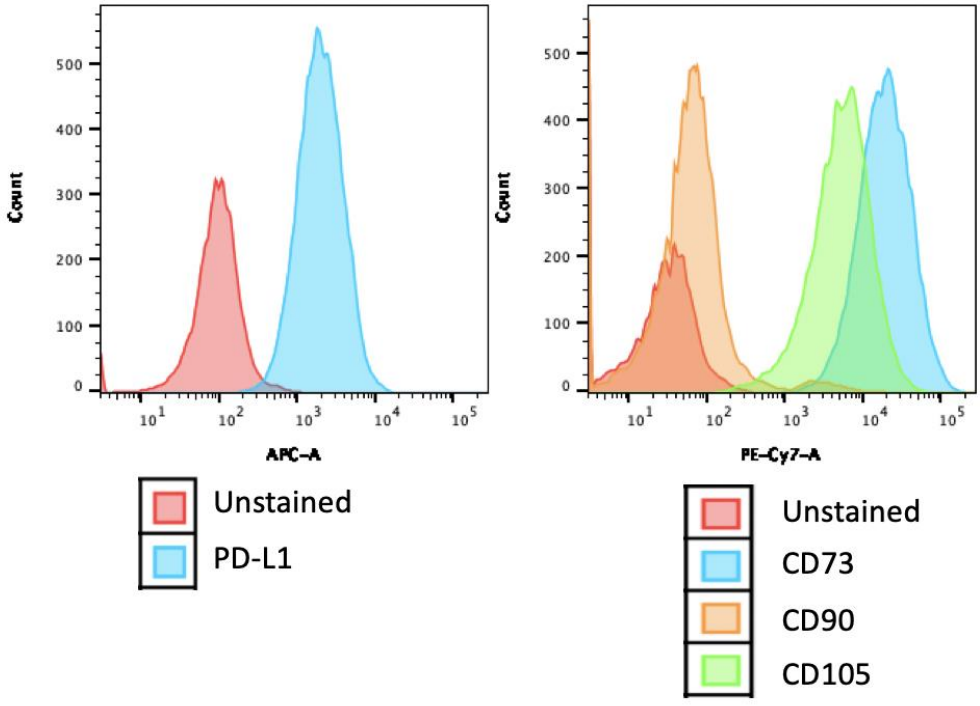

MPP89 flow cytometry screen

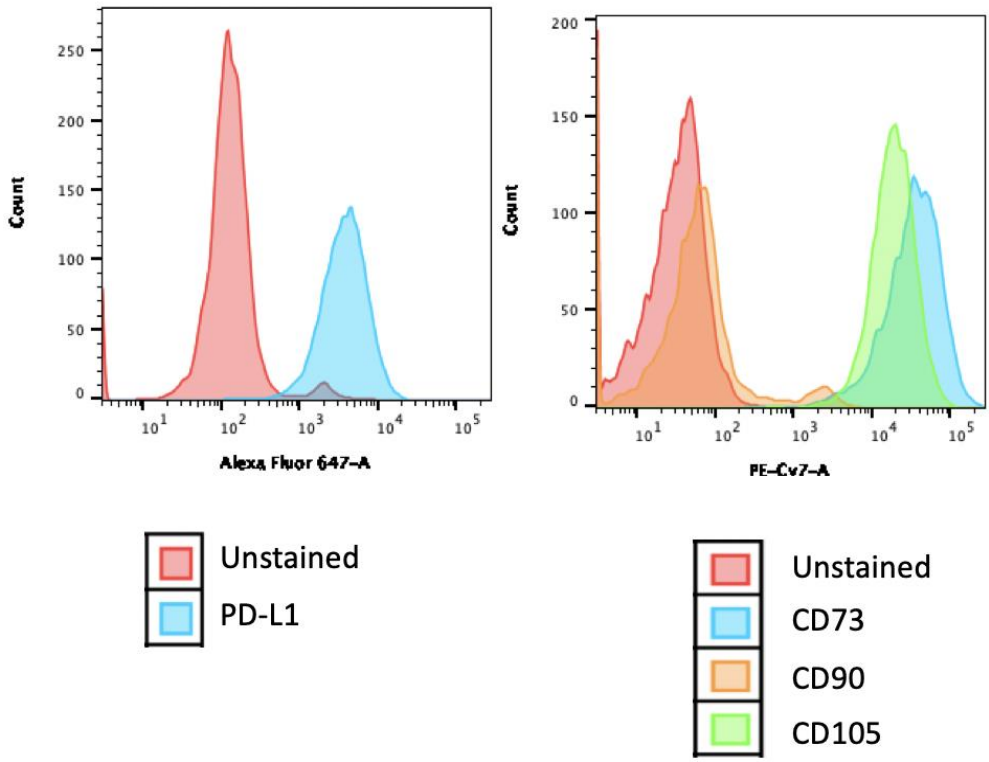

Figure 4. 19 – Flow cytometry of MPM cell lines

Flow cytometry confirms H513, H226 and MPP89 are all CD90 negative, a marker that can be used to differentiate cell types from MSCs. Assistance was offered by Dr Krishna Kolluri.

These apoptosis assays remain ongoing for these cell lines. The complexity encountered in these assays has led to some delays but work continues to identify a protocol that works well. My expectation is the apoptosis measurements match the cell viability results in the same cell lines and the non MPM cells lines.

4.3 Use of immunomodulatory agents do not amplify this effect further

Immunomodulatory agents targeting PD-1, PD-L1 and CTLA-4 have made it to the clinic in other tumour types such as melanoma, lung cancer and renal cell carcinoma (79, 302, 303). Immune checkpoint inhibition has been shown to synergise with chemotherapy (304). In addition, MSCTRAIL has demonstrated the same synergistic relationship with chemotherapy (250).

PD-1 and PD-L1 blockade

Treatment with monoclonal antibodies targeting the PD-1 / PD-L1 axis have revolutionised cancer treatment years over the past few years.

To explore the relationship between this immune regulatory axis and MSCTRAIL, A549 cells were initially labelled with DiI and seeded in a 96 well plate at 3000 cells per well in triplicate. Following 24 hours of incubation, the cells were treated with MSCTRAIL (5000 / well), MSCTRAIL (5000 / well) and PBMCs (200,000/well) or MSCTRAIL with activated PBMCs with or without the anti PD-1 antibody pembrolizumab. Following 48 hours of incubation, cells were collected via trypsinisation, washed and stained with DAPI and Annexin V antibody to assess for apoptosis. Cancer cells were analysed using flow cytometry.

As expected, A549 cells treated with MSCTRAIL led to little apoptosis given its inherent resistance to TRAIL. Adding allogeneic PBMCs led to a 33% drop in cell death and a further

31% when PBMCs were activated with CD3/CD28 Dynabeads. Surprisingly, there was little difference when pembrolizumab was added.

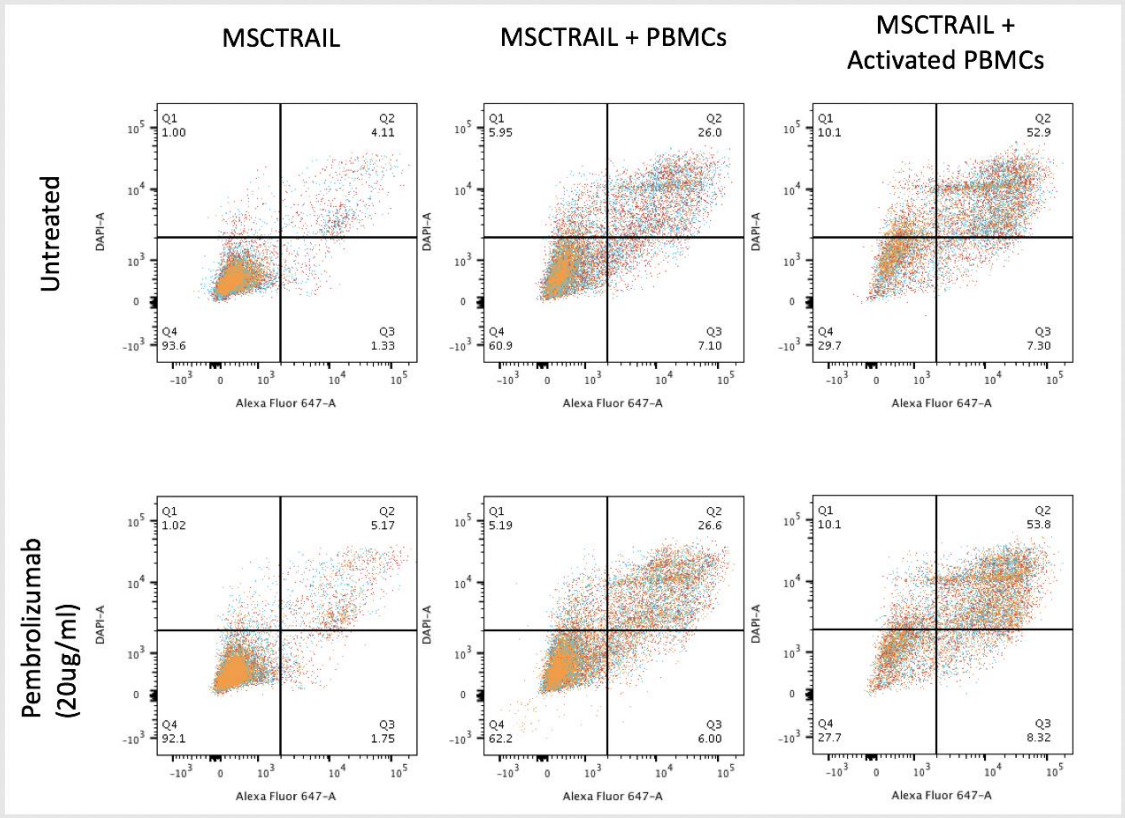

Figure 4. 20 - A549 treated with MSCTRAIL and allogeneic PBMCs

DiI labelled A549 cells were co-cultured with MSCTRAIL, PBMCs and activated PBMCs. Cell death was recorded following 48 hours of incubation using DAPI and Annexin V antibody.

The unsuccessful blockade of PD-1 was likely to be replicated when blocking PD-L1. This was explored using A549 transduced to express luciferase. Cells were seeded in a 96 well plate at 3000 cells per well in triplicate. Following 24 hours of incubation, the cells were treated with MSC (5000 / well), MSCTRAIL (5000 / well), PBMCs (200,000/well) and anti PD-L1 at increasing concentrations. Following 48 hours of incubation, bioluminescence was

recorded, a proxy for cell viability. Results showed that MSCTRAIL was sensitive to volunteer PBMCs, however similar to the flow cytometry PD-1 assay, the sensitivity was not improved when increasing doses of anti PD-L1 were added.

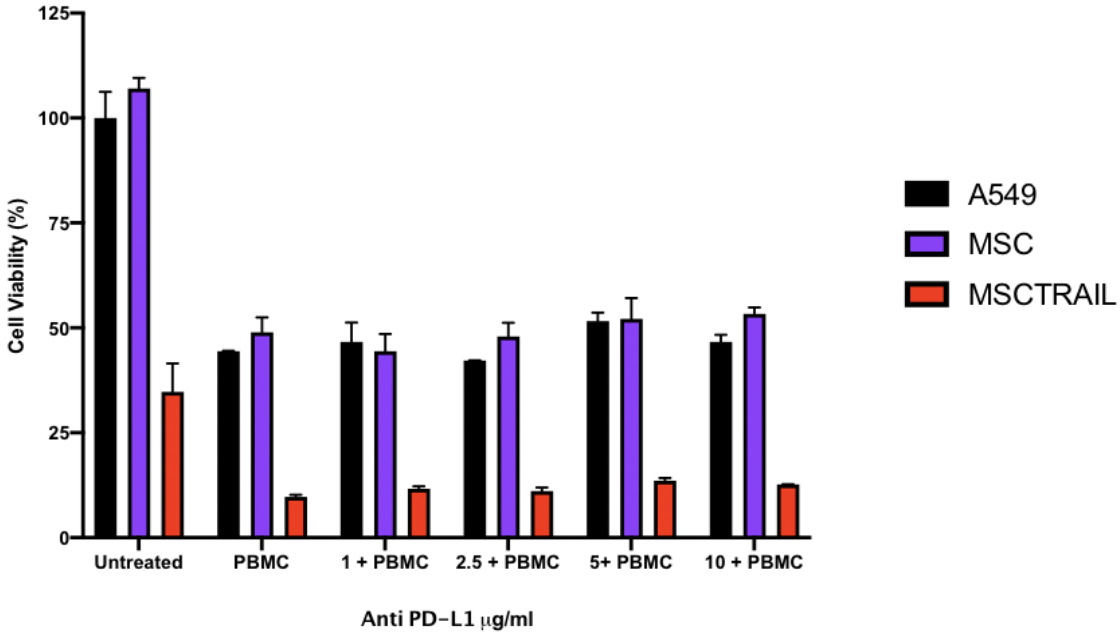

Figure 4. 21 - Cell viability assay of A549 cells treated with anti PD-L1

Co-culture cell viability assay over 48 hours. Luciferase labelled A459 cells treated with MSCs, MSCTRAIL, allogeneic PBMCs and increasing doses of anti PD-L1 antibody. Cells were either incubated without PBMC and anti PD-L1 antibody (untreated), with PBMCs alone and with a combination of PBMCs and anti PD-L1 antibody in increasing concentrations. Paired t test comparing MSCTRAIL + PBMC v MSCTRAIL + PBMC + 10ug/ml p=0.0633.

CTLA-4 blockade

Demonstrating pre-clinical and clinical efficacy by targeting the immune checkpoint receptor CTLA-4 paved the way for immune checkpoint inhibition in cancer (305). Its exploration in mesothelioma has been subdued with little on the horizon regarding licensing in this tumour type.

Using the reference cell line A549 transduced to express luciferase, cells were seeded in a 96 well plate at 3000 cells per well in triplicate. Following 24 hours of incubation, the cells were treated with MSC (5000 / well), MSCTRAIL (5000 / well), PBMCs (200,000/well) and an anti CTLA-4 monoclonal antibody, at increasing concentrations. Following 48 hours of incubation, bioluminescence was recorded, a proxy for cell viability. Results again showed that MSCTRAIL was sensitive to volunteer PBMCs, however disappointingly this sensitivity was not amplified further when increasing doses of anti CTLA-4 antibody were added.

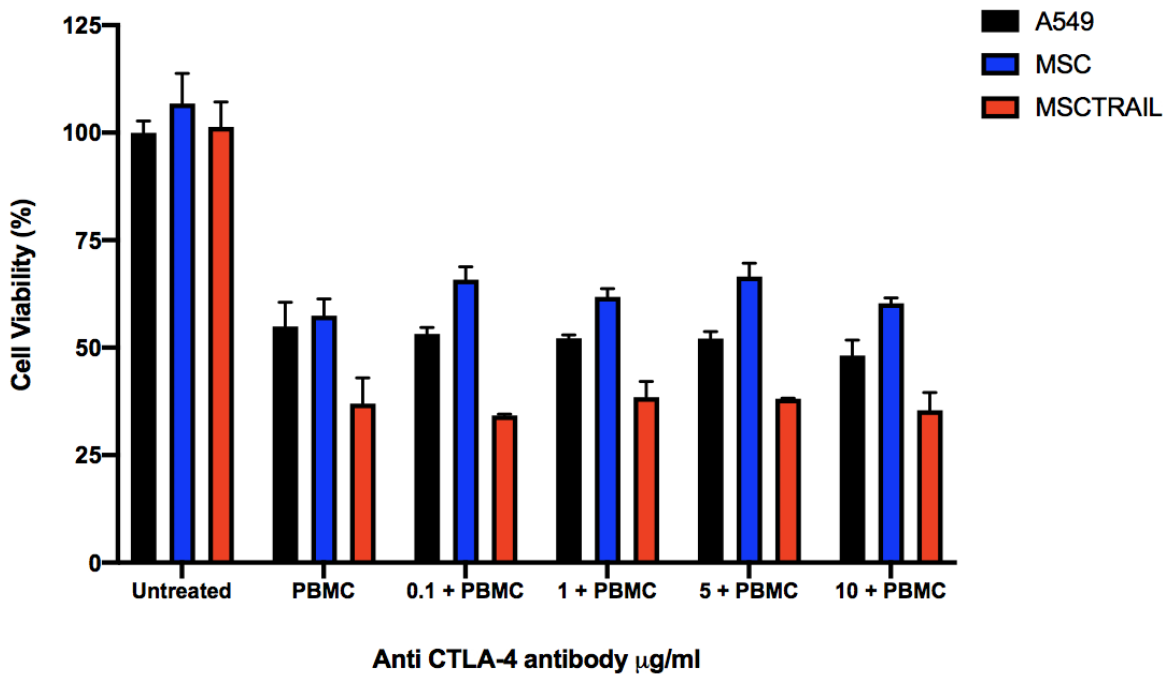

Figure 4. 22 - Cell viability assay of A549 cells treated with CTLA-4 blockade

Co-culture cell viability assay over 48 hours. Luciferase labelled A459 cells treated with MSCs, MSCTRAIL, allogeneic PBMCs and increasing doses of anti CTLA-4 antibody. Cells were either incubated without PBMC and anti CTLA-4 antibody (untreated), with PBMCs alone and with a combination of PBMCs and anti CTLA-4 antibody in increasing concentrations. Paired t test comparing MSCTRAIL + PBMC v MSCTRAIL + PBMC + 10ug/ml p=0.4266

Studying immune checkpoint blockade *in vitro* has great limitations. Immune diversity relies not just on the interaction with cancer cells, but a region where they can process this information, develop antigen specific T cell receptors and divide accordingly to an adequate number so as to tackle these tumours efficiently. *In vivo* this is done through the lymphatic system where lymphocytes migrate to lymph nodes following antigen recognition. *In vitro* this system is very much absent.

To explore this further an *in vivo* study is required. The caveat to murine studies in this work is murine MSCs have a totally different phenotype to human MSCs, a crucial issue with animal studies. To use human MSCs in a mouse model this would require human PBMCs which complicates this work necessitating the need for a humanised mouse model, a resource I was unable to acquire up during my time in research.

IDO inhibition

As discussed, activation of immune cells by MSCs is balanced by the release of indoleamine 2,3-dioxygenase (IDO), which downregulates T cells and chemokine receptors such as CXCR3 and CCR5 on immune cells, which are activated by CXCR5/CCR5 ligands (228).

IDO inhibitors have had mixed success in the clinic when combined with anti PD-1 (306), however the rationale for testing it is supported here. Pharmacological inhibition of IDO leads to the removal of the inhibitory signal to immune cells allowing the balance to shift to a more MSC activating phenotype.

Immunoregulation of immune cells by MSCs

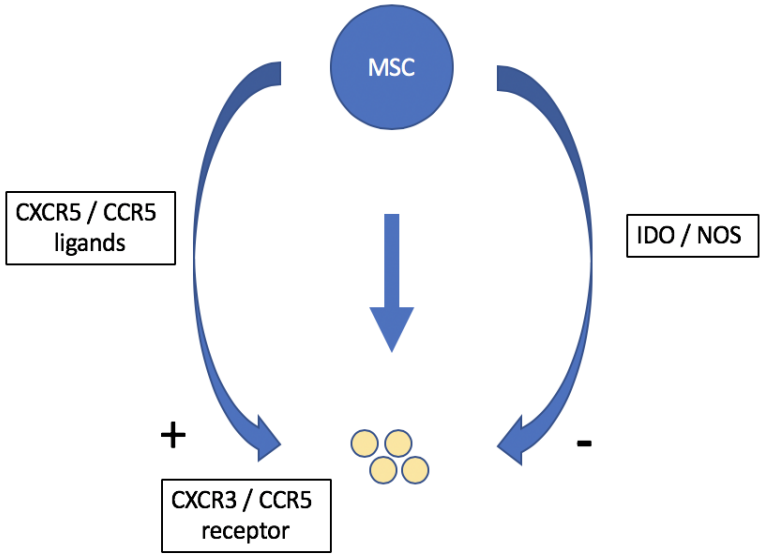

Figure 4. 23 - The balance between activation and inhibition of T cells by MSC's.

Luciferase labelled A549 cells were plated in a 96 well plate at 3000 cells per well in triplicate. Following 24 hours of culture, cells were treated with MSCs (5000 / well), MSCTRAIL (5000 / well) and allogeneic PBMCs (200,000 / well). An increased dose of IDO inhibitor was added from 0.1 µmol/L to 10 µmol/L and re-cultured for 48 hours. Bioluminescence was recorded to measure cell viability.

When PBMC's were added to A549 cells a significant reduction in cell viability was noted, more so in the MSCTRAIL arm. As IDO inhibitor concentration increases in combination with PBMCs the effect remains unchanged. Failure of this inhibitor could be a consequence of concentration used, although the highest dose used was guided by previously published *in vitro* studies. In addition to the possibility of poor IDO inhibition it may not be the most critical enzyme in MSC mediated immune regulation. MSCs secrete a plethora of cytokines

many of which may also contribute to immune inhibition a paradigm supporting the idea that inhibiting one enzyme is not enough.

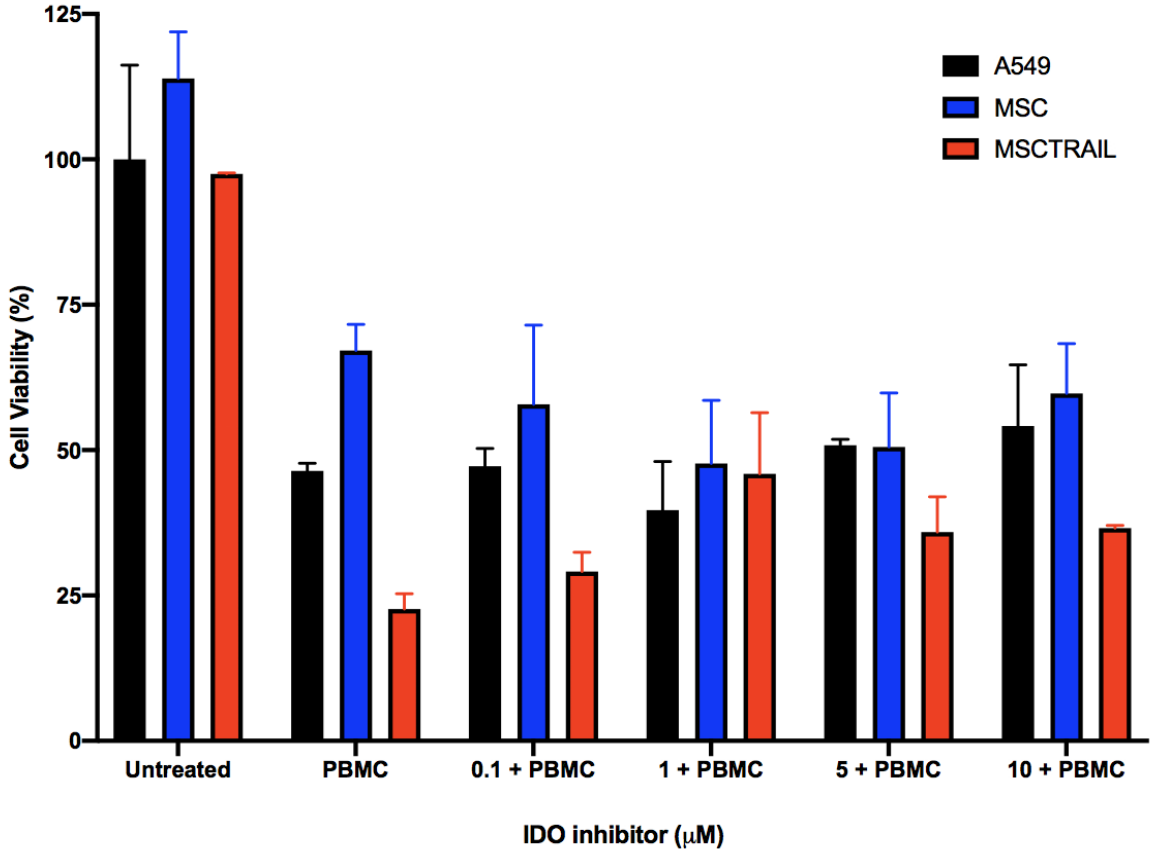

Figure 4. 24- Cell viability assay of A549 cells treated with an IDO inhibitor

Co-culture cell viability assay over 48 hours. Luciferase labelled A549 cells were treated MSCs, MSCTRAIL and PBMCs and increasing doses of an IDO inhibitor. Cells were either incubated without PBMC and inhibitor (untreated), with PBMCs alone and with a combination of PBMCs and inhibitor in increasing concentrations. Paired t test comparing MSCTRAIL + PBMC v MSCTRAIL + PBMC + 10uM p= 0.0989

4.4 Development of a syngeneic model

The allogeneic model presented has invited much criticism. The most important of these is the synergistic relationship described between MSCTRAIL and PBMCs which is thought reflective of a non self immune response. Mitigating this was always going to be a challenge using established cell lines with unpaired PBMCs, which has led to the development of a syngeneic model. This section describes both its inception and translation to a more relevant model.

Development of cell lines from pleural effusion samples

Cases were identified in conjunction with the respiratory team at University College London Hospital (UCLH) and the cardiovascular team at the satellite unit at Westmoreland Street Hospital (UCLH). Cases were screened on a weekly basis and considered for participation if appropriate. Patients with suspected malignant pleural effusions in particular those suspicious of pleural origin were identified. Patients 18 and over with the ability provide informed consent were approached. Patients were approached by managing clinical teams initially asking permission for me to discuss my programme of work with them. Written consent was mandatory and obtained from each patient (see supplementary for patient information sheet and consent forms). A blood sample was collected at the time of consent (20-25ml) for the isolation of PBMCs. Patients were taken to theatre for either intra-pleural drain insertion or video assisted thoracoscopic surgery (VATS) to treat the pleural effusion. Fluid was collected for clinical diagnostics followed by fluid donated for cell line development.

Fluid was transported to the lab alongside matched PBMCs for each patient. A sample of fluid was collected and immediately frozen for future proteomic work. The remainder of the

sample was diluted in PBS, centrifuged to form a cell pellet, subjected to red lysis to remove red blood cells, and finally seeded in T175 and T75 flasks for cell culture and subsequent -150^{o}C storage. A sample of fluid was collected for immune cell isolation (CD45+) and stored at -150^{o}C for future use. In parallel, the blood sample was subjected to FICCOL separation to generate a buffy coat. This was then isolated and diluted in RPMI culture media. Following centrifugation, a pellet of PBMCs are formed, which are then counted and frozen at -150^{o}C for future use.

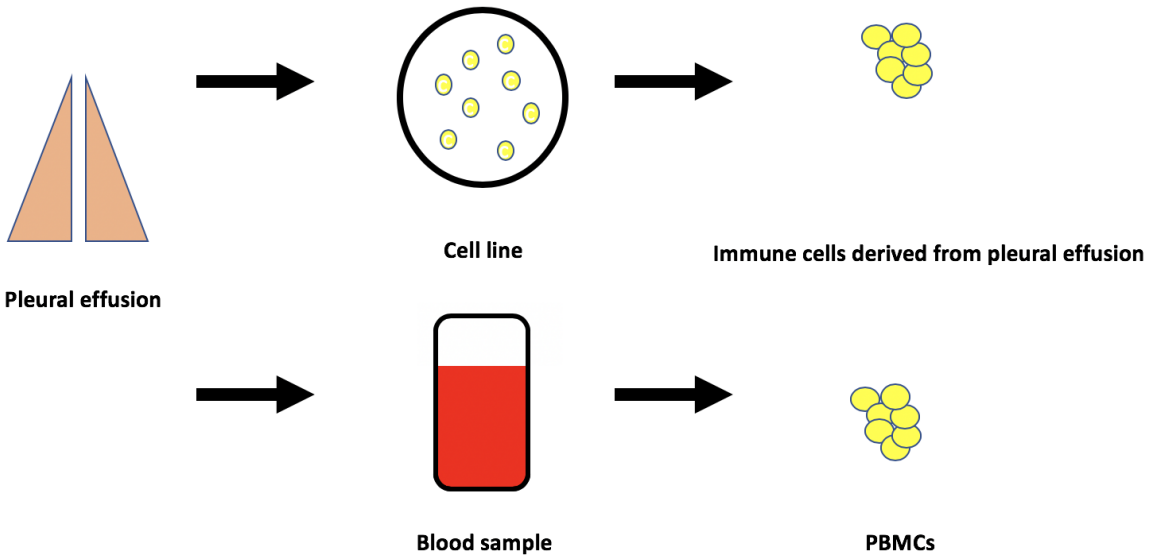

Figure 4. 25 – Sample collection pathway

A schematic demonstrating the development of cell lines from malignant pleural effusions. Patients with malignant pleural effusions identified with particular emphasis on mesothelioma. See materials and methods for detailed description of development.

Cancer subtype	No. of total cases	No. of successful cell lines
Mesothelioma	6	4
Lung	9	3
Gynaecological	5	1
Breast	4	0
Sarcoma	3	2
Other	4	0
TOTAL	31	10

Figure 4. 26 – List of patients and tumour types collected

A table summarising the total number of cases collected, the tumour subtype and whether the cell line grew successfully or not. A successful cell line was defined as greater than 10 passages.

Sample collection was an increasingly difficult task particularly when performed alone. Without the help of the relevant teams it would be almost impossible to collect these cases. Theatre based co-ordination and thorough communication was key to acquiring these samples, although many fell through despite this effort.

Collecting mesothelioma cases was a particular challenge. Many patients were identified and underwent pleural drainage without my knowledge, a result of many issues but commonly due to prioritising good quality care rather than pre-clinical exploration. A more robust pathway of tissue collection for research is needed where patient care is not compromised and clinicians are largely uninterrupted in their day to day work but all cases are highlighted to pre-clinical research teams for consideration of consent.

The syngeneic model is comparable to the non-syngeneic model

The benefit of developing a syngeneic model to confirm synergy centres around the concept of non-self recognition driven by human leukocyte antigen (HLA) molecules. All cells express these antigens and are unique for each patient. Organ transplantation is the commonest example of tissue rejection through this process. To mitigate this the syngeneic model described has been used to test this relationship between MSCTRAIL and immune cells in an attempt to avoid this issue.

MDA-MB-231, used in the allogenic platform was tested alongside the first mesothelioma syngeneic model as a comparative assessment. MDA-MB-231 and the effusion derived mesothelioma cell line GF230519 were co-cultured with volunteer and matched PBMCs respectively (Matched PBMCs weren't used with the MDA-MB-231 given their preciousness but is accepted as a limitation). Cell viability was compared over 24 and 48 hours. Similar to previous assays GF230519 was initially transduced to express luciferase. Cells were seeded in a 96 well plate at 3000 cells per well in triplicate. Following 24 hours of incubation the two cell types were treated with MSCs (5000 / well), MSCTRAIL (5000 / well), PBMCs (100,000 / well) and cisplatin (2μM). The dose of cisplatin was dropped to 2μM on account of previous work showing similar outcomes compared to 5μM. Some of the cells used were platinum sensitive and to avoid losing a synergistic signal with higher doses of cisplatin I decided to drop the concentration. In addition, the immune cells were reduced by 50% as the cells isolated were in limited supply. To perform an adequate assay with appropriate controls the immune cells were limited for the subsequent syngeneic luciferase assays. Following 24 and 48 hours of incubation, bioluminescence was recorded.

Bioluminescence recorded after 24 hours demonstrated little fall in cell viability in the allogeneic model compared with a much greater drop (27%) in the syngeneic mesothelioma model. This was repeated 48 hours post incubation with an even greater drop in the syngeneic model (37% compared with 12% in the allogeneic model). This issue with non-self recognition is not just negated but in fact using a paired model provides even greater efficiency.

24 hours

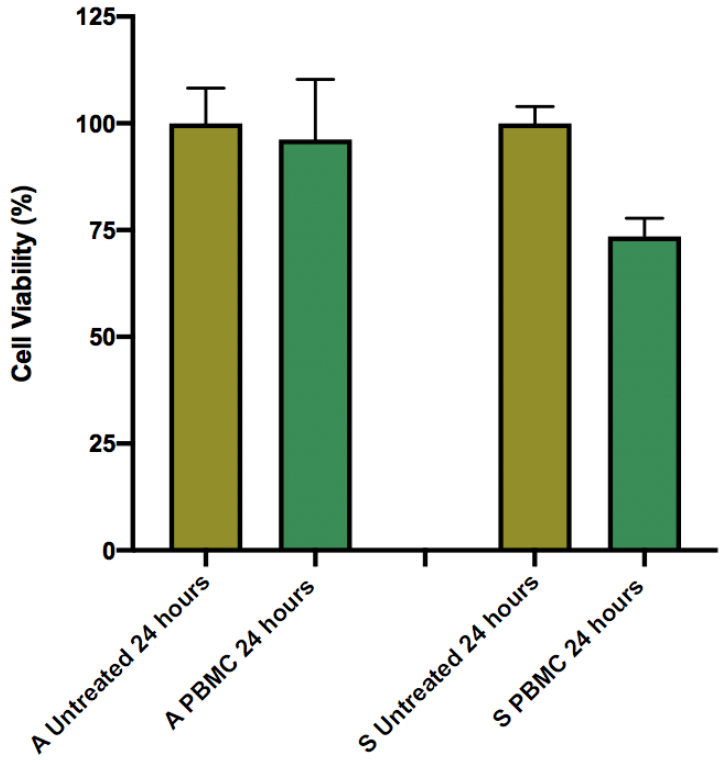

48 hours

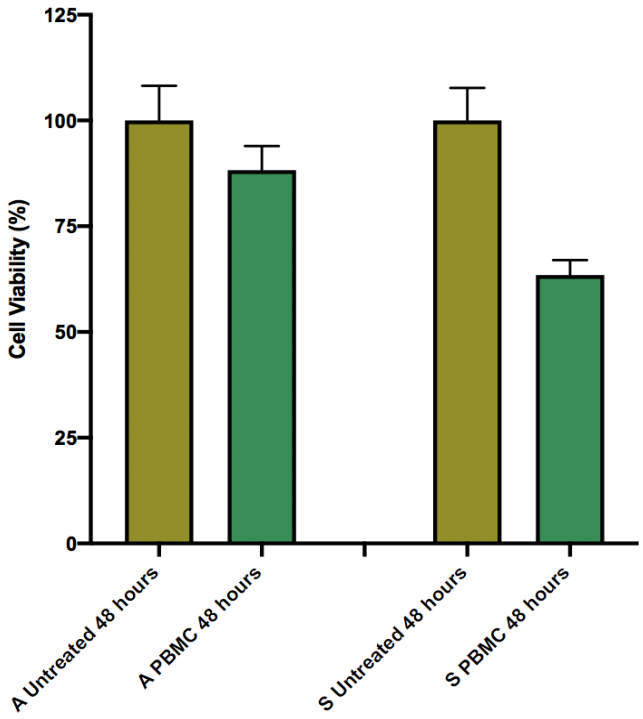

Figure 4. 27 - Cell viability assay - allogeneic versus syngeneic model 24 & 48 hours

A cell viability assay comparing luciferase labelled MDA-MB-231 and GF230519 cell lines, following 24 and 48 hours of incubation with allogeneic and syngeneic PBMCs. Paired t test between allogeneic and syngeneic untreated p=0.9933 (24 hours), allogeneic and syngeneic with 24 hours of PBMCs p=0.1264 (24 hours). Paired t test between allogeneic and syngeneic untreated p=0.9995 (48 hours), allogeneic and syngeneic with 48 hours of PBMCs p=0.0428 (48 hours).

Syngeneic model – cell viability luciferase assay's

Once the developed cell lines were shown to thrive (>10 passages or more) they were transduced to express luciferase (see materials and methods). Cells were sorted for GFP expression at the Institute of Child Health (ICH) with the kind help of Dr Ayad Eddaoudi and re-expanded in culture. Once cells were shown to thrive and divide, they were collected, counted and plated in a 96 well plate at 3000 cells / well in triplicate. Cells were treated in the same way as the allogeneic cell lines earlier in the chapter. Following 24 hours of incubation cells were treated with MSCs (5000 / well), MSCTRAIL (5000 / well), matched PBMCs (100,000 / well) and cisplatin (2μM).

The following syngeneic cases are examples of patients to date who have undergone cell viability assessment:

Case 1: GF230519 – Effusion derived cell line co-culture with syngeneic PBMCs

This first case represents a patient with *epithelioid MPM*. The cell line is partially TRAIL sensitive (approximately 25% reduction in cell viability). The cells are partially sensitive to matched PBMCs although the addition of MSCTRAIL offers little in this circumstance. Supported by the allogeneic model, anti PD-1 therapy offers no change. The greatest reduction in cell viability is associated with cisplatin. It would be interesting to know the BAP1 status of this patient as those with loss of function mutations are more susceptible to TRAIL as per our previous work (144).

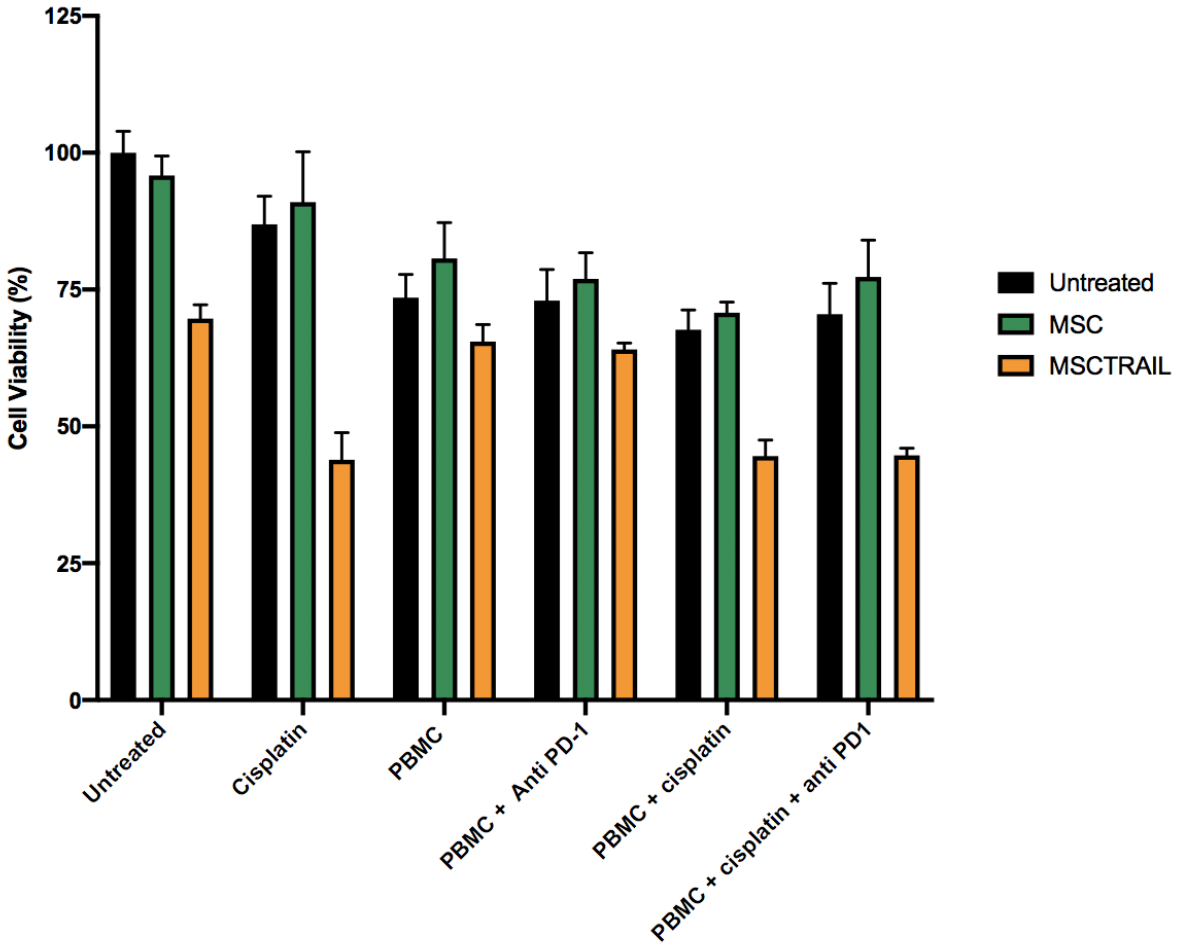

Figure 4. 28 – GF230519: Effusion derived cell line with syngeneic PBMCs (24 hours)

Co-culture assay of luciferase labelled MPM cell line - GF230519. Treated with MSCs, MSCTRAIL, PBMCs, cisplatin and anti PD-1 antibody for 24 hours. Paired t test comparing MSCTRAIL v MSCTRAIL + PBMC p=0.1164, MSCTRAIL v PBMC + anti PD-1 p=0.0399, MSCTRAIL v PBMC + cisplatin p=0.0022 and MSCTRAIL v PBMC + anti PD-1 + cisplatin p=0.0032.

Following 48 hours of culture the patterns are similar however with greater loss in cell viability observed across all arms. This patient was particularly sensitive to cisplatin when combined with MSCTRAIL. The patient demonstrated sensitivity to PBMCs, although little was achieved when MSCTRAIL was added. This patient would benefit best from single agent cisplatin with MSCTRAIL, according to this *in vitro* assay.

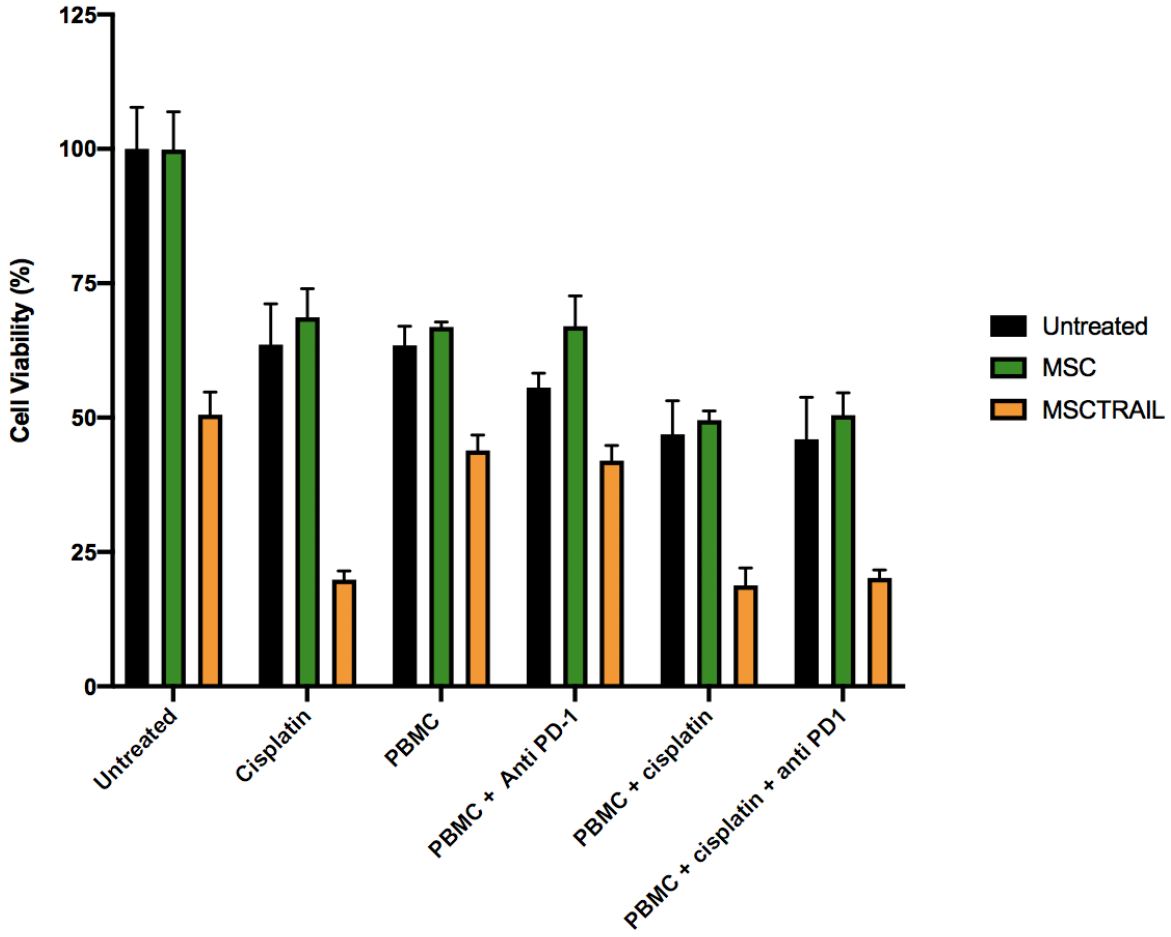

Figure 4. 29 – GF230519: Effusion derived cell line + syngeneic PBMCs (48 hours)

Co-culture assay of luciferase labelled MPM cell line - GF230519. Treated with MSCs, MSCTRAIL, PBMCs, cisplatin and anti PD-1 antibody for 48 hours. Paired t test comparing MSCTRAIL v MSCTRAIL + PBMC p=0.0819, MSCTRAIL v PBMC + anti PD-1 p=0.1119, MSCTRAIL v PBMC + cisplatin p=0.0055 and MSCTRAIL v PBMC + anti PD-1 + cisplatin p=0.0026

Case 2: WL270319 – Effusion derived cell line co-culture with syngeneic PBMCs

This patient was proven to have non-small cell lung cancer (adenocarcinoma) previously treated with platinum therapy. As previous, transduced cells to express luciferase were cultured with MSCs, MSCTRAIL, matched PBMCs, cisplatin (2μM); standard backbone chemotherapy for MPM/NSCLC and anti PD-1 antibody treatment.

This is a particularly interesting case. The tumour did not respond at all to the PBMCs following 24 hours of incubation. The sensitivity to MSCTRAIL was truly spectacular. Regardless of the situation, the fall in cell viability was almost 90% across all treatment arms. Given the level of sensitivity it was difficult to confirm any synergistic relationship. As a patient with previous platinum use this level of response supports exploration of MSCTRAIL in later lines of therapy. Isolation of this patients PBMCs was limited therefore only 1 time point was performed.

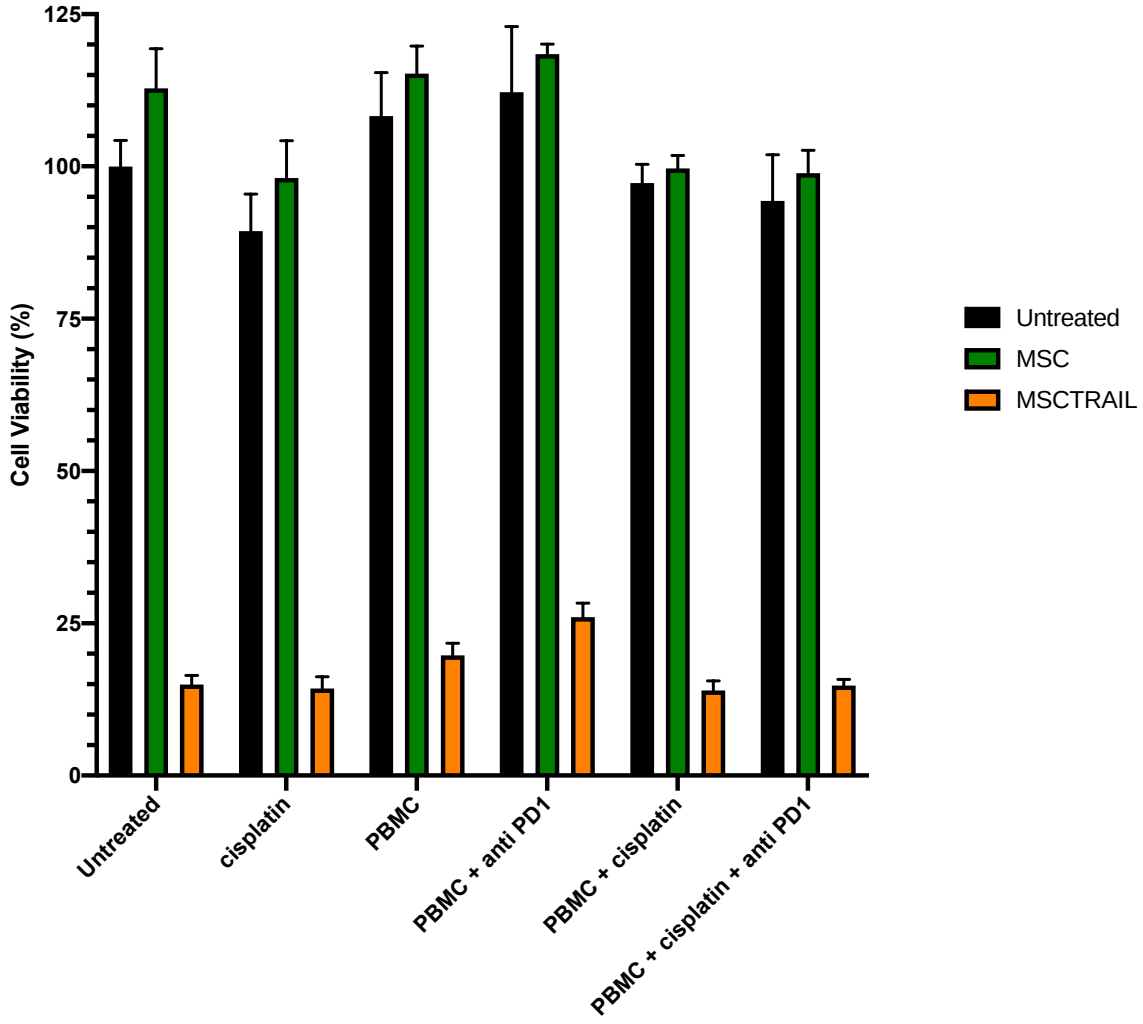

Figure 4. 30 – WL270319: Effusion derived cell line with syngeneic PBMCs (24 hours)

Co-culture assay of luciferase labelled cell line – WL270319. Treated with MSCs, MSCTRAIL, PBMCs, cisplatin and anti PD-1 antibody for 24 hours. Paired t test comparing MSCTRAIL v MSCTRAIL + PBMC p=0.088, MSCTRAIL v PBMC + anti PD-1 p=0.0068, MSCTRAIL v PBMC + cisplatin p=0.0055 and MSCTRAIL v PBMC + anti PD-1 + cisplatin p=0.11144

Case 3: PK061219 – Effusion derived cell line co-culture with syngeneic PBMCs

This case of PK061219 represents cells grown from a pleural effusion secondary to epithelioid mesothelioma. The cells are sensitive to MSCTRAIL from the outset. The syngeneic PBMCs led to a reduction in cell viability in the non-MSC arms of 20%. MSCTRAIL and PBMCs led to a fall in cell viability of 16% when compared with MSCTRAIL alone. No further treatment interventions offered improvements. A 48 hour assay was not possible given the limited supply of PBMCs available.

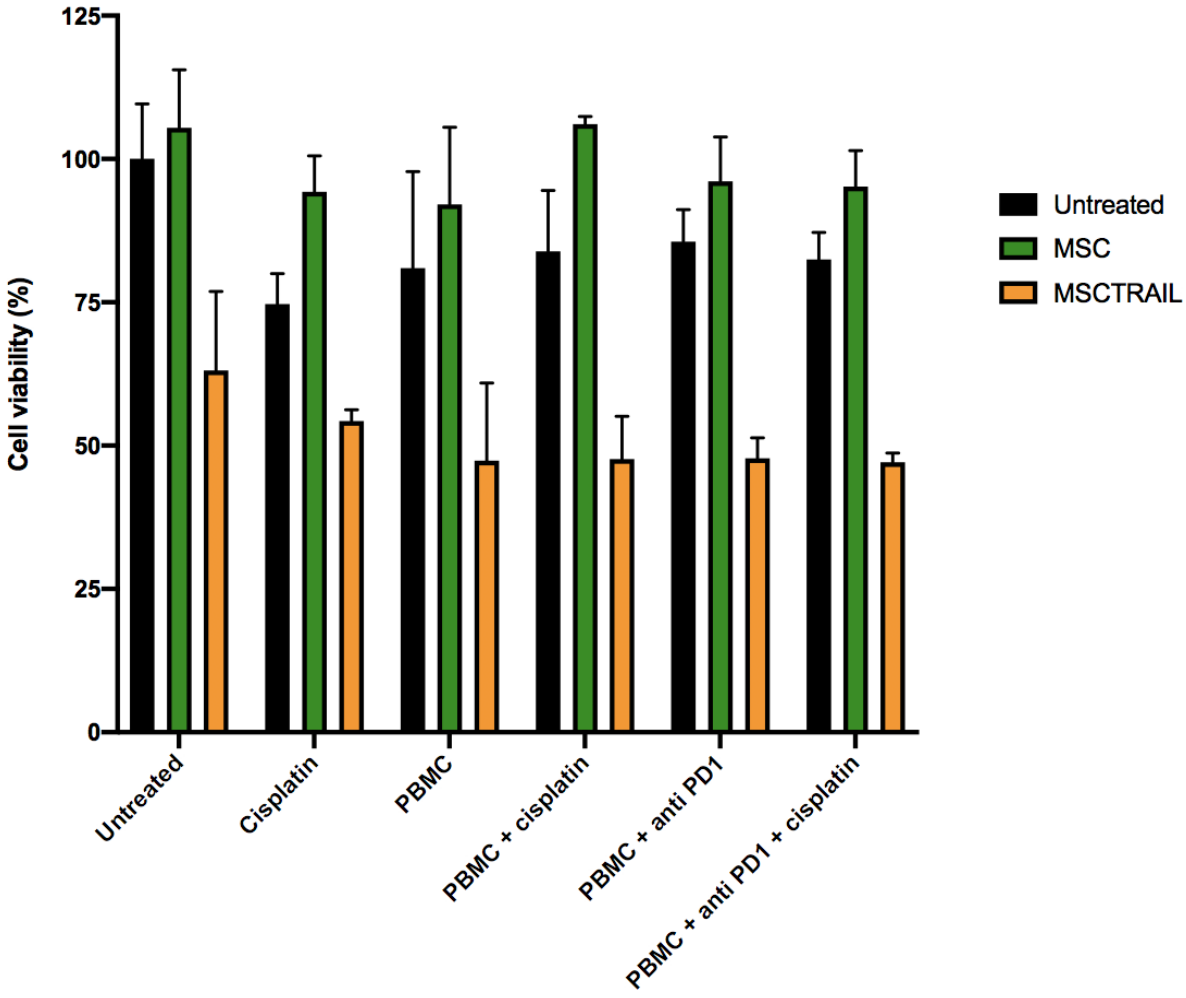

Figure 4. 31 - PK061219: Effusion derived cell line with syngeneic PBMCs 24 hours

Co-culture assay of luciferase labelled cell line – PK061219. Treated with MSCs, MSCTRAIL, PBMCs, cisplatin and anti PD-1 antibody for 24 hours. Paired t test comparing MSCTRAIL v MSCTRAIL + PBMC p=0.0051, MSCTRAIL v PBMC + anti PD-1 p=0.1570, MSCTRAIL v PBMC + cisplatin p=0.3147 and MSCTRAIL v PBMC + anti PD-1 + cisplatin p=0.1555

Case 4: AH040619 – Effusion derived cell line co-culture with syngeneic PBMCs

The final cell line tested originated from a myxoid chondrosarcoma. Following only 24 hours of treatment, cells were sensitive to MSCTRAIL, further augmented with the addition of syngeneic PBMCs leading to a drop in cell viability of 20% when compared with MSCTRAIL alone, an impressive signal given it was only 24 hours.

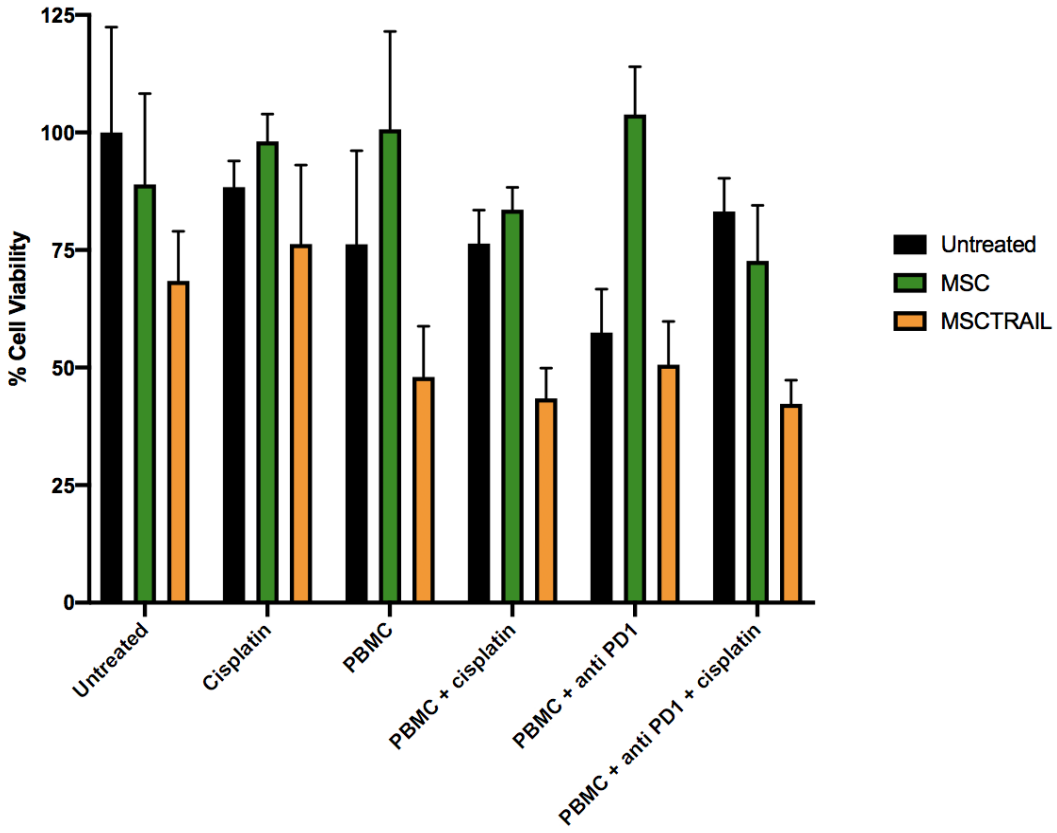

Figure 4. 32 - AH040619 - Effusion derived cell line with syngeneic PBMCs (24 hours)

Co-culture assay of luciferase labelled cell line – AH040619. Treated with MSCs, MSCTRAIL, PBMCs, cisplatin and anti PD-1 antibody for 24 hours. Paired t test comparing MSCTRAIL v MSCTRAIL + PBMC p=0.0021, MSCTRAIL v PBMC + anti PD-1 p=0.0076, MSCTRAIL v PBMC + cisplatin p=0.0551 and MSCTRAIL v PBMC + anti PD-1 + cisplatin p=0.0396

Discrepancies were noted at 48 hours. MSCTRAIL performed less well than the 24 hour assay in the untreated arms. Cisplatin and MSCTRAIL led to a huge drop in cell viability. Moreover, matched PBMCs and MSCTRAIL led to a reduction of cell viability and the combination of cisplatin and PBMCs with MSCTRAIL led to the greatest drop. In the non-MSC arms, the effect of PBMCs led to a 42% drop in cell viability when compared with untreated cells. Again, anti PD1 therapy added nothing to the treatment effect.

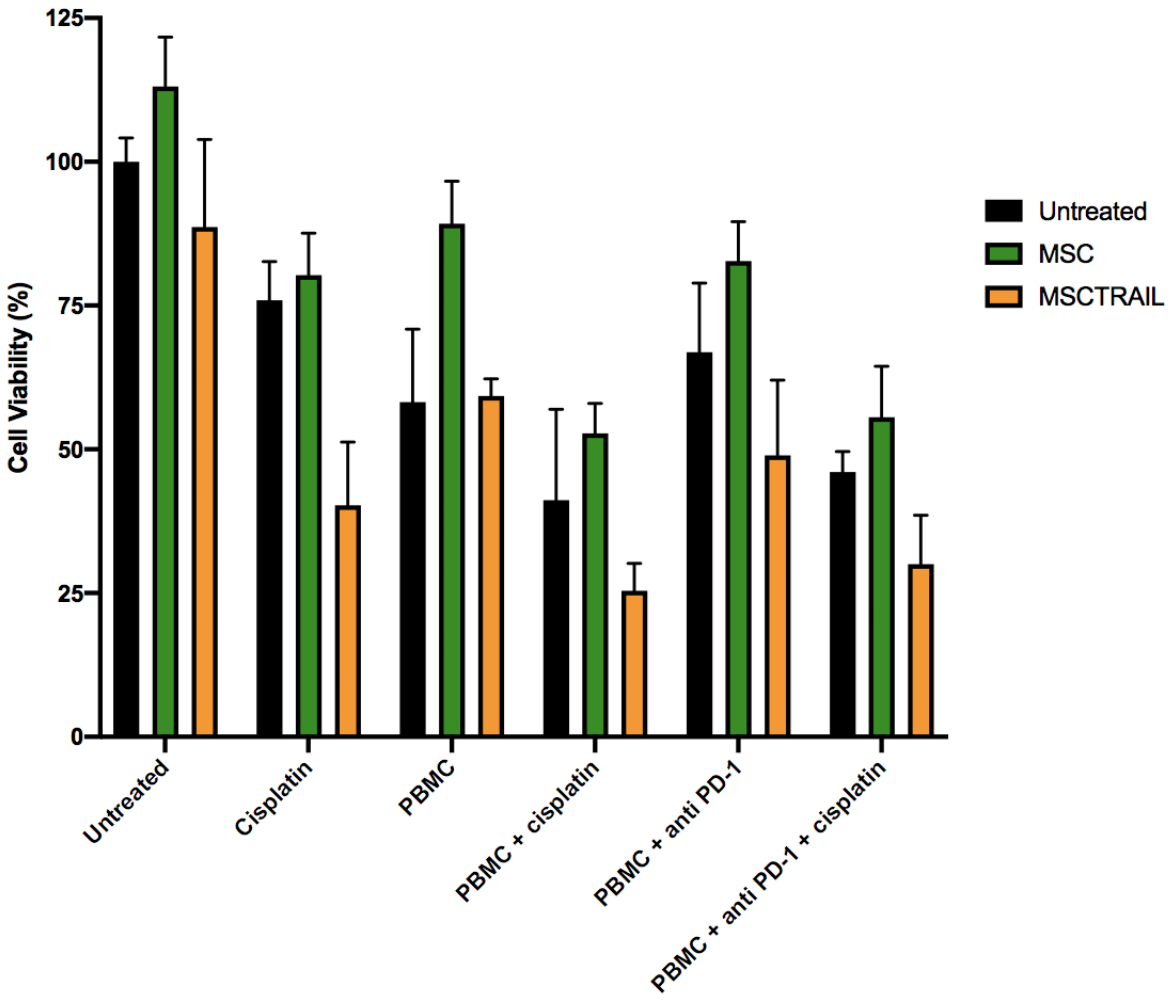

Figure 4. 33 - AH040619 - Effusion derived cell line with syngeneic PBMCs (48 hours)

Co-culture assay of luciferase labelled cell line – AH040619. Treated with MSCs, MSCTRAIL, PBMCs, cisplatin and anti PD-1 antibody for 24 hours. Paired t test comparing MSCTRAIL v MSCTRAIL + PBMC p=0.1071, MSCTRAIL v PBMC + anti PD-1 p=0.1317, MSCTRAIL v PBMC + cisplatin p=0.0182 and MSCTRAIL v PBMC + anti PD-1 + cisplatin p=0.0472

Syngeneic model - effusion derived immune cells

Immune cells residing in pleural effusion fluid may harbour T cell receptors more focused towards tumour antigens compared with circulating immune cells. Isolation of CD45+ cells from the fluid were compared with circulating PBMCs and allogeneic PBMCs.

The MPM luciferase labelled cell line PK061219 was seeded in a 96 well plate at 3000 cells per well in triplicate. Following 24 hours of incubation the PBMCs were cultured at 100,000 cells per well. Following a further 24 hours, bioluminescence was measured.

Allogenic PBMCs lead to a drop in cell viability of 16%, syngeneic 20% and effusion specific over 24%. When MSCTRAIL is added the fall is greater compared with untreated. Allogeneic PBMCs led to a drop in cell viability of 42%, syngeneic PBMCs 53% and the greatest drop was in effusion specific cells 61%.

This suggests that immune cells collected from pleural effusion samples may offer a greater sensitivity when co-cultured with MSCTRAIL, compared with syngeneic circulating PBMCs.

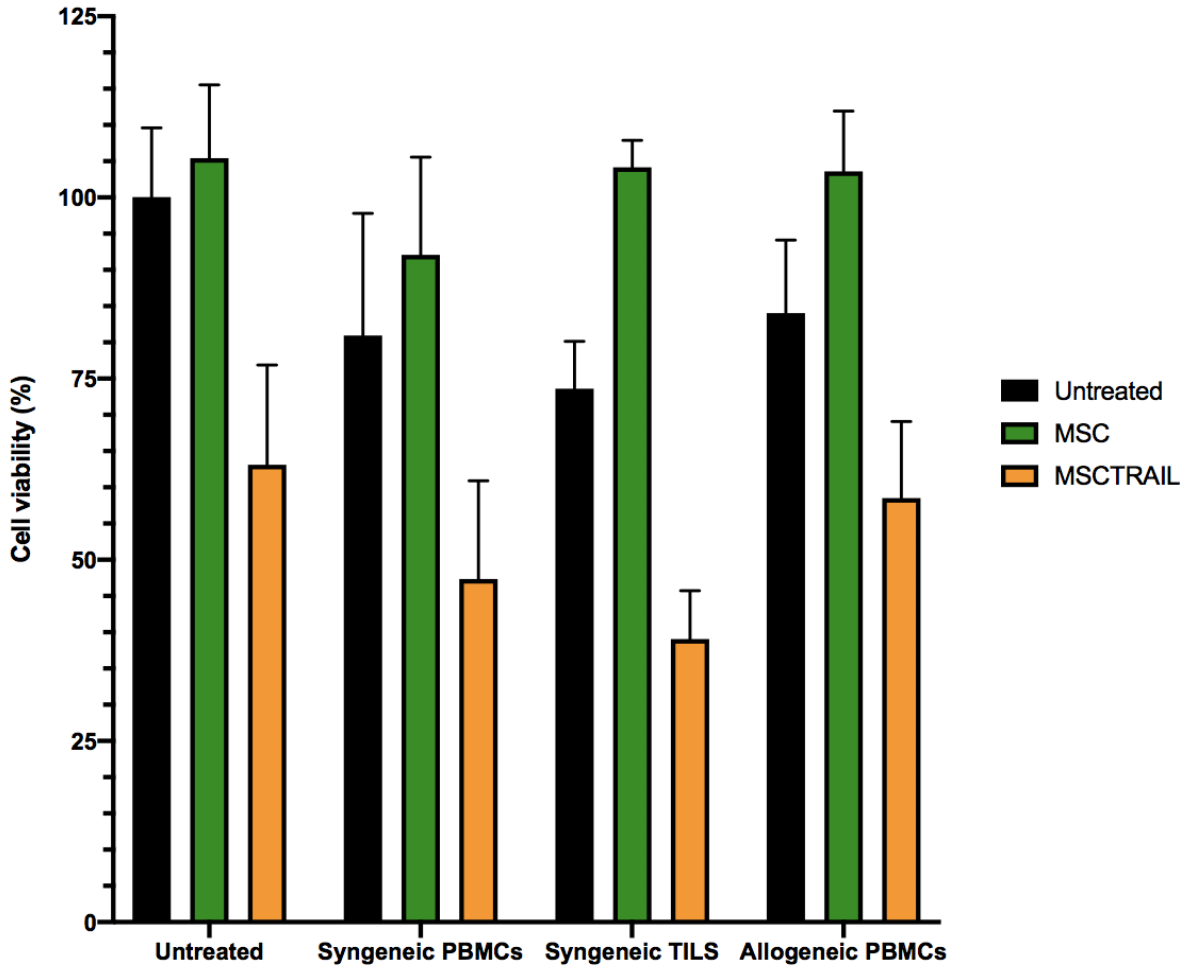

Figure 4. 34 – PK061219: Effusion derived CD45+ cells 'v' syngeneic 'v' allogeneic PBMCs (24 hours)

Co-culture assay of luciferase labelled MPM cell line – PK061219. Treated with syngeneic PBMCS, effusion derived PBMCs and allogeneic PBMCs over 24 hours. Paired t test comparing untreated MSCTRAIL v syngeneic PBMCs, p=0.0051, untreated MSCTRAIL v syngeneic TILS p=0.0333 and untreated MSCTRAIL v allogeneic PBMCs p=0.7687

Development of patient derived xenograft (PDX) models

Cells derived from the pleural effusion samples are unlikely to be purified cancer cells. Following initial seeding of cells into a culture flask more than one cell type can be seen under the microscope. Growth of cells in culture conditions are not exclusive to malignant cells and other cells such as fibroblasts also have the ability to grow and adhere to plastic.

Many cancer cells including mesothelioma do not have distinct extracellular markers that differentiate from other cells precluding the use of flow cytometry sorting methods.

An alternative approach is to develop patient derived xenograft (PDX) models. Cell lines that have passaged several times and thrive in culture conditions were collected into a pellet, resuspended in Matrigel and subcutaneously implanted into the flank of an immunocompromised mouse. With the assistance of Dr Krishna Kolluri and Dr Rob Hynds, following the development of subcutaneous tumours, the mice were culled and the tumours extracted and re-cultured.

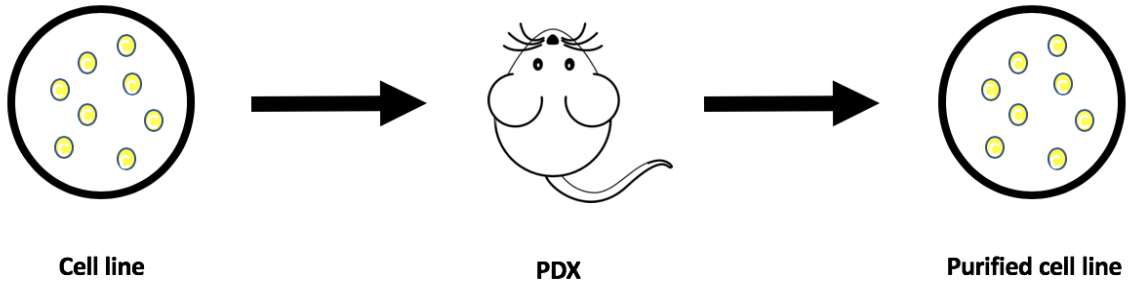

PDX cell lines	
WL270319	lung Adenocarcinoma
GF230419	MPM
EM120919	lung Adenocarcinoma
PK061219	MPM

Figure 4. 35 – Cell lines used in the PDX programme

Exome sequencing of cell lines

I was keen to explore the genomic landscape of these acquired cell lines, in particular in mesothelioma. Acquisition of somatic mutations through several cell line passages; the act of trypsinisation and splitting cells once cells reach confluency, is well recognised (307).

Cells were identified that were both early (up to 5 passages) and late (10 or more passages) passages. Cell lines collected and cultured following PDXs were also included. Matched PBMCs were collected as a germline control for the samples. DNA was extracted using a PureLink Genomic DNA kit (Qiagen, cat no. K182001). Cells were collected following a process of trypsinisation, and subjected to enzymatic digestion. A digestion buffer was used to aid protein denaturation i.e. unfolding of proteins to aid digestion. RNase A was used to remove an unwanted RNA. Ethanol and a binding buffer were added to aid binding to the spin columns, allowing for washing of the sample to remove impurities. The samples were then finally eluted in a low salt elution buffer and the DNA collected. DNA was quantified and assessed for quality using a Nanodrop One.

Sample ID	Volume supplied (µl)	Sample concentration (ng/µl)	A260/A280	A260 / A230
WL270319-EP	50	124.9	1.78	2.02
WL270319-LP	50	44	1.77	2.50
WL270319-PDX	50	370.4	1.93	2.73
WL230519-Germline	50	68	1.79	2.46
GF230519-EP	50	100.6	1.66	1.82
GF230519-LP	50	1787.7	2.01	2.23
GF230519-PDX	50	99.7	1.86	6.09
GF230519-Germline	50	12.4	1.84	2.94
MK020419-EP	50	191.4	1.91	1.79
MK020410-LP	50	184.1	1.97	2.04
MK020419-Germline	50	21.6	1.84	2.27
PK061219-EP	50	1216.9	2.02	2.04
PK061219-LP	50	212.3	1.91	2.13
PK061219-Germline	50	28.4	1.78	2.87
EM120919-EP	50	43.9	1.58	3.96
EM120919-LP	50	166	1.93	2.31
EM120919-Germline	50	53	1.76	2.54
AH020419-EP	50	114.5	1.92	2.09
AH020419-LP	50	162.8	1.92	2.26
AH020419-Germline	50	23.4	1.86	3.66

Figure 4. 36 – Cell lines and PBMC DNA extraction

A table of cell lines and PBMCs subjected to DNA isolation. The sample concentration (ng/ml), sample purity ratios A260/A280 and A260/A230 were measured. A260/A280 is a measure of protein / reagent contamination. A ratio of around 1.80 is widely accepted as satisfactory for purity. A260/A230 is a secondary measure of purity which is accepted to be between 2.0 – 2.20. WL270319: lung adenocarcinoma, GF230519: MPM, MK: sarcomatoid, PK061219: MPM, EM120919: lung adenocarcinoma, AH040619: sarcomatoid tumour. Highlighted blue = MPM cell lines.

Sadly, as a result of COVID19 these samples were sent in February 2020 for whole exome sequencing to Great Ormond Street Hospital and Institute of Cancer Research, however results are yet to be returned with no outcome in sight.

As a result of this I plan to report these findings in a separate manuscript at a later date once they are finally processed and analysed (timing of which is dependent on the government and academic approach to the pandemic). For the purposes of the thesis submission I halt any further description at this point but am keen to describe my efforts given the time investment made.

4.5 Mechanism behind synergy

The synergistic relationship between MSCTRAIL and PBMCs was established in both the allogeneic and syngeneic cell line models earlier in the chapter. It is hypothesised that the relationship between MSCTRAIL and PBMCs is driven by two possible methods.

MSCTRAIL targets cancer cells leading to apoptosis. As cells die and fragment, an immune response is potentially evoked. This *in vitro* system has several limitations including inhibited immune cell recognition and expansion given there is no lymphatic system available to perform selection and T cell expansion. An alternative hypothesis is this is driven by an amplified TRAIL effect.

Granzyme B ELISA (syngeneic)

To assess whether the immune system has a role to play in this synergism, I attempted to quantify the functional ability of cytotoxic T cells and NK cells in the presence of MSCs. Granzyme B, a serine protease, is an enzyme that works in partnership with perforin to mediate apoptosis.

This sandwich Enzyme Linked ImmunoSorbent Assay (ELISA) was used to measure the amount of protein, using paired antibodies. A plate coated with target bound antibody within each well was used. The MPM cell line GF230519 was initially seeded into two identical standard 96 well plates at 3000 cells per well. 24 hours later, MSCs, MSCTRAIL and PBMC's were co-cultured in different wells depending on the pre-exiting arrangement. Tumour cells were cultured alone, with MSCs and MSCTRAIL. PBMCs were cultured alone, with MSCs and with MSCTRAIL. Tumour cells were co-cultured with PBMCs followed by

either MSCs or MSCTRAIL. The fluid in each well was collected and deposited into the prepared antibody coated wells at 24 and 48 hours. A secondary antibody was then added followed by a manufacturer substrate to generate a signal representative of protein detection. This was measured using a colorimetric microplate reader. Granzyme B was measured at 24 and 48 hours as a surrogate for anti-cancer immunity.

Following 24 hours, wells absent of PBMC's released low levels of granzyme B compared with PBMCs only. This is likely to be due to experimental variation / background signal as opposed to actual granzyme B detection given there are no PBMCs in these wells. MSCs secreted the most granzyme B (355 pg/ml of versus 275 pg/ml in PBMCs alone, similar to PBMC + MSCTRAIL 250 pg/ml). When cultured with tumour cells, MSCs again secreted the most granzyme B (627 pg/ml versus 537 pg/ml in tumour).

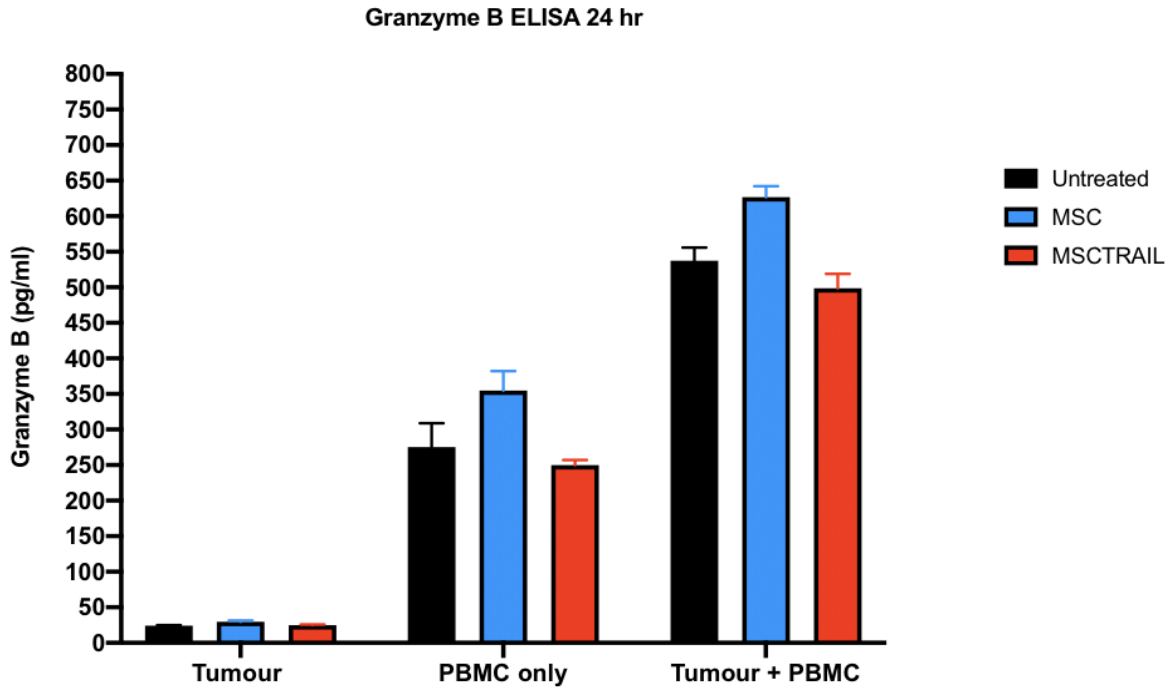

Figure 4. 37 – Granzyme B ELISA 24 hours

Co-culture assay of tumour cells alone, PBMCs alone and the combination of the two in the presence of MSCs and MSCTRAIL following 24 hours. Paired t test between MSCTRAIL + tumour v MSCTRAIL + PBMCs adjusted p=0.0120, MSCTRAIL + tumour v MSCTRAIL + tumour + PBMC p=0.0202 and MSCTRAIL + PBMCs v MSCTRAIL v MSCTRAIL + PBMCs + tumour p=0.0493.

Following 48 hours, similar findings were seen. Where PBMCs were co-cultured with MSCTRAIL this secreted the most granzyme B with a 17% increase compared to PBMC alone (PBMC 439, MSC 491, MSCTRAIL 515 pg/ml). This was not shown in the tumour and PBMC co-culture arm where untransduced MSCs secreted slightly higher levels of PBMCs (PBMC 792, MSC 879 and MSCTRAIL 828 pg/ml).

Although MSCTRAIL was not found to secrete the highest levels of granzyme B, this can be explained by the direct killing effect TRAIL has on PBMC's. It is likely MSCTRAIL induces immune cell death, hence the reduction in granzyme B. In addition to this, it was interesting to see MSCs associated with higher granzyme B levels compared with control, a finding suggestive of immune potentiation. These so called immune privileged cells are likely to modify their immune-phenotype depending on the circumstance. This paradigm of MSC potentiation is one of great interest.

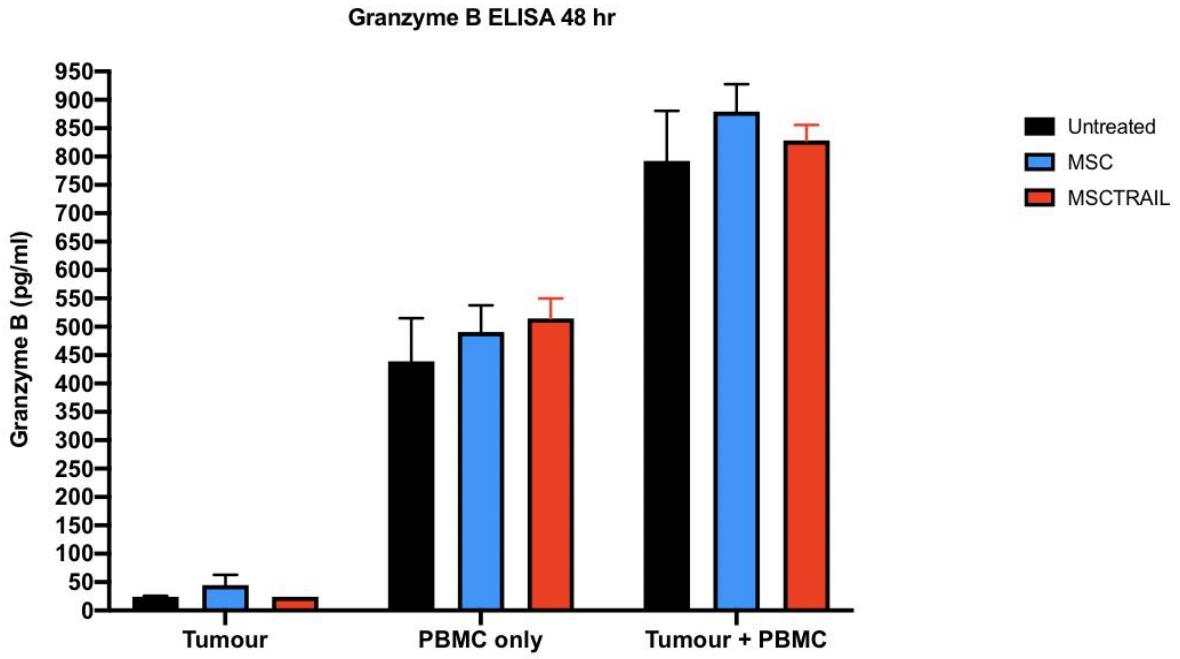

Figure 4. 38 - Granzyme B ELISA 48 hours

A co-culture assay of tumour cells alone, PBMCs alone and the combination of the two in the presence of MSCs and MSCTRAIL following 48 hours. Paired t test between MSCTRAIL + tumour v MSCTRAIL + PBMCs adjusted p=0.0174, MSCTRAIL + tumour v MSCTRAIL + tumour + PBMC p=0.0237 and MSCTRAIL + PBMCs v MSCTRAIL v MSCTRAIL + PBMCs + tumour p=0.0889.

A cytokine array which was running through initial optimisation steps has been postponed until after COVID19. A plan was made to measure a panel of cytokines following culture of tumour cells with PBMCs, MSCTRAIL, co-culture of both and tumour cells alone. A revealing experiment and one needed to support the immune mediated hypothesis of the aforementioned synergistic relationship.

Determination of a TRAIL mediated cause

To explore the role of TRAIL in this proposed synergistic relationship, i attempted to mitigate its function. TRAIL antagonistic antibodies were assessed but no suitable options were identified. The development of a knockout model was also reviewed, however given the time constraints this will be explored outside the remit of this thesis.

The best option was to develop a dominant negative construct of FADD, a critical protein in the external apoptosis pathway. By eliminating the intracellular function of FADD, apoptosis cannot be activated by TRAIL and so the cell relies on other means of contributing to death such as the immune mediated approach via perforin and granzyme B.

Granzyme B activates apoptosis through caspase activation such as caspase 3. Moreover, it also cleaves Bid a crucial intracellular protein which regulates mitochondria permeability via Bax and Bak. A more porous mitochondria allows for release of a plethora of proteins important in apoptosis such as cytochrome C release, which activated caspase 9.

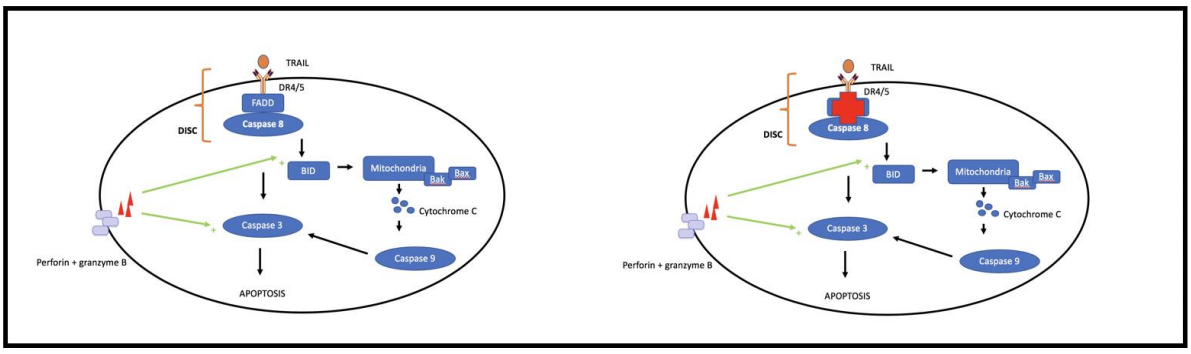

Figure 4. 39 – TRAIL mediated versus immune mediated cell death

Schematic describing the relationship between TRAIL induced and immune mediated apoptosis. TRAIL induces apoptosis through death receptor 4 and 5 (DR4/5). This leads to activation of caspase 8 via FADD, a component of the DISC and subsequent activation of a caspase cascade leading to cleaving of procaspase 3 to caspase 3 and subsequent apoptosis. By removing FADD, TRAIL is no longer able to induce apoptosis and immune cell direct death takes over via activation of BID and caspase 3, leading to apoptosis.

Luciferase labelled MDA-MB-231 cells, a TRAIL sensitive cell line, were transfected with a plasmid that expresses a truncated non-functioning form of FADD, i.e. a dominant negative construct (see methods section). Cells were treated with puromycin, an antibiotic used for selection and maintenance of cell lines with a transfected pac gene (S.alboniger). Cells were grown to confluency of 80-90%, harvested and plated in 96 well plate at 3000 cells per well in triplicate. In the same plate luciferase labelled cells with an intact FADD protein were seeded in triplicate at the same cellular concertation.

Cells were treated with recombinant TRAIL to validate the cell line. In the dominant negative constructs, it would be expected to lead to limited cell death, however in the non-transfected cell line, a reduction of cell viability in the order of 40-50% would be expected. The control cell line (luciferase labelled MDA-MB-231) was resistant to TRAIL on several occasions, a finding inconsistent with historical findings in our lab. Moreover the dnFADD construct was shown to be more sensitive inconsistent with the expected findings. This cell line was therefore abandoned and mesothelioma cell lines selected for transfection. A defect with the purchased plasmid was not ruled out.

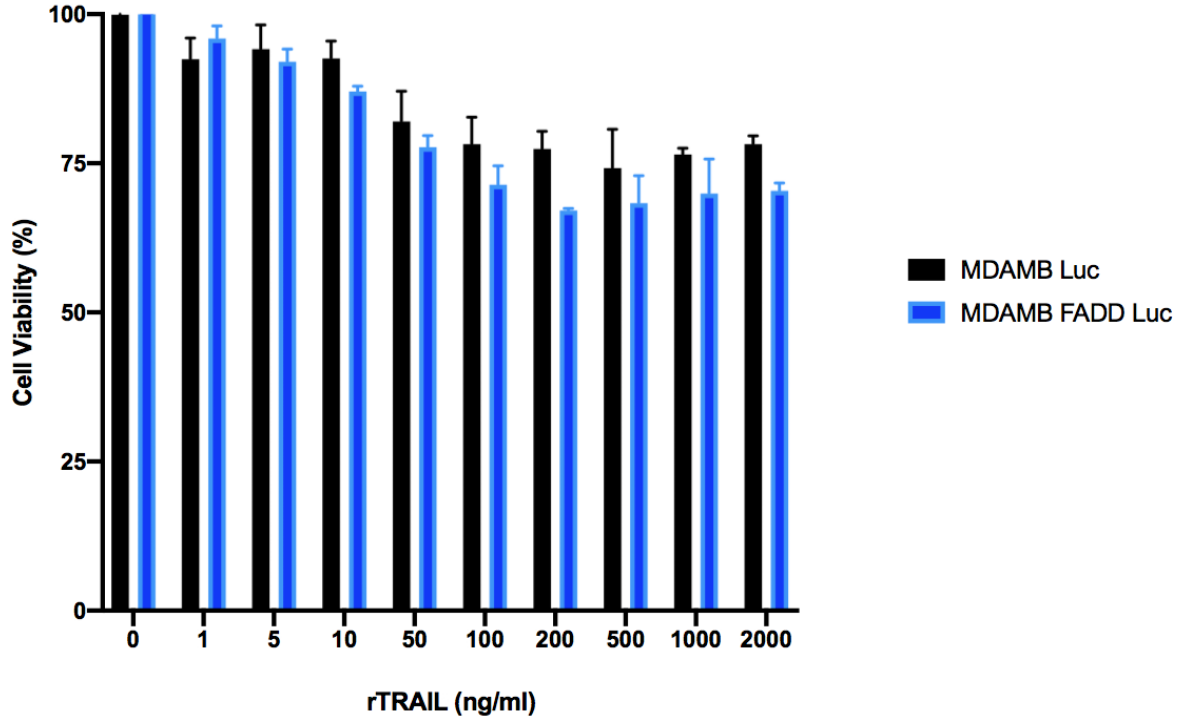

Figure 4. 40 – Cell viability assay comparing MDA-MB-231 and dnFADD MDA-MB-231

A cell viability assay comparing luciferase labelled MDA-MB-231 with luciferase labelled MDA-MB-231 expressing a dominant negative FADD. Sidak's multiple comparison test comparing MDAMB luc v MDAMB FADD luc 0 – p=>0.999, 1 - p=0.9091, 5 - p=0.9972, 10 - p=0.4094, 50 – p=0.7401, 100 – p=0.1703, 200 – p=0.0059, 500 – p=0.3244, 1000 – p=0.2093 and 2000 – p=0.0683

4.6 Discussion

Identification of synergy between MSCTRAIL and immune cells

The signal achieved between MSCTRAIL and PBMCs both in the allogeneic and syngeneic setting is exciting. The premise of MSCs downregulating the immune system is expected to promote cancer growth, however following genetic manipulation of MSCs to express TRAIL, a balance emerges between TRAIL mediate cancer cell death and downregulation of the immune system, tipping the balance towards cancer cell death.

This data offers further encouragement where both volunteer and matched PBMCs demonstrate clear synergy with MSCTRAIL. The logarithmic scale provides context to the level of synergism in the cell viability assays. Data is limited by the use of allogeneic PBMCs however matched PBMCs were later used and demonstrate similar yet less impressive findings. Like results chapter I H513 was used in these assays which is a further limitation given it is now known to be of adeno-squamous pathology. Use of MSCTRAIL in MPM remains in its clinical infancy, however pre-clinical data, in particular where MPM harbours mutations in BAP1, leads to sensitisation to TRAIL. Exploring the impact BAP1 has in this space would be immensely valuable, in particular *in vivo*. The significance of this is particularly pertinent as it ties in with the set-up of our clinical trial; *STRATEGIC, a genetically engineered allogeneic cell therapy for mesothelioma patients with loss of functional BAP1*. This phase II randomised controlled study explores the synergistic potential of front-line MSCTRAIL and chemotherapy in MPM. As immune checkpoint inhibition gathers pace in mesothelioma its clear it will soon have a role in the treatment of patients with MPM including an expected amendment to the treatment arms of this study. The addition of PBMCs and documented synergism is relevant in human models. It first questions the role MSCTRAIL has on the immune system, in particular cells that make up PBMCs. Its

delivery in human models can be potentiated when the immune system is alert and activated. In patients with cancer, immune evasion is a key mechanism of tumour growth. Utilising methods to overcome this with immune checkpoint inhibitors or similar is imperative in generating significant responses in patients receiving MSCTRAIL. The lack of improved activity when anti PD-1 treatment was added was disappointing, however I highlight earlier that this may not be the perfect model to test anti PD-1 treatment and in fact an *in vivo* system is critical to offer a more reliable conclusion. This adds further complexity to the issue as this would require murine MSCs which are phenotypically different to human MSCs, discussed later.

The synergistic potential can be extended further when cisplatin is added. As a backbone chemotherapy agent to MPM, MSCTRAIL is well placed to offer clinical value in this setting. Cisplatin has been extensively reviewed in the literature and where agents have been explored for activity in MPM, they are always combined with cisplatin. The addition of pemetrexed extends median survival by only a few months and so it seemed sensible to test MSCTRAIL alongside cisplatin only to keep potential toxicities low. Exploration of PD-L1 was key as the only licensed biomarker for sensitivity to anti PD-1 antibodies, although this is not necessarily used in every indication.

Performing apoptosis assays on the 3 selected MPM cell lines following flow cytometry MSC marker stratification is important. Although the cell viability data supports synergy, further validation is necessary to confirm this relationship. The screening process to identify cells that had a negative MSC marker (CD90) was crucial to be able to differentiate between MSCs and MPM cells. Without this differentiating factor it would be very difficult to ascertain which cell type was dying as both MPM and MSCs are co-cultured. Plans to

complete this panel are likely to pick up again post COVID19 – towards the end of the year. Without cell death data complimenting the viability assays, this remains a significant limitation of the work and is acknowledged as an area that requires completion.

Development of a syngeneic model

A clear criticism of the volunteer immune cell work was a non-self effect (dissimilar HLA subtype to cell line). The development of the syngeneic platform to address this non-self effect was based around identifying cases with malignant pleural effusion. Biopsy collection was a far more complex affair. Biopsy samples were collected and frozen where the opportunity arose however not enough samples were achieved to come to a meaningful conclusion. As more samples are collected and frozen these can be digested and developed into cell lines for later work. More MPM pleural effusion samples are desperately needed. Reviewing other centres with a significant number of MPM patients offers an opportunity to expand this cohort of samples. A dedicated pathway to identify cases with minimal disruption to clinical activity is needed. Surgical cases identified from the front end is key to initiating the process. Keen and enthusiastic surgical colleagues alerting us to potential suitable samples is paramount. Occasionally, patients were consented by surgical teams to avoid repeated visits to centres. Dedicated personnel to obtain samples at the time of surgery and bring back to the lab would be extremely helpful and avoid wasted time. This would allow immediate processing of samples and avoid stagnation minimising the risk of a wasted sample. Some samples required repeated trips to surgical medical facilities compromising the quality of the sample given the repeated delays. Once the samples were back in the lab, they were put through a rigorous experimental pipeline as described earlier.

The success of developing a cell line was low. Of the 31 cases formally brought to the lab for culture, only 9 were deemed successful (> 10 passages). Success was not based on the number of cells isolated but rather the aggressive dividing potential of the cells. Samples where 5 million cells were seeded in a T175 flask led to no cell division whereas cases of 100,000 cells in a T75 grew to confluency within days. Predicting which cell lines grow and which die remains a mystery. The inherent behaviour of a malignant cell and its surrounding microenvironment plays a role.

The consistency of the cells isolated was another problem. Transduction of cells to express luciferase occurs in all cell types not just cancer cells. Purification of these cells were sought through persistent passage to clear non-malignant cells from the sample. Cells were transduced to express luciferase and following subcutaneous implantation into mice (patient derived xenograft) and subsequent tumour growth, mice were culled, cells re-collected and re-cultured.

The synergistic relationship was extended to matched PBMC and tumour samples, a reassuring testament to the originally identified relationship. Of particular note, Fig 4.30 showed a phenomenal response to MSCTRAIL in a patient previously treated with cisplatin. Reasons behind this remain unclear, however homing of the MSCs to the tumour and upregulation of death receptors are likely to influence this outcome. The greatest disappointment stemmed from lack of efficacy of any of the biological immunomodulatory agents currently investigated in the clinic. In particular, it was disappointing to see immune checkpoint inhibition designed to disturb the PD-1/PD-L1 axis not have any impact whatsoever. The model is not an ideal platform to test immunogenic agents and an *in vivo* platform is preferred. The reasons behind not pursuing this were 2-fold. Firstly, human MSCs

are phenotypically different to murine MSCs. To conduct a mouse experiment would require murine MSCs which are not representative of human developed MSCTRAIL. Secondly, our routinely use immune SCID mice would not be suitable for an experiment which relies on an immune response to cancer. The only option would be humanised models, which are characteristically difficult to acquire and manage. A heavily discussed future prospect but not one within the remit of this current programme of work. Functional testing of anti PD-1 *in vitro* was a further challenge evidenced by using the well known B16 melanoma murine cell line (transduced to express luciferase) cultured with murine collected PBMCs and anti PD-1. This led to no change in cell viability (data not shown) questioning again the validity of assay.

A collection of early and late passage cell lines and their extracted DNA was planned for exome sequencing however these samples have now been halted until following COVID19. Hugely disappointing given this was the product of 2 years of worth. Once the data is finally processed, retrieved and analysed its I plan to report it in a separate manuscript.

A further limitation to this work was the lack of evaluation of the proportion of immune cells in each PBMC sample prior to the assays being performed rather than assume the population based on historical assays. This could also have implications on immune checkpoint blockade efficiency.

Understanding the mechanism behind the synergy

The mechanism underlying this synergism remains unknown. Several theories emerged including the possibility of tumour specific apoptosis debris following MSCTRAIL treatment. This plethora of tumour antigen was thought to play a role in immune potentiation,

although this remains limited with the model used. Developing the dnFADD construct seemed easy in principle, however it was hugely difficult to optimise. Sensitivity of untransduced MDA-MB-231 to TRAIL was lacking. Discarding the cell line, re-thawing and culturing a new version as well as 1 or 2 new MPM cell lines are planned followed by repeat transduction with the plasmid. Moreover, uncertainty regarding the credibility of the plasmid has led to plans to re-purchase it (yet to receive due to COVID19). A direct knockout of FADD is also being explored, which requires CRISPR-Cas9, a huge time investment but one that may be worth pursuing.

The granzyme B ELISA was not as informative as I'd hoped. MSCTRAIL secreted less granzyme B thought partly due to apoptosis of immune cells by MSCTRAIL. Of interest, MSCs were associated with higher granzyme B levels compared with control, a finding suggestive of immune potentiation, supporting the premise that their immune-phenotype can change depending on the environment. The planned cytokine assay will offer more support to this premise.

RESULTS CHAPTER III

Exploring the role of HSP90 inhibition in combination with TRAIL in malignant pleural mesothelioma

Hypothesis

I hypothesise that inhibition of HSP90 leads to sensitisation to TRAIL in MPM, in particular when loss of function mutations of BAP1 are present.

5 RESULTS III EXPLORING THE ROLE OF HSP90 INHIBITION IN COMBINATION WITH TRAIL IN MALIGNANT PLEURAL MESOTHELIOMA

HSP90 inhibition has been explored across many tumour types. Data has emerged reporting its inhibition leading to cell cycle arrest and apoptosis in MPM, which is associated with reduction in AKT and survivin levels (290). Moreover, the HSP90 inhibitor ganetespib has demonstrated synergy with standard of care chemotherapy in MPM (291). As described, HSP90 inhibition in colon cancer leads to upregulation of death receptor 5 (DR5), which binds TRAIL, triggering apoptosis. This upregulation may pave the way for combination therapy using HSP90 inhibitors with TRAIL in BAP1 mutant MPM, given the previous published work from our lab (144, 292).

5.1 MPM is associated with sensitivity to ganetespib and human recombinant TRAIL

Exploration of sensitivity to HSP90 inhibition with and without rTRAIL is best performed using a co-culture assay assessing for cell viability and death.

4 cell lines were selected based on their historical resistance to TRAIL. A549 a common reference lung cancer cell line was used alongside 3 other MPM cell lines; MPP89, H226 and H513.

MPM is associated with greater loss in cell viability when rTRAIL is combined with ganetespib

Luciferase labelled cells were grown in standard culture conditions to a confluency of 80-90%. Cells were harvested via trypsinisation and seeded in black clear bottom 96 well plates at 3000 cells per well. Following 24 hours of incubation, cells were treated with a dose range of ganetespib (0-100 nM) and a fixed dose (100ng/ml) of rTRAIL. Cells were incubated for a further 48 hours followed by measurement of bioluminescence.

Both A549 and MPP89 demonstrated reduction in cell viability where TRAIL resistance was clearly evident from the outset. The combination of ganetespib and rTRAIL led to synergy. H226 and H513 exhibited some sensitivity to TRAIL in the absence of ganetespib, progressing to impressive losses of cell viability at higher doses of ganetespib. These lines may all be related to TRAIL effect.

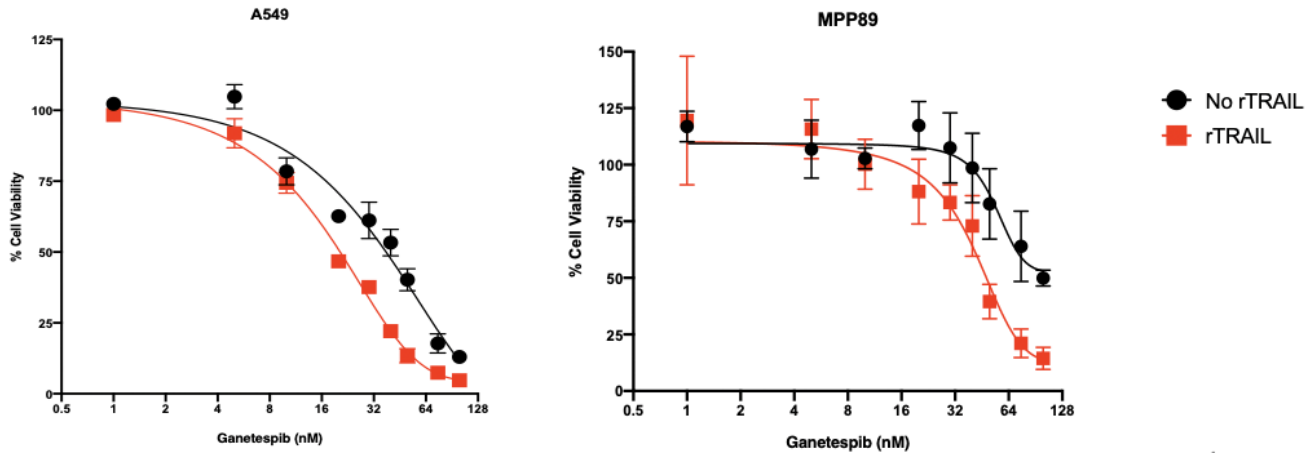

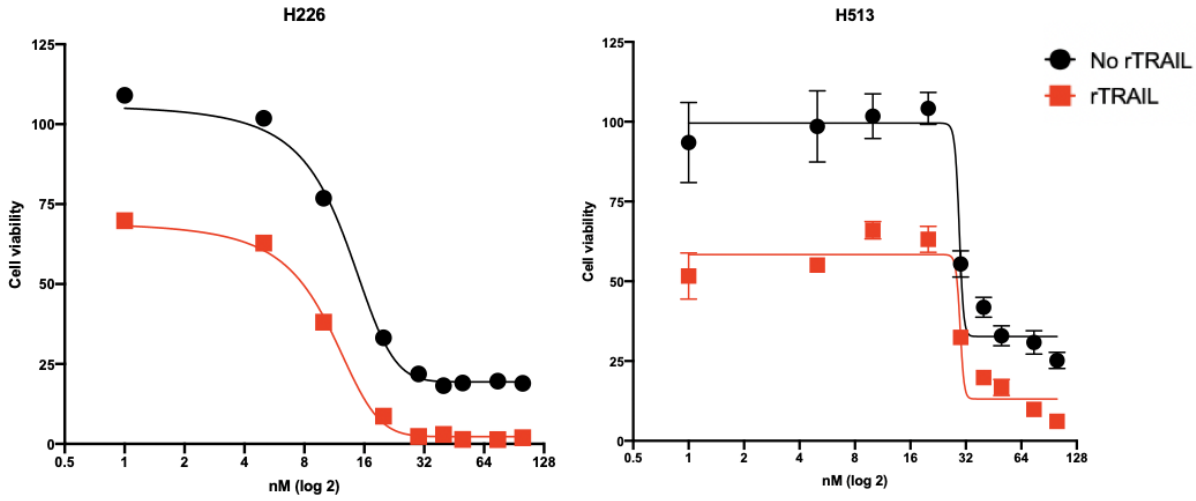

Figure 5. 1 - Cell viability (bioluminescence) of 4 cell lines comparing ganetespib +/- rTRAIL

4 luciferase labelled cell lines underwent a cell viability assay when treated with a dose range of ganetespib and rTRAIL. Following 48 hours cell viability was measured using bioluminescence (logarithmic scale – first dose 0nM). Two way ANOVA to assess interaction between ganetespib and ganetespib + trail – A549 P<0.0001, MPP89 p=0.0020, H226 <0.0001, H513 p<0.0001.

An alternative method of measuring cell viability uses an MTT assay. Cells transduced to express luciferase are no longer needed. Untransduced cells were grown in standard culture conditions. When cells reached 80-90% confluency they were harvested via trypsinization and seeded in a 96 well plate at 3000 cells per well. Following 24 hours of incubation cells were treated in the same way as the luciferase assay above with a dose range of ganetespib and fixed dose of (100ng/ml) rTRAIL. At 48 hours MTT reagent was added to the cells and replaced with DMSO 3 hours later. Cells were carefully agitated for 5 minutes before measuring metabolic activity using a spectrophotometer.

TRAIL sensitivity was reproducible in both assays and similar patterns of response to treatment were seen. A dose of 30nM of ganetespib was taken forward for future experiments as this appeared to be a turning point in the cell viability curves, in particular when MPP89 and H513 were treated.

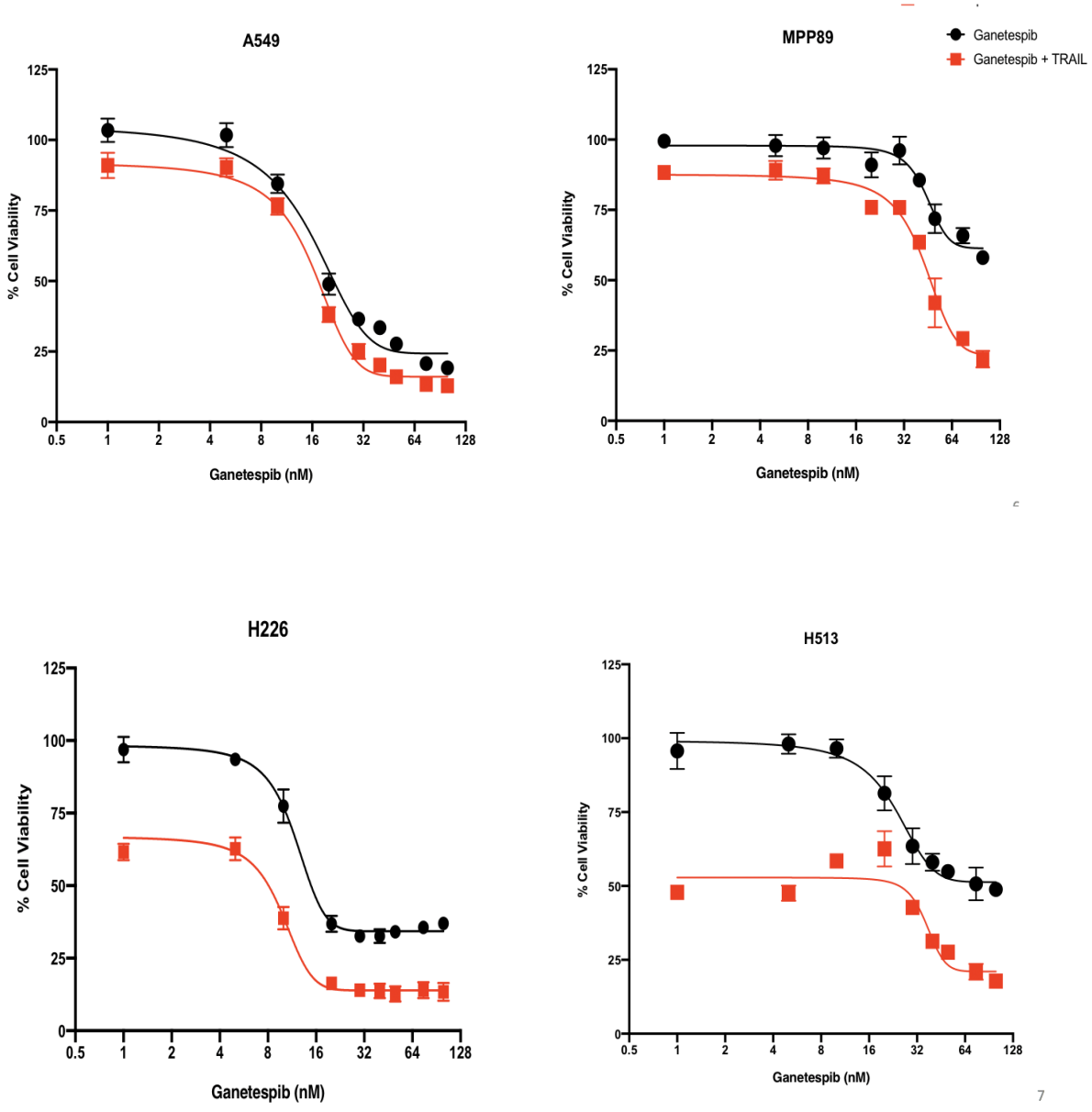

Figure 5. 2 - Cell viability (MTT) of 4 cell lines comparing ganetespib +/- rTRAIL

4 untransduced cell lines underwent a cell viability assay when treated with a dose range of ganetespib and rTRAIL. Following 48 hours cell viability was measured using an MTT assay. Two way ANOVA to assess interaction between ganetespib and ganetespib + trail – A549 P=0.8008, MPP89 p=<0.0001, H226 <0.0001, H513 p<0.0001.

To validate these findings further an apoptosis assay was performed assessing for cell death following treatment. 4 MPM cell lines including H513, H2818, H2803 and CRL2081 were assessed.

Cells were grown in standard culture conditions and once a confluency of 80-90% was reached they were harvested via trypsinisation and subjected to centrifugation. Cancer cells were stained for DiI as a labelling tool and seeded into a 96 well plate at 3000 cells per well. Following 24 hours of incubation, cells were treated with 30nM of ganetespib and 100ng/ml rTRAIL.

Following a further 48 hours of incubation, cells were transferred to a V shaped 96 well plate following washing with PBS and trypsinization of the desired wells. Cells were stained, subjected to centrifugation and stained with Annexin V and DAPI, markers of early and late apoptosis respectively. Cells were then assessed using flow cytometry. CRL2081 and H2803 were both particularly sensitive to the combination of therapy at 24 and 48 hours.

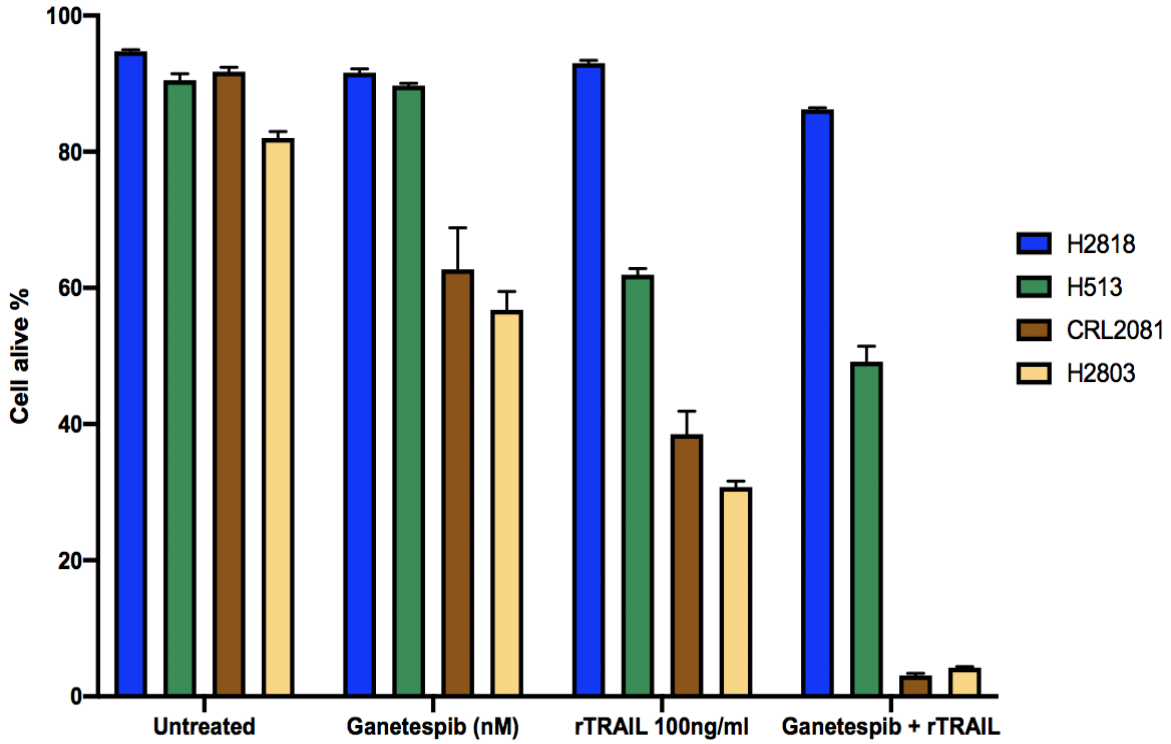

Figure 5. 3 – Assessment of apoptosis in MPM following 24 hours of HSP90i/rTRAIL

4 MPM cell lines treated with 30nM of ganetespib and 100ng/ml of rTRAIL. Paired t test comparing untreated with ganetespib (G), rTRAIL (T) and ganetespib + rTRAIL (G+T). H2818 p=0.0167 (G), p=0.0320 (T) and p=0.0006 (G+T), H513 p=0.1946 (G), p=0.0011 (T) and p=0.0018 (G+T), CRL2081 p=0.0134 (G), p=0.0010 (T) and p<0.0001 (G+T) and H2803 p=0.0016 (G), p<0.0001 (T) and p<0.0001 (G+T),

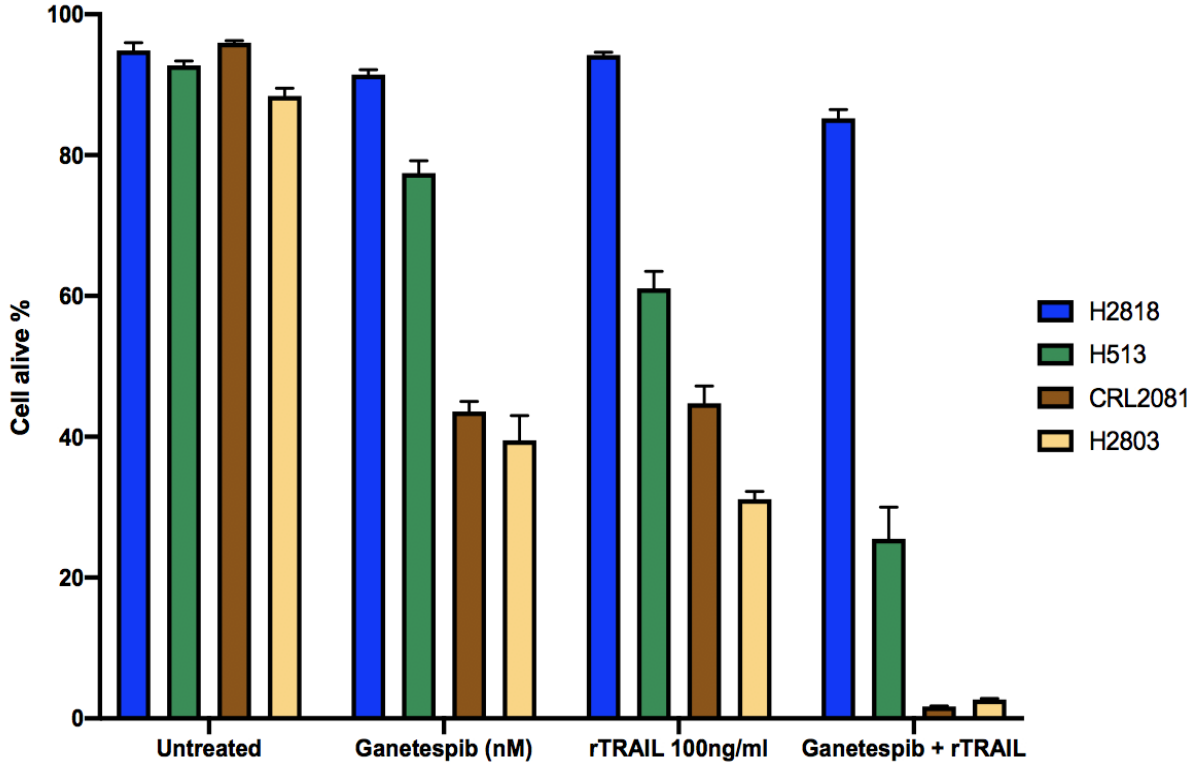

Figure 5. 4 - Assessment of apoptosis in MPM following 48 hours of treatment

4 MPM cell lines treated with 30nM of ganetespib and 100ng/ml of rTRAIL. Paired t test comparing untreated with ganetespib (G), rTRAIL (T) and ganetespib + rTRAIL (G+T). H2818 p=0.0551 (G), p=0.2451 (T) and p=0.0190 (G+T), H513 p=0.0073 (G), p=0.0023 (T) and p=0.0012 (G+T), CRL2081 p=0.0002 (G), p=0.0009 (T) and p<0.0001 (G+T) and H2803 p=0.0.0009 (G), p<0.0003 (T) and p<0.0001 (G+T),

5.2 MPM is associated with sensitivity to ganetespib and MSCTRAIL

MSCs remain viable in the presence of ganetespib

Prior to conducting co-culture experiments, it was important to identify whether HSP90 inhibition had an impact on the cell viability of MSCs. To explore this, MSCs and MSCTRAIL were cultured in a 96 well plate in triplicate. Following 24 hours of incubation, cells were treated with a dose range of ganetespib (0-100 nM). Following a further 48 hours, cell viability was assessed using an MTT assay. MSCs were not significantly affected but MSCTRAIL suffered some loss in viability. There is no clear explanation for this. In spite of this, the drop in MSCTRAIL viability of approximately 20% was deemed acceptable to continue its assessment with ganetespib. Based on these experiments, further co-culture assays were performed using MSCTRAIL and ganetespib.

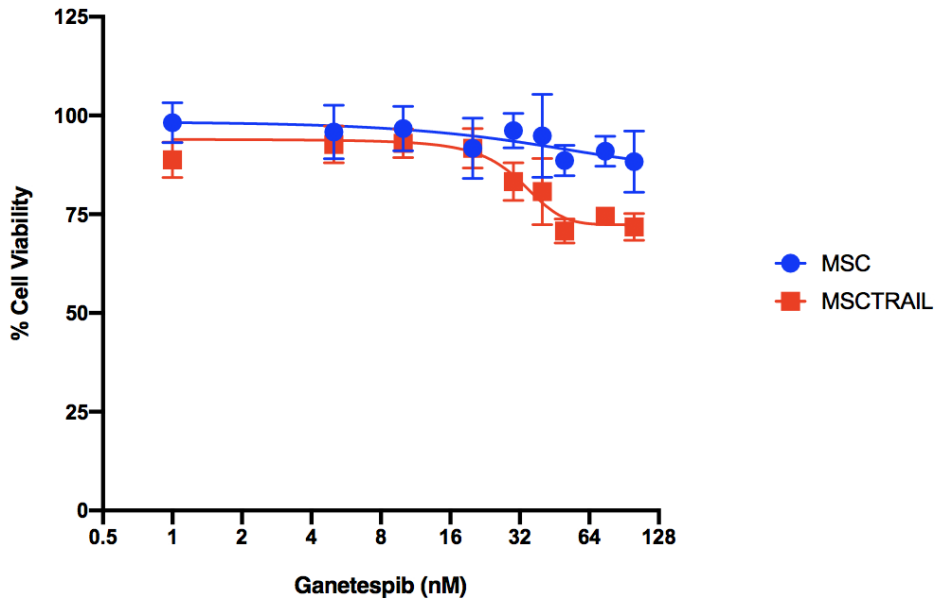

Figure 5. 5 – Cell viability assay of MSCs and MSCTRAIL

MSC and MSCTRAIL were independently cultured for 48 hours with a dose range of ganetespib (0 – 100nM). Two way ANOVA to assess interaction between MSC and MSCTRAIL p=0.1688

As described in previous chapters clinical use of human recombinant TRAIL offers little bioavailability given its short half-life. The attraction of using MSCTRAIL is not just its ability to remain *in vivo* longer but also its homing potential to the tumour.

MPM is associated with greater loss in cell viability when MSCTRAIL is combined with ganetespib

MPM cell lines were cultured and seeded in 96 well plates in triplicate (3000 cells per well). Following 24 hours of incubation MSCTRAIL was added (2500 cells per well) and a dose range of ganetespib. At 48 hours post treatment cells were measured for bioluminescence and reported below.

Some of the cell lines were sensitive to MSCTRAIL upfront but led to further reductions in cell viability when ganetespib was added and the dose increased.

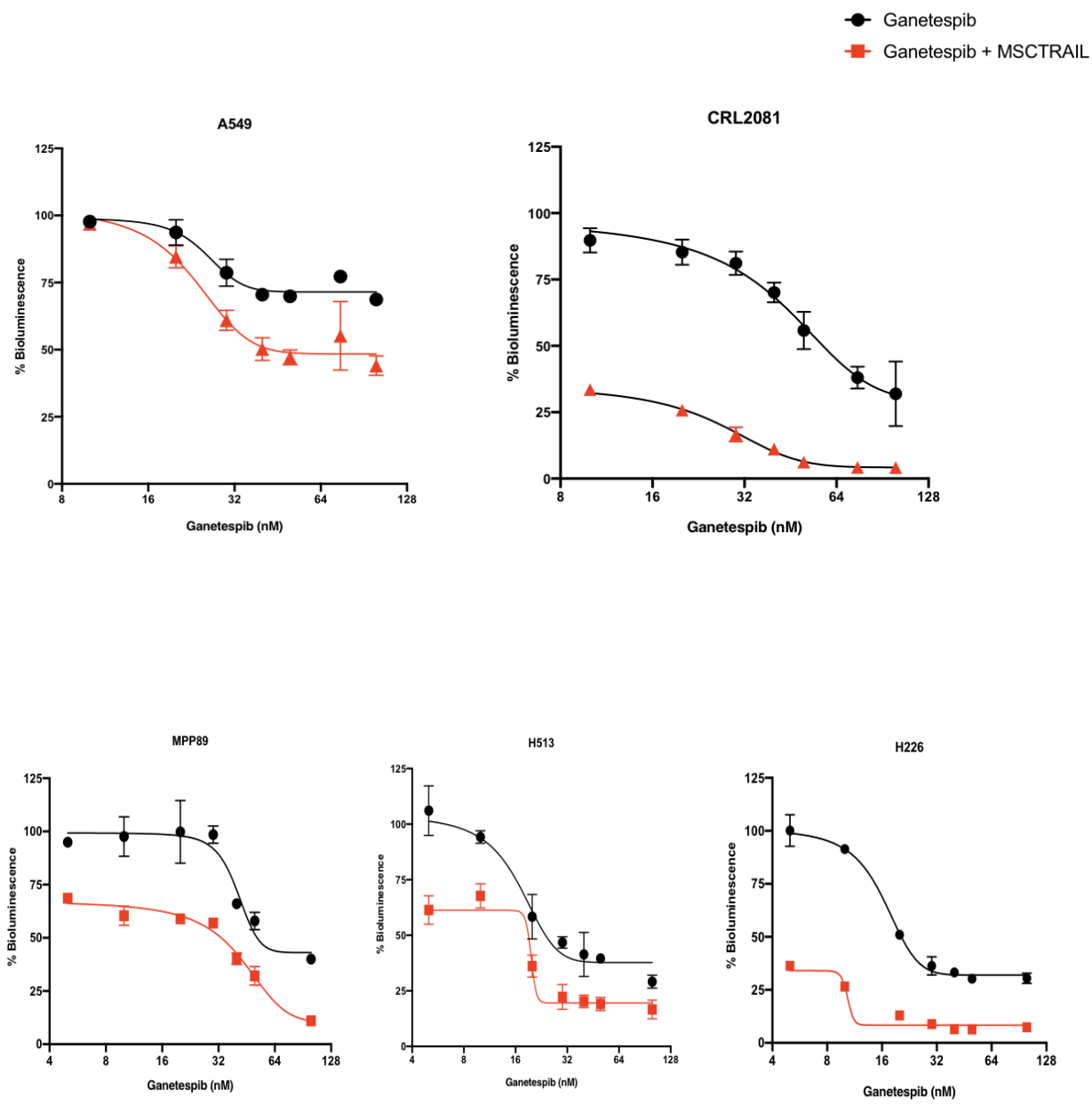

Figure 5. 6 – Cell viability (luciferase assay) of MPM cells treated with MSCTRAIL and ganetespib

5 cell lines transduced to express luciferase underwent a cell viability assay when treated with a dose range of ganetespib and MSCTRAIL. Following 48 hours bioluminescence was measured (logarithmic scale – starting dose 0nM). Two way ANOVA to assess interaction between ganetespib and ganetespib + MSCTRAIL – A549 P<0.0001, CRL2081 p<0.0001, MPP89 p=0.0699, H513 p<0.0002 H226 <0.0001.

MPM is associated with greater cell death when MSCTRAIL is combined with ganetespib

To validate this finding further an apoptosis assay was performed. Untransduced MPM cell lines were cultured and seeded in a 96 well plate at 3000 cells per well. Following 24 hours of incubation rTRAIL (100ng/ml), MSCTRAIL (2500 cells per well) and ganetespib (30nM) were all added followed by a further 48 hours of incubation.

Cells were transferred to a V shaped 96 well plate following washing with PBS and trypsinization of the desired wells. Cells were stained, subjected to centrifugation and stained with Annexin V and DAPI. Cells were then assessed using flow cytometry. Independent of TRAIL sensitivity the combination of HSP90 inhibition and TRAIL effect led to the greatest cell death.

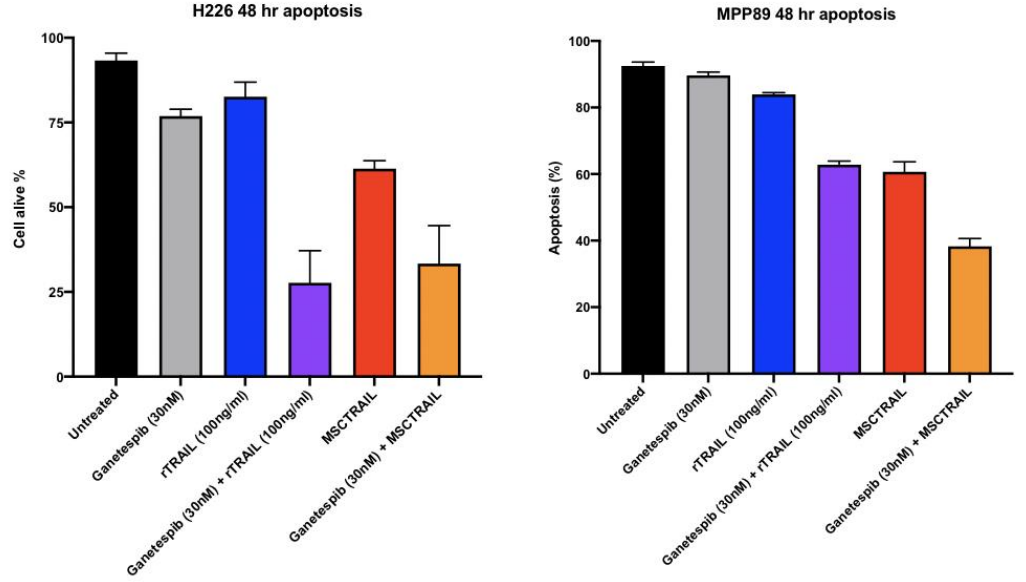
H226 48 hr apoptosis
Cell alive %
100
75
50
25
0
Untreated
Ganetespib (30nM)
rTRAIL (100ng/ml)
Ganetespib (30nM) + rTRAIL (100ng/ml)
MSCTRAIL
Ganetespib (30nM) + MSCTRAIL
MPP89 48 hr apoptosis
Apoptosis (%)
100
80
60
40
20
0
Untreated
Ganetespib (30nM)
rTRAIL (100ng/ml)
Ganetespib (30nM) + rTRAIL (100ng/ml)
MSCTRAIL
Ganetespib (30nM) + MSCTRAIL
Untreated
Ganetespib (30nM)
rTRAIL (100ng/ml)
Ganetespib (30nM) + rTRAIL (100ng/ml)
MSCTRAIL
Ganetespib (30nM) + MSCTRAIL

16

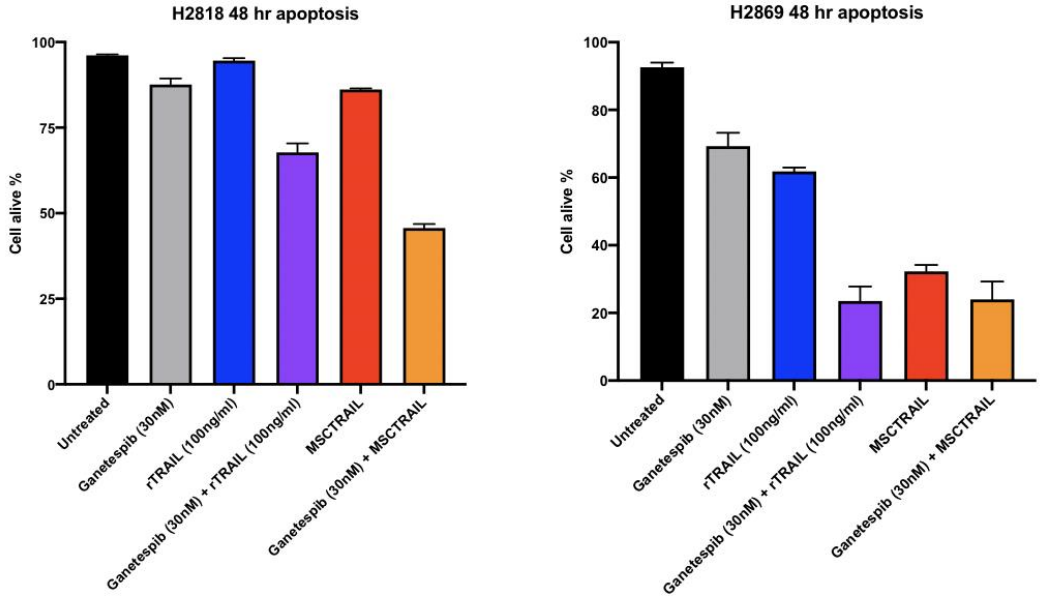
H2818 48 hr apoptosis
Cell alive %
100
75
50
25
0
Untreated
Ganetespib (30nM)
rTRAIL (100ng/ml)
Ganetespib (30nM) + rTRAIL (100ng/ml)
MSCTRAIL
Ganetespib (30nM) + MSCTRAIL
H2869 48 hr apoptosis
Cell alive %
100
80
60
40
20
0
Untreated
Ganetespib (30nM)
rTRAIL (100ng/ml)
Ganetespib (30nM) + rTRAIL (100ng/ml)
MSCTRAIL
Ganetespib (30nM) + MSCTRAIL

Figure 5. 7 – Assessment of apoptosis in MPM following 48 hours of treatment

4 MPM cell lines subjected to a cell death assay when cultured with rTRAIL, MSCTRAIL and a fixed dose of ganetespib. Flow cytometry was performed and cell live measured and reported above. Paired t test comparing untreated (U) to ganetespib (G), MSCTRAIL (M) and ganetespib + MSCTRAIL (G+M). H226 p=0.0009 (G), p<0.0001 (M), p=0.0152. MPP89 p=0.0083(G), p=0.0018 (M), p=0.0003 (G+M). H2818 p=0.0139 (G), p=0.0010 (M), p=0.0003. H2869 p=0.0041 (G), p=0.0010 (M), p=0.0031 (G+M).

5.3 Mutations in BAP1 do not sensitise to ganetespib and rTRAIL

Mutations in BAP1 sensitise to TRAIL leading me to study whether this can be augmented further with the addition of HSP90 inhibition.

The H226 BAP1 cell line constructs were used to explore this further. Untransduced H226 and wild type were cultured and seeded in a 96 well plate at 3000 cells per well. Following 24 hours of incubation 100ng/ml rTRAIL and a dose range of ganetespib was added. MSCTRAIL was excluded from this analysis as the untransduced (non luciferase) MPM cells required an MTT assay to assess for a cell viability meaning only 1 cell type in question could be Included in the wells.

Following 48 further hours of incubation, MTT reagent was added to each well and replaced with DMSO 3 hours later followed by measurement of cell viability. Untransduced BAP1 (mutant BAP1 cell line) led to a fall in cell viability when rTRAIL was added, however the

BAP1 wild type construct led to the same impressive effect making interpretation of this challenging.

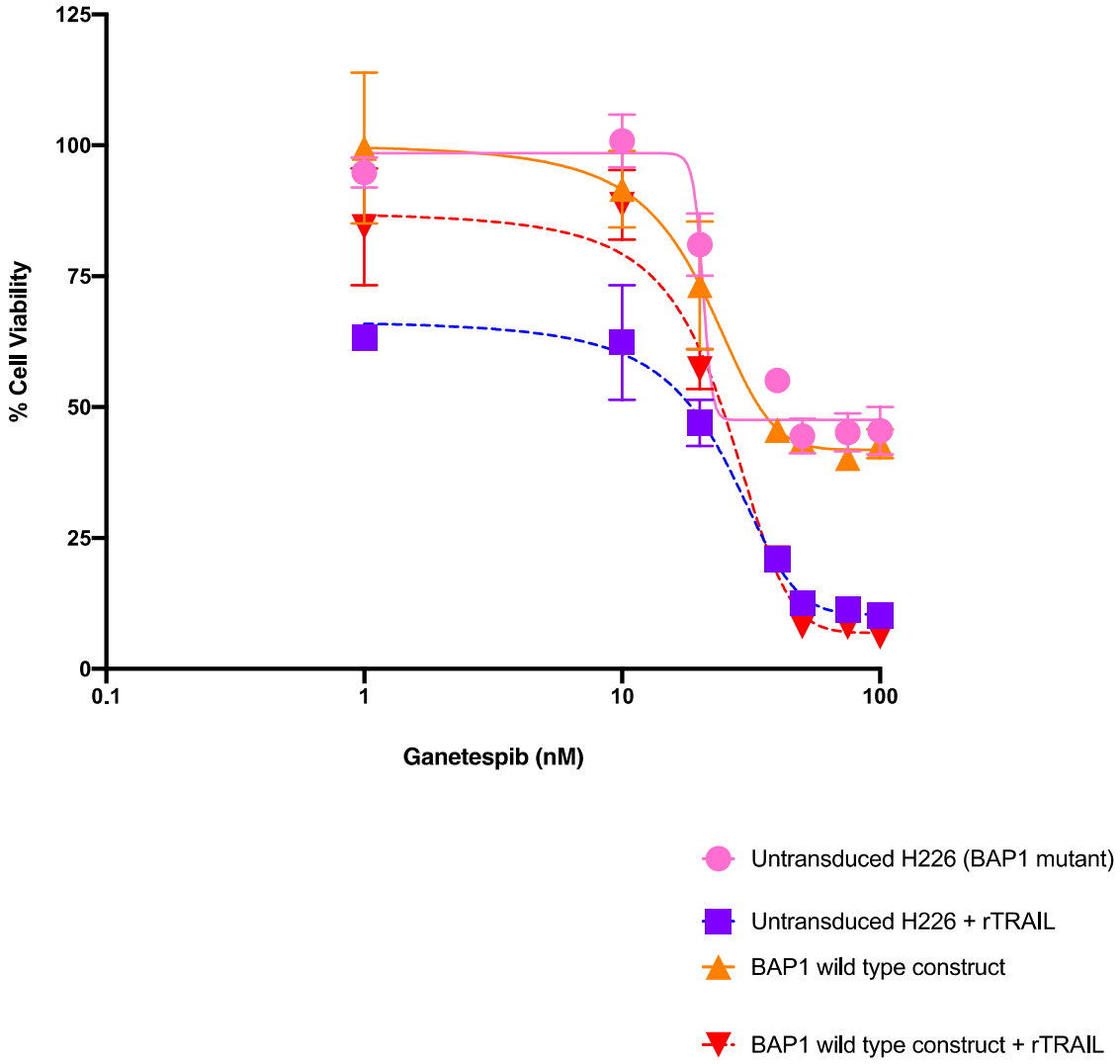

Figure 5. 8 - Cell viability of BAP1 mutant H226 and its BAP1 wild type construct

H226 cell line constructs were (untransduced H226 and wild type constructs) treated with / without rTRAIL and a dose range of ganetespib. Following 48 hours, cell viability was measured. Two way ANOVA to assess interaction between curves – untransduced H226 v addition of rTRAIL (p=0.9547), untransduced H226 v wild type construct (p=0.4491), BAP1

wild type construct v BAP1 wild type construct + rTRAIL (p=0.0009) and untransduced H226 + rTRAIL v BAP1 wild type construct + rTRAIL (p<0.0001).

5.4 HSP partner proteins are upregulated following treatment with TRAIL

To explore the relationship between HSP90 inhibition and TRAIL / apoptosis, an apoptosis array (R&D systems) was performed. A panel of 35 human apoptosis proteins can be analysed simultaneously (see methods section for detailed description).

CRL2081 was used for this experiment based on the cell viability data described earlier. Cells were cultured in a 96 well plate for 24 hours and treated with 30nM of ganetespib and 100ng/ml of rTRAIL or 30nM of ganetespib alone.

Following a further 24 hours of incubation the cells were retrieved and target proteins bound by the various assay antibodies and measured using a chemiluminescent reaction.

Of the 35 proteins, a select few have been highlighted on the array and represented in graphical form below. HSP60 and particularly HSP70 increase following the combination of HSP90 inhibition and rTRAIL.

CRL2081 apoptosis array

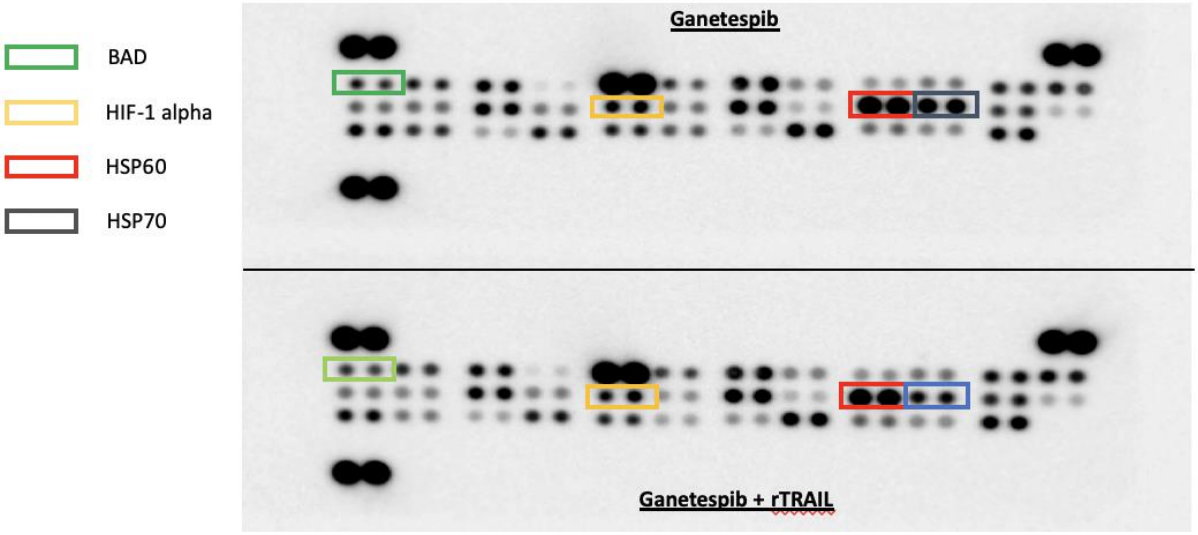

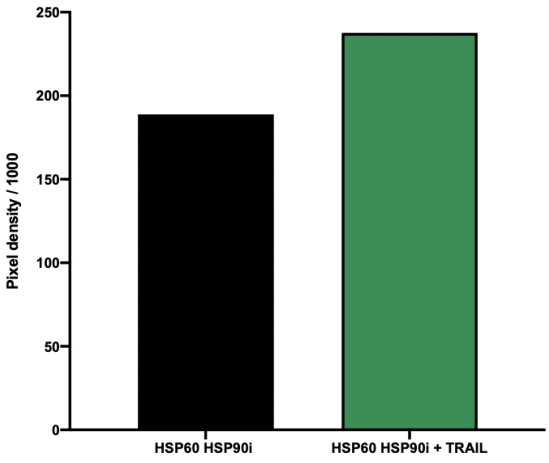

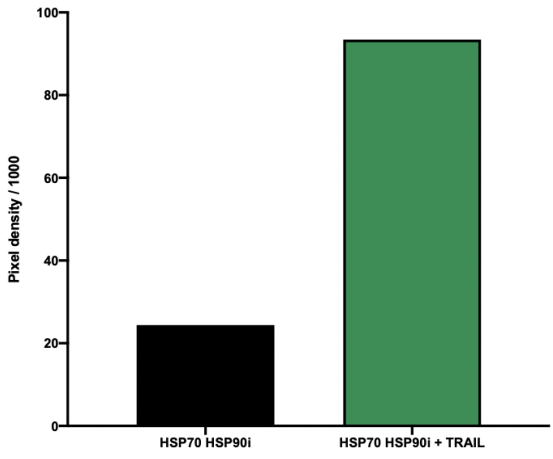

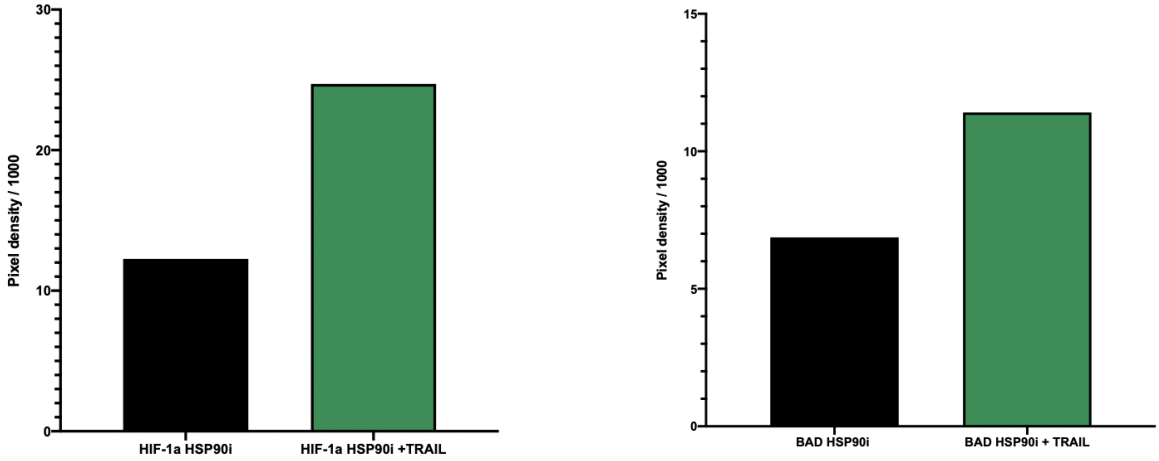

Figure 5. 9 – Apoptosis array of CRL2081

An apoptosis array demonstrating differences in pixel density between HSP90 inhibition and the addition of rTRAIL. Pixel density was reduced by a factor of 1000 to ease data interpretation. The top array represents CRL2081 treated with ganetespib alone and the bottom array in combination with rTRAIL Assistance was offered by Dr Krishna Kolluri.

5.5 Discussion

Exploration of HSP90 inhibition was triggered by clinical data showing that in MPM significant activity has been demonstrated (294). The rationale for combining this with TRAIL was supported by pre-clinical work showing upregulation of death receptors likely to synergise with TRAIL (292).

The different cell viability assays confirmed that when TRAIL resistant cell lines where treated with ganetespib further loss of cell viability was achieved as the dose increased. Some of the cell lines had some sensitivity to TRAIL upfront making assessment more difficult however despite this, activity can be seen in the combination. Cell lines used in the apoptosis assays differed to the initial cell viability assays. Repeated experiments were performed and where cell lines had been passaged repeatedly these were discarded and replaced with the same cell lines. Where issues occurred during cell line culture these were replaced with alternative mesothelioma cell lines. Following identification of a signal when ganetespib was combined with rTRAIL (Fig 5.1 and 5.2) I purposefully screened our catalogue of cell lines known to be TRAIL resistant in an attempt to demonstrate a reversal of this resistance phenotype. Although a further exchange of cell lines occurred in the apoptosis assay in figure 5.7 when MSCTRAIL was introduced this was controlled with simultaneous rTRAIL to minimise selection bias.

Using MSCTRAIL adds further to this, although this may be best demonstrated in an *in vivo* model which was planned for March 2020 (pre COVID19 pandemic plan). Work is still needed to characterise further the mechanism underlying this relationship as both exploration of the role of BAP1 and key apoptosis proteins failed to add further to this.

The BAP1 mutant and knock in cell line assays require more work. The IC50 for each arm confirms the BAP1 mutant (H226 untransduced)/TRAIL/HSP90 treatment arm performs best supporting my initial hypothesis. Moreover, the BAP1 knock in cell line (wild type) leads to a similar end cell viability suggesting resistance might be overcome by the addition of ganetespib. Far too many caveats exist to draw any reliable conclusions but with a further time investment to optimise this assay I predict a clearer separation of the treatment arms can be achieved. Moreover, BAP1 knockdown cell lines can be used to illustrate this point further as can pure BAP1 knock out cell line constructs, although as mentioned the latter is a much more challenging endeavor. Without good knock in / knockdown validation its uncertain whether BAP1 has a role in HSP90 inhibition.

The apoptosis array revealed interesting findings. Upregulation of partner HSP proteins as a result of the addition of recombinant TRAIL may not fully explain the sensitivity to HSP90 inhibition. It is well documented that pharmacological inhibition of HSP90 results in upregulation of other partner proteins such as HSP70, known as a heat shock response (308) a speculated mechanism of resistance to these drugs. It's less well known whether rTRAIL augments this further. The excellent response seen earlier in the apoptosis and cell viability assays to the combination could be due to the overwhelming sensitivity to TRAIL upfront masking any resistance mechanisms to HSP90 inhibition. Equally we know HSP90 inhibition leads to upregulation of death receptors 4 and 5 which is also confirmed in this array (data not represented in graphical form) which might explain the sensitivity to the combination. Measuring death receptors can be challenging as both normal and malignant tissue express these proteins. Detection using immunohistochemistry can be user dependent meaning more sophisticated methods may be needed such as qPCR or similar.

Moreover, HIF 1a was upregulated following rTRAIL and HSP90i treatment (Fig 5.9). It's found to be upregulated in many cancers and implicates processes such as angiogenesis and cell proliferation. Considering the difficultly in not having an untreated control arm, this suggests the addition of rTRAIL leads to further upregulation of HIF 1a. This however may not necessarily lead to reduced efficacy of TRAIL. Data published shows that the level of hypoxia is important in regulating TRAIL mediated death. It has been shown that conditions of moderate hypoxia lead to no growth retardation despite HIF 1a upregulation (309). The implications of this may manifest as a resistance mechanism as treatment continues and hypoxia builds. To validate upregulation of these proteins a western blot is necessary.

The mechanism of action of ganetespib and newer generations of HSP inhibitors leads one to wonder what the off-target effects are. Its unselective approach is likely to cause a higher toxicity profile, although clinical trials suggest this drug is very tolerable; a key characteristic when considering drug combination therapy for patients.

6 SUMMARY AND FUTURE DIRECTION

Clinicians treating patients with advanced MPM have struggled to find successful therapeutic strategies over the years. Several avenues have been explored but other than front-line chemotherapy little else has been licensed and shown to provide significant benefit.

Initial data from our lab suggests loss of function mutations in BAP1 sensitise to TRAIL. This is yet to be tested in a clinical trial, however the projected time line is 12 – 18 months from now once ongoing phase I data is available. As the treatment paradigm in MPM is soon to change with the introduction of immune checkpoint blockade, this creates a greater challenge for MSCTRAIL to compete and demonstrate efficacy in this patient group.

Several opportunities to augment the effect of TRAIL have been explored in this thesis in particular its relationship with the immune system, which is particularly pertinent given the anticipated future change to the treatment pathway. As MSCTRAIL finds its place in MPM with the upcoming clinical trial STRATEGIC, further avenues of investigation are warranted to augment this effect further.

6.1 DNA damage response and TRAIL

Data presented in results chapter III shows that BAP1 has a non-critical role in synthetic lethality. Its influence on DNA damage and repair provides some evidence that it may modulate this process through BAP1 knockdown assays, however grouped cell line work stratified for BAP1 mutant and wild type failed to statistically show a difference in foci per

nuclei or proportion of yH2AX, independent of ionising radiation. Analysis of cell viability using a number of BAP1 mutant and wild type cell lines showed a marginal statistically significant difference but the gap between the two groups was small with one cell line being an outlier. Moreover, knockdown cell line assays only demonstrated a difference between empty vector and its respective BAP1 knockdown cell line in 2 out of 4. Without testing further knockdown / knock in models to support this or use of more sophisticated and efficient ways of abrogating BAP1 such as CRISPR-Cas9 it is challenging to categorically say BAP1 is key in response to olaparib. A question mark looms over the activity of MSCTRAIL in this group of patients as all the assays include rTRAIL only. The benefit of using MSCs to deliver TRAIL have been described earlier but fundamentally include the homing of these cells to tumours and increased half life. Identifying regions within BAP1 that sensitise to PARP inhibition / synthetic lethality revealed sensitivity when the catalytic domain responsible for deubiquitination and the BRCA binding domain were knocked down. Areas of interest include targeting other DNA damaging proteins outside of ATM and ATR such as CHK1 and WEE1. Patients with MPM may benefit from assessment of a panel of genes responsible for DNA damage response and treatment of the defective regions accordingly. Genomic platforms such as FoundationOne can offer this assessment both intra-tumour or liquid based, facilitating the development of an umbrella trial. This personalised approach to cancer medicine allows for identification of niche foci which can be targeted with relevant agents.

6.2 MSCTRAIL and the immune system

As described, the school of thought has been that MSCs lead to downregulation of the immune system. Their use as vectors for delivering TRAIL to cancer cells can revolutionise

the way these patients are managed given the homing ability these cells have and the selectivity of TRAIL for cancer cells, sparing normal cells. A balance emerges between use of MSCs expressing TRAIL and potentiation of the immune system. This synergistic relationship between the two was a surprising find given our understanding of the field. The biggest disappointment was the lack of further amplification of the signal when immunomodulatory agents such as pembrolizumab were used. It is likely the *in vitro* model I utilised limited further synergy and the complexities associated with the development of murine models as discussed restricted this further. Once apoptosis assays validate the viability studies it can be argued to proceed straight to human models as Phase 1 data supporting the use of chemotherapy and pembrolizumab with MSCTRAIL are underway (NCT03298763). As we expect MPM to move to an immune checkpoint blockade treatment paradigm it's important to integrate these methods of treatment in future research. Given the exceptional synergistic relationship seen between MSCTRAIL and PBMCs this challenges our understanding of how they actually interact. Its role with BAP1 is yet to be ascertained but as this sensitises to TRAIL it would be fitting to robustly explore this relationship with knockdown / knockout cell models in a separate piece of work. The mechanism underlying this synergy remains unknown and further work to decipher this is expected.

6.3 HSP90 inhibition and MPM

Following data supporting the use of HSP90 inhibition with front-line chemotherapy in MPM, I explored the role this strategy had when combined with TRAIL. Cell viability and apoptosis assays confirmed in several cell lines that at least an additive effect and in some cell lines a synergistic effect was seen. As more work is needed to validate these findings including a mouse study, it's clear that TRAIL can augment this effect. Exploration of its

relationship with death receptors can strengthen our understanding of the underlying mechanism. Agents with limited toxicities such as ganetespib can be combined with cancer selective agents like MSCTRAIL to amplify tumour kill further at little cost to patient quality of life.

7 BIBLIOGRAPHY

REFERENCES

1. Travis WD, Brambilla E, Nicholson AG, Yatabe Y, Austin JHM, Beasley MB, et al. The 2015 World Health Organization Classification of Lung Tumors: Impact of Genetic, Clinical and Radiologic Advances Since the 2004 Classification. J Thorac Oncol. 2015;10(9):1243-60.
2. Baumann F, Ambrosi JP, Carbone M. Asbestos is not just asbestos: an unrecognised health hazard. Lancet Oncol. 2013;14(7):576-8.
3. Liu B, van Gerwen M, Bonassi S, Taioli E, International Association for the Study of Lung Cancer Mesothelioma Task F. Epidemiology of Environmental Exposure and Malignant Mesothelioma. J Thorac Oncol. 2017;12(7):1031-45.
4. Camidge DR, Stockton DL, Bain M. Factors affecting the mesothelioma detection rate within national and international epidemiological studies: insights from Scottish linked cancer registry-mortality data. Br J Cancer. 2006;95(5):649-52.
5. Carbone M, Ly BH, Dodson RF, Pagano I, Morris PT, Dogan UA, et al. Malignant mesothelioma: facts, myths, and hypotheses. J Cell Physiol. 2012;227(1):44-58.
6. Allen LP, Baez J, Stern MEC, Takahashi K, George F. Trends and the Economic Effect of Asbestos Bans and Decline in Asbestos Consumption and Production Worldwide. Int J Environ Res Public Health. 2018;15(3).
7. Attanoos RL, Churg A, Galateau-Salle F, Gibbs AR, Roggli VL. Malignant Mesothelioma and Its Non-Asbestos Causes. Arch Pathol Lab Med. 2018;142(6):753-60.
8. Marsh GM, Riordan AS, Keeton KA, Benson SM. Non-occupational exposure to asbestos and risk of pleural mesothelioma: review and meta-analysis. Occup Environ Med. 2017;74(11):838-46.
9. Carbone M, Baris YI, Bertino P, Brass B, Comertpay S, Dogan AU, et al. Erionite exposure in North Dakota and Turkish villages with mesothelioma. Proc Natl Acad Sci U S A. 2011;108(33):13618-23.
10. Carbone M, Emri S, Dogan AU, Steele I, Tuncer M, Pass HI, et al. A mesothelioma epidemic in Cappadocia: scientific developments and unexpected social outcomes. Nat Rev Cancer. 2007;7(2):147-54.
11. Ortega-Guerrero MA, Carrasco-Nunez G, Barragan-Campos H, Ortega MR. High incidence of lung cancer and malignant mesothelioma linked to erionite fibre exposure in a rural community in Central Mexico. Occup Environ Med. 2015;72(3):216-8.
12. Baumann F, Buck BJ, Metcalf RV, McLaurin BT, Merkler DJ, Carbone M. The Presence of Asbestos in the Natural Environment is Likely Related to Mesothelioma in Young Individuals and Women from Southern Nevada. J Thorac Oncol. 2015;10(5):731-7.
13. Bocchetta M, Di Resta I, Powers A, Fresco R, Tosolini A, Testa JR, et al. Human mesothelial cells are unusually susceptible to simian virus 40-mediated transformation and asbestos cocarcinogenicity. Proc Natl Acad Sci U S A. 2000;97(18):10214-9.
14. Gordon R, Fitzgerald S, Millette J. Asbestos in commercial cosmetic talcum powder as a cause of mesothelioma in women. Int J Occup Environ Health. 2015;21(4):347-8.

15. Xu A, Wu LJ, Santella RM, Hei TK. Role of oxyradicals in mutagenicity and DNA damage induced by crocidolite asbestos in mammalian cells. Cancer Res. 1999;59(23):5922-6.
16. Qi F, Okimoto G, Jube S, Napolitano A, Pass HI, Laczko R, et al. Continuous exposure to chrysotile asbestos can cause transformation of human mesothelial cells via HMGB1 and TNF-alpha signaling. Am J Pathol. 2013;183(5):1654-66.
17. Betti M, Casalone E, Ferrante D, Aspesi A, Morleo G, Biasi A, et al. Germline mutations in DNA repair genes predispose asbestos-exposed patients to malignant pleural mesothelioma. Cancer Lett. 2017;405:38-45.
18. Churg A, Galateau-Salle F, Roden AC, Attanoos R, von der Thusen JH, Tsao MS, et al. Malignant mesothelioma in situ: morphologic features and clinical outcome. Mod Pathol. 2020;33(2):297-302.
19. Woolhouse I, Bishop L, Darlison L, De Fonseka D, Edey A, Edwards J, et al. British Thoracic Society Guideline for the investigation and management of malignant pleural mesothelioma. Thorax. 2018;73(Suppl 1):i1-i30.
20. Finn RS, Brims FJH, Gandhi A, Olsen N, Musk AW, Maskell NA, et al. Postmortem findings of malignant pleural mesothelioma: a two-center study of 318 patients. Chest. 2012;142(5):1267-73.
21. Gillezeau C, van Gerwen M, Ramos J, Liu B, Flores R, Taioli E. Biomarkers for malignant pleural mesothelioma: a meta-analysis. Carcinogenesis. 2019.
22. Pei D, Li Y, Liu X, Yan S, Guo X, Xu X, et al. Diagnostic and prognostic utilities of humoral fibulin-3 in malignant pleural mesothelioma: Evidence from a meta-analysis. Oncotarget. 2017;8(8):13030-8.
23. Grigoriu BD, Scherpereel A, Devos P, Chahine B, Letourneux M, Lebailly P, et al. Utility of osteopontin and serum mesothelin in malignant pleural mesothelioma diagnosis and prognosis assessment. Clin Cancer Res. 2007;13(10):2928-35.
24. Henderson DW, Reid G, Kao SC, van Zandwijk N, Klebe S. Challenges and controversies in the diagnosis of mesothelioma: Part 1. Cytology-only diagnosis, biopsies, immunohistochemistry, discrimination between mesothelioma and reactive mesothelial hyperplasia, and biomarkers. J Clin Pathol. 2013;66(10):847-53.
25. Galateau-Salle F, Churg A, Roggli V, Travis WD, World Health Organization Committee for Tumors of the P. The 2015 World Health Organization Classification of Tumors of the Pleura: Advances since the 2004 Classification. J Thorac Oncol. 2016;11(2):142-54.
26. Ray M, Kindler HL. Malignant pleural mesothelioma: an update on biomarkers and treatment. Chest. 2009;136(3):888-96.
27. Berg KB, Churg A. GATA3 Immunohistochemistry for Distinguishing Sarcomatoid and Desmoplastic Mesothelioma From Sarcomatoid Carcinoma of the Lung. Am J Surg Pathol. 2017;41(9):1221-5.
28. Righi L, Duregon E, Vatrano S, Izzo S, Giorcelli J, Rondon-Lagos M, et al. BRCA1-Associated Protein 1 (BAP1) Immunohistochemical Expression as a Diagnostic Tool in Malignant Pleural Mesothelioma Classification: A Large Retrospective Study. J Thorac Oncol. 2016;11(11):2006-17.
29. Carbone M, Yang H, Pass HI, Krausz T, Testa JR, Gaudino G. BAP1 and cancer. Nat Rev Cancer. 2013;13(3):153-9.

30. Chiosea S, Krasinskas A, Cagle PT, Mitchell KA, Zander DS, Dacic S. Diagnostic importance of 9p21 homozygous deletion in malignant mesotheliomas. Mod Pathol. 2008;21(6):742-7.
31. Parker C, Neville E. Lung cancer * 8: Management of malignant mesothelioma. Thorax. 2003;58(9):809-13.
32. Hallifax RJ, Haris M, Corcoran JP, Leyakathalikhan S, Brown E, Srikantharaja D, et al. Role of CT in assessing pleural malignancy prior to thoracoscopy. Thorax. 2015;70(2):192-3.
33. Elboga U, Yilmaz M, Uyar M, Zeki Celen Y, Bakir K, Dikensoy O. The role of FDG PET-CT in differential diagnosis of pleural pathologies. Rev Esp Med Nucl Imagen Mol. 2012;31(4):187-91.
34. Armato SG, 3rd, Blyth KG, Keating JJ, Katz S, Tsim S, Coolen J, et al. Imaging in pleural mesothelioma: A review of the 13th International Conference of the International Mesothelioma Interest Group. Lung Cancer. 2016;101:48-58.
35. Rusch VW, Chansky K, Kindler HL, Nowak AK, Pass HI, Rice DC, et al. The IASLC Mesothelioma Staging Project: Proposals for the M Descriptors and for Revision of the TNM Stage Groupings in the Forthcoming (Eighth) Edition of the TNM Classification for Mesothelioma. J Thorac Oncol. 2016;11(12):2112-9.
36. Curran D, Sahmoud T, Therasse P, van Meerbeeck J, Postmus PE, Giaccone G. Prognostic factors in patients with pleural mesothelioma: the European Organization for Research and Treatment of Cancer experience. J Clin Oncol. 1998;16(1):145-52.
37. Courtiol P, Maussion C, Moarii M, Pronier E, Pilcer S, Sefta M, et al. Deep learning-based classification of mesothelioma improves prediction of patient outcome. Nat Med. 2019;25(10):1519-25.
38. Pastorino S, Yoshikawa Y, Pass HI, Emi M, Nasu M, Pagano I, et al. A Subset of Mesotheliomas With Improved Survival Occurring in Carriers of BAP1 and Other Germline Mutations. J Clin Oncol. 2018:JCO2018790352.
39. Carbone M, Adusumilli PS, Alexander HR, Jr., Baas P, Bardelli F, Bononi A, et al. Mesothelioma: Scientific clues for prevention, diagnosis, and therapy. CA Cancer J Clin. 2019;69(5):402-29.
40. Treasure T, Lang-Lazdunski L, Waller D, Bliss JM, Tan C, Entwisle J, et al. Extra-pleural pneumonectomy versus no extra-pleural pneumonectomy for patients with malignant pleural mesothelioma: clinical outcomes of the Mesothelioma and Radical Surgery (MARS) randomised feasibility study. Lancet Oncol. 2011;12(8):763-72.
41. Stahel RA, Riesterer O, Xyrafas A, Opitz I, Beyeler M, Ochsenbein A, et al. Neoadjuvant chemotherapy and extrapleural pneumonectomy of malignant pleural mesothelioma with or without hemithoracic radiotherapy (SAKK 17/04): a randomised, international, multicentre phase 2 trial. Lancet Oncol. 2015;16(16):1651-8.
42. Bayman N, Appel W, Ashcroft L, Baldwin DR, Bates A, Darlison L, et al. Prophylactic Irradiation of Tracts in Patients With Malignant Pleural Mesothelioma: An Open-Label, Multicenter, Phase III Randomized Trial. J Clin Oncol. 2019:JCO1801678.
43. Clive AO, Taylor H, Dobson L, Wilson P, de Winton E, Panakis N, et al. Prophylactic radiotherapy for the prevention of procedure-tract metastases after surgical and large-bore pleural procedures in malignant pleural mesothelioma (SMART): a multicentre, open-label, phase 3, randomised controlled trial. Lancet Oncol. 2016;17(8):1094-104.
44. Ashton M, O'Rourke N, Macleod N, Laird B, Stobo J, Kelly C, et al. SYSTEMS-2: A randomised phase II study of radiotherapy dose escalation for pain control in malignant pleural mesothelioma. Clin Transl Radiat Oncol. 2018;8:45-9.

45. Vogelzang NJ, Rusthoven JJ, Symanowski J, Denham C, Kaukel E, Ruffie P, et al. Phase III study of pemetrexed in combination with cisplatin versus cisplatin alone in patients with malignant pleural mesothelioma. J Clin Oncol. 2003;21(14):2636-44.
46. Santoro A, O'Brien ME, Stahel RA, Nackaerts K, Baas P, Karthaus M, et al. Pemetrexed plus cisplatin or pemetrexed plus carboplatin for chemonaive patients with malignant pleural mesothelioma: results of the International Expanded Access Program. J Thorac Oncol. 2008;3(7):756-63.
47. Castagneto B, Botta M, Aitini E, Spigno F, Degiovanni D, Alabiso O, et al. Phase II study of pemetrexed in combination with carboplatin in patients with malignant pleural mesothelioma (MPM). Ann Oncol. 2008;19(2):370-3.
48. Ceresoli GL, Zucali PA, Favaretto AG, Grossi F, Bidoli P, Del Conte G, et al. Phase II study of pemetrexed plus carboplatin in malignant pleural mesothelioma. J Clin Oncol. 2006;24(9):1443-8.
49. van Meerbeeck JP, Gaafar R, Manegold C, Van Klaveren RJ, Van Marck EA, Vincent M, et al. Randomized phase III study of cisplatin with or without raltitrexed in patients with malignant pleural mesothelioma: an intergroup study of the European Organisation for Research and Treatment of Cancer Lung Cancer Group and the National Cancer Institute of Canada. J Clin Oncol. 2005;23(28):6881-9.
50. van Meerbeeck JP, Baas P, Debruyne C, Groen HJ, Manegold C, Ardizzoni A, et al. A Phase II study of gemcitabine in patients with malignant pleural mesothelioma. European Organization for Research and Treatment of Cancer Lung Cancer Cooperative Group. Cancer. 1999;85(12):2577-82.
51. Nowak AK, Byrne MJ, Williamson R, Ryan G, Segal A, Fielding D, et al. A multicentre phase II study of cisplatin and gemcitabine for malignant mesothelioma. Br J Cancer. 2002;87(5):491-6.
52. Byrne MJ, Davidson JA, Musk AW, Dewar J, van Hazel G, Buck M, et al. Cisplatin and gemcitabine treatment for malignant mesothelioma: a phase II study. J Clin Oncol. 1999;17(1):25-30.
53. Steele JP, Shamash J, Evans MT, Gower NH, Tischkowitz MD, Rudd RM. Phase II study of vinorelbine in patients with malignant pleural mesothelioma. J Clin Oncol. 2000;18(23):3912-7.
54. Muers MF, Stephens RJ, Fisher P, Darlison L, Higgs CM, Lowry E, et al. Active symptom control with or without chemotherapy in the treatment of patients with malignant pleural mesothelioma (MS01): a multicentre randomised trial. Lancet. 2008;371(9625):1685-94.
55. Fennell DA, JP CS, Shamash J, Sheaff MT, Evans MT, Goonewardene TI, et al. Phase II trial of vinorelbine and oxaliplatin as first-line therapy in malignant pleural mesothelioma. Lung Cancer. 2005;47(2):277-81.
56. Caliandro R BC, Perol M, Monnet I, Dabouis G, Guerin JC, Le Chevalier T, Ruffie P. 62 Phase II study of paclitaxel (Taxol®) and cisplatin (CDDP) in advanced pleural malignant mesothelioma (MM). Lung Cancer. 1999;18:19.
57. Samuels BL, Herndon JE, 2nd, Harmon DC, Carey R, Aisner J, Corson JM, et al. Dihydro-5-azacytidine and cisplatin in the treatment of malignant mesothelioma: a phase II study by the Cancer and Leukemia Group B. Cancer. 1998;82(8):1578-84.
58. Eisenhauer EA, Evans WK, Murray N, Kocha W, Wierzbicki R, Wilson K. A phase II study of VP-16 and cisplatin in patients with unresectable malignant mesothelioma. An NCI Canada Clinical Trials Group Study. Invest New Drugs. 1988;6(4):327-9.

59. Chahinian AP, Antman K, Goutsou M, Corson JM, Suzuki Y, Modeas C, et al. Randomized phase II trial of cisplatin with mitomycin or doxorubicin for malignant mesothelioma by the Cancer and Leukemia Group B. J Clin Oncol. 1993;11(8):1559-65.
60. Nakano T, Chahinian AP, Shinjo M, Togawa N, Tonomura A, Miyake M, et al. Cisplatin in combination with irinotecan in the treatment of patients with malignant pleural mesothelioma: a pilot phase II clinical trial and pharmacokinetic profile. Cancer. 1999;85(11):2375-84.
61. Kindler HL, Karrison TG, Gandara DR, Lu C, Krug LM, Stevenson JP, et al. Multicenter, double-blind, placebo-controlled, randomized phase II trial of gemcitabine/cisplatin plus bevacizumab or placebo in patients with malignant mesothelioma. J Clin Oncol. 2012;30(20):2509-15.
62. Zalcman G, Mazieres J, Margery J, Greillier L, Audigier-Valette C, Moro-Sibilot D, et al. Bevacizumab for newly diagnosed pleural mesothelioma in the Mesothelioma Avastin Cisplatin Pemetrexed Study (MAPS): a randomised, controlled, open-label, phase 3 trial. Lancet. 2016;387(10026):1405-14.
63. Reck M, Kaiser R, Mellemgaard A, Douillard JY, Orlov S, Krzakowski M, et al. Docetaxel plus nintedanib versus docetaxel plus placebo in patients with previously treated non-small-cell lung cancer (LUME-Lung 1): a phase 3, double-blind, randomised controlled trial. Lancet Oncol. 2014;15(2):143-55.
64. Scagliotti GV, Gaafar R, Nowak AK, Reck M, Tsao AS, van Meerbeeck J, et al. LUME-Meso: Design and Rationale of the Phase III Part of a Placebo-Controlled Study of Nintedanib and Pemetrexed/Cisplatin Followed by Maintenance Nintedanib in Patients With Unresectable Malignant Pleural Mesothelioma. Clin Lung Cancer. 2017;18(5):589-93.
65. Scagliotti GV, Gaafar R, Nowak AK, Nakano T, van Meerbeeck J, Popat S, et al. Nintedanib in combination with pemetrexed and cisplatin for chemotherapy-naive patients with advanced malignant pleural mesothelioma (LUME-Meso): a double-blind, randomised, placebo-controlled phase 3 trial. Lancet Respir Med. 2019.
66. Wozniak AJ SB, Kalemkerian GP, Daly RM, Chen W, Ventimiglia J, Nagasaka M, Zauderer MG A phase II trial of nintedanib in recurrent malignant pleural mesothelioma (MPM). Journal of Clinical Oncology. 2019.
67. Jahan T, Gu L, Kratzke R, Dudek A, Otterson GA, Wang X, et al. Vatalanib in malignant mesothelioma: a phase II trial by the Cancer and Leukemia Group B (CALGB 30107). Lung Cancer. 2012;76(3):393-6.
68. Buikhuisen WA, Scharpfenecker M, Griffioen AW, Korse CM, van Tinteren H, Baas P. A Randomized Phase II Study Adding Axitinib to Pemetrexed-Cisplatin in Patients with Malignant Pleural Mesothelioma: A Single-Center Trial Combining Clinical and Translational Outcomes. J Thorac Oncol. 2016;11(5):758-68.
69. Szlosarek PW, Klabatsa A, Pallaska A, Sheaff M, Smith P, Crook T, et al. In vivo loss of expression of argininosuccinate synthetase in malignant pleural mesothelioma is a biomarker for susceptibility to arginine depletion. Clin Cancer Res. 2006;12(23):7126-31.
70. Delage B, Fennell DA, Nicholson L, McNeish I, Lemoine NR, Crook T, et al. Arginine deprivation and argininosuccinate synthetase expression in the treatment of cancer. Int J Cancer. 2010;126(12):2762-72.
71. Szlosarek PW, Steele JP, Nolan L, Gilligan D, Taylor P, Spicer J, et al. Arginine Deprivation With Pegylated Arginine Deiminase in Patients With Argininosuccinate Synthetase 1-Deficient Malignant Pleural Mesothelioma: A Randomized Clinical Trial. JAMA Oncol. 2017;3(1):58-66.

72. Allen MD, Luong P, Hudson C, Leyton J, Delage B, Ghazaly E, et al. Prognostic and therapeutic impact of argininosuccinate synthetase 1 control in bladder cancer as monitored longitudinally by PET imaging. Cancer Res. 2014;74(3):896-907.
73. Beddowes E, Spicer J, Chan PY, Khadeir R, Corbacho JG, Repana D, et al. Phase 1 Dose-Escalation Study of Pegylated Arginine Deiminase, Cisplatin, and Pemetrexed in Patients With Argininosuccinate Synthetase 1-Deficient Thoracic Cancers. J Clin Oncol. 2017;35(16):1778-85.
74. Pardoll DM. The blockade of immune checkpoints in cancer immunotherapy. Nat Rev Cancer. 2012;12(4):252-64.
75. Alexandrov LB, Nik-Zainal S, Wedge DC, Aparicio SA, Behjati S, Biankin AV, et al. Signatures of mutational processes in human cancer. Nature. 2013;500(7463):415-21.
76. Hmeljak J, Sanchez-Vega F, Hoadley KA, Shih J, Stewart C, Heiman D, et al. Integrative Molecular Characterization of Malignant Pleural Mesothelioma. Cancer Discov. 2018;8(12):1548-65.
77. Suzuki K, Kadota K, Sima CS, Sadelain M, Rusch VW, Travis WD, et al. Chronic inflammation in tumor stroma is an independent predictor of prolonged survival in epithelioid malignant pleural mesothelioma patients. Cancer Immunol Immunother. 2011;60(12):1721-8.
78. Ujiie H, Kadota K, Nitadori JI, Aerts JG, Woo KM, Sima CS, et al. The tumoral and stromal immune microenvironment in malignant pleural mesothelioma: A comprehensive analysis reveals prognostic immune markers. Oncoimmunology. 2015;4(6):e1009285.
79. Larkin J, Chiarion-Sileni V, Gonzalez R, Grob JJ, Rutkowski P, Lao CD, et al. Five-Year Survival with Combined Nivolumab and Ipilimumab in Advanced Melanoma. N Engl J Med. 2019;381(16):1535-46.
80. Thapa B WM, Murone C, Ameratunga M, Asadi K, Deb S, Lin X, Salcedo A, Barnett S, Knight S, Mitchell P, Boutros PC, Watkins N, John T Correlation of PD-L1 expression with immune cell infiltrates, genome-wide copy number aberrations and survival in mesothelioma. Journal of Clinical Oncology. 2017.
81. Mansfield AS, Roden AC, Peikert T, Sheinin YM, Harrington SM, Krco CJ, et al. B7-H1 expression in malignant pleural mesothelioma is associated with sarcomatoid histology and poor prognosis. J Thorac Oncol. 2014;9(7):1036-40.
82. Kindler H, Scherpereel A, Calabro L, Aerts J, Perez SC, Bearz A. Tremelimumab as second- or third-line treatment of unresectable malignant mesothelioma (MM): Results from the global, double-blind, placebo-controlled DETERMINE study. Journal of Clinical Oncology. 2016;34(15_suppl pp.):8502-.
83. Alley EW, Lopez J, Santoro A, Morosky A, Saraf S, Piperdi B, et al. Clinical safety and activity of pembrolizumab in patients with malignant pleural mesothelioma (KEYNOTE-028): preliminary results from a non-randomised, open-label, phase 1b trial. Lancet Oncol. 2017;18(5):623-30.
84. Quispel-Janssen J, Zago G, Schouten R, Buikhuisen W, Monkhorst K, Thunissen E, et al. OA13.01 A Phase II Study of Nivolumab in Malignant Pleural Mesothelioma (NivoMes): with Translational Research (TR) Biopies. Journal of Thoracic Oncology. 2017;12(1):S292-S3.
85. Popat S C-FA, Polydoropoulou V, Shah R, O'Brien M, Pope A, Fisher P, Spicer J, Roy A, Gilligan D, Gautschi O, Nadal E, Janthur W-D, Lopez Castro R, Garcia Campelo R, Roschotzki-Voser H, Ruepp B, Rusakiewicz S, Peters S, Stahel RA. A multicentre randomized phase III trial comparing pembrolizumab (P) vs single agent chemotherapy (CT) for advanced pre-treated malignant pleural mesothelioma (MPM): Results from the European Thoracic

Oncology Platform (ETOP 9-15) PROMISE-meso trial. In: Oncology Ao, editor. ESMO 2019; Barcelona
86. Nowak A KP, Lesterhuis WJ, Hughes BGM, Brown C, Kao SC, Karikios DJ, John T, Pavlakis N, O'Byrne KJ, Yip S, Lam WS, Briscoe K, Karapetis C, Stockler MR,. DREAM - A Phase 2 Trial of Durvalumab with First Line Chemotherapy in Mesothelioma: Final Result. Journal of Thoracic Oncology. 2018;13(10):S338-S9.
87. Scherpereel A, Mazieres J, Greillier L, Lantuejoul S, Do P, Bylicki O, et al. Nivolumab or nivolumab plus ipilimumab in patients with relapsed malignant pleural mesothelioma (IFCT-1501 MAPS2): a multicentre, open-label, randomised, non-comparative, phase 2 trial. Lancet Oncol. 2019;20(2):239-53.
88. Disselhorst MJ, Quispel-Janssen J, Lalezari F, Monkhorst K, de Vries JF, van der Noort V, et al. Ipilimumab and nivolumab in the treatment of recurrent malignant pleural mesothelioma (INITIATE): results of a prospective, single-arm, phase 2 trial. Lancet Respir Med. 2019;7(3):260-70.
89. Hassan R, Kindler HL, Jahan T, Bazhenova L, Reck M, Thomas A, et al. Phase II clinical trial of amatuximab, a chimeric antimesothelin antibody with pemetrexed and cisplatin in advanced unresectable pleural mesothelioma. Clin Cancer Res. 2014;20(23):5927-36.
90. Blumenschein GR HR, Moore KN, Santin A, Kindler HL, Nemunaitis JJ, Seward SM, Rajagopalan P, Walter A, Sarapa N, Bendell JC. Phase I study of anti-mesothelin antibody drug conjugate anetumab ravtansine (AR). Journal of Clinical Oncology. 2017.
91. Kindler HL NS, Fennell D, Blumenschein G, Bearz A, Ceresoli G, Aerts J, Spicer J, Taylor P, Greystoke A, Nackaerts K, Calabro L, Burgers S, Jennens R, Sporchia A, Walter A, Siegel J, Childs B, Elbi C, Hassan R. OA 02.01 Randomized Phase II Study of Anetumab Ravtansine or Vinorelbine in Patients with Metastatic Pleural Mesothelioma. Journal of Thoracic Oncology. 2017;12(1152).
92. Adusumilli PS ZM, Rusch VW, O'Cearbhaill RE, Zhu A, Ngai DA, McGee E, Chintala NK, Messinger JC, Vincent A, Halton EF, Diamonte C, Pineda J, Modi S, Solomon SB, Jones DR, Brentjens RJ, Rivière I, Sadelain M. . CT036 - A phase I clinical trial of malignant pleural disease treated with regionally delivered autologous mesothelin-targeted CAR T cells: Safety and efficacy. Clin Cancer Res. 2019.
93. Peikert T, Mandrekar S, Mansfield A, Keulen VV, Albelda S, Aderca S, et al. Intrapleural Modified Vaccine Strain Measles Virus Therapy for Patients with Malignant Pleural Mesothelioma. Journal of Thoracic Oncology. 2017;12.
94. Cornelissen R, Hegmans JP, Maat AP, Kaijen-Lambers ME, Bezemer K, Hendriks RW, et al. Extended Tumor Control after Dendritic Cell Vaccination with Low-Dose Cyclophosphamide as Adjuvant Treatment in Patients with Malignant Pleural Mesothelioma. Am J Respir Crit Care Med. 2016;193(9):1023-31.
95. Jahan T, Hassan R, Alley E, Kindler H, Antonia S, Whiting C, et al. 208O_PR: CRS-207 with chemotherapy (chemo) in malignant pleural mesothelioma (MPM): Results from a phase 1b trial. J Thorac Oncol. 2016;11(4 Suppl):S156.
96. Zauderer MG, Tsao AS, Dao T, Panageas K, Lai WV, Rimner A, et al. A Randomized Phase II Trial of Adjuvant Galinpepimut-S, WT-1 Analogue Peptide Vaccine, After Multimodality Therapy for Patients with Malignant Pleural Mesothelioma. Clin Cancer Res. 2017;23(24):7483-9.
97. Krug LM ZM, Adusumili PS, McGee E, Sepkowitz K, Yu MKA, Scigalla P, Rusch VW Phase I study of intra-pleural administration of GL-ONC1, an oncolytic vaccinia virus, in patients with malignant pleural effusion. Journal of Clinical Oncology. 2015.

98. Hassan R, Sharon E, Thomas A, Zhang J, Ling A, Miettinen M, et al. Phase 1 study of the antimesothelin immunotoxin SS1P in combination with pemetrexed and cisplatin for front-line therapy of pleural mesothelioma and correlation of tumor response with serum mesothelin, megakaryocyte potentiating factor, and cancer antigen 125. Cancer. 2014;120(21):3311-9.
99. Hegmans JP, Hemmes A, Hammad H, Boon L, Hoogsteden HC, Lambrecht BN. Mesothelioma environment comprises cytokines and T-regulatory cells that suppress immune responses. Eur Respir J. 2006;27(6):1086-95.
100. Meniawy TM, Creaney J, Lake RA, Nowak AK. Existing models, but not neutrophil-to-lymphocyte ratio, are prognostic in malignant mesothelioma. Br J Cancer. 2013;109(7):1813-20.
101. Pinato DJ, Mauri FA, Ramakrishnan R, Wahab L, Lloyd T, Sharma R. Inflammation-based prognostic indices in malignant pleural mesothelioma. J Thorac Oncol. 2012;7(3):587-94.
102. Miki Y, Swensen J, Shattuck-Eidens D, Futreal PA, Harshman K, Tavtigian S, et al. A strong candidate for the breast and ovarian cancer susceptibility gene BRCA1. Science. 1994;266(5182):66-71.
103. Testa JR, Cheung M, Pei J, Below JE, Tan Y, Sementino E, et al. Germline BAP1 mutations predispose to malignant mesothelioma. Nat Genet. 2011;43(10):1022-5.
104. Panou V, Gadiraju M, Wolin A, Weipert CM, Skarda E, Husain AN, et al. Frequency of Germline Mutations in Cancer Susceptibility Genes in Malignant Mesothelioma. J Clin Oncol. 2018;36(28):2863-71.
105. Goodman AM, Kato S, Bazhenova L, Patel SP, Frampton GM, Miller V, et al. Tumor Mutational Burden as an Independent Predictor of Response to Immunotherapy in Diverse Cancers. Mol Cancer Ther. 2017;16(11):2598-608.
106. Bueno R, Stawiski EW, Goldstein LD, Durinck S, De Rienzo A, Modrusan Z, et al. Comprehensive genomic analysis of malignant pleural mesothelioma identifies recurrent mutations, gene fusions and splicing alterations. Nat Genet. 2016;48(4):407-16.
107. Carbone M, Yang H, Gaudino G. Does Chromothripsis Make Mesothelioma an Immunogenic Cancer? J Thorac Oncol. 2019;14(2):157-9.
108. Yoshikawa Y, Emi M, Hashimoto-Tamaoki T, Ohmuraya M, Sato A, Tsujimura T, et al. High-density array-CGH with targeted NGS unmask multiple noncontiguous minute deletions on chromosome 3p21 in mesothelioma. Proc Natl Acad Sci U S A. 2016;113(47):13432-7.
109. Mansfield AS, Peikert T, Smadbeck JB, Udell JBM, Garcia-Rivera E, Elsbernd L, et al. Neoantigenic Potential of Complex Chromosomal Rearrangements in Mesothelioma. J Thorac Oncol. 2019;14(2):276-87.
110. Chau C, van Doorn R, van Poppelen NM, van der Stoep N, Mensenkamp AR, Sijmons RH, et al. Families with BAP1-Tumor Predisposition Syndrome in The Netherlands: Path to Identification and a Proposal for Genetic Screening Guidelines. Cancers (Basel). 2019;11(8).
111. Roushdy-Hammady I, Siegel J, Emri S, Testa JR, Carbone M. Genetic-susceptibility factor and malignant mesothelioma in the Cappadocian region of Turkey. Lancet. 2001;357(9254):444-5.
112. Emri SA. The Cappadocia mesothelioma epidemic: its influence in Turkey and abroad. Ann Transl Med. 2017;5(11):239.

113. Nasu M, Emi M, Pastorino S, Tanji M, Powers A, Luk H, et al. High Incidence of Somatic BAP1 alterations in sporadic malignant mesothelioma. J Thorac Oncol. 2015;10(4):565-76.
114. Yoshikawa Y, Sato A, Tsujimura T, Emi M, Morinaga T, Fukuoka K, et al. Frequent inactivation of the BAP1 gene in epithelioid-type malignant mesothelioma. Cancer Sci. 2012;103(5):868-74.
115. Guo G, Chmielecki J, Goparaju C, Heguy A, Dolgalev I, Carbone M, et al. Whole-exome sequencing reveals frequent genetic alterations in BAP1, NF2, CDKN2A, and CUL1 in malignant pleural mesothelioma. Cancer Res. 2015;75(2):264-9.
116. Dey A, Seshasayee D, Noubade R, French DM, Liu J, Chaurushiya MS, et al. Loss of the tumor suppressor BAP1 causes myeloid transformation. Science. 2012;337(6101):1541-6.
117. Jensen DE, Rauscher FJ, 3rd. Defining biochemical functions for the BRCA1 tumor suppressor protein: analysis of the BRCA1 binding protein BAP1. Cancer Lett. 1999;143 Suppl 1:S13-7.
118. Ventii KH, Devi NS, Friedrich KL, Chernova TA, Tighiouart M, Van Meir EG, et al. BRCA1-associated protein-1 is a tumor suppressor that requires deubiquitinating activity and nuclear localization. Cancer Res. 2008;68(17):6953-62.
119. Eletr ZM, Yin L, Wilkinson KD. BAP1 is phosphorylated at serine 592 in S-phase following DNA damage. FEBS Lett. 2013;587(24):3906-11.
120. Jensen DE, Proctor M, Marquis ST, Gardner HP, Ha SI, Chodosh LA, et al. BAP1: a novel ubiquitin hydrolase which binds to the BRCA1 RING finger and enhances BRCA1-mediated cell growth suppression. Oncogene. 1998;16(9):1097-112.
121. Mallery DL, Vandenberg CJ, Hiom K. Activation of the E3 ligase function of the BRCA1/BARD1 complex by polyubiquitin chains. EMBO J. 2002;21(24):6755-62.
122. Nishikawa H, Wu W, Koike A, Kojima R, Gomi H, Fukuda M, et al. BRCA1-associated protein 1 interferes with BRCA1/BARD1 RING heterodimer activity. Cancer Res. 2009;69(1):111-9.
123. Wei R, Liu X, Yu W, Yang T, Cai W, Liu J, et al. Deubiquitinases in cancer. Oncotarget. 2015;6(15):12872-89.
124. Wilkinson KD. Ubiquitination and deubiquitination: targeting of proteins for degradation by the proteasome. Semin Cell Dev Biol. 2000;11(3):141-8.
125. Scheffner M, Nuber U, Huibregtse JM. Protein ubiquitination involving an E1-E2-E3 enzyme ubiquitin thioester cascade. Nature. 1995;373(6509):81-3.
126. Nalepa G, Rolfe M, Harper JW. Drug discovery in the ubiquitin-proteasome system. Nat Rev Drug Discov. 2006;5(7):596-613.
127. Yu H, Pak H, Hammond-Martel I, Ghram M, Rodrigue A, Daou S, et al. Tumor suppressor and deubiquitinase BAP1 promotes DNA double-strand break repair. Proc Natl Acad Sci U S A. 2014;111(1):285-90.
128. Yu H, Mashtalir N, Daou S, Hammond-Martel I, Ross J, Sui G, et al. The ubiquitin carboxyl hydrolase BAP1 forms a ternary complex with YY1 and HCF-1 and is a critical regulator of gene expression. Mol Cell Biol. 2010;30(21):5071-85.
129. Kuznetsov JN AT, Kurtenbach S, Field MG, King ML and Harbour JW. The tumor suppressor BAP1 promotes a developmental switch from pluripotency to differentiation. Cancer Research 2017;77(13).

130. Bononi A, Giorgi C, Patergnani S, Larson D, Verbruggen K, Tanji M, et al. BAP1 regulates IP3R3-mediated Ca(2+) flux to mitochondria suppressing cell transformation. Nature. 2017;546(7659):549-53.
131. Zhang Y, Shi J, Liu X, Feng L, Gong Z, Koppula P, et al. BAP1 links metabolic regulation of ferroptosis to tumour suppression. Nat Cell Biol. 2018;20(10):1181-92.
132. Scheuermann JC, de Ayala Alonso AG, Oktaba K, Ly-Hartig N, McGinty RK, Fraterman S, et al. Histone H2A deubiquitinase activity of the Polycomb repressive complex PR-DUB. Nature. 2010;465(7295):243-7.
133. LaFave LM, Beguelin W, Koche R, Teater M, Spitzer B, Chramiec A, et al. Loss of BAP1 function leads to EZH2-dependent transformation. Nat Med. 2015;21(11):1344-9.
134. Zauderer MGSP, Le Moulec S, Popat S, Taylor P, Planchard D, Scherpereel A, Jahan T, Koczywas M, Forster M, Cameron RB, Peikert T, Campbell C, Sapir I, McDonald A, Oei C, Clawson A, Roche M, Fennell D. Phase 2, multicenter study of the EZH2 inhibitor tazemetostat as monotherapy in adults with relapsed or refractory (R/R) malignant mesothelioma (MM) with BAP1 inactivation. J Clin Oncol. 2018.
135. Machida YJ, Machida Y, Vashisht AA, Wohlschlegel JA, Dutta A. The deubiquitinating enzyme BAP1 regulates cell growth via interaction with HCF-1. J Biol Chem. 2009;284(49):34179-88.
136. Eletr ZM, Wilkinson KD. An emerging model for BAP1's role in regulating cell cycle progression. Cell Biochem Biophys. 2011;60(1-2):3-11.
137. Tyagi S, Chabes AL, Wysocka J, Herr W. E2F activation of S phase promoters via association with HCF-1 and the MLL family of histone H3K4 methyltransferases. Mol Cell. 2007;27(1):107-19.
138. Ji Z, Mohammed H, Webber A, Ridsdale J, Han N, Carroll JS, et al. The forkhead transcription factor FOXK2 acts as a chromatin targeting factor for the BAP1-containing histone deubiquitinase complex. Nucleic Acids Res. 2014;42(10):6232-42.
139. Okino Y, Machida Y, Frankland-Searby S, Machida YJ. BRCA1-associated protein 1 (BAP1) deubiquitinase antagonizes the ubiquitin-mediated activation of FoxK2 target genes. J Biol Chem. 2015;290(3):1580-91.
140. White AE, Harper JW. Cancer. Emerging anatomy of the BAP1 tumor suppressor system. Science. 2012;337(6101):1463-4.
141. Ruan HB, Han X, Li MD, Singh JP, Qian K, Azarhoush S, et al. O-GlcNAc transferase/host cell factor C1 complex regulates gluconeogenesis by modulating PGC-1alpha stability. Cell Metab. 2012;16(2):226-37.
142. Bononi A, Yang H, Giorgi C, Patergnani S, Pellegrini L, Su M, et al. Germline BAP1 mutations induce a Warburg effect. Cell Death Differ. 2017;24(10):1694-704.
143. Kuznetsov JN, Aguero TH, Owens DA, Kurtenbach S, Field MG, Durante MA, et al. BAP1 regulates epigenetic switch from pluripotency to differentiation in developmental lineages giving rise to BAP1-mutant cancers. Sci Adv. 2019;5(9):eaax1738.
144. Kolluri KK, Alifrangis C, Kumar N, Ishii Y, Price S, Michaut M, et al. Loss of functional BAP1 augments sensitivity to TRAIL in cancer cells. Elife. 2018;7.
145. Sacco JJ, Kenyani J, Butt Z, Carter R, Chew HY, Cheeseman LP, et al. Loss of the deubiquitylase BAP1 alters class I histone deacetylase expression and sensitivity of mesothelioma cells to HDAC inhibitors. Oncotarget. 2015;6(15):13757-71.
146. Krug LM, Kindler HL, Calvert H, Manegold C, Tsao AS, Fennell D, et al. Vorinostat in patients with advanced malignant pleural mesothelioma who have progressed on previous

chemotherapy (VANTAGE-014): a phase 3, double-blind, randomised, placebo-controlled trial. Lancet Oncol. 2015;16(4):447-56.
147. Harper JW, Elledge SJ. The DNA damage response: ten years after. Mol Cell. 2007;28(5):739-45.
148. Ayoub N, Jeyasekharan AD, Bernal JA, Venkitaraman AR. HP1-beta mobilization promotes chromatin changes that initiate the DNA damage response. Nature. 2008;453(7195):682-6.
149. Cleaver JE, Feeney L, Revet I. Phosphorylated H2Ax is not an unambiguous marker for DNA double-strand breaks. Cell Cycle. 2011;10(19):3223-4.
150. Paull TT, Rogakou EP, Yamazaki V, Kirchgessner CU, Gellert M, Bonner WM. A critical role for histone H2AX in recruitment of repair factors to nuclear foci after DNA damage. Curr Biol. 2000;10(15):886-95.
151. Mailand N, Bekker-Jensen S, Faustrup H, Melander F, Bartek J, Lukas C, et al. RNF8 ubiquitylates histones at DNA double-strand breaks and promotes assembly of repair proteins. Cell. 2007;131(5):887-900.
152. Nakada S. Opposing roles of RNF8/RNF168 and deubiquitinating enzymes in ubiquitination-dependent DNA double-strand break response signaling and DNA-repair pathway choice. J Radiat Res. 2016;57 Suppl 1:i33-i40.
153. Price BD, D'Andrea AD. Chromatin remodeling at DNA double-strand breaks. Cell. 2013;152(6):1344-54.
154. Scully R, Xie A. Double strand break repair functions of histone H2AX. Mutat Res. 2013;750(1-2):5-14.
155. Chapman JR, Taylor MR, Boulton SJ. Playing the end game: DNA double-strand break repair pathway choice. Mol Cell. 2012;47(4):497-510.
156. Bekker-Jensen S, Lukas C, Kitagawa R, Melander F, Kastan MB, Bartek J, et al. Spatial organization of the mammalian genome surveillance machinery in response to DNA strand breaks. J Cell Biol. 2006;173(2):195-206.
157. Essers J, Houtsmuller AB, van Veelen L, Paulusma C, Nigg AL, Pastink A, et al. Nuclear dynamics of RAD52 group homologous recombination proteins in response to DNA damage. EMBO J. 2002;21(8):2030-7.
158. Kaufman B, Shapira-Frommer R, Schmutzler RK, Audeh MW, Friedlander M, Balmana J, et al. Olaparib monotherapy in patients with advanced cancer and a germline BRCA1/2 mutation. J Clin Oncol. 2015;33(3):244-50.
159. Ledermann J, Harter P, Gourley C, Friedlander M, Vergote I, Rustin G, et al. Olaparib maintenance therapy in platinum-sensitive relapsed ovarian cancer. N Engl J Med. 2012;366(15):1382-92.
160. Robson M, Im SA, Senkus E, Xu B, Domchek SM, Masuda N, et al. Olaparib for Metastatic Breast Cancer in Patients with a Germline BRCA Mutation. N Engl J Med. 2017;377(6):523-33.
161. Brown JS, O'Carrigan B, Jackson SP, Yap TA. Targeting DNA Repair in Cancer: Beyond PARP Inhibitors. Cancer Discov. 2017;7(1):20-37.
162. Wei H, Yu X. Functions of PARylation in DNA Damage Repair Pathways. Genomics Proteomics Bioinformatics. 2016;14(3):131-9.
163. Beck C, Robert I, Reina-San-Martin B, Schreiber V, Dantzer F. Poly(ADP-ribose) polymerases in double-strand break repair: focus on PARP1, PARP2 and PARP3. Exp Cell Res. 2014;329(1):18-25.

164. Plummer R. Poly(ADP-ribose) polymerase inhibition: a new direction for BRCA and triple-negative breast cancer? Breast Cancer Res. 2011;13(4):218.
165. Langelier MF, Riccio AA, Pascal JM. PARP-2 and PARP-3 are selectively activated by 5' phosphorylated DNA breaks through an allosteric regulatory mechanism shared with PARP-1. Nucleic Acids Res. 2014;42(12):7762-75.
166. Bi FF, Li D, Yang Q. Hypomethylation of ETS transcription factor binding sites and upregulation of PARP1 expression in endometrial cancer. Biomed Res Int. 2013;2013:946268.
167. Li D, Bi FF, Cao JM, Cao C, Li CY, Liu B, et al. Poly (ADP-ribose) polymerase 1 transcriptional regulation: a novel crosstalk between histone modification H3K9ac and ETS1 motif hypomethylation in BRCA1-mutated ovarian cancer. Oncotarget. 2014;5(1):291-7.
168. Pritchard CC, Mateo J, Walsh MF, De Sarkar N, Abida W, Beltran H, et al. Inherited DNA-Repair Gene Mutations in Men with Metastatic Prostate Cancer. N Engl J Med. 2016;375(5):443-53.
169. Farmer H, McCabe N, Lord CJ, Tutt AN, Johnson DA, Richardson TB, et al. Targeting the DNA repair defect in BRCA mutant cells as a therapeutic strategy. Nature. 2005;434(7035):917-21.
170. Helleday T. The underlying mechanism for the PARP and BRCA synthetic lethality: clearing up the misunderstandings. Mol Oncol. 2011;5(4):387-93.
171. Murai J, Huang SY, Das BB, Renaud A, Zhang Y, Doroshow JH, et al. Trapping of PARP1 and PARP2 by Clinical PARP Inhibitors. Cancer Res. 2012;72(21):5588-99.
172. Pommier Y, O'Connor MJ, de Bono J. Laying a trap to kill cancer cells: PARP inhibitors and their mechanisms of action. Sci Transl Med. 2016;8(362):362ps17.
173. Zhou W, Wang X, Rosenfeld MG. Histone H2A ubiquitination in transcriptional regulation and DNA damage repair. Int J Biochem Cell Biol. 2009;41(1):12-5.
174. Shanbhag NM, Rafalska-Metcalf IU, Balane-Bolivar C, Janicki SM, Greenberg RA. ATM-dependent chromatin changes silence transcription in cis to DNA double-strand breaks. Cell. 2010;141(6):970-81.
175. Butler LR, Densham RM, Jia J, Garvin AJ, Stone HR, Shah V, et al. The proteasomal de-ubiquitinating enzyme POH1 promotes the double-strand DNA break response. EMBO J. 2012;31(19):3918-34.
176. Shao G, Lilli DR, Patterson-Fortin J, Coleman KA, Morrissey DE, Greenberg RA. The Rap80-BRCC36 de-ubiquitinating enzyme complex antagonizes RNF8-Ubc13-dependent ubiquitination events at DNA double strand breaks. Proc Natl Acad Sci U S A. 2009;106(9):3166-71.
177. Ismail IH, Davidson R, Gagne JP, Xu ZZ, Poirier GG, Hendzel MJ. Germline mutations in BAP1 impair its function in DNA double-strand break repair. Cancer Res. 2014;74(16):4282-94.
178. Srinivasan G, Sidhu GS, Williamson EA, Jaiswal AS, Najmunnisa N, Wilcoxen K, et al. Synthetic lethality in malignant pleural mesothelioma with PARP1 inhibition. Cancer Chemother Pharmacol. 2017;80(4):861-7.
179. Parrotta R, Okonska A, Ronner M, Weder W, Stahel R, Penengo L, et al. A Novel BRCA1-Associated Protein-1 Isoform Affects Response of Mesothelioma Cells to Drugs Impairing BRCA1-Mediated DNA Repair. J Thorac Oncol. 2017;12(8):1309-19.
180. Borchert S, Wessolly M, Schmeller J, Mairinger E, Kollmeier J, Hager T, et al. Gene expression profiling of homologous recombination repair pathway indicates susceptibility

for olaparib treatment in malignant pleural mesothelioma in vitro. BMC Cancer. 2019;19(1):108.
181. Hassan R, Morrow B, Thomas A, Walsh T, Lee MK, Gulsuner S, et al. Inherited predisposition to malignant mesothelioma and overall survival following platinum chemotherapy. Proc Natl Acad Sci U S A. 2019;116(18):9008-13.
182. Busacca S, Sheaff M, Arthur K, Gray SG, O'Byrne KJ, Richard DJ, et al. BRCA1 is an essential mediator of vinorelbine-induced apoptosis in mesothelioma. J Pathol. 2012;227(2):200-8.
183. Krug LM, Wozniak AJ, Kindler HL, Feld R, Koczywas M, Morero JL, et al. Randomized phase II trial of pemetrexed/cisplatin with or without CBP501 in patients with advanced malignant pleural mesothelioma. Lung Cancer. 2014;85(3):429-34.
184. Kato S, Tomson BN, Buys TP, Elkin SK, Carter JL, Kurzrock R. Genomic Landscape of Malignant Mesotheliomas. Mol Cancer Ther. 2016;15(10):2498-507.
185. Illei PB, Rusch VW, Zakowski MF, Ladanyi M. Homozygous deletion of CDKN2A and codeletion of the methylthioadenosine phosphorylase gene in the majority of pleural mesotheliomas. Clin Cancer Res. 2003;9(6):2108-13.
186. Takeda M, Kasai T, Enomoto Y, Takano M, Morita K, Kadota E, et al. Genomic gains and losses in malignant mesothelioma demonstrated by FISH analysis of paraffin-embedded tissues. J Clin Pathol. 2012;65(1):77-82.
187. Quelle DE, Zindy F, Ashmun RA, Sherr CJ. Alternative reading frames of the INK4a tumor suppressor gene encode two unrelated proteins capable of inducing cell cycle arrest. Cell. 1995;83(6):993-1000.
188. Sherr CJ. Divorcing ARF and p53: an unsettled case. Nat Rev Cancer. 2006;6(9):663-73.
189. Cheng JQ, Jhanwar SC, Klein WM, Bell DW, Lee WC, Altomare DA, et al. p16 alterations and deletion mapping of 9p21-p22 in malignant mesothelioma. Cancer Res. 1994;54(21):5547-51.
190. Dacic S, Kothmaier H, Land S, Shuai Y, Halbwedl I, Morbini P, et al. Prognostic significance of p16/cdkn2a loss in pleural malignant mesotheliomas. Virchows Arch. 2008;453(6):627-35.
191. Kratzke RA, Otterson GA, Lincoln CE, Ewing S, Oie H, Geradts J, et al. Immunohistochemical analysis of the p16INK4 cyclin-dependent kinase inhibitor in malignant mesothelioma. J Natl Cancer Inst. 1995;87(24):1870-5.
192. Hirao T, Bueno R, Chen CJ, Gordon GJ, Heilig E, Kelsey KT. Alterations of the p16(INK4) locus in human malignant mesothelial tumors. Carcinogenesis. 2002;23(7):1127-30.
193. Frizelle SP, Kratzke MG, Carreon RR, Engel SC, Youngquist L, Klein MA, et al. Inhibition of both mesothelioma cell growth and Cdk4 activity following treatment with a TATp16INK4a peptide. Anticancer Res. 2008;28(1A):1-7.
194. Frizelle SP, Rubins JB, Zhou JX, Curiel DT, Kratzke RA. Gene therapy of established mesothelioma xenografts with recombinant p16INK4a adenovirus. Cancer Gene Ther. 2000;7(11):1421-5.
195. Thurneysen C, Opitz I, Kurtz S, Weder W, Stahel RA, Felley-Bosco E. Functional inactivation of NF2/merlin in human mesothelioma. Lung Cancer. 2009;64(2):140-7.
196. McClatchey AI, Giovannini M. Membrane organization and tumorigenesis--the NF2 tumor suppressor, Merlin. Genes Dev. 2005;19(19):2265-77.

197. Zanconato F, Cordenonsi M, Piccolo S. YAP/TAZ at the Roots of Cancer. Cancer Cell. 2016;29(6):783-803.
198. Liu-Chittenden Y, Huang B, Shim JS, Chen Q, Lee SJ, Anders RA, et al. Genetic and pharmacological disruption of the TEAD-YAP complex suppresses the oncogenic activity of YAP. Genes Dev. 2012;26(12):1300-5.
199. Song S, Xie M, Scott AW, Jin J, Ma L, Dong X, et al. A Novel YAP1 Inhibitor Targets CSC-Enriched Radiation-Resistant Cells and Exerts Strong Antitumor Activity in Esophageal Adenocarcinoma. Mol Cancer Ther. 2018;17(2):443-54.
200. Lopez-Lago MA, Okada T, Murillo MM, Socci N, Giancotti FG. Loss of the tumor suppressor gene NF2, encoding merlin, constitutively activates integrin-dependent mTORC1 signaling. Mol Cell Biol. 2009;29(15):4235-49.
201. Altomare DA, You H, Xiao GH, Ramos-Nino ME, Skele KL, De Rienzo A, et al. Human and mouse mesotheliomas exhibit elevated AKT/PKB activity, which can be targeted pharmacologically to inhibit tumor cell growth. Oncogene. 2005;24(40):6080-9.
202. Ou SH, Moon J, Garland LL, Mack PC, Testa JR, Tsao AS, et al. SWOG S0722: phase II study of mTOR inhibitor everolimus (RAD001) in advanced malignant pleural mesothelioma (MPM). J Thorac Oncol. 2015;10(2):387-91.
203. Dolly SO, Wagner AJ, Bendell JC, Kindler HL, Krug LM, Seiwert TY, et al. Phase I Study of Apitolisib (GDC-0980), Dual Phosphatidylinositol-3-Kinase and Mammalian Target of Rapamycin Kinase Inhibitor, in Patients with Advanced Solid Tumors. Clin Cancer Res. 2016;22(12):2874-84.
204. Yoon H, Dehart JP, Murphy JM, Lim ST. Understanding the roles of FAK in cancer: inhibitors, genetic models, and new insights. J Histochem Cytochem. 2015;63(2):114-28.
205. Shapiro IM, Kolev VN, Vidal CM, Kadariya Y, Ring JE, Wright Q, et al. Merlin deficiency predicts FAK inhibitor sensitivity: a synthetic lethal relationship. Sci Transl Med. 2014;6(237):237ra68.
206. Soria JC, Gan HK, Blagden SP, Plummer R, Arkenau HT, Ranson M, et al. A phase I, pharmacokinetic and pharmacodynamic study of GSK2256098, a focal adhesion kinase inhibitor, in patients with advanced solid tumors. Ann Oncol. 2016;27(12):2268-74.
207. Fennell DA BP, Kindler HL, Krug LM, Nowak A, Zauderer M. COMMAND: A phase II randomized, double-blind, placebo-controlled, multicenter study of defactinib as maintenance therapy in subjects with malignant pleural mesothelioma that has not progressed on at least four cycles of pemetrexed/platinum therapy. Journal of Clinical Oncology. 2017.
208. Bueno R GR, Lizotte PH, Sprott K, Jackman DM, Barlow J, Sharma S, Yeap BY, Chirieac LR, Lebenthal A, Cavanaugh M, Rode AJ, Kirschmeier P, Kwiatkowski DJ, Wong KK, Richards WG, Weaver DT. Effect of FAK inhibitor defactinib on tumor immune changes and tumor reductions in a phase II window of opportunity study in malignant pleural mesothelioma (MPM). Journal of Clinical Oncology. 2017.
209. Dominici M, Le Blanc K, Mueller I, Slaper-Cortenbach I, Marini F, Krause D, et al. Minimal criteria for defining multipotent mesenchymal stromal cells. The International Society for Cellular Therapy position statement. Cytotherapy. 2006;8(4):315-7.
210. Uccelli A, Moretta L, Pistoia V. Mesenchymal stem cells in health and disease. Nat Rev Immunol. 2008;8(9):726-36.
211. Fibbe WE, Noort WA. Mesenchymal stem cells and hematopoietic stem cell transplantation. Ann N Y Acad Sci. 2003;996:235-44.

212. Ryan JM, Barry FP, Murphy JM, Mahon BP. Mesenchymal stem cells avoid allogeneic rejection. J Inflamm (Lond). 2005;2:8.
213. Horwitz EM, Le Blanc K, Dominici M, Mueller I, Slaper-Cortenbach I, Marini FC, et al. Clarification of the nomenclature for MSC: The International Society for Cellular Therapy position statement. Cytotherapy. 2005;7(5):393-5.
214. Herrera MB, Bussolati B, Bruno S, Morando L, Mauriello-Romanazzi G, Sanavio F, et al. Exogenous mesenchymal stem cells localize to the kidney by means of CD44 following acute tubular injury. Kidney Int. 2007;72(4):430-41.
215. Shi M, Zhang Z, Xu R, Lin H, Fu J, Zou Z, et al. Human mesenchymal stem cell transfusion is safe and improves liver function in acute-on-chronic liver failure patients. Stem Cells Transl Med. 2012;1(10):725-31.
216. Augello A, Tasso R, Negrini SM, Amateis A, Indiveri F, Cancedda R, et al. Bone marrow mesenchymal progenitor cells inhibit lymphocyte proliferation by activation of the programmed death 1 pathway. Eur J Immunol. 2005;35(5):1482-90.
217. Lourenco S, Teixeira VH, Kalber T, Jose RJ, Floto RA, Janes SM. Macrophage migration inhibitory factor-CXCR4 is the dominant chemotactic axis in human mesenchymal stem cell recruitment to tumors. J Immunol. 2015;194(7):3463-74.
218. Roccaro AM, Sacco A, Purschke WG, Moschetta M, Buchner K, Maasch C, et al. SDF-1 inhibition targets the bone marrow niche for cancer therapy. Cell Rep. 2014;9(1):118-28.
219. Dasari VR, Kaur K, Velpula KK, Gujrati M, Fassett D, Klopfenstein JD, et al. Upregulation of PTEN in glioma cells by cord blood mesenchymal stem cells inhibits migration via downregulation of the PI3K/Akt pathway. PLoS One. 2010;5(4):e10350.
220. Kletukhina S, Neustroeva O, James V, Rizvanov A, Gomzikova M. Role of Mesenchymal Stem Cell-Derived Extracellular Vesicles in Epithelial-Mesenchymal Transition. Int J Mol Sci. 2019;20(19).
221. Gong M, Yu B, Wang J, Wang Y, Liu M, Paul C, et al. Mesenchymal stem cells release exosomes that transfer miRNAs to endothelial cells and promote angiogenesis. Oncotarget. 2017;8(28):45200-12.
222. Barcellos-de-Souza P, Comito G, Pons-Segura C, Taddei ML, Gori V, Becherucci V, et al. Mesenchymal Stem Cells are Recruited and Activated into Carcinoma-Associated Fibroblasts by Prostate Cancer Microenvironment-Derived TGF-beta1. Stem Cells. 2016;34(10):2536-47.
223. Poggi A, Musso A, Dapino I, Zocchi MR. Mechanisms of tumor escape from immune system: role of mesenchymal stromal cells. Immunol Lett. 2014;159(1-2):55-72.
224. Kalluri R. The biology and function of fibroblasts in cancer. Nat Rev Cancer. 2016;16(9):582-98.
225. Ridge SM, Sullivan FJ, Glynn SA. Mesenchymal stem cells: key players in cancer progression. Mol Cancer. 2017;16(1):31.
226. Ramasamy R, Lam EW, Soeiro I, Tisato V, Bonnet D, Dazzi F. Mesenchymal stem cells inhibit proliferation and apoptosis of tumor cells: impact on in vivo tumor growth. Leukemia. 2007;21(2):304-10.
227. Lu YR, Yuan Y, Wang XJ, Wei LL, Chen YN, Cong C, et al. The growth inhibitory effect of mesenchymal stem cells on tumor cells in vitro and in vivo. Cancer Biol Ther. 2008;7(2):245-51.
228. Shi Y, Wang Y, Li Q, Liu K, Hou J, Shao C, et al. Immunoregulatory mechanisms of mesenchymal stem and stromal cells in inflammatory diseases. Nat Rev Nephrol. 2018;14(8):493-507.

229. Prendergast GC, Malachowski WP, DuHadaway JB, Muller AJ. Discovery of IDO1 Inhibitors: From Bench to Bedside. Cancer Res. 2017;77(24):6795-811.
230. Kronsteiner B, Wolbank S, Peterbauer A, Hackl C, Redl H, van Griensven M, et al. Human mesenchymal stem cells from adipose tissue and amnion influence T-cells depending on stimulation method and presence of other immune cells. Stem Cells Dev. 2011;20(12):2115-26.
231. Barcia RN, Santos JM, Filipe M, Teixeira M, Martins JP, Almeida J, et al. What Makes Umbilical Cord Tissue-Derived Mesenchymal Stromal Cells Superior Immunomodulators When Compared to Bone Marrow Derived Mesenchymal Stromal Cells? Stem Cells Int. 2015;2015:583984.
232. Galland S, Stamenkovic I. Mesenchymal stromal cells in cancer: a review of their immunomodulatory functions and dual effects on tumor progression. J Pathol. 2019.
233. Nasef A, Chapel A, Mazurier C, Bouchet S, Lopez M, Mathieu N, et al. Identification of IL-10 and TGF-beta transcripts involved in the inhibition of T-lymphocyte proliferation during cell contact with human mesenchymal stem cells. Gene Expr. 2007;13(4-5):217-26.
234. Romieu-Mourez R, Francois M, Boivin MN, Stagg J, Galipeau J. Regulation of MHC class II expression and antigen processing in murine and human mesenchymal stromal cells by IFN-gamma, TGF-beta, and cell density. J Immunol. 2007;179(3):1549-58.
235. Davies LC, Heldring N, Kadri N, Le Blanc K. Mesenchymal Stromal Cell Secretion of Programmed Death-1 Ligands Regulates T Cell Mediated Immunosuppression. Stem Cells. 2017;35(3):766-76.
236. Ren G, Zhao X, Zhang L, Zhang J, L'Huillier A, Ling W, et al. Inflammatory cytokine-induced intercellular adhesion molecule-1 and vascular cell adhesion molecule-1 in mesenchymal stem cells are critical for immunosuppression. J Immunol. 2010;184(5):2321-8.
237. Le Blanc K, Mougiakakos D. Multipotent mesenchymal stromal cells and the innate immune system. Nat Rev Immunol. 2012;12(5):383-96.
238. Spaggiari GM, Capobianco A, Becchetti S, Mingari MC, Moretta L. Mesenchymal stem cell-natural killer cell interactions: evidence that activated NK cells are capable of killing MSCs, whereas MSCs can inhibit IL-2-induced NK-cell proliferation. Blood. 2006;107(4):1484-90.
239. Jiang XX, Zhang Y, Liu B, Zhang SX, Wu Y, Yu XD, et al. Human mesenchymal stem cells inhibit differentiation and function of monocyte-derived dendritic cells. Blood. 2005;105(10):4120-6.
240. Chen HW, Chen HY, Wang LT, Wang FH, Fang LW, Lai HY, et al. Mesenchymal stem cells tune the development of monocyte-derived dendritic cells toward a myeloid-derived suppressive phenotype through growth-regulated oncogene chemokines. J Immunol. 2013;190(10):5065-77.
241. Bernardo ME, Fibbe WE. Mesenchymal stromal cells: sensors and switchers of inflammation. Cell Stem Cell. 2013;13(4):392-402.
242. Prigione I, Benvenuto F, Bocca P, Battistini L, Uccelli A, Pistoia V. Reciprocal interactions between human mesenchymal stem cells and gammadelta T cells or invariant natural killer T cells. Stem Cells. 2009;27(3):693-702.
243. Jiang W, Xu J. Immune modulation by mesenchymal stem cells. Cell Prolif. 2020;53(1):e12712.

244. Shirjang S, Mansoori B, Solali S, Hagh MF, Shamsasenjan K. Toll-like receptors as a key regulator of mesenchymal stem cell function: An up-to-date review. Cell Immunol. 2017;315:1-10.
245. Waterman RS, Tomchuck SL, Henkle SL, Betancourt AM. A new mesenchymal stem cell (MSC) paradigm: polarization into a pro-inflammatory MSC1 or an Immunosuppressive MSC2 phenotype. PLoS One. 2010;5(4):e10088.
246. Ferguson SW, Wang J, Lee CJ, Liu M, Neelamegham S, Canty JM, et al. The microRNA regulatory landscape of MSC-derived exosomes: a systems view. Sci Rep. 2018;8(1):1419.
247. Reagan MR, Kaplan DL. Concise review: Mesenchymal stem cell tumor-homing: detection methods in disease model systems. Stem Cells. 2011;29(6):920-7.
248. Melzer C, Rehn V, Yang Y, Bahre H, von der Ohe J, Hass R. Taxol-Loaded MSC-Derived Exosomes Provide a Therapeutic Vehicle to Target Metastatic Breast Cancer and Other Carcinoma Cells. Cancers (Basel). 2019;11(6).
249. Yang X, Du J, Xu X, Xu C, Song W. IFN-gamma-secreting-mesenchymal stem cells exert an antitumor effect in vivo via the TRAIL pathway. J Immunol Res. 2014;2014:318098.
250. Loebinger MR, Sage EK, Davies D, Janes SM. TRAIL-expressing mesenchymal stem cells kill the putative cancer stem cell population. Br J Cancer. 2010;103(11):1692-7.
251. Matuskova M, Hlubinova K, Pastorakova A, Hunakova L, Altanerova V, Altaner C, et al. HSV-tk expressing mesenchymal stem cells exert bystander effect on human glioblastoma cells. Cancer Lett. 2010;290(1):58-67.
252. Elzaouk L, Moelling K, Pavlovic J. Anti-tumor activity of mesenchymal stem cells producing IL-12 in a mouse melanoma model. Exp Dermatol. 2006;15(11):865-74.
253. Liu X, Hu J, Sun S, Li F, Cao W, Wang YU, et al. Mesenchymal stem cells expressing interleukin-18 suppress breast cancer cells in vitro. Exp Ther Med. 2015;9(4):1192-200.
254. Xin H, Sun R, Kanehira M, Takahata T, Itoh J, Mizuguchi H, et al. Intratracheal delivery of CX3CL1-expressing mesenchymal stem cells to multiple lung tumors. Mol Med. 2009;15(9-10):321-7.
255. Wang S, El-Deiry WS. TRAIL and apoptosis induction by TNF-family death receptors. Oncogene. 2003;22(53):8628-33.
256. Ashkenazi A, Dixit VM. Death receptors: signaling and modulation. Science. 1998;281(5381):1305-8.
257. Pitti RM, Marsters SA, Ruppert S, Donahue CJ, Moore A, Ashkenazi A. Induction of apoptosis by Apo-2 ligand, a new member of the tumor necrosis factor cytokine family. J Biol Chem. 1996;271(22):12687-90.
258. Gura T. How TRAIL kills cancer cells, but not normal cells. Science. 1997;277(5327):768.
259. Boldin MP, Varfolomeev EE, Pancer Z, Mett IL, Camonis JH, Wallach D. A novel protein that interacts with the death domain of Fas/APO1 contains a sequence motif related to the death domain. J Biol Chem. 1995;270(14):7795-8.
260. Kischkel FC, Hellbardt S, Behrmann I, Germer M, Pawlita M, Krammer PH, et al. Cytotoxicity-dependent APO-1 (Fas/CD95)-associated proteins form a death-inducing signaling complex (DISC) with the receptor. EMBO J. 1995;14(22):5579-88.
261. Bodmer JL, Holler N, Reynard S, Vinciguerra P, Schneider P, Juo P, et al. TRAIL receptor-2 signals apoptosis through FADD and caspase-8. Nat Cell Biol. 2000;2(4):241-3.
262. Shakeri R, Kheirollahi A, Davoodi J. Apaf-1: Regulation and function in cell death. Biochimie. 2017;135:111-25.

263. Fulda S, Debatin KM. Extrinsic versus intrinsic apoptosis pathways in anticancer chemotherapy. Oncogene. 2006;25(34):4798-811.
264. Johnstone RW, Ruefli AA, Lowe SW. Apoptosis: a link between cancer genetics and chemotherapy. Cell. 2002;108(2):153-64.
265. Cuello M, Ettenberg SA, Nau MM, Lipkowitz S. Synergistic induction of apoptosis by the combination of trail and chemotherapy in chemoresistant ovarian cancer cells. Gynecol Oncol. 2001;81(3):380-90.
266. Galligan L, Longley DB, McEwan M, Wilson TR, McLaughlin K, Johnston PG. Chemotherapy and TRAIL-mediated colon cancer cell death: the roles of p53, TRAIL receptors, and c-FLIP. Mol Cancer Ther. 2005;4(12):2026-36.
267. Kataoka T, Schroter M, Hahne M, Schneider P, Irmler M, Thome M, et al. FLIP prevents apoptosis induced by death receptors but not by perforin/granzyme B, chemotherapeutic drugs, and gamma irradiation. J Immunol. 1998;161(8):3936-42.
268. Gill C, Dowling C, O'Neill AJ, Watson RW. Effects of cIAP-1, cIAP-2 and XIAP triple knockdown on prostate cancer cell susceptibility to apoptosis, cell survival and proliferation. Mol Cancer. 2009;8:39.
269. Danish L, Imig D, Allgower F, Scheurich P, Pollak N. Bcl-2-mediated control of TRAIL-induced apoptotic response in the non-small lung cancer cell line NCI-H460 is effective at late caspase processing steps. PLoS One. 2018;13(6):e0198203.
270. Trepel J, Mollapour M, Giaccone G, Neckers L. Targeting the dynamic HSP90 complex in cancer. Nat Rev Cancer. 2010;10(8):537-49.
271. Imai J, Maruya M, Yashiroda H, Yahara I, Tanaka K. The molecular chaperone Hsp90 plays a role in the assembly and maintenance of the 26S proteasome. EMBO J. 2003;22(14):3557-67.
272. Pratt WB, Galigniana MD, Morishima Y, Murphy PJ. Role of molecular chaperones in steroid receptor action. Essays Biochem. 2004;40:41-58.
273. Lang SA, Klein D, Moser C, Gaumann A, Glockzin G, Dahlke MH, et al. Inhibition of heat shock protein 90 impairs epidermal growth factor-mediated signaling in gastric cancer cells and reduces tumor growth and vascularization in vivo. Mol Cancer Ther. 2007;6(3):1123-32.
274. Garcia-Carbonero R, Carnero A, Paz-Ares L. Inhibition of HSP90 molecular chaperones: moving into the clinic. Lancet Oncol. 2013;14(9):e358-69.
275. Chen B, Piel WH, Gui L, Bruford E, Monteiro A. The HSP90 family of genes in the human genome: insights into their divergence and evolution. Genomics. 2005;86(6):627-37.
276. Pearl LH, Prodromou C. Structure, function, and mechanism of the Hsp90 molecular chaperone. Adv Protein Chem. 2001;59:157-86.
277. Duval M, Le Boeuf F, Huot J, Gratton JP. Src-mediated phosphorylation of Hsp90 in response to vascular endothelial growth factor (VEGF) is required for VEGF receptor-2 signaling to endothelial NO synthase. Mol Biol Cell. 2007;18(11):4659-68.
278. Mollapour M, Tsutsumi S, Donnelly AC, Beebe K, Tokita MJ, Lee MJ, et al. Swe1Wee1-dependent tyrosine phosphorylation of Hsp90 regulates distinct facets of chaperone function. Mol Cell. 2010;37(3):333-43.
279. Kurokawa M, Zhao C, Reya T, Kornbluth S. Inhibition of apoptosome formation by suppression of Hsp90beta phosphorylation in tyrosine kinase-induced leukemias. Mol Cell Biol. 2008;28(17):5494-506.

280. Yang Y, Rao R, Shen J, Tang Y, Fiskus W, Nechtman J, et al. Role of acetylation and extracellular location of heat shock protein 90alpha in tumor cell invasion. Cancer Res. 2008;68(12):4833-42.
281. Martinez-Ruiz A, Villanueva L, Gonzalez de Orduna C, Lopez-Ferrer D, Higueras MA, Tarin C, et al. S-nitrosylation of Hsp90 promotes the inhibition of its ATPase and endothelial nitric oxide synthase regulatory activities. Proc Natl Acad Sci U S A. 2005;102(24):8525-30.
282. Choo A, Palladinetti P, Passioura T, Shen S, Lock R, Symonds G, et al. The role of IRF1 and IRF2 transcription factors in leukaemogenesis. Curr Gene Ther. 2006;6(5):543-50.
283. Zhao R, Houry WA. Hsp90: a chaperone for protein folding and gene regulation. Biochem Cell Biol. 2005;83(6):703-10.
284. Maloney A, Clarke PA, Naaby-Hansen S, Stein R, Koopman JO, Akpan A, et al. Gene and protein expression profiling of human ovarian cancer cells treated with the heat shock protein 90 inhibitor 17-allylamino-17-demethoxygeldanamycin. Cancer Res. 2007;67(7):3239-53.
285. Kabakov AE, Makarova YM, Malyutina YV. Radiosensitization of human vascular endothelial cells through Hsp90 inhibition with 17-N-allilamino-17-demethoxygeldanamycin. Int J Radiat Oncol Biol Phys. 2008;71(3):858-65.
286. Tse AN, Klimstra DS, Gonen M, Shah M, Sheikh T, Sikorski R, et al. A phase 1 dose-escalation study of irinotecan in combination with 17-allylamino-17-demethoxygeldanamycin in patients with solid tumors. Clin Cancer Res. 2008;14(20):6704-11.
287. Hubbard J, Erlichman C, Toft DO, Qin R, Stensgard BA, Felten S, et al. Phase I study of 17-allylamino-17 demethoxygeldanamycin, gemcitabine and/or cisplatin in patients with refractory solid tumors. Invest New Drugs. 2011;29(3):473-80.
288. Busacca S, Law EW, Powley IR, Proia DA, Sequeira M, Le Quesne J, et al. Resistance to HSP90 inhibition involving loss of MCL1 addiction. Oncogene. 2016;35(12):1483-92.
289. Kamal A, Thao L, Sensintaffar J, Zhang L, Boehm MF, Fritz LC, et al. A high-affinity conformation of Hsp90 confers tumour selectivity on Hsp90 inhibitors. Nature. 2003;425(6956):407-10.
290. Okamoto J, Mikami I, Tominaga Y, Kuchenbecker KM, Lin YC, Bravo DT, et al. Inhibition of Hsp90 leads to cell cycle arrest and apoptosis in human malignant pleural mesothelioma. J Thorac Oncol. 2008;3(10):1089-95.
291. di Martino S, Amoreo CA, Nuvoli B, Galati R, Strano S, Facciolo F, et al. HSP90 inhibition alters the chemotherapy-driven rearrangement of the oncogenic secretome. Oncogene. 2018;37(10):1369-85.
292. Yao Z, Chen A, Li X, Zhu Z, Jiang X. Hsp90 inhibitor sensitizes TRAIL-mediated apoptosis via chop-dependent DR5 upregulation in colon cancer cells. Am J Transl Res. 2017;9(11):4945-53.
293. Eccles SA, Massey A, Raynaud FI, Sharp SY, Box G, Valenti M, et al. NVP-AUY922: a novel heat shock protein 90 inhibitor active against xenograft tumor growth, angiogenesis, and metastasis. Cancer Res. 2008;68(8):2850-60.
294. Fennell D DS, Forster M, Talbot D, Woll P, Child J, Ngai Y, Farrelly L, Hackshaw A, Sharkey A, Busacca S, Hastings R, Barnes D, Nicolson M, Taylor P, Ahmed S, Wheeler G. Phase 1 Study of HSP90 Inhibitor Ganetespib with Pemetrexed and Cisplatin/Carboplatin Chemotherapy for Pleural Mesothelioma. Journal of Thoracic Oncology. 2018;13(10):S397.
295. Wood RD, Mitchell M, Lindahl T. Human DNA repair genes, 2005. Mutat Res. 2005;577(1-2):275-83.

296. Lange SS, Takata K, Wood RD. DNA polymerases and cancer. Nat Rev Cancer. 2011;11(2):96-110.
297. Ronen A, Glickman BW. Human DNA repair genes. Environ Mol Mutagen. 2001;37(3):241-83.
298. Aravind L, Walker DR, Koonin EV. Conserved domains in DNA repair proteins and evolution of repair systems. Nucleic Acids Res. 1999;27(5):1223-42.
299. Hong R, Ma F, Zhang W, Yu X, Li Q, Luo Y, et al. 53BP1 depletion causes PARP inhibitor resistance in ATM-deficient breast cancer cells. BMC Cancer. 2016;16(1):725.
300. Mohni KN, Kavanaugh GM, Cortez D. ATR pathway inhibition is synthetically lethal in cancer cells with ERCC1 deficiency. Cancer Res. 2014;74(10):2835-45.
301. Brin E, Wu K, Dagostino E, Meng-Chiang Kuo M, He Y, Shia WJ, et al. TRAIL stabilization and cancer cell sensitization to its pro-apoptotic activity achieved through genetic fusion with arginine deiminase. Oncotarget. 2018;9(97):36914-28.
302. Motzer RJ, Rini BI, McDermott DF, Aren Frontera O, Hammers HJ, Carducci MA, et al. Nivolumab plus ipilimumab versus sunitinib in first-line treatment for advanced renal cell carcinoma: extended follow-up of efficacy and safety results from a randomised, controlled, phase 3 trial. Lancet Oncol. 2019;20(10):1370-85.
303. Gandhi L, Garassino MC. Pembrolizumab plus Chemotherapy in Lung Cancer. N Engl J Med. 2018;379(11):e18.
304. Emens LA, Middleton G. The interplay of immunotherapy and chemotherapy: harnessing potential synergies. Cancer Immunol Res. 2015;3(5):436-43.
305. Leach DR, Krummel MF, Allison JP. Enhancement of antitumor immunity by CTLA-4 blockade. Science. 1996;271(5256):1734-6.
306. Long GV, Dummer R, Hamid O, Gajewski TF, Caglevic C, Dalle S, et al. Epacadostat plus pembrolizumab versus placebo plus pembrolizumab in patients with unresectable or metastatic melanoma (ECHO-301/KEYNOTE-252): a phase 3, randomised, double-blind study. Lancet Oncol. 2019;20(8):1083-97.
307. Kim M, Rhee JK, Choi H, Kwon A, Kim J, Lee GD, et al. Passage-dependent accumulation of somatic mutations in mesenchymal stromal cells during in vitro culture revealed by whole genome sequencing. Sci Rep. 2017;7(1):14508.
308. Morimoto RI. Regulation of the heat shock transcriptional response: cross talk between a family of heat shock factors, molecular chaperones, and negative regulators. Genes Dev. 1998;12(24):3788-96.
309. Weinmann M, Marini P, Jendrossek V, Betsch A, Goecke B, Budach W, et al. Influence of hypoxia on TRAIL-induced apoptosis in tumor cells. Int J Radiat Oncol Biol Phys. 2004;58(2):386-96.

8 SUPPLEMENTARY DOCUMENTS

8.1 Patient information sheet for pleural procedures

UCL Respiratory
Rayne Institute
5, University Street
London
WC1E 6JF

Tel (+44) 0203 549 5979

Version 4: Pleural procedures
Date: 15 November 2018
Project ID: 245471

Participant Information Sheet

1. Study title

An investigation into the molecular pathogenesis (cause) of lung disease II

2. Invitation paragraph

You are being invited to take part in a research study. Before you decide whether or not to participate it is important to understand why the research is being done and what it will involve for you. Please take time to read the following information carefully and discuss it with others if you wish. Ask us if there is anything that is not clear or if you would like more information.

3. What is the purpose of the study?

Lung diseases, such as asthma, COPD and lung cancer, are a major cause of illness and death in the UK. This project is trying to understand the causes of lung disease. To do this we need to be able to compare normal and abnormal samples from the respiratory tract (lining of the airway). By exploring the molecular pathways which underlie these conditions we hope to identify new treatment targets.

4. Why have I been invited?

You have been invited because we are interested in patients who are due to undergo a pleural procedure. This may be a pleural fluid aspiration; which is where fluid, that has built up in the lining of the lungs, is removed or pleural biopsy; which is where small biopsies of the lung lining are taken. The exact procedure that you are having would be planned as part of your clinical care and discussed with you by your doctor. You would not undergo any additional procedures for this research project.

5. Do I have to take part?

No. It is entirely up to you to decide whether or not to take part. If you do decide to take part you will be given this information sheet to keep and be asked to sign a consent form. If you decide to take part you are still free to withdraw at any time before the research samples are taken and without giving a reason. A decision to withdraw at any time, or a decision not to take part, will not affect your care.

6. What is involved in the study?

This study will fit into your planned attendance at hospital for your procedure. If you agree to take part you will be asked to provide some additional samples for this study, which may include;

- Pleural fluid sample (requested if you are having pleural fluid aspiration)
- Pleural biopsies (requested if you are having pleural biopsies)
- Blood sample

The processes around these are explained in more detail below.

During a pleural fluid aspiration, once the necessary fluid samples have been collected for diagnostic purposes, a further fluid sample would be collected for research. This fluid would otherwise be removed from the lining of your lungs and discarded as waste.

During a pleural biopsy you may be asked to have 1-6 extra biopies taken for research (usually you would have 4-6 taken as part of your clinical care).

Patients may also be asked to give a blood sample, which will be approximately 40ml or 8 teaspoons. The blood sample is taken so that we have a sample of cells from you that is not from the respiratory tract, in order to compare with this.

Any samples that are taken for research purposes will be taken after the diagnostic samples have been acquired and only if it is felt safe to do so by the doctor performing the procedure.

No expenses will be paid.

7. What are known risks of the study or the side effects of any treatment received?

When you are consented for your pleural procedure, the doctor will explain the risks and benefits and you will be able to ask questions. In terms of participation in the research specifically, there are no additional risks associated with providing a research pleural fluid sample. Having a pleural biopsy is considered overall to be a safe procedure but there is a small risk of bleeding associated with having a biopsy taken. This risk would be minimised by stopping any anticoagulants beforehand and the clinician would be prepared for such complications.

Obtaining blood via a cannula is very minimally invasive and you would not experience any discomfort. If the blood could not be taken at the point of cannulation, we may ask you to undergo a blood test, in which case there is a small risk of developing a bruise, which would be minimalised through applying pressure.

8. What are the possible benefits of taking part?

There will be no intended clinical benefit to you personally from taking part in the trial. It may be that research carried out on the samples you provide will help future patients.

9. The information held about the research subject

Some details will be collected about you including your age and sex, a record of your personal medical and drug history particularly with reference to lung disease, any relevant family history, your smoking history and lung function tests. Details of any lung disease including diagnosis, date of

diagnosis, method of diagnosis, biopsy reports and clinical outcome may also be collected if applicable.

All information which is collected about you during the course of the research will be kept strictly confidential. The samples that you provide will be labelled with a unique study number and will not have any identifiable information (name, NHS number, date of birth) on them. University College London will be the organisation involved in collecting the data. The principal investigator, Professor Sam Janes, will be responsible for safety and security of any data we collect.

If you are agreeable, we will notify your GP of your participation in this project. This is standard practice when the GP is not directly involved but is entirely at your discretion.

10. How will my information be used?

UCL is the sponsor for this study based in the United Kingdom. We will be using information from you and/or your medical records in order to undertake this study and UCL will act as the data controller for this study. This means that we are responsible for looking after your information and using it properly. UCL will keep identifiable information about you for 12 years after the study has finished.

Your rights to access, change or move your information are limited, as we need to manage your information in specific ways in order for the research to be reliable and accurate. To safeguard your rights, we will use the minimum personally identifiable information possible.

UCL will collect information from you and/or your medical records for this research study in accordance with its instructions. UCL will use your name, NHS number and contact details to contact you about the research study, and make sure that relevant information about the study is recorded for your care, and to oversee the quality of the study. Individuals from UCL and regulatory organisations may look at your medical and research records to check the accuracy of the research study. The hospital will pass these details to UCL along with the information collected from you and/or your medical records. The only people in UCL who will have access to information that identifies you will be people who need to contact you to check information or audit the data collection process. The people who analyse the information will not be able to identify you and will not be able to find out your name, NHS number or contact details.

The information about your health and care may be provided to researchers running other research studies in this organisation or other organisations. This information will not identify you and will not be combined with other information in a way that could identify you. The information will only be used for the purpose of health and care research, and cannot be used to contact you or to affect your care. It will not be used to make decisions about future services available to you, such as insurance. These organisations may be universities, NHS organisations or companies involved in health and care research in this country or abroad. Your information will only be used by organisations and researchers to conduct research in accordance with the UK Policy Framework for Health and Social Care Research.

You can find out more about how we use your information by contacting Sam Janes at s.janes@ucl.ac.uk or at http://www.ctc.ucl.ac.uk/Privacy.

11. What will happen to the samples I provide?

The samples collected in this study and the data obtained from them will be stored and used at University College London. Your samples will be used to carry out research into how respiratory diseases develop and to identify new treatment strategies.

The types of experiment that we may do on your tissue sample include;

- Freezing the tissue and/or embedding it in paraffin so that we may perform molecular analysis, including genetic analysis, of the cells

- Growing the cells from the tissue so that we can manipulate the surrounding environment e.g. to find out if certain treatments (which may underpin future medicines) work. Cells from biopsy samples do not survive for very long outside of the body. Therefore in order for us to study the cells, we must place them in culture, which enables them to survive for a longer period ('culture' refers to an environment which provides factors necessary for cell survival). In some instances, we would look to alter the cells in order that they would continue to survive, in theory, forever. This is known as creating a 'cell line' and has a number of benefits, including being able to repeat experiments on the same cell type.

Some of these projects may be carried out in collaboration with commercial organisations, including the pharmaceutical industry. At the end of the study, samples will be disposed in accordance with all applicable legal and regulatory requirements, including the Human Tissue Act 2004 and any amendments thereafter.

12. Possibility of future studies

When a biopsy is taken as part of this study it is regarded as a gift to the institution and could be used for future investigations into the molecular causes of lung disease. At the end of the study any surplus tissue may be transferred to a registered tissue bank for use in future research. Any future studies will be reviewed by a research ethics committee. Consent from you for future studies would only be required if the committee considers that the study is likely to substantially affect the subjects' interests.

13. Gene studies

As part of the project we will be storing the samples taken to investigate genes and genetic pathways potentially involved in causing lung disease. There will be no attempt made to use your samples without your explicit consent to investigate any disorder, particularly any inherited disorder, other than lung disease.

14. What willl happen if the findings may affect the subject personally?

The findings of this project will not affect you personally.

15. What if something goes wrong?

Every care will be taken in the course of this research. In the unlikely event that something goes wrong and you suspect that the injury is the result of the sponsor (UCL), or hospitals negligence you many be able to claim compensation. Please make the claim in writing to Professor Sam Janes, Chief Investigator for the study. If you wish to complain or have any concerns about any aspect of the way you have been approached or treated by members of staff or about any adverse events you may have experienced due to your participation in the study, the normal National Health Service complaints mechanisms are available to you.

16. What will happen to the results of the research study?

The results of the research will be presented at national and international meetings and submitted to peer-reviewed journals for publication. We will be very happy to inform you at your request of any such publication. If you are one of the patients who we biopsy with a view to creating a cell line then we will be happy to update you, again at your request, of the success or otherwise of the attempt to create a cell line.

You will not be identified in any report or publication.

17. Who is organising and funding the research?

University College London is the sponsor of this research.

The study is primarily funded by the Wellcome Trust.

Neither your doctor nor the investigators are paid for including you in this project.

18. Inducements

As with standard practice you will not be paid for entering this project.

19. Withdrawal from the project

Your participation in the trial is entirely voluntary. You are free to decline to enter or to withdraw from the study prior to the procedure without having to give a reason. If you choose not to enter the study, or to withdraw subsequently but prior to the procedure, this will in no way affect your future medical care. Participation in this study will in no way affect your legal rights.

Who has reviewed the study?

This project has been reviewed and given favourable opinion by Hampshire Research Committee and by the Health Research Authority.

20. Contact for further information

Your contact point for further information is Professor Sam Janes.

Email: s.janes@ucl.ac.uk,

Telephone: 02035495976

We would like to take this opportunity to thank you very much for considering being a participant in this project.

You will be given a copy of this information sheet for your records.

8.2 Patient information sheet for video assisted thoracoscopic surgery (VATS)

UCL Respiratory
Rayne Institute
5, University Street
London
WC1E 6JF

Tel (+44) 0203 549 5979

Version 4: Video-assisted thoracoscopic surgery
Date: 15th November 2018
Project ID: 245471

Participant Information Sheet

1. Study title

An investigation into the molecular pathogenesis (cause) of lung disease.

2. Invitation paragraph

You are being invited to take part in a research study. Before you decide it is important for you to understand why the research is being done and what it will involve. Please take time to read the following information carefully and discuss it with others if you wish. Ask us if there is anything that is not clear or if you would like more information.

3. What is the purpose of the study?

Lung diseases, such as asthma, COPD and lung cancer, are a major cause of illness and death in the UK. This project is trying to understand the causes of lung disease. To do this we need to be able to compare normal and abnormal samples from the lungs. By exploring the molecular pathways which underlie these conditions we hope to identify new treatment targets.

4. Why have I been invited?

You have been invited because we are interested in patients who are undergoing video assisted thoracoscopic surgery (VATS) for diagnostic and treatment purposes.

5. Do I have to take part?

No. It is entirely up to you to decide whether or not to take part. If you do decide to take part you will be given this information sheet to keep and be asked to sign a consent form. If you decide to take part you are still free to withdraw at any time before your operation without giving a reason. A decision to withdraw at any time, or a decision not to take part, will not affect your care.

6. What is involved in the study?

This study will fit into your planned attendance at hospital for your operation and you will not have any additional operations/procedures for this study.

If you agree to take part you will be asked to provide some additional samples for this study, which may include;

- Biopsies from the lining of the lung (taken during VATS)
- Pleural fluid sample (taken during VATS)
- Blood sample

The processes around these are explained in more detail below.

During your VATS procedure, the surgeon will take all the biopsies necessary for diagnostic purposes first. Following this, the surgeon would take up to 4 extra biopsies for research (usually you would have 2-6 taken as part of your clinical care). A biopsy is around 1cm in size.

During your VATS procedure, the surgeon will drain any fluid that has built up in the lining of the lung. Samples will be sent usually for diagnostic purposes to the laboratory and, once this has been done, a sample may be taken for research.

Patients may also be asked to give a blood sample, which will be approximately 40ml or 8 teaspoons. The blood sample is taken so that we have a sample of cells from you that is not from the lungs, in order to compare with this. We would aim to take this at the point of having a cannula inserted, which is needed as part of your planned procedure in order to give you medicine for sedation purposes. If it were not possible to obtain the blood from the cannula then we may ask if you would be willing to undergo a blood test specifically for research purposes.

No expenses will be paid.

7. What are known risks of the study or the side effects of any treatment received?

You will be consented for the procedure by the surgeon who will explain the risks and benefits and give you time to answer any questions. When biopsies are taken there is a small risk of bleeding. There is no additional risk from providing a sample of pleural fluid, as any excess fluid would be usually be discarded. Taking blood via a cannula is a painless procedure. If we needed to perform a blood test, there is a small risk of developing a bruise.

8. What are the possible benefits of taking part?

There will be no intended clinical benefit to you personally from taking part in the trial. It may be that research carried out on the samples you provide will help future patients.

9. The information held about the research subject

Some details will be collected about you including your age and sex, a record of your personal medical and drug history particularly with reference to lung disease, any relevant family history, your smoking history and lung function tests. Details of any lung disease including diagnosis, date of diagnosis, method of diagnosis, biopsy reports and clinical outcome may also be collected if applicable.

All information which is collected about you during the course of the research will be kept strictly confidential. The samples that you provide will be labelled with a unique study number and will not

have any identifiable information (name, NHS number, date of birth) on them. University College London will be the organisation involved in collecting the data. The principal investigator, Professor Sam Janes, will be responsible for safety and security of any data we collect.

If you are agreeable, we will notify your GP of your participation in this project. This is standard practice when the GP is not directly involved but is entirely at your discretion.

10. How will my information be used?

UCL is the sponsor for this study based in the United Kingdom. We will be using information from you and/or your medical records in order to undertake this study and UCL will act as the data controller for this study. This means that we are responsible for looking after your information and using it properly. UCL will keep identifiable information about you for 12 months after the study has finished.

Your rights to access, change or move your information are limited, as we need to manage your information in specific ways in order for the research to be reliable and accurate. To safeguard your rights, we will use the minimum personally identifiable information possible.

UCL will collect information from you and/or your medical records for this research study in accordance with its instructions. UCL will use your name, NHS number and contact details to contact you about the research study, and make sure that relevant information about the study is recorded for your care, and to oversee the quality of the study. Individuals from UCL and regulatory

organisations may look at your medical and research records to check the accuracy of the research study. The hospital will pass these details to UCL along with the information collected from you and/or your medical records. The only people in UCL who will have access to information that identifies you will be people who need to contact you to check information or audit the data collection process. The people who analyse the information will not be able to identify you and will not be able to find out your name, NHS number or contact details.

The information about your health and care may be provided to researchers running other research studies in this organisation or other organisations. This information will not identify you and will not be combined with other information in a way that could identify you. The information will only be used for the purpose of health and care research, and cannot be used to contact you or to affect your care. It will not be used to make decisions about future services available to you, such as insurance. These organisations may be universities, NHS organisations or companies involved in health and care research in this country or abroad. Your information will only be used by organisations and researchers to conduct research in accordance with the UK Policy Framework for Health and Social Care Research.

You can find out more about how we use your information by contacting Sam Janes at s.janes@ucl.ac.uk or at http://www.ctc.ucl.ac.uk/Privacy.

11. What will happen to the samples I provide?

The samples collected in this study and the data obtained from them will be stored and used at University College London. Your samples will be used to carry out research into how respiratory diseases develop and to identify new treatment strategies.

The types of experiment that we may do on your tissue sample include;

- Freezing the tissue and/or embedding it in paraffin so that we may perform molecular analysis, including genetic analysis, of the cells
- Growing the cells from the tissue so that we can manipulate the surrounding environment e.g. to find out if certain treatments (which may underpin future medicines) work. Cells from biopsy samples do not survive for very long outside of the body. Therefore in order for us to study the cells, we must place them in culture, which enables them to survive for a longer period ('culture' refers to an environment which provides factors necessary for cell survival). In some instances, we would look to alter the cells in order that they would continue to survive, in theory, forever. This is known as creating a 'cell line' and has a number of benefits, including being able to repeat experiments on the same cell type.

Some of these projects may be carried out in collaboration with commercial organisations, including the pharmaceutical industry. At the end of the study, samples will be disposed in accordance with all applicable legal and regulatory requirements, including the Human Tissue Act 2004 and any amendments thereafter.

12. Possibility of future studies

When a biopsy is taken as part of this study it is regarded as a gift to the institution and could be used for future investigations into the molecular causes of lung disease. At the end of the study, any surplus tissue may be transferred to a registered tissue bank for use in future research projects. Any future studies will be reviewed by a research ethics committee. Consent from you for future studies would only be required if the committee considers that the study is likely to substantially affect the subjects' interests.

13. Gene studies

As part of the project we will be storing the samples taken to investigate genes and genetic pathways potentially involved in causing lung disease. There will be no attempt made to use your samples without your explicit consent to investigate any disorder, particularly any inherited disorder, other than lung disease.

14. What will happen if the findings may affect the subject personally?

The findings of this project will not affect you personally.

15. What if something goes wrong?

Every care will be taken in the course of this research. In the unlikely event that something goes wrong and you suspect that the injury is the result of the sponsor (UCL) or hospitals negligence you many be able to claim compensation. Please make the claim in writing to Professor Sam Janes, Chief Investigator for the study. If you wish to complain or have any concerns about any aspect of the way you have been approached or treated by members of staff or about any adverse events you may have experienced due to your participation in the study, the normal National Health Service complaints mechanisms are available to you.

16. What will happen to the results of the research study?

The results of the research will be presented at national and international meetings and submitted to peer-reviewed journals for publication. We will be very happy to inform you at your request of any such publication. If you are one of the patients who we biopsy with a view to creating a cell line then we will be happy to update you, again at your request, of the success or otherwise of the attempt to create a cell line.

You will not be identified in any report or publication.

17. Who is organising and funding the research?

University College London is the sponsor of this research.

The study is primarily funded by the Wellcome Trust.

Neither your doctor nor the investigators are paid for including you in this project.

18. Inducements

As with standard practice you will not be paid for entering this project.

19. Withdrawal from the project

Your participation in this study is entirely voluntary. You are free to decline to enter or withdraw from the study prior to the procedure without having to give a reason. If you choose not to enter the study, or to withdraw subsequently but prior to the procedure, this will in no way affect your future medical care. Participation in this study will in no way affect your legal rights.

20. Who has reviewed the study?

This project has been reviewed and given a favourable opinion by Hampshire Research Ethics Committee and by the Health Research Authority.

21. Contact for further information

Your first contact point for further information is Professor Sam Janes,

Email: s.janes@ucl.ac.uk,

Telephone 02035495976

We would like to take this opportunity to thank you very much for considering being a participant in this project.

You will be given a copy of this information sheet for your records.

8.3 Consent form for pleural procedures

UCL Respiratory
Rayne Institute
5 University Street
London
WC1E 6JF
Tel (+44) 0203 549 5979

Version 4: Pleural procedures
Date: 15 November 2018
Project ID: 245471
Patient identification number for this study:

CONSENT FORM

Title of project: An investigation into the molecular pathogenesis of lung disease II

Name of Principal Investigator: Professor Sam Janes

Please initial box

1. I confirm that I have read and understood the information sheet dated 15/11/18 (version 4) for the above study, have had the opportunity to ask questions and have had sufficient time to consider whether or not I want to be involved. ☐

2. I understand that my participation is voluntary and that I am free to withdraw at any time before any biopsy/sample collection occurs, without giving any reason, without my medical care or legal rights being affected. ☐

3. I understand that relevant sections of my medical notes and data collected during the study may be looked at by individuals from the sponsor (University College London), persons authorised by the sponsor, regulatory authorities or individuals from the NHS Trust. I give permission for these individuals to have access to my records. ☐

4. I understand that my tissue is regarded as a gift to the institution and that I will not retain any future rights to it. ☐

5. I consent to molecular and genetic assessment of my samples to determine whether genetic makeup has any influence on disease. ☐

6. I understand that the researchers may try to create a cell line using my biopsy tissue. ☐

7. I consent for any surplus tissue to be archived at the end of the study for future research. ☐

8. I understand that some of these projects may be carried out in collaboration with commercial organisations to include the pharmaceutical industry and I agree to this in the knowledge my personal data will not be shared. ☐

9. I understand that my GP will be informed of my participation in the study, unless I request otherwise. ☐

10. I agree to take part in the above study. ☐

CONSENT FORM

Title of project: An investigation into the molecular pathogenesis of lung disease II

Name of Principal Investigator: Professor Sam Janes

_____ _____ _____

Name of patient Date Signature

_____ _____ _____

Name of person taking consent Date Signature

____Professor Sam Janes ___ _____ _____

Chief Investigator Date Signature

8.4 Consent form for VATS procedures

UCL Respiratory
Rayne Institute
5 University Street
London
WC1E 6JF
Tel (+44) 0203 549 5979

Version 4: Video-assisted thoracoscopic surgery
Date: 15 November 2018
Project ID: 245471
Patient identification number for this study:

CONSENT FORM

Title of project: An investigation into the molecular pathogenesis of lung disease II

Name of Principal Investigator: Professor Sam Janes

Please initial box

1. I confirm that I have read and understood the information sheet dated 15/11/18 (version 4) for the above study, have had the opportunity to ask questions and have had sufficient time to consider whether or not I want to be involved. ☐

2. I understand that my participation is voluntary and that I am free to withdraw at any time before any biopsy/sample collection occurs, without giving any reason, without my medical care or legal rights being affected. ☐

3. I understand that relevant sections of my medical notes and data collected during the study may be looked at by individuals from the sponsor (University College London), persons authorised by the sponsor, regulatory authorities or individuals from the NHS Trust. I give permission for these individuals to have access to my records. ☐

4. I understand that my tissue is regarded as a gift to the institution and that I will not retain any future rights to it. ☐

5. I consent to molecular and genetic assessment of my samples to determine whether genetic makeup has any influence on disease. ☐

6. I understand that the researchers may try to create a cell line using my biopsy tissue. ☐

7. I consent for any surplus tissue to be archived at the end of the study for future research. ☐

8. I understand that some of these projects may be carried out in collaboration with commercial organisations to include the pharmaceutical industry and I agree to this in the knowledge my personal data will not be shared. ☐

9. I understand that my GP will be informed of my participation in the study, unless I request otherwise. ☐

10. I agree to take part in the above study. ☐

CONSENT FORM

Title of project: An investigation into the molecular pathogenesis of lung disease II

Name of Principal Investigator: Professor Sam Janes

_____	_____	
Name of patient	Date	Signature
_____	_____	
Name of person taking consent	Date	Signature
____Professor Sam Janes ___	_____	
Chief Investigator	Date	Signature

9 LIST OF PUBLICATIONS DURING THIS RESEARCH PERIOD

9.1 Journal articles

- **Alrifai D,** Forster MD, Janes SM. Emerging resistance pathways in lung cancer: what has ROS-1 taught us? Transl Lung Cancer Res. 2018; 7(Suppl 1): S9-S12

- Kolluri KK, Alifrangis C, Kumar N, Ishii Y, Price S, Michaut M, Williams S, Barthorpe S, Lightfoot H, Busacca S, Sharkey A, Yuan Z, Sage EK, Vallath S, Le Quesne J, Tice DA, **Alrifai D,** von Karstedt S, Montinaro A, Guppy N, Waller DA, Nakas A, Good R, Holmes A, Walczak H, Fennell DA, Garnett M, Iorio F, Wessels L, McDermott U, Janes SM. Loss of functional BAP1 augments sensitivity to TRAIL in cancer cells. eLIFE. 2018; 7:e30224

- Kumar N, **Alrifai D**, Kolluri KK, Sage EK, Ishii Y, Guppy N, Borg E, Falzon M, Nankivell M, Nicholson AG, Janes SM. Retrospective response analysis of BAP1 expression to predict the clinical activity of systemic cytotoxic chemotherapy in mesothelioma. Lung Cancer. 2019; 127:164-6

- Kumar N, **Alrifai D**, Psallidas I. Palliative care in mesothelioma: are current services RESPECT-able enough?. Thorax. 2019; 74(4):326-7

- Ishii Y, Kolluri KK, Pennycuick A, Nigro E, **Alrifai D**, Borg E, Falzon M, Shah K, Kumar N, Janes SM, BAP1 and YY1 regulate expression of death receptors in malignant pleural mesothelioma, pre print bioRxiv 2020

- Patel P*, **Alrifai D* (joint first author)**, McDonald F, Forster M. Beyond chemoradiation: Improving treatment outcomes for patients with stage III non-small cell lung cancer through immuno-oncology and durvalumab. British Journal of Cancer. Nov 2020 (in press)

9.2 Abstracts

- Kumar N, Kolluri K, **Alrifai D**, Ishii Y, Borg E, Falzon M, Nicholson A, Janes S. BAP1 expression and treatment outcomes in malignant pleural mesothelioma, in a prospective UK based clinical trial, In: Thorax 2018. British Thoracic Society Winter meeting. 2017. Dec 6-8, London, UK. p.A16-A17

- Alnajjar HM*, **Alrifai D*** (joint 1st author), Kolluri K, Mitra A, Feber A, Ben-Salha I, Muneer A, Alifrangis C. BAP1 protein loss in squamous cell carcinoma of the penis is associated with less nodal and distant metastasis at presentation. In: European Urology 2018. Proceedings of Annual European association of Urology. Copenhagen, Denmark. p.e43-e44

- Kolluri KK, Alifrangis C, Kumar N, Ishii Y, Price S, Michaut M, Williams S, Barthorpe S, Lightfoot H, Busacca S, Sharkey A, Yuan Z, Sage EK, Vallath S, Le Quesne J, Tice DA, **Alrifai D**, von Karstedt S, Montinaro A, Guppy N, Waller DA, Nakas A, Good R, Holmes A, Walczak H, Fennell DA, Garnett MJ, Iorio F, Wessels LFA, McDermott U, Janes SM. Loss of BAP1 function leads to trail sensitivity in malignant mesothelioma. Proceedings of iMig; 2018. May 2-5. Ottawa, Canada

- Zaki K, **Alrifai D**, Ulahannan D, Ahmad T, Papadatos-Pastos D, Lee SM, Swanton C, Bennett P, Falzon M, Borg E, Navani N, Janes S, Forster M. Molecular characterisation of lung adenocarcinoma using a 22-gene panel: A United Kingdom tertiary cancer centre experience. In: British Journal of Cancer 2018. Proceedings of the NCRI conference; 2018. Nov 4-6, Glasgow, UK

- Kolluri KK, Alifrangis C, Kumar N, Ishii Y, Price S, Michaut M, Williams S, Barthorpe S, Lightfoot H, Busacca S, Sharkey S, Yuan Q, Sage EK, Vallath S, Le Quesne J, Tice DA, **Alrifai D***, von Karstedt S, Montinaro A, Guppy N, Waller DA, Nakas A, Good R, Holmes A, Walczak H, Fennel DA, Garnett M, Iorio F, Wessels L, McDermott U, Janes SM. Loss of BAP1 is a biomarker for TRAIL sensitivity in malignant pleural mesothelioma. Proceedings of CRUK Lung Cancer Centre of Excellence, Student and Postdoc workshop; 2018. Nov 29-30, York, UK

- Kumar N, Kolluri KK, Alifrangis C, Ishii Y, Price S, Michaut M, Williams S, Barthorpe S, Lightfoot H, Busacca S, Sharkey S, Yuan Q, Sage EK, Vallath S, Le Quesne J, Tice DA, **Alrifai D**, von Karstedt S, Montinaro A, Guppy N, Waller DA, Nakas A, Good R, Holmes A, Walczak H, Fennel DA, Garnett M, Iorio F, Wessels L, McDermott U, Janes SM. Loss of BAP1 function leads to TRAIL sensitivity in mesothelioma. In: Thorax 2018. Proceedings of British Thoracic Society Winter meeting. 2018; Dec 5-7, London UK p.A1

- Davies A, Sage B, Kolluri K, **Alrifai D**, Graham R, Weil B, Rego R, Bain O, Patrick PS, Champion K, Day A, Popova B, Wheeler G, Fullen D, Kalbur T, Forster M, Lowdell M, Janes S. TACTICAL: A phase I/II trial to assess the safety and efficacy of MSCTRAIL in the treatment of metastatic lung adenocarcinoma. In: Journal of Clinical Oncology 2019. Proceedings of ASCO Annual Meeting 2019; May 31-June 4, Chicago USA p.9116

- Sage EK, Davies A, Kolluri K, **Alrifai D**, Graham R, Weil B, Rego R, Pereira VT, Edwards A, Bain O, Santilli G, Champion K, Day A, Popova B, Wheeler G, Fullen D, Forster M, Lowdell M, Janes S. TACTICAL: A phase I/II trial to assess the safety and efficacy of MSCTRAIL in metastatic lung adenocarcinoma. Proceedings of annual conference of the British Society of Gene and Cell Therapy; 2019; Aug 1, Sheffield, UK. p.A8

- Davies A, Sage EK, Kolluri K, Graham R, **Alrifai D**, Weil B, Patrick PS, Champion K, Day A, Popova B, Wheeler G, Fullen D, Kalber T, Lowdell M, Janes S, Forster M. Novel biomarker-driven trial of a cell and gene therapy for the treatment of malignant pleural mesothelioma (MPM): the STRATEGIC trial. In: Lung Cancer 2020.

Proceedings of the 18th BTOG annual conference 2020; Jan 29-31, Dublin, Ireland. p.S70

- Kolluri KK, Davies A, **Alrifai D**, Graham R, Day A, Champion K, Wheeler G, Popova B, Kalber T, Stephen PS, Weil B, Lowdell M, Fullen D, Sage EK, Forster M, Janes SM. STRATEGIC – A genetically engineered allogeneic cell therapy for mesothelioma patients with loss of functional BAP1. Proceedings of iMig; 2021. TBC. Brisbane, Australia (delayed as a result of COVID19)